Optimal Scheduling of Micro-Sources and Load Frequency Control in Multi-Microgrid System using Meta-heuristic Techniques

Submitted in partial fulfillment of requirement for the award of the degree of

Doctor of Philosophy

By

C. Srinivasarathnam

(Roll No. 716009)

Under the supervision of

Dr. Chandrasekhar Yammani
Assistant professor
&
Prof. Maheswarapu Sydulu

DEPARTMENT OF ELECTRICAL ENGINEERING
NATIONAL INSTITUTE OF TECHNOLOGY
(AN INSTITUTE OF NATIONAL IMPORTANCE)
WARANGAL, TELANGANA, INDIA – 506004

FEBRUARY-2021

APPROVAL SHEET

This Thesis entitled "**Optimal Scheduling of Micro-Sources and Load Frequency Control in Multi-Microgrid System using Meta-heuristic Techniques**" by **C.Srinivasarathnam** is approved for the degree of Doctor of Philosophy

Examiners

____

____

Supervisor (s)

Dr. Chandrasekhar Yammani
Assistant Professor

Prof. Maheswarapu Sydulu

Chairman

Dr. M. Sailaja Kumari
Professor & Head,
Department of Electrical Engineering,
NIT Warangal

Place: ____________

Date: ____________

DEPARTMENT OF ELECTRICAL ENGINEERING
NATIONAL INSTITUTE OF TECHNOLOGY-WARANGAL
(An Institute of National Importance)
506 004, TELANGANA, INDIA

CERTIFICATE

This is to certify that the dissertation work entitled **"Optimal Scheduling of Micro-Sources and Load Frequency Control in Multi-Microgrid System using Meta-Heuristic Techniques**", which is being submitted by **Mr. C. Srinivasarathnam** (Roll No: 716009), is a bonafide work submitted to National Institute of Technology, Warangal in partial fulfilment of the requirement for the award of the degree of **Doctor of Philosophy** in Electrical Engineering. To the best of our knowledge, the work incorporated in this thesis has not been submitted elsewhere for the award of any degree.

Dr. Chandrasekhar Yammani
(Supervisor)
Asst. Professor
Department of Electrical Engineering
National Institute of Technology
Warangal – 506004

Prof. Maheswarapu Sydulu
(Co-Supervisor)
Professor (HAG)
Department of Electrical Engineering
National Institute of Technology
Warangal – 506004

DECLARATION

This is to certify that the work presented in the thesis entitled "**Optimal Scheduling of Micro-Sources and Load Frequency Control in Multi-Microgrid System using Meta-Heuristic Techniques"** is a bonafide work done by me under the supervision of **Dr. Chandrasekhar Yammani, Assistant Professor and Prof. Maheswarapu Sydulu**, Department of Electrical Engineering, National Institute of Technology, Warangal, India and was not submitted elsewhere for the award of any degree.

I declare that this written submission represents my ideas in my own words and where others ideas or words have been included, I have adequately cited and referenced the original sources. I also declare that I have adhered to all principles of academic honesty and integrity and have not misrepresented or fabricated or falsified any idea/data/fact/source in my submission. I understand that any violation of the above will be a cause for disciplinary action by the Institute and can also evoke penal action from the sources which have thus not been properly cited or from whom proper permission has not been taken when needed.

C. Srinivasarathnam
(Roll No: 716009)

Date: 04.02.2021
Place: NIT Warangal

ACKNOWLEDGEMENTS

It gives me immense pleasure to express my deep sense of gratitude and thanks to my Supervisor **Dr. Chandrasekhar Yammani, Assistant Professor** and Co-Supervisor **Prof. Maheswarapu Sydulu,** Department of Electrical Engineering, National Institute of Technology Warangal, for their invaluable guidance, support and suggestions. Their knowledge, suggestions, and discussions helped me to become a capable Researcher. They have shown me the interesting side of this wonderful and potential research area. Their encouragement helped me to overcome the difficulties encountered in my research as well in my life.

I am very much thankful to **Prof. M.Sailaja Kumari**, **Chairman of DSC & Head**, Department of Electrical Engineering for her constant encouragement, support and cooperation.

I wish to express my sincere thanks to **Prof. N.V.Ramana Rao**, Director, NIT Warangal for his official support and encouragement

I take this privilege to thank all my Doctoral Scrutiny Committee (DSC) members, **Prof. M.Sailaja Kumari, Dr. T.Vinay Kumar, Asst. Professor,** Department of Electrical Engineering and **Prof.V.Ramana Murthy**, Department of Civil Engineering for their detailed review, constructive suggestions and excellent advice during the progress of this research work. I also express my sincere thanks to former DSC member, **Dr. P.Chandrasekhar**, Asst.Professor, Department of Electrical Engineering.

I also appreciate the encouragement from teaching, non-teaching members and fraternity of Department of Electrical Engineering of NIT Warangal. They have always been encouraging and supportive.

I convey my special thanks to contemporary Research Scholars Mr.A.Anil Kumar, Dr.B.Gurappa, Mr.S.Sreekantha Reddy, Dr.B.Kiran Babu, Dr.Pranay Kumar, Mr.Hemasundar, Dr.Kunisetti.V.Praveen Kumar, Dr.Ratna Rahul, Dr.Jammy Rahul of Department of Electrical Engineering.

I acknowledge my gratitude to Co-Scholars at NIT Warangal for their moral support and technical suggestions.

I acknowledge my gratitude to all my teachers and colleagues at various places for supporting and encouraging me to complete the work.

Finally, I render my respect to all my family members (My father Late Sri. C.Krishnama Chary, mother Smt.C.Kamalamma, brother Sri.C.Pavan Kumar, Sisters Smt.K.Sridevi & Smt.A.Soubhagya, Brother-in-laws Sri.K.Manohara Chary & Sri.A.Krishna, Sister-in-law Smt.C.Saritha, my wife Smt.C.Priyanka and my lovely Daughter Baby C.Adhvaitha) for giving me moral support and inspiration. They have motivated and helped me to complete my thesis work successfully.

C. Srinivasarathnam

ж

CONTENTS

ABSTRACT

Electrical Power Systems is gigantic in size with complex structure consisting of thousands of generators, hundreds of thousands of Kilometers length transmission & Distribution lines, millions of electrical consumers. Because of its complex structure, electrical network is prone to faults due to many reasons. A local and small event may get cascaded to cause major failures across Power Grid affecting millions of people, with severe economic and political consequents. Thus, providing reliable power to the consumer is of major concern.

Though electrical power generation was started in 1882, many countries in the world are not electrified fully. As per World Bank open data 2018, only 89.59% of World's population has electricity access. Majority of the unelectrified places are found to be rural areas. Lack of reliable electricity supply is one of the biggest hurdles for socio-economic development of the Nation. Thus, it is a challenge to the Power Systems Engineer to supply Electrical power to the remote locations where geographically grid expansion is not feasible.

Deregulation in Power System has given the scope for Distributed Generation. To address the challenges non-electrification of remote locations, the Power Systems Engineer converted the passive electrical network into active electrical network with Distributed Energy Sources. The IEEE guidelines 1547.4 states that the operation and reliability of the electrical system can be improved by sectionalizing the system into Multiple Networks. Thus, by sectionalizing the system into multiple networks, the blackouts can be avoided. Considering the above, in this thesis, the active Distribution System has been assumed to be sectionalized into multiple self-adequate networks, each network named as Microgrid System. Thus, the active Distribution System is modelled as Multi-Microgrid System.

The Microgrids are proposed to operate independently or combined with other Microgrids. Further, three objectives are aimed in Multi-Microgrid System operation. The first objective is aimed at economic operation, is achieved by minimizing the operating cost. The second objective is addressed to improve the energy efficiency of the system by minimizing the Active Power Losses and the third objective is focused on minimization of the System node's voltage deviation from its nominal value, is the Squared Voltage Deviation. The above objectives are achieved by Optimal Scheduling of the Micro-Sources.

It helps the Microgrid Central Control to schedule the Micro-Sources based on the desired objective.

Higher the reliability, lower the chance of power failure. Thus, to increase the reliability of power supply, the Forced Outage Rate (FOR) of Micro-Sources have to be considered for optimal scheduling of Micro-Sources with the constraint that Energy Index of Reliability should be greater than or equal to 0.97 along with equality and inequality constraints. Now, the objective functions like minimization of operating cost, active power losses and voltage deviation are need to be evaluated with the above constraints. This aspect helps the System Operator in promising the reliability of Multi-Microgrid System.

Further, optimizing one objective function may lead to compromise on other objective functions. Thus, the problem of Multi-Objective optimal scheduling of Micro-Sources with and without considering Energy Index of Reliability Criterion is also to be addressed. Three scenarios are formulated considering two objectives at a time. *Non-dominated Sortin*g and *Crowding Distance methodologies* are used to obtain the pareto optimal solution set. The Best Compromised Solution among the pareto front need to be evaluated. Based on the required objectives and constraints, the Microgrid Central Controller would operate the Multi-Microgrid System.

Considering the global warming due to consumption of fossil fuel sources, more attention is being paid on the Renewable Energy Sources especially Wind Power and Solar Power. As these sources are intermittent in nature, they cause frequency and Tie-lines power flow deviations in the Multi-Microgrid System. Thus, there is a need to identify the robust Secondary Load Frequency Controller in handling the fluctuations caused by sudden load changes, incorporation of Renewable Energy Sources and with Parametric uncertainty.

LIST OF FIGURES

LIST OF TABLES

NOMENCLATURE

ACE	Area Control Error
ACO	Ant Colony Optimization
AGC	Automatic Generation Control
BCS	Best Compromised Solution
BESS	Battery Energy Storage System
CD	Crowding Distance
CERTS	Consortium for Electric Reliability Technology Solutions
DEG	Diesel Engine Generator
DER	Distributed Energy Resources
DG	Distributed Generator/Micro-Sources
EA	Evolutionary Algorithms
EER	Energy Export Rate
EIR	Energy Index of Reliability
ESS	Energy Storage System
FC	Fuel Cell
FOR	Forced Outage Rate
FW	Fly Wheel
GA	Genetic Algorithm
GDP	Gross Domestic Product
GW	Giga Watts
GWO	Grey Wolf Optimization
HS	Harmony Search
IAE	Integral Absolute Error
IPFC	Internal Power Flow Controller
IEEE	Institute of Electrical and Electronics Engineers
ISE	Integral Square Error
IST	Indian Standard Time
ITAE	Integral Time multiplied Absolute Error
ITSE	Integral Time-weighted Squared Error
iter	iteration

kW	Kilo Watts
kWh	Kilo Watt Hour
kV	Kilo Volts
kVAR	Kilo Volt Ampere Reactive
LFC	Load Frequency Control
MG	Microgrid
MGCC	Microgrid Central Controller
MMG	Multi-Microgrid
MOJA	Multi-Objective Jaya Algorithm
MOO	Multi-Objective Optimization
MW	Mega Watts
PCC	Point of Common Coupling
PID Controller	Proportional Integral Derivative Controller
PSO	Particle Swarm Optimization
P.U	Per Unit
RES	Renewable Energy Sources
SA	Simulated Annealing
SI	Swarm Intelligence
SPV	Solar Photo Voltaic
SSO	Social-Spider Optimizer
TLBO	Teacher Learner Based Optimization
VD	Voltage Deviation
w.r.t	With respect to
WTG	Wind Turbine Generator

CHAPTER-1

Introduction

1.1 Introduction

Human life is very much dependent on energy. Industries, commercial, and day-to-day activities cannot be progressed without energy. However, energy is available in different forms such as Chemical energy, Thermal energy, Radiant energy, Nuclear energy, Electrical energy, Motion energy, etc. as shown in Fig-1.1[1]. According to the "*Law of Conservation of energy*," energy can be transformed from one form to another, but neither can it be created nor destroyed. Out of various forms of energy, electrical energy is the most important as it can efficiently be generated (converted from other forms of energy), easily transmitted, and for a reasonable cost, it can be utilized. The ease of transmission of electrical energy gives rise to a possibility of generating electrical energy in bulk at centralized places and transmit it over a long distance to be used ultimately by a large number of users[2]. Because of ease in generation, transmission, and utilization, throughout the world, the demand for electrical energy is increasing day-by-day.

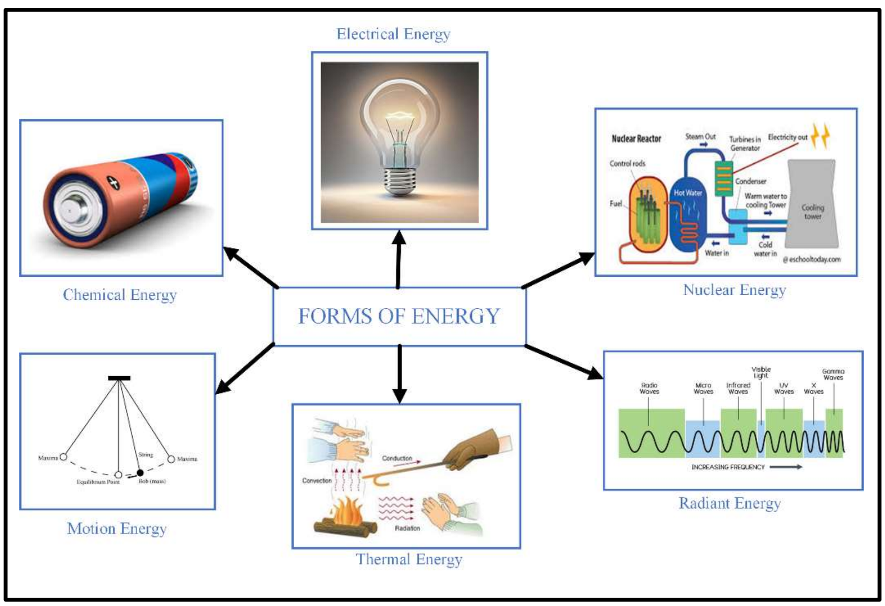

Fig-1.1: Various form of Energy

As stated in [3], Electrical Power Systems is a technical wonder, and according to the National Academy of Engineering, electricity and its accessibility are the greatest engineering achievements of the twentieth century, ahead of computers and airplanes. The authors in [4][5] stated that adult literacy rate, life expectancy at birth, GDP per capita (the level of economic development), consumption expenditure per capita, urbanization rate are the five indices that reflect the human development. The per capita electricity consumption should be strengthened to enhance the level of welfare of society and human development.

Therefore, special attention is being paid to the generation of electricity[4]. India has installed a capacity of 1.36GW during Independence [6], whereas it has raised to 365GW as on 31.10.2019 [7]. As a reflection, the per capita energy consumption of electricity in India has grown from 16kWh during 1946-47 to 1181kWh in the year 2018-19, as shown in Fig-1.2. The per capita energy consumption of electricity by various countries is shown in Fig-1.3[6]. It is clear from Fig-1.3 that the per capita energy consumption of electricity in India is much lower than the developed countries and is lesser than the World's average consumption. Further, the Worlds' average electricity consumption is much lower than the developed countries' electricity consumption. Thus, there is a need to think of supplying reliable power to the consumer at an affordable price.

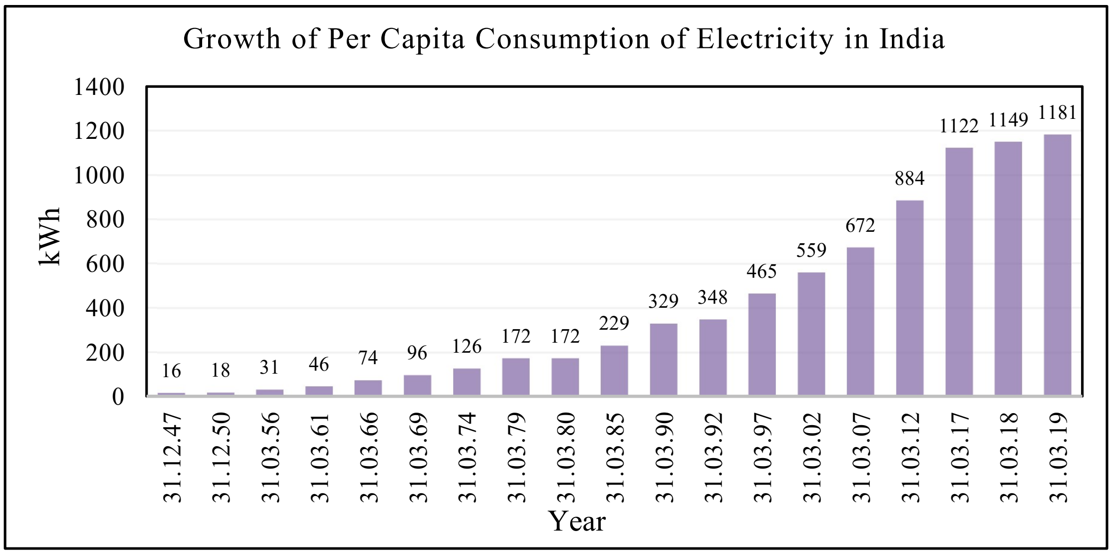

Fig-1.2: Growth in Per Capita Consumption of Electrical Energy in India

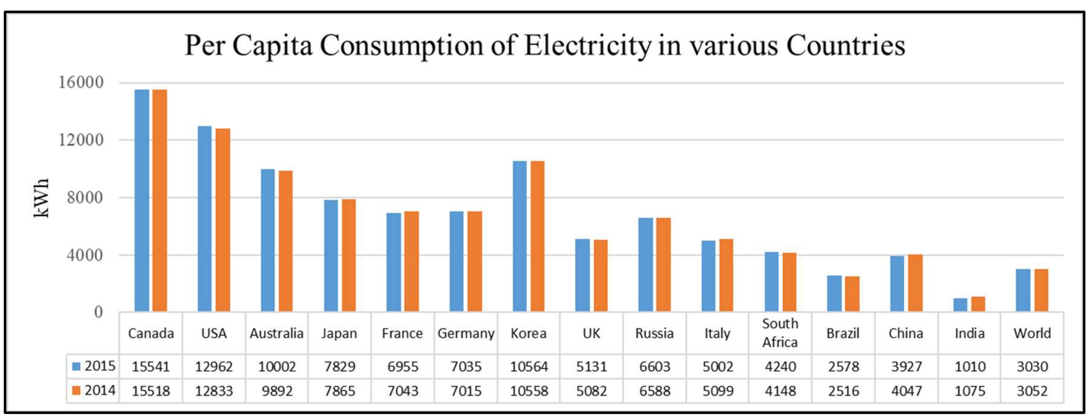

Fig-1.3: Per Capita energy Consumption of Electrical Energy in various Countries

As the Power System network is vast, at each node, a real-time energy requirement should be sensed, and it shall be balanced with the amount of produced energy. The balancing of generated power and demand is the main challenge in the Power Systems. The power demand varies from time to time, which depends on the end-user's usage of electric appliances. Further, due to highly unpredictable factors, such as weather conditions, energy pricing, and increasing of penetration of electric transportation, electrical energy usage is profoundly affected[3].

In addition to the above problem, for developing countries with spurring social and economic progress, it is pivotal to have affordable and reliable electricity in rural areas. It is proclaimed by Ministry of Power, Government of India [4] that still 13.90 Lakhs households in India are yet to be electrified as on 31.10.2019, and as per the World Bank report, the percentage of the World's population having access of electricity up to 2018 is 89.59% [5] as depicted in Fig-1.4. The Indian Government, by grid expansion, has made remarkable progress on rural electrification. However, copious householders have no electricity access[6]. Thus, it is a challenge to the Power Systems Engineer to supply electrical power to the remote locations where geographically grid expansion is not feasible.

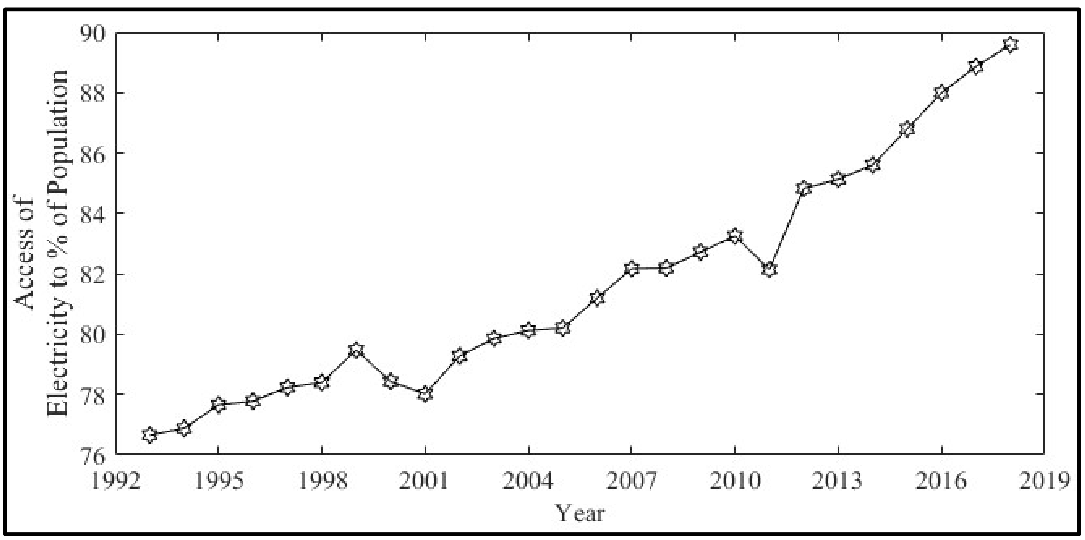

Fig-1.4: Access of Electricity to Percentage of Population in the World

It is a well-known fact that Power Systems is prone to faults without prior warning. Tree contacts, animal contacts, lightning, equipment failure, wind, ice/snowfall, dig-in, vehicle accidents, vandalism, construction activities, etc. are some of the causes of faults in the Power Systems. If a particular region of the system is affected by a fault, it may lead to overloading or isolation of other regions due to load redistribution. Continuous load redistribution to other regions, often leads to cascading phenomena, causes catastrophic failure, which has an enormous social and economic impact on society due to power disruptions.

As proclaimed in [7], a blackout was experienced by the Northeast United States and Canada in August 2003, which plunged thirty million people into darkness. The cause for it was identified as a single faulty relay at the Sir Adam Beck Station Number 2 in Ontario, Canada. The failure caused a transmission line to open. This fault, in turn, caused a cascade of line overloads that ultimately caused power generation plants throughout the region to shut down automatically.

Similarly, on 28th September 2003, Italy was in a blackout. The root cause for the blackout, as reported by UTEC in [8], was tripping off the first line from Switzerland - the so-called "Lukmanier" line - was caused by a tree flashover. The automatic reclosure was failed to switch-on the breaker, even after the carbonization of the affected tree. This failure of reclosure is due to phase angle difference over the line exceeded 30^0. The islanding operation of the system was found to be failed due to angular instability and voltage collapse, which caused a blackout, pushed 56 million people into darkness.

In India, the Northern region consisting of 8 states, has experienced a major blackout on 30th July 2012 affecting 400 million people. The cause was identified as circuit breakers on the 400kV Bina-Gwalior line got tripped. As this line fed into the Agra-Bareilly transmission section, breakers at that station tripped, and power failures cascaded through the grid. All major power stations were shut down in the affected states, causing an estimated shortage of 32GW. Again on 31st July, 2012, the system failed, due to a relay problem in substation near the Taj-Mahal. As a result, power stations across the affected parts of India again went offline. Over 600 million people, nearly half of India's population, in 22 out of 29 states in India, were without power [9].

To avoid such blackouts, the IEEE Power Engineering Society has made a report on remedial measures and restoration practices from blackout condition [10]. The report proclaimed that grid strengthening, remote emergency control for severe contingencies, out-of-step islanding were the remedial solutions.

Considering the challenges faced by the Power Systems i.e., (a) Electrification of remote locations where grid expansion is impossible and (b) To avoid blackout due to cascading effect on other parts, Power Systems Researchers have started contemplating for a feasible solution. Instigation of deregulation in the electrical systems has provided a realizable solution to Power Systems Researchers, thus evolved the *Microgrid* concept.

1.1.1 Formulation of Multi-Microgrid System

According to the U.S. Department of Energy, Microgrids are defined as "*a group of interconnected loads and Distributed Energy Resources (DERs) with clearly defined boundaries that acts as a single, controllable entity and can connect and disconnect from the main grid to operate in both Grid-connected or Island mode*"[11]. The schematic diagram of a typical Microgrid System is presented in Fig-1.5.

A Microgrid is characterized as the ability to interact with the main grid in real-time, and thereby optimize system performance and operational savings [12].

Microgrids have the ability to:

- ✓ Reduce Greenhouse gas emissions
- ✓ Enable integration of Renewable Energy Sources
- ✓ Support and modernize the local electricity Distribution System
- ✓ Provide energy resilience for critical facilities during electrical grid outages

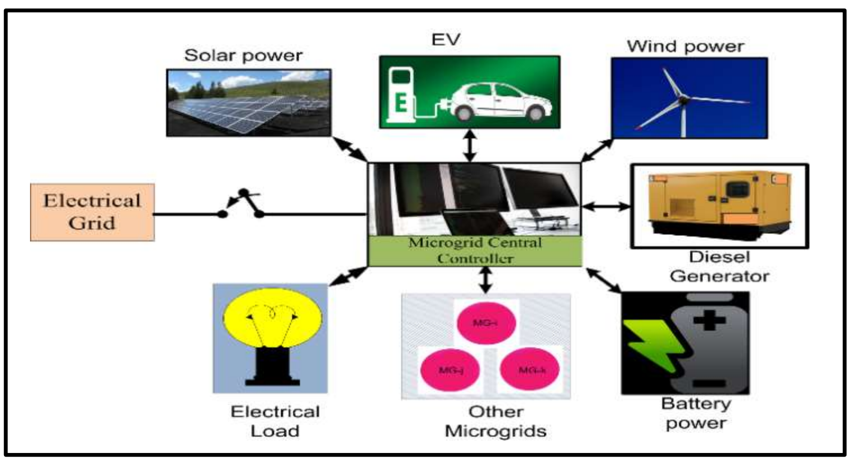

Fig-1.5: Schematic view of Microgrid System

The incredible feature of a Microgrid is, it functions in the *grid-connected mode* as well as in *islanded mode*[13]. A Microgrid is coupled to the main grid with one or more Points of Common Coupling (PCC) during the normal operating condition. Mostly Microgrids operate in islanded mode, unless the islanded mode of operation causes a problem of the safety and reliability of service [12]. Furthermore, whenever the main grid demands immediate restoration of voltage problems, islanding operation can safeguard the voltage-sensitive devices from significant voltage drops. The schematic view of the grid-connected mode of operation and the islanded mode of operation of a Microgrid are shown in Fig-1.6 and Fig-1.7, respectively.

The potential benefits of a Microgrid are the economical operation, environmental compliance, reliable, flexible, upgradable, dynamic islanding, enhancement of operational efficiency, and customer service. Considering these advantages, in addition to sophisticated metering in the Distribution System, advanced communication technologies, modern control strategies have changed the conventional structure of the active Distribution System into the "Multi-Microgrid System" over the past decade[14][15].

The IEEE Standard 1547.4, "IEEE Guide for Design, Operation, and Integration of Distributed Resource Island Systems with Electric Power Systems,"[16] proclaims that the Distribution System operation and reliability can be enhanced by sectionalizing the network into Multi-Microgrids. The schematic view of a typical Multi-Microgrid System is shown in Fig-1.8.

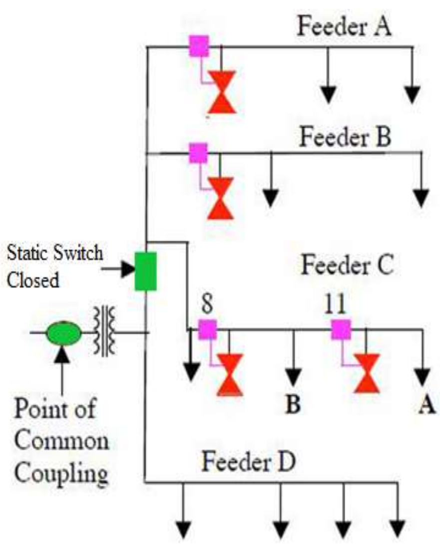

Fig-1.6: Schematic view of Microgrid System operation in Grid-connected mode

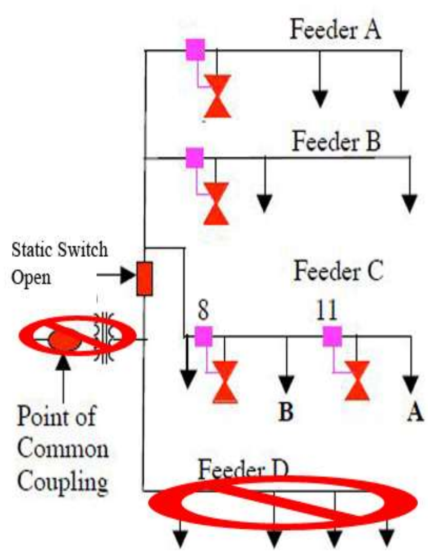

Fig-1.7: Schematic view of Microgrid System operation in Islanded mode

The implementation of Microgrid projects have increased throughout the World, majorly in Europe, the United States, Australia, China and Brazil. Recent analysis of global '*Microgrid Deployment Tracker 1Q20*' has identified 6610 grid-tied and remote Microgrid projects of capacity 31,784 MW which are operating, under development, or proposed around the World[17]. In India, the Indian Coast Guard operates a Microgrid in Andaman

Island of 75kW capacity[18], The Kalkeri Sangeet Vidyalaya, a musical school situated in Kalkeri village, Dharwad District in Karnataka operated as a Microgrid of capacity 14kW.

In [12], it is pronounced that Hurricane Sandy, which knocked out power to more than 8 million people, had islanded New York University and Princeton University. Two Microgrids were interconnected, and a total load of 15MW between two Universities had been shared. Thus, Microgrids enhance the reliability of the operation of the electrical system.

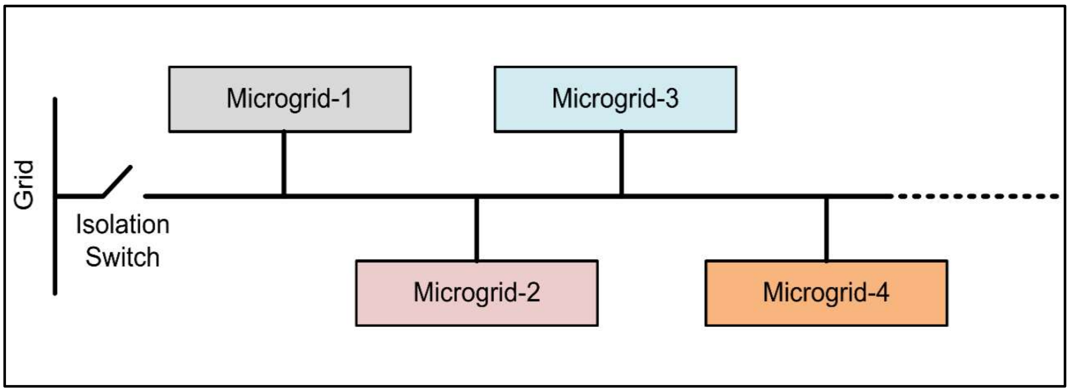

Fig-1.8: Schematic view of Multi-Microgrid System

Considering above, upon sectionalizing the islanded active Distribution System into Multi-Microgrids, advantages associated with the Microgrid system are achievable. Further, to achieve the advantages, there is a need to attempt the optimal scheduling of controllable DGs, similar to that of the conventional system, i.e., economical operation, minimization of active power losses, voltage deviation minimization, even in the Multi-Microgrid System. To supply the electricity reliably, as each DG has Forced Outage Rate (FOR), and to increase the customer satisfaction, a reliability constraint optimal scheduling shall be performed such that DG with higher FOR will contribute less power output. Optimizing one objective function value may lead to an increase in other objective function value. Thus, to get a trade-off among various objectives, Multi-objective optimization problem is to be addressed.

1.1.2 Multi-Microgrid System Frequency Control

The frequency of the system is dependent on the active power balance. The frequency of the system must be maintained nearly constant for the satisfactory operation of the electrical system [19]. The need for maintaining constant frequency is that: (a) The blades of the steam turbine are designed to operate in a narrow band of frequency. Gradual or immediate damage to the turbine may be caused by the continuous operation of the turbine beyond the band of frequency. (b) Electrical appliances are generally designed to operate at nominal frequency. Operating the system at off-nominal frequency may cause deteriorated performance/reduced output of loads and affects power system operation, security, reliability, overloading of transmission lines, triggering of protective devices [20]. For instance, the output of power plant auxiliaries like pumps or fans which supply combustion air to the thermal power plant or which supply coolant to Nuclear power plant may reduce, causing a reduction in power plant output. Further, relatively close control of frequency ensures constancy of the speed of induction motors and synchronous motors. The magnetizing current in an induction motor and transformer is also dependent on frequency. Thus, a considerable drop in frequency leads to high magnetizing currents and lower efficiency. Considering the above, it is essential to maintain the frequency of the system near to nominal value.

The frequency control levels are categorized into three levels: Primary, Secondary, and Tertiary control [21]. Governor is a primary controller. The primary controller is the immediate control of the relationship between turbine speed and power i.e., it is responsible for intercepting the frequency decline before triggering the under/over frequency protection relays. The primary controller controls the relation between speed and power as per Equation-(1.1).

$$\omega = \omega_{ref} - RP \tag{1.1}$$

Where R - Governor droop setting, ω - running speed of the turbine, ω_{ref} - speed-load reference setting of the turbine, P – output power of turbine.

The primary controller of power plants is autonomous and will function continuously without requiring inputs from any external source. Whenever an event occurs, the primary frequency controller of the generators responds immediately within a few seconds. Once the balance of power generation and demand is re-established, the system frequency is fixed for that balancing condition but does not restore to the nominal value, thus causing a steady-state error. This is because of the proportional action of the generator's droop characteristics. Consequently, in a multi-area system, tie-line power flows differ from the scheduled values.

The secondary frequency controller is also called Automatic Generation Control (AGC) or Load Frequency Control (LFC). It is responsible for regulating the frequency of the system to the nominal value [21]. The goals of the LFC are: (a) Maintaining the frequency in acceptable range and (b) Control the power exchange through Tie-lines between different control areas. The time taken by the LFC to restore frequency lies between tens of seconds to a few minutes [20][22].

As stated, balancing power generation and demand is critical for the Power System Operator for maintaining the stability of the Power System. As proclaimed in [22], in India, the energy deficit has been declined over the past years, and the grid frequency has been improved since 2014 by the inception of the secondary frequency controller in the system. The average grid frequency profile and variation in minimum & maximum frequency in India have been presented in Fig-1.9 and Fig-1.10, respectively [23]. Thus, it is evident that the secondary frequency controller restores the system frequency to the nominal value.

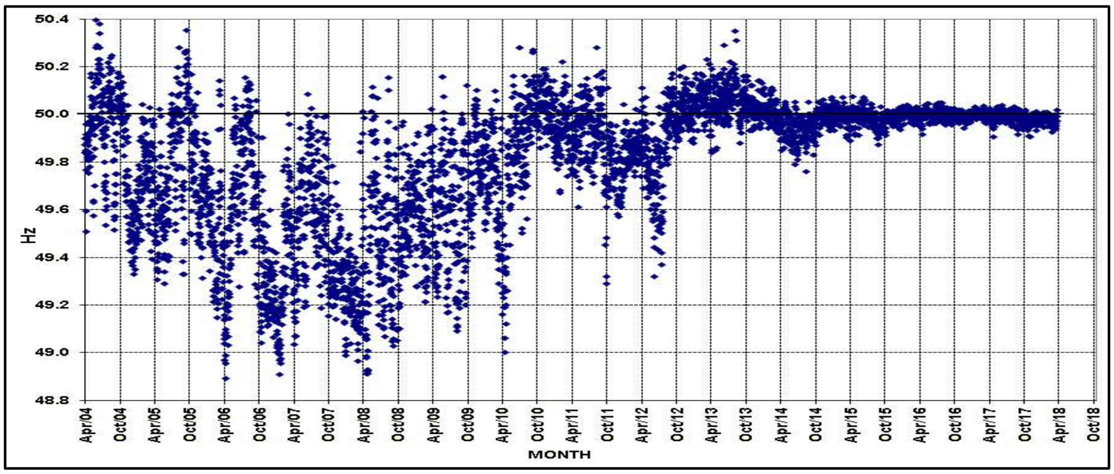

Fig-1.9: Average Grid Frequency Profile of India since 2004

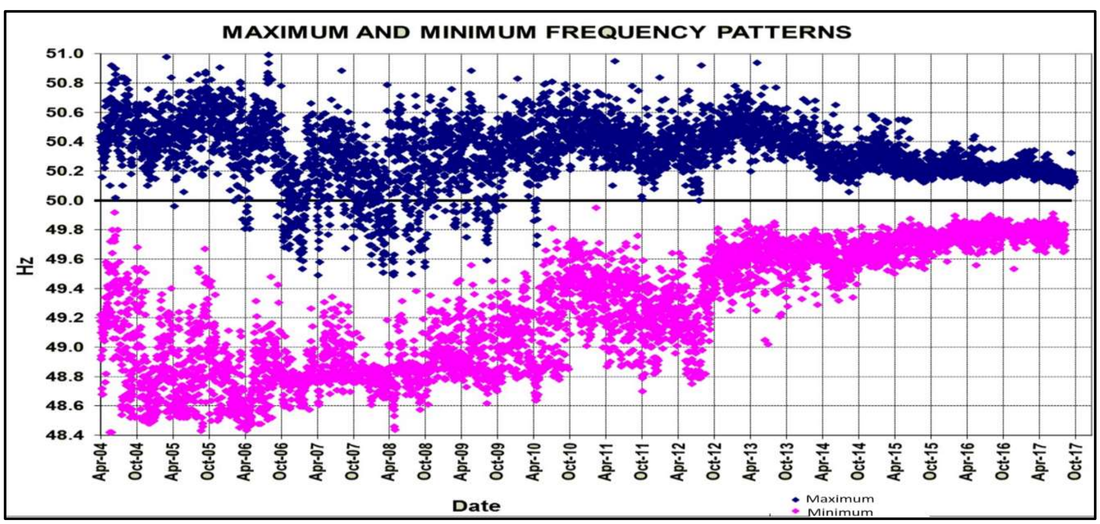

Fig-1.10: Variation in Maximum and Minimum Frequency of the Indian Grid since 2004

Whenever system frequency quickly drops to a critical value due to severe event in the system, due to under frequency, the other generating units may trip, which leads to the blackout of the system. In this situation, to avoid cascading failure, a tertiary frequency controller or emergency control plan is adopted to restore the frequency and tie-line flow to the nominal value. In addition, the tertiary controller manages congestion in the transmission system, restores the secondary reserve, and is achieved by on/off of ancillary reserves, demand-side control, rescheduling of LFC participating units [20]. The characteristics of various controllers are presented in Table-1.1.

Table-1.1: Characteristics of Various Frequency Controllers[22]

Response / Attribute	Inertia	Primary	Secondary	Tertiary
Time	First Few Secs	Few Secs - 5 mins	30 Secs - 15 mins	5mins – 30 mins
Manual/Automatic	Automatic	Automatic	Automatic	Manual
Centralized/ Decentralized	Decentralized	Decentralized	Centralized	Centralized

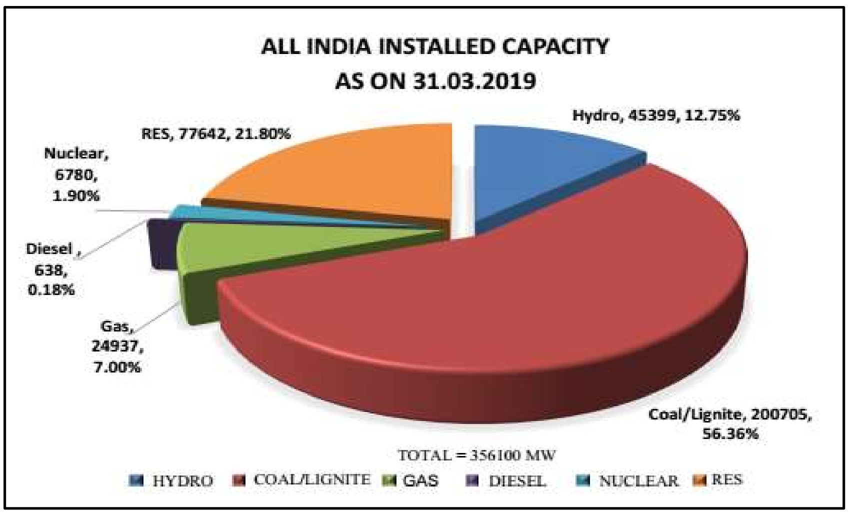

Fig-1.11: All India Installed capacity as on 31.03.2019

Throughout the World, Environmentalists are making policies to protect the Earth from global warming. Kyoto protocol in 1997, Paris Agreement-2015 are agreed by the parties of United Nations Framework Convention on Climate Change (UNFCCC), with the aim of long-term temperature goal, to keep the increase in global average temperature to well below 2 °C relative to pre-industrial levels and to pursue efforts to limit the increase to 1.5 °C, recognizing that this would substantially reduce the risks and impacts of climate change. Further, it states that, if global warming is to be limited to between 1.5 °C and 2 °C by the year 2100, global emissions must peak before 2020 and then begin to rapidly decline.

Considering this, Renewable Energy Sources (RES) are integrated into Power System. The share of RES in electricity generation has raised to 33% in the World and, in India, as presented in the CEA report [24], the RES have an installed capacity of 77.64MW as on 31.03.2019 which is 21.80% as shown in Fig-1.11. As RES are intermittent in nature, they cause an imbalance in power generation and demand, as a consequence, frequency deviation and tie-line power flow deviation arise in the system[25]. Thus, there is a need to contemplate the design of a robust Load Frequency Controller for mitigation of frequency deviation and scheduled tie-line flow deviations in the system. This design aspect must be supported by good algorithms.

1.2 Meta-Heuristic Techniques

Most conventional or classic algorithms are deterministic. For example, the Simplex method in Linear programming is deterministic. Some deterministic optimization algorithms have used gradient information, and they are called Gradient-based algorithms. A well-known Newton-Raphson algorithm is a gradient-based approach, as it uses the function values and their derivatives, and it works exceptionally well for smooth uni-modal problems. However, if there is some discontinuity in the objective function, it does not work well. In this case, a non-gradient algorithm is preferred. Non-gradient based or gradient-free algorithms do not use any derivative, and they make use of only the function values.

Stochastic algorithms are of two types in general, i.e. Heuristic and Meta-Heuristic, however, their difference is small. Generally speaking, heuristic means “to find” or “to discover by trial and error.” Quality solutions to a tough optimization problem can be found in a reasonable amount of time, but there is no guarantee that the solutions have reached the optimal solutions. It can be expected that these heuristic algorithms work most, but not all the time. This is good when we do not necessarily want the best solutions, or rather good solutions are easily reachable.

Further development of heuristic algorithms is the so-called Meta-Heuristic algorithms. Here meta means “beyond” or “higher level,” and these algorithms generally perform better than simple heuristics. In addition, all meta-heuristic algorithms use certain trade-offs of randomization and local search. It is worth pointing out that no agreed definitions of heuristics and meta-heuristics exist in the literature; some use the terms heuristics and meta-heuristics interchangeably. However, the recent trend is to name all Stochastic algorithms with randomization and local search property as meta-heuristic.

Considering this, in this present research work, the convention is followed. Randomization provides an excellent way to move away from local search to another search on a global scale. Therefore, almost all meta-heuristics algorithms tend to be suitable for global optimization.

Two significant components of any meta-heuristic algorithm are intensification and diversification, or exploitation, and exploration. Diversification means to generate diverse solutions to explore the search space on a global scale. Intensification means to focus on the search in a local region by exploiting the information that a current good solution is found in this region. This is in combination with the selection of the best solutions. The selection of the best solution ensures that the solutions will converge to the optimality, whereas the diversification via randomization avoids the solutions being trapped at local optima and, at the same time, increases the diversity of the solutions. The good combination of these two major components will usually ensure that the global optimality is achievable [26].

Meta-heuristics, in their original definition, are solution methods that organize interaction between local improvement procedures and higher-level strategies to create a process capable of escaping from local optima and performing a robust search of a solution space. Over time, these methods have also come to include some procedures that employ strategies for overcoming the trap of local optimality in complex solution spaces.

A number of tools and mechanisms that have emerged from the creation of meta-heuristic methods and they have proved to be remarkably effective. With that, meta-heuristics have moved into the spotlight in recent years as the preferred line of attack for solving many types of complex optimization problems, particularly those of a non-linear constrained nature.

The problem considered in this Thesis is "Optimal Scheduling of Micro-Sources and Load Frequency Control in Multi-Microgrid System," and it is a complex non-linear optimization problem with many constraints. To obtain the optimal solution for these types of problems, a suitable optimization algorithm is required.

More attention is being paid on the Multi-Microgrid concept due to its numerous advantages. Small scale energy resources are integrated into the system. As the Power System Engineers, our aim is to operate the system in an economical manner, improving the energy efficiency, and supply the quality power to the consumers. To achieve 'or' realise these, optimal scheduling of energy sources is to be addressed on prominent note. As the

Renewable Energy Sources in the Multi-Microgrid System cause deviation in system frequency and tie-line power flow, the Secondary Load Frequency Controller is to be incorporated to mitigate the fluctuations.

Multi-Objective study can be defined as the problem of finding “a vector of decision variables which satisfies the constraints and optimize a vector function whose elements represent the objective function.” These objective functions are from the mathematical description of relevant performance criterion and are usually conflicting with each other. Hence, the term ‘optimize’ means finding a solution that gives the values of various objective functions that are acceptable.

Though the Multi-Objective Optimization offers a set of solutions which are all optimal, the user needs only one final solution. The user requires some higher-level information to choose one solution from the set of optimal solutions. Often, such higher-level information is non-technical, qualitative, and experience-driven. Therefore, in multi-objective optimization, better effort must be made in finding the set of trade-off optimal solutions by considering various objectives simultaneously. After a set of such trade-off solutions are found, the user can use high-level information to make a choice. Higher-level information is usually taken from domain expertise.

As the conventional techniques fail to identify the global solution in a nonlinear constraint optimization problem, meta-heuristic techniques are required to address the Optimal Scheduling of Micro-Sources and Load Frequency Control (LFC) problem in Multi-Microgrid System.

1.3 Literature Review

1.3.1 Optimal Scheduling of Micro-Sources in Multi-Microgrid System

A transformative architecture for the optimal operation and self-healing of autonomous networked Microgrids was attempted by Zhaoyu Wang and et al. in [27]. It was stated that multiple Microgrids were connected to a common bus. For information exchange and coordinated control, the Microgrids were connected through a cyber-communication network. In the normal operation mode, each Microgrid operates independently. The operating cost was minimized by optimally controlling the dispatchable DGs and loads. When a fault or generation deficiency happens in a Microgrid, the framework enters the self-healing mode. The on-emergency Microgrid receives power support from other Microgrids that were under normal operation. A Consensus algorithm was used to distribute portions of the desired power support to individual Microgrid in a decentralized way.

Carlos A. Hernandez-Aramburo and et al. in [28] proposed an operating cost minimization strategy in Microgrid System. The proposed test system consists of a reciprocating engine, combined heat and power plant, Solar Photo Voltaic and Wind Turbine Generator. The optimization problem was formulated as a minimization of operating cost subjected to power balance active power demand and thermal energy demand. The authors have introduced a penalty factor for the production of excess heat than the demand. However, this paper has not focused on the economic operation of interconnected Microgrid Systems.

The authors in [29] attempted economic power dispatching in an islanded Microgrid System. The test system had included Photovoltaic, Geothermal and Biomass generators. The forecasted load profile and PV power generation for 24 hours have been considered for economic dispatching of controllable DGs. However, loss minimization and Voltage Deviation minimization aspects have not been attempted by the authors. Also, the economic dispatch in the Multi-Microgrid system has not been concentrated by the authors.

The authors in [30] proposed two modes of operation of the Distribution System, which were Normal operating condition and Self-healing condition. During the Normal operating condition, the controllable DGs in the Distribution System were optimally dispatched to achieve operating cost minimization. Whenever a fault/faults occurred in the system, the system entered into Self-healing mode. The on-outage areas were optimally sectionalized into networked self-adequate MGs. A Rolling-Horizon optimization method was used to schedule the outputs of dispatchable DGs. The above methodology was tested on a modified IEEE 123 node Distribution System. However, the authors have not considered Forced Outage Rate (FOR) of DGs while optimally scheduling the DGs in the Multi-Microgrid System for reliability improvement.

Javier Matamoros and et al. in [31] presented energy trading among the interconnected Microgrids. The Microgrids were isolated from the main grid. The goal was to minimize the total cost, which includes energy generation costs plus energy transportation costs while satisfying the local power demand at each Microgrid. The optimization was addressed in a centralized fashion and also in a distributed fashion. It was stated that the centralized approach required all information about energy generation and transportation costs to be available at a central controller. The authors asserted that the central controller is the best approach wherein Microgrids belong to the same energy operator. On the contrary, if privacy needs to be protected, the distributed approach was a better choice. In the distributed approach, each Microgrid iteratively solved a local optimization problem by exchanging energy estimate information with the other Microgrids. It is stated that in the distributed approach case, the solution converged (under some mild assumption on the cost functions) to the centralized optimal solution. The authors focused on energy exchange among Microgrids, but optimal scheduling of DGs in individual Microgrids was not tackled. Further, the authors has not considered reliability constraint while optimally scheduling.

In [32], the authors proposed energy and operation management in a Microgrid System. Minimization of total energy and operating cost by optimally adjusting the control variables and satisfying operating constraints have been addressed. Particle Swarm Optimization (PSO) technique was employed by the authors to solve the stated problem. The authors have implemented the PSO on a typical Grid-connected Microgrid System. However, the authors have not concentrated on the minimization of operating cost in a Multi-Microgrid System.

Nima Nikmehr and et al. in [33] proposed optimal power dispatch among interconnected Microgrids. The authors propounded that the system not only exchanges power among Microgrids but also with the main grid. The power exchange among Microgrids and the main grid was regarded as sold or purchase of power among Microgrids and the main grid. It is regulated to realize total cost minimization. The load and small-scale energy resources are modelled as probabilistic models. PSO and Imperialist competitive algorithm were used for optimizing the problem. However, the authors have not focused on the islanded operation of Microgrids system and reliability constraint optimal scheduling of resources.

S. Najafi Ravadanegh and et al. [34] attempted the economic operation of the Multi-Microgrid System with the objective of cost minimization. The proposed test system consists of three Microgrids connected to the main distribution grid. The proposed problem was to minimize the total cost of power generation in each MG and also that of power interchange between MGs and the main distribution grid. The optimal power dispatch problem was addressed considering uncertainty and probabilistic behaviour of power demand and power generation from small scale energy resources. PSO was used to solve the scheduling problem. However, the authors had paid attention to cost minimization only when Microgrids connected to main grid, but not investigated the islanded operation of

Microgrids. Further, Power loss minimization and Voltage Deviation minimization problems in the Multi-Microgrid System have not been attempted by the authors.

Sicong Tan and et al. in [35] proposed reconfiguration of the distribution network for isolation of the faulty section in the network. Upon isolation, economic dispatch of energy sources has been performed. The stochastic nature of small-scale energy resources and the load was considered. The optimization problem was solved using four bio-inspired algorithms named: Vaccine-enhanced Artificial Immune System, PSO, GA, and Artificial Immune System. However, the authors have not tackled the problem of multiple faults in the network. Furthermore, active power loss minimization and voltage deviation minimization problems are not attempted by the authors.

1.3.2 Reliability constraint optimal Scheduling of Micro-Sources in Multi-Microgrid System

The authors in [36] proposed optimal Distributed Energy Resources (DER) within the framework of an optimal Microgrid architecture. The objective function was formed considering deployment cost of DGs and savings gained by the use of Combined Heat and Power (CHP) with Energy Index of Reliability (EIR) as a constraint. The problem was formulated as Non-linear Programming and Simulated Annealing optimization was applied. Six bus test system was used by the authors for demonstration purpose.

Optimal sizing and siting of Distributed Generation units in a Microgrid were attempted by Mallikarjuna R. Vallem and et al., in [37]. The authors considered EIR criterion for solving the stated optimization problem. The authors proclaimed that with reliability criterion, the cost increases minimally. The cost function was modelled as a Nonlinear Programming problem, and Simulated Annealing (SA) optimization was used to achieve global optimum. However, the reliability criterion based optimal scheduling of DGs has not been applied for Multi-Microgrid System.

In [38], the authors investigated the optimal dispatch strategy of DGs in a Microgrid System. The Energy Index of Reliability (EIR) was taken as criterion for minimization of system losses, system voltage deviation and cost of DGs. The methodology was implemented for four seasons: Winter, Spring, Summer and Autumn with future load enhancement. Dispatch strategy was attempted by Bat Optimization Algorithm on IEEE 33 Bus Distribution System. However, the formulation of the Distribution System into the

Multi-Microgrid System and Multi-objective optimal scheduling of DGs in Multi-Microgrid System have not been covered by the authors.

Logenthiran T and et al. in [39] proposed a Multi-Agent System based scheduling of energy resources in an islanded power system consisting of integrated microgrids. The authors have solved the proposed problem in three-stages. In the initial stage, the optimal scheduling of energy sources has been attempted to satisfy each Microgrid's internal demand. In the next stage, the best possible bids for the energy-exporting to the other microgrids were evaluated and in the final stage, Microgrids energy resources were rescheduled to meet their internal demand and the energy export demand. However, the authors have not considered FOR of energy resources while attempting economic scheduling.

1.3.3 Multi-objective Optimal Scheduling of Micro-Sources in Multi-Microgrid System with and without Reliability constraint.

Amin Kargarian and et al. in [40] attempted the Multi-Objective optimal power flow among interconnected Microgrids. Interline Power Flow Controller (IPFC) was used to control the power flow among Microgrids. Minimization of total operating cost, total energy losses and voltage deviation were treated as objective functions in the Multi-Objective Optimization problem considering the power injection of IPFC as control variables. Sequential Quadratic Programming technique was employed to evaluate the control variables. Reliability constraint was not studied by the authors in [40] while solving Multi-objective optimization.

The authors addressed the optimal scheduling of Distributed Generators in a Microgrid System in [41]. A multi-objective optimization problem was formulated considering minimization of squared voltage deviation, minimization of active power losses, reducing the cost of energy imported from the grid and levelling the active power at the interconnected buses. The multi-objective optimization problem was solved using the Weighted Sum approach with the Rank Order Centroid method. However, the authors have not considered the reliability constraint of the optimal scheduling of DGs.

In [42], the authors attempted the optimal scheduling of DGs in a Microgrid System. The Maximum Fuzzy Satisfaction Degree method was adopted to transform the multi-objective optimization problem into a nonlinear single-objective optimum problem. The improved Genetic Algorithm was used to optimize Micro-Sources' active power output, reactive power output. In [42], the effort has not been extended to cover multi-objective optimal scheduling of DGs in the Multi-Microgrid environment with reliability criterion.

Gholamreza Aghajani and et al. in [43] attempted optimal scheduling of energy resources in Microgrid environment. Multi-objective optimization problem was addressed by the authors considering minimization of operating cost and emission as objective functions. The test Microgrid was operated in grid-connected mode. Multi-objective Particle Swarm Optimization technique was pursued by the authors to realize the pareto-optimal front. Fuzzy decision-making technique was applied to evaluate the interactive solution. The authors have not attempted the optimal scheduling of energy resources in Multi-Microgrid system and also the reliability constraint was not tackled by the authors.

1.3.4 Load Frequency Control of Multi-Microgrid System considering Renewable Energy Sources

Dong-Jing Lee and et al. in [44] addressed small-signal stability analysis of an islanded hybrid Renewable Energy power generation/energy storage system. The test system consists of a Diesel Engine Generator (DEG), three Wind Power Generators, a Photovoltaic System, an Acqu-electrolyser, Battery Energy Storage System (BESS) and two Fuel Cells. Three case studies were formulated considering power supply from different power sources. In the initial case, power supply only from the combination of Wind Power Plant, DEG & Energy Storage devices was considered, in the next case power supply only from the combination of Solar Power, DEG & Energy Storage devices, and in the final case power supply from DEG, Wind Power integration at different time slots & Energy Storage devices. From the case studies, the authors claimed that Energy Storage Systems could effectively meet the varying load demand and thus arrest the system frequency deviations.

K.V. Vidyanandan and et al. in [45] attempted the LFC problem on a Microgrid System consisting of a Diesel Engine Generator (DEG), Fuel-cell (FC), Wind Power and Electrolyzer. The FC and electrolyser were used to regulate the frequency fluctuation originated from the intermittent nature of Wind Power. Electrolysis was performed to generate Hydrogen gas. The generated Hydrogen gas was used as fuel to FC. Being uncontrollable, whenever excess power was produced by the Wind Power plant than the power demand, the surplus power was used for electrolysis action. On the other hand, during deficient power generation, FC used Hydrogen gas to generate electrical power along with DEG. However, it was noticed that the Fuel Cell being an electrochemical device, its response time was not quick to meet the varying load conditions. Thus, it does not restore the frequency quickly. Besides, parametric uncertainty has not been addressed by the authors in this paper.

Jeya Veronica and et la. in [46], considered a Microgrid System consisting of Diesel engine generator, Wind power, Solar power, Fuel cell, Battery Energy Storage System. The authors stated that because of the weak inertia nature of the RES, regulating the frequency to the nominal value of the system is of more importance. Internal Model-Based Controller was attempted by the authors for better frequency regulation in Microgrid System. The Multi-Microgrid System consisting of RES and parametric uncertainty were not given attention by the authors.

G. Mallesham and et al. in [47] proposed the Ziegler Nichols method for frequency regulation in a Microgrid System. A test system consisting of Wind Power, Solar Power, Fuel Cell, Diesel Engine Generator as power generation sources and Batter, Flywheel, Acqa-electrolyzer as energy storage systems, was considered for case studies. The authors have evaluated the frequency bias and gains of the PID controllers for the dynamic stability of the Microgrid System. However, the authors have considered one PID controller for each energy storage element and also the output power from RES was treated as constant.

The authors in [48] presented a control strategy for the frequency regulation in a Wind–Diesel powered Microgrid. To reduce the adverse effects caused by Wind's variability, intermittency and uncertainty on the system frequency and improve the performance of Diesel Engine Generator (DEG), two different energy storage technologies were explored. Fuel cell (FC) for long-term energy storage and a Flywheel (FW) for short-term energy storage devices for regulating the system frequency. The authors proclaimed that the integration of energy storage in the Wind dominated generation improves the overall system performance by way of improved frequency profile. The effectiveness of energy storage devices in frequency regulation was demonstrated on a test system. The role of parametric uncertainty in the Microgrid System frequency regulation was not addressed.

Hassan Bevrani and et al. [49] addressed the Load Frequency Control problem in an islanded Microgrid System. The test system consists of Micro-Sources (Diesel Engine Generator, Micro-turbines, Fuel-Cells) and RES (Wind Power and Solar Power). The authors have used $H\infty$ and μ-synthesis methods for secondary frequency controller designing with the linearized state-space model of the MG system. The robustness of the proposed controller has been verified considering perturbations in RES, system load and dynamic perturbations. However, the calculation process is tedious [50] and stability to be demonstrated for each case study.

A. Hasib Chowdhury and et al. [51] attempted Load Frequency Control of Multi-Microgrid System. The test MG consists of Synchronous Generator, Wind Power, Solar Power, Energy Storage System (ESS). Integral Square Error (ISE) has been considered as a performance index by the authors. The output of ESS is regulated using feedback of frequency deviation and Area Control Error (ACE). The intermittent nature of RES and parametric variation were not given attention by the authors.

Attia A. El-Fergany and et al. [52] proposed the Load Frequency Controller for standalone two-area hybrid Microgrid System. The gains of PID controllers and Integral Time multiplied Absolute Error (ITAE) were considered as control variables and the fitness function respectively. Diesel Engine Generator, Wind turbine, Solar panel and various energy storage devices were considered in the two-area Hybrid Microgrid System. Social-Spider Optimizer (SSO) was applied to fine-tune the gains of the Proportional–Integral–Derivative (PID) controllers. Scenarios such as load fluctuations, variations in Wind speed and Sun irradiance were considered. It was demonstrated that the SSO Algorithm diminuting the signal deviations in a short time. In the proposed LFC for hybrid Multi-Microgrid System, the possibility of parametric uncertainty aspect was not investigated.

Grey Wolf Optimization was used by Esha Gupta and Akash Saxena in [53] for AGC of two areas' interconnected power system consisting of Thermal units only. In this article, the authors have verified the superiority of the algorithm with load change in steps of 10%, 20% and 25% in different areas. However, the authors have not considered Renewable Energy Sources, which are highly intermittent in nature and the parametric variations of the system to verify the robustness of the algorithm.

1.4 Motivation

From the above introduction and literature review, it is observed that maximum benefits can be obtained from sectionalizing the islanded active Distribution System into Multi-Microgrid System. But, operation of the Multi-Microgrid System without optimally scheduling the controllable DGs for the long run leads to increased expenditure, unsatisfactory operation of appliances due to voltage violations, deteriorating the life of current-carrying elements due to increased losses. Further, integrating the RES in the Multi-

Microgrid System leads to frequency deviations in such a Multi-Microgrid System. Thus, it is necessary to address these challenges associated with the system

To overcome the above-mentioned problems, the optimal scheduling of controllable DGs in the Multi-Microgrid System is required. Further, the Energy Index of Reliability (EIR) criterion in optimal scheduling of DGs is to be addressed for reliable power supply to the customers.

Multi-objective optimal scheduling of DGs has to be developed to optimize the generators' Operating cost, Active power losses in the system and system Voltage Deviation ***without EIR criterion*** and ***with EIR criterion***.

Next, to mitigate the impact of RES and parametric uncertainty on the Multi-Microgrid System frequency and tie-line power flow deviation, a robust secondary load frequency controller, is to be investigated.

The conventional optimization techniques fail to identify the global optimal solution for the above stated non-linear constraint optimization problems. Thus, there is a need for simple and effective meta-heuristic optimization techniques to address the same.

1.5 Objectives of Thesis

The objectives of this thesis include:

1. To optimally schedule the Micro-Sources in the Multi-Microgrid System, which is formed by sectionalizing the islanded active Distribution System into self-adequate Microgrids with the aim of minimization of Operating Cost, Active Power Losses and Voltage Deviation.
2. To develop reliability constraint optimal scheduling model in Multi-Microgrid System with Cost minimization, Loss minimization and Voltage Deviation minimization as objectives.
3. To develop a Multi-Objective Optimization model for optimal scheduling of DGs in the Multi-Microgrid System with reliability constraint and without reliability constraint.
4. To improve the stability of the Multi-Microgrid System consisting of Renewable Energy Sources, the secondary frequency controller gains are proposed to tune with various meta-heuristic techniques.

1.6 Description of Research Work

From the literature, it has been noticed that, for minimizing the number of customers affected by a fault at a distinct location in the active Distribution System, the aspect of sectionalization of active Distribution Network into self-adequate Microgrids is essential. Further, it is stated that islanding operation can safeguard the voltage-sensitive devices from significant voltage drops, whenever the main grid encounters immediate restoration of voltage problem. It is manifested in the literature that mostly Microgrids operate in islanded mode owing to the advantages associated with it unless the islanded mode of operation causes an issue of the safety and reliability of service.

The meta-heuristic techniques are more popular to solve the non-linear combinatorial complex optimization problems. To date, there are numerous meta-heuristic optimization algorithms available in the literature. The more popular meta-heuristic algorithms are the Genetic Algorithm (GA), Particle Swarm Optimization (PSO), Ant Colony Optimization (ACO), Teaching-Learning-Based Optimization (TLBO), Grey Wolf Optimization (GWO), Jaya Algorithm, etc. Most of the meta-heuristic optimization required common control parameters (population size, maximum no. of generations) and algorithm-specific parameters (cross over probability, mutation probability and elitism probability in GA, inertia weight, social and cognitive parameters in PSO). It is a well-known fact that improper tuning of algorithm-specific parameters either increases the computational effort or yields the local optimal solution. In view of this, the Jaya Algorithm, which is independent of algorithm-specific parameters, is used in this research work.

It is evident from the majority of the previous works, optimal scheduling approach for Micro-Sources has been performed by the authors before sectionalizing the active Distribution System into Microgrids. Upon sectionalizing, the islanded Microgrids are being power supplied either by dispatching the DGs without considering optimal scheduling approach or by power exchange from other Microgrids. Improper dispatching of Micro-Sources leads to increased active power losses or escalation in operating cost or increased Voltage Deviation from the nominal value at the system buses.

In view of the above, in the present research work, the islanded active Distribution System has been sectionalized into self-adequate Microgrids based on the locations of the DGs. These Microgrids are proposed to operate either in isolated mode or in amalgamated with other Microgrids. Various case studies are formulated considering the individual operation or networked operation of Microgrids. The DGs in the Microgrids are optimally scheduled, considering different scenarios. The scenarios include Cost minimization or Active power loss minimization or Voltage Deviation minimization as objective functions. A single-objective optimization problem has been formulated considering one of the scenarios. Jaya Algorithm has been used for optimal dispatch of Micro-Sources in Multi-Microgrid System. The test results are validated upon comparison with the Genetic Algorithm (GA). The results reveal that the Jaya Algorithm is superior in all scenarios for various case studies. *This part of the work is published in the IEEE International Conference on Sustainable Energy, Electronics and Computing Systems (SEEMS), I.T.S Engineering College, Greater Noida, India, 2018 with DOI: 10.1109/SEEMS.2018.8687370.*

Further, the Energy Index of Reliability (EIR) has been considered as additional constraint along with equality and inequality constraints for optimal scheduling of Micro-Sources in Multi-Microgrid System considering different case studies under each scenario. Higher the value of EIR, the greater the probability of reliable power supply to customers. The optimization problem has been solved using Jaya Algorithm. Genetic Algorithm is used to validate the results obtained using Jaya Algorithm. *This part of the work is published in the 9th National Power Electronics Conference, NIT Tiruchirappalli, 13th-15th December 2019 with DOI:10.1109/NPEC47332.2019.9034703.*

To get the trade-off among various objectives, multi-objective optimization cases have been formulated considering two objectives at a time, for various case studies. Non-dominated Sorting Technique and Crowding Distance methodology have been adopted for obtaining the Pareto-optimal solution set. This multi-objective optimization problem has been solved initially without considering EIR criterion and then extended by considering EIR criterion. To get the Best Compromised Solution (BCS) among various solutions in the Pareto-front, the Fuzzy Decision-making approach has been used. A Part of this work is published in *Smart Science - Taylor & Francis Group Publishers, Vol-7, Issue-1, pp. 59-78, 2018. DOI:10.1080/23080477.2018.1540381 (ESCI Indexed).*

Due to the tremendous advantages of Renewable Energy Sources (RES), more importance is being given to integrating the RES in the Microgrid System. As a part of this research work, RES are integrated into the Multi-Microgrid System. Since the RES are intermittent in nature, frequency deviation in Microgrids and tie-line flow deviation have been investigated. To stabilize the oscillations, secondary load frequency controller gains are tuned with various meta-heuristic techniques. The robustness of the controller has been established by comparing the performance index and time domain specifications of the system. The results could reveal that the Grey Wolf Optimization based Proportion Integral Derivative (GWO-PID) controller is superior over the conventional Proportion Integral Derivative Controller, Particle Swarm Optimization based Proportion Integral Derivative Controller (PSO-PID), Jaya optimization based Proportion Integral Derivative Controller (JAYA-PID) and Teaching Learning Based Optimization tuned Proportion Integral Derivative Controller (TLBO-PID). Part of this work is published in *Smart Science – Taylor & Francis Group Publishers, Vol-7, Issue-3, pp. 198-217, 2018. DOI: 10.1080/23080477.2019.1630057 (ESCI Indexed)* and remaining part of this work is published in *the 9th National Power Electronics Conference, NIT Tiruchirappalli, 13th -15th December 2019 with DOI: 10.1109/NPEC47332.2019.9034751.*

The organization of research work is shown Fig-1.12.

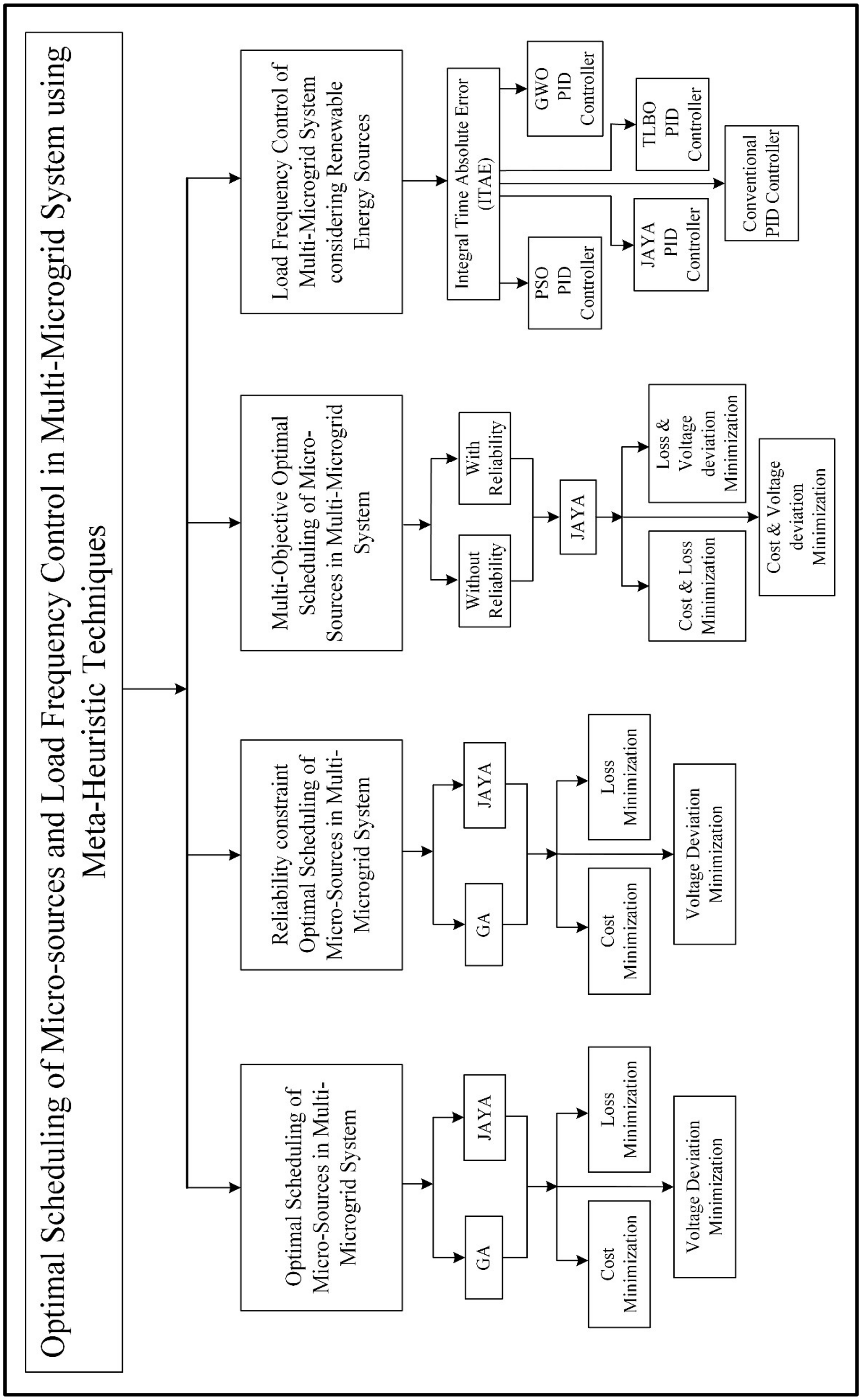

Fig-1.12: Flow chart for organization of Research work

1.7 Thesis Organization

The thesis is organized into six chapters and presented as below:

The **First Chapter** presents the literature survey, important observations and motivation for this research work in the area of "Optimal Scheduling of Micro-Sources (DGs) with and without considering Energy Index of Reliability (EIR) criterion and Load Frequency Control (LFC) in Multi-Microgrid System considering Renewable Energy Sources (RES)". In this chapter, a detailed literature review is carried out for the Optimal Scheduling of DGs and Dynamic Stability aspects of the Multi-Microgrid System consisting of RES. The motivation, objectives of the thesis and the chapter wise summary are also outlined.

The **Second Chapter** presents the need to sectionalize the active Distribution System into the self-adequate Multi-Microgrid System. Upon sectionalizing, the Micro-Sources in Multi-Microgrid System are scheduled optimally satisfying equality and inequality constraints. Several case studies are formulated considering the independent operation of Microgrids and amalgamated functioning of Microgrid(s). To increase the energy efficiency of the system, to stabilize the system node Voltage Deviation from nominal value and for economical operation of the system, minimization of Active power losses, minimization of Voltage Deviation and minimization of Operating cost of DGs are considered as objective functions. The proposed methodology is tested on IEEE 33 Bus Distribution System and Practical Indian 85 Bus Distribution System. A novel algorithm-specific parameter-free meta-heuristic algorithm named Jaya Algorithm is employed for an optimally scheduling approach of DGs. The performance of the Jaya Algorithm is validated by comparing it with the well-known algorithm in the literature i.e., the Genetic Algorithm.

The **Third Chapter** presents "the Optimal Scheduling approach of Micro-Sources in Multi-Microgrid System considering Energy Index of Reliability (EIR) as a criterion in addition to equality constraint (i.e. power balance) and inequality constraints (generator power output limits, Bus voltage limits). Considering the independent operation of Microgrid and combined operation of Microgrid with other Microgrid(s), various case studies are formulated. Cost minimization, Active power loss minimization and Voltage Deviation minimization are considered as objective functions. IEEE 33 Bus Distribution System and Practical Indian 85 Bus Distribution System are considered as test systems for testing the proposed methodology. The optimization is performed using Jaya Algorithm and the obtained results are validated by comparing with the Genetic Algorithm (GA). The variation in Operating cost, Active power losses and system Voltage Deviation with and without consideration of EIR criterion are analyzed for various case studies.

The **Fourth Chapter** elaborates on the need for Multi-Objective Optimization (MOO). In this chapter, the procedure for the formation of Pareto-front in MOO is explained in detail. Since the results produced by the Jaya Algorithm are superior to that of the Genetic Algorithm in optimal scheduling of single-objective optimization problems performed in the above chapters, Jaya Algorithm is applied for the MOO problem. The necessary modifications in the procedure for Multi-Objective-Jaya Algorithm are explained in detail in this chapter. MOO using Jaya Algorithm is performed with EIR and without considering EIR. Three scenarios are formulated considering two objective functions out of three objectives (i.e. Cost minimization, Active power loss minimization and Voltage Deviation minimization) at a time, and the DGs are optimally scheduled. The Best Compromised Solution (BCS) from the Pareto-front is evaluated using the Fuzzy Decision-making approach. The work is executed on IEEE 33 Bus Distribution System and Practical Indian 85 Bus Distribution Systems for the various case studied.

The **Fifth Chapter** presents the need of Load Frequency Control (LFC) in the Multi-Microgrid System. As the primary frequency controller cannot restore the frequency to the nominal value, the secondary frequency controller (PID) is considered. The gains of the secondary frequency controllers are tuned with various meta-heuristic techniques. The dynamics in the Multi-Microgrid System frequency and tie-line flow deviations are analyzed for multiple scenarios, which include single-step load change, multi-step load change, multi-step load with the integration of RES, parametric variation without the integration of RES and parametric variation with the integration of RES. The robustness of the various controllers is analyzed by considering the performance index (Integral Time multiplied Absolute Error) and the time domain specifications.

Finally, the **Sixth Chapter** highlights the conclusions and the significant contributions of research work and provides scope for future research in this area.

CHAPTER-2

Optimal Scheduling of Micro-Sources in Multi-Microgrid System

2.1 Introduction

The topology of the Distribution Network, location of DGs and loads could play a crucial role in supplying the Microgrid loads with diverse reliability requirements. Locating DG nearer to load will decrease the power outage duration and the frequency of power outages as well as the level of energy not supplied at a Microgrid [54]. In the Grid-connected mode, outages of the main grid could lead to the Microgrid islanding.

The planning of any system is an off-line study that needs to consider both technical aspects and economic analysis for aiming quality power supply to customers in a reliable manner. In order to avoid the stated difficulties, arise due to a fault in the Distribution System and to avail the potential benefits of the Microgrid system, it is proposed in this work to sectionalize the islanded active Distribution System into several Microgrids. Further, sectionalization has been made considering the topology of the network, size & location of DGs in the network and load demand at each bus. Besides, non-violation of operational constraints such that each Microgrid DGs can feed power to its load, i.e. self-adequate Microgrids [55], so as to provide reliable power supply to as many customers as possible. Furthermore, these on-outage Microgrids share power among themselves. The existing Micro-Sources are optimally scheduled in individual Microgrids or among on-outage Microgrids for obtaining the following objectives: (i) Minimization of Operating cost, (ii) Minimization of Active power losses and (iii) Minimization of Voltage Deviation. This proposal has been attempted, for optimal scheduling of the Micro-Sources in the sectionalized Microgrids. The effectiveness of the proposed model is analyzed on a modified IEEE 33 Bus Distribution System and a modified Practical Indian 85 Bus Distribution System. A novel meta-heuristic algorithm named Jaya Algorithm is used for optimal scheduling of controllable DGs and the results obtained are compared with the Genetic Algorithm.

The contributions of this Chapter are as follows:

1. Sectionalized the islanded Active Distribution System into self-adequate Microgrids based on the DGs position, the topology of the Distribution System and the possible fault locations.
2. Optimally schedule the controllable DGs in each Microgrid for single-objective optimization problem i.e., Operating cost minimization or Active power loss

minimization or Voltage Deviation minimization. A novel, meta-heuristic optimization named Jaya Algorithm, has been considered for optimization.

3. In this chapter, a modified IEEE 33 Bus Distribution System and a modified Practical Indian 85 Bus Distribution System are considered as test case study systems for illustrating the proposed strategy and the test results are compared with the Genetic Algorithm.

2.2 Sectionalizing of Distribution System:

The strategy considered is to operate the system effectively to supply power to as many consumers as possible during normal and faulty conditions.

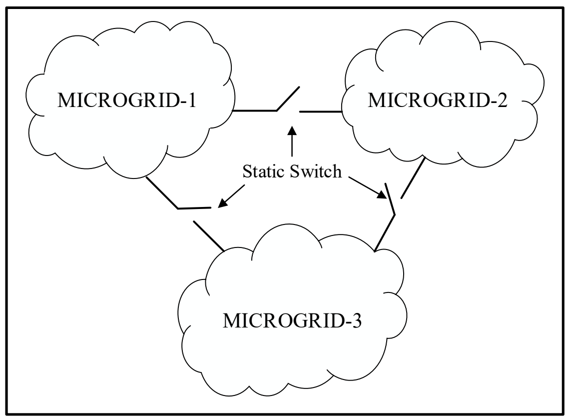

Fig-2.1: Sectionalisation of Distribution System into Multi-Microgrid System with Tie-line connection.

During normal operating conditions, the controllable Micro-Sources in the entire Distribution System are optimally scheduled to realize the desired objective functions such as minimization of Operating cost, Minimization of system Active power losses, Minimization of Voltage Deviation.

Whenever a fault occurs in the system, the traditional Distribution System enters into self-healing mode and reconfiguration of the system has to be made for interconnection of on-outage areas and isolating the faulty region from the rest of the system. In general, as the Distribution Networks are radial in nature, while reconfiguring these networks, this quality of the Distribution Network has been preserved. A tie switch and a sectionalizing switch are composed by each loop in the network such that each time anyone is opened, the other one is closed to maintain the radial nature of the network [56].

Sectionalisation of the Distribution System has been made based on the self-adequate of supply and demand, which in turn is necessary for the stability of Multi-Microgrid System. It is assumed that Microgrid Central Controller (MGCC) will take the decision of sectionalizing the system into self-adequate Microgrids. In this chapter, transient stability and dynamic stability aspects of the system are ignored, considering that stability will be maintained while sectionalizing the network [35][57].

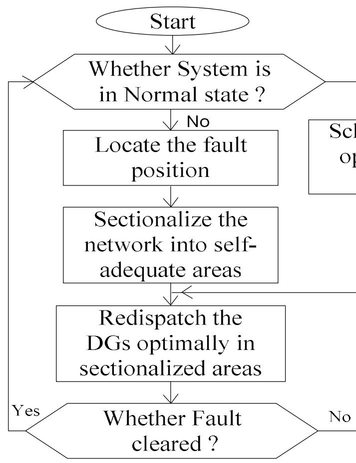

Fig-2.2: Flow chart for sectionalizing the islanded active Distribution System into Multi-Microgrid System.

A simple Distribution System with three Microgrids is shown in the Fig-2.1. It is assumed that three Microgrids are self-adequate. From the Fig-2.1, it can be analyzed that whenever a fault occurs in any one of the Microgrids say Microgrid-1, then Microgrid-1 will be disconnected from the rest of the system (Microgrid-2 and Microgrid-3) by opening the static switches of tie-lines of Microgrid-2 and Microgrid-3. Similarly, whenever a multi-area fault occurs, then faulted Microgrids will be disconnected from the rest of the system. During the fault condition also, the various objectives considered for the case of normal state operation are also been considered for minimization in on-outage area. On clearing the fault, the system goes back to the normal state. The flowchart for Distribution System sectionalisation is shown in the Fig-2.2.

2.3 Problem Formulation

Identifying the best solution from an exponentially large set of feasible solution is defined as the optimization problem. The objective of the optimization problem will be either minimization or maximization. In this chapter, single-objective optimization has been executed. In single-objective optimization problem, one of these objective functions

(i) Minimization of Generation Cost, (ii) Minimization of Active power losses and (iii) Minimization of System Voltage Deviation, has been considered for optimization at a time, to get the optimal scheduled output power of DGs. The control variables for these optimization problems is the controllable DGs output. Equality constraints and inequality constraints are considered while optimally scheduling the DGs output power, which is explained in section-2.3.4 below. The optimization problem has been formulated as follows:

2.3.1 Minimization of Generation Cost

Minimization of total Generation cost or total Operating cost in an isolated Microgrid or Multi-Microgrid System by optimally scheduling the controllable DGs output is considered as an objective function. The cost function of each DG is expressed as quadratic cost function. The total generation cost is obtained by summing up the quadratic cost model of all the generators [58] and is defined as per Equation-(2.1).

$$F_1(X) = \sum_{q=1}^{m}\sum_{k=1}^{N_{gen}}(a_{qk}P_{qk}^2 + b_{qk}P_{qk} + c_{qk})\frac{\$}{hr} \tag{2.1}$$

$$[X] = [P_{q1i}\ \ P_{q2i}\ \ P_{q3i} \dots \dots P_{qk-1i}\ \ P_{qki}] \tag{2.2}$$

where m is the total number of Microgrids in the system, N_{gen} is the total number of generators in each Microgrid-q. The a_{qk}, b_{qk} and c_{qk} are the fuel cost coefficients of k^{th}generator in q^{th} Microgrid, P_{qki} is active power generation value of k^{th}generator in q^{th} Microgrid at i^{th} iteration, X is a control variable relating any P_{qk}, which is defined as per Equation-(2.2). However, while optimizing the generation cost, equality constraint (i.e., power balance constraint) as well as inequality constraints (i.e., Generators capacity constraints and Bus voltage constraints) are need to be satisfied.

2.3.2 Minimization of Active Power Loss

This loss minimization objective function is achieved by optimally scheduling the controllable DGs such that total Active power losses in the isolated Microgrid or Multi-Microgrids are minimum and these are expressed in Equation-(2.3) and Equation-(2.4)[59]. While scheduling to attain the objective function, the equality constraint and inequality constraints need to comply. The objective function is defined as follows:

$$F_2\,(X) = Minimize(P_{loss}\,) \tag{2.3}$$

$$P_{loss} = \sum_{q=1}^{m} P_{q,loss} = \sum_{q=1}^{m}\left[\sum_{k=1}^{N_{gen}} P_{qk} - P_{q\,demand}\right] \tag{2.4}$$

Where $P_{q,loss}$ is Active power loss in q^{th} Microgrid, P_{qk} is active power generation value of k^{th}generator in q^{th} Microgrid, $P_{q\,demand}$ is total active power demand in q^{th} Microgrid and P_{loss} is total active power losses of all active Microgrids.

2.3.3 Minimization of Voltage Deviation

Third objective function of investigation in this chapter is minimization of Voltage Deviation. It is defined as the square of the difference between the bus voltage V_i and its specified nominal voltage value upon total buses in the system as per Equation-(2.5). To attain the desired objective, the DGs are optimally scheduled satisfying both equality and inequality constraints. The Voltage Deviation is defined as follows [41] .

$$F_3(x_{i,k}) = Minimize\left[\frac{1}{n_{bus}}\sum_{q=1}^{m}\sum_{k=1}^{nbus_q}\left(|V_{qk}| - |V_{qk}^{sp}|\right)^2\right] \tag{2.5}$$

Where V_{qk} and V_{qk}^{sp} are the absolute voltage value and the specified voltage value at k^{th} bus of q^{th} Microgrid respectively, $nbus_q$ is total number of buses in q^{th} Microgrid and n_{bus} is total number of buses in all active Microgrids.

2.3.4 Equality and Inequality constraints

The system constraints are generally defined as equality constraint and inequality constraints. The equality constraint is power generation and demand balance whereas the inequality constraints are boundaries of active power output, voltage magnitude at bus. These constraints are mathematically defined as follows.

2.3.4.1 Power balance constraint

The total power generation in the Microgrid(s) System must be equal to the total power demand and the total power losses in the Microgrids considered for the operation, to maintain the stability of the system as per Equation-(2.6). Since the network is a radial system, with multiple buses and loads in each feeder, there is a need to consider power losses in the system.

$$\sum_{q=1}^{m}\left[\sum_{k=1}^{N_{gen}} P_{qk}\right] = \sum_{q=1}^{m}\left[P_{q\ demand} + P_{q\ loss}\right] \tag{2.6}$$

Where $P_{q\ demand}$ is total active power demand in q^{th} Microgrid, $P_{q,loss}$ is Active power losses in q^{th} Microgrid, P_{qk} is active power generation value of k^{th}generator in q^{th} Microgrid, m is the total number of Microgrids in the system and N_{gen} is the total number of generators in each Microgrid-q.

2.3.4.2 Generation capacity constraints

For stable operation, the real power output of each generator P_{qk} is restricted by lower and upper limits. While scheduling the DGs output, the power limits have to be enforced for stable operation of the system. Thus, the active power generation boundaries of a DG are defined as per Equation-(2.7).

$$P_{qk}^{min} \leq P_{qk} \leq P_{qk}^{max} \tag{2.7}$$

Where P_{qk}^{min} and P_{qk}^{max} are the minimum and maximum active power operating limits of k^{th} unit in q^{th} Microgrid.

2.3.4.3 Bus voltage constraints

For voltage stability of the system, the Bus voltage magnitude of the k^{th} bus in any Microgrid System must be within lower and upper limits [60]. Thus, the boundaries of the bus voltages magnitudes are defined in Equation-(2.8). The voltage limits considered in this research work are ±5%.

$$V_k^{min} \leq V_k \leq V_k^{max} \tag{2.8}$$

2.4 Implementation of the Proposed Jaya Algorithm

The traditional optimization algorithms, such as Dynamic Programming, Nonlinear Programming, Geometric Programming, Sequential Programming, etc., have certain limitations in their search mechanism. The search mechanism of these algorithms depends on the type of objective and constraint functions, modelling of variables type. The efficiency of these algorithms relies on the solution space size, the structure of solution space, the number of variables. The above problems associated with traditional techniques have been surmounted with population-based optimization techniques over the past two decades.

There are different type of population-based algorithms such as Evolutionary Algorithms (EA) and Swarm Intelligence (SI) algorithms. These probabilistic algorithms require tuning of control parameters, some of which are common parameters of all algorithms such as population size, number of iterations etc. and the rest are algorithm-specific parameters such as crossover probability, mutation probability, elitism probability in the Genetic Algorithm (GA), inertia weight, maximum velocity, and cognitive parameters in Particle Swarm Optimization (PSO) algorithm, harmony memory in Harmon Search (HS) algorithm. These parameters play a vital role in finding the global optimum in the search space and improper tuning of these parameters leads to premature convergence.

Considering the stated facts, a novel meta-heuristic algorithm which is independent of algorithm-specific parameters rather needs only common control parameters such as population size and the maximum number of iterations i.e., Jaya Algorithm has been considered in this chapter. Jaya Algorithm was proposed by Prof. R.Venkata Rao in 2016 and it is a simple and powerful global optimization algorithm[61]. The Jaya Algorithm procedure is described as follows.

Let 'f' be the objective function to be minimized. Assuming that there are k number of *design variables* of the objective function f. In this algorithm, at the beginning, generate P_{size}(Population size) number of initial solutions (X) randomly. The random solutions must be within the search space, bounded by the lower and upper limits of the design variables. Now, evaluate the objective function value for all the P_{size} initial solutions. Upon evaluation of objective function value, the three common phases of Jaya Algorithm are to be followed to produce the next generation population.

2.4.1 Evaluation of the Best solution candidate and the Worst solution candidate Phase

In each iteration, the candidate solution which provides minimum objective function value and maximum objective function value are treated as the Best solution candidate ($X_{i,best,\mathrm{k}}$) and the Worst solution candidate ($X_{i,worst,k}$) among the total population ($X_{i,j,\mathrm{k}}$) respectively.

where 'i' stands for iteration number, varies from zero to maximum number of iterations/generations, 'j' indicates the candidate number in the population, which varies from one to population size (P_{size}) and 'k' points out the design variable, varies from one to maximum number of design variables of the objective function. On identification of Best solution candidate and Worst solution candidate, the candidate has to be modified as specified in the '*Update Phase*' which is as follows.

2.4.2 Updation Phase

On obtaining the Best solution candidate and the Worst candidate solution of the population, each candidate solution will be updated using the Equation-(2.9).

$$X_{i,j,k}^{1} = X_{i,j,k} + r_{i,j,1}\left(X_{i,best,\mathrm{k}} - |X_{i,j,k}|\right) - r_{i,j,2}\left(X_{i,worst,k} - |X_{i,j,k}|\right) \tag{2.9}$$

where $X_{i,j,k}$ indicate the value of the k^{th} variable for the j^{th} candidate during the i^{th} iteration, $X_{i,best,k}$ and $X_{i,worst,k}$ represents the Best candidate solution and the Worst candidate solution in i^{th} iteration respectively, $r_{i,j,1}$ & $r_{i,j,2}$ represents the two random numbers of the k^{th} variable during i^{th} iteration in the range [0,1] and $X_{i,j,k}^{1}$ represents corresponding updated candidate.

The term " $r_{i,j,1}\left(X_{i,best,\mathrm{k}} - |X_{i,j,k}|\right)$ " implies that the candidate tendency to move towards the Best candidate solution and the term " $- r_{i,j,2}\left(X_{i,worst,k} - |X_{i,j,k}|\right)$ " indicates the tendency of the candidate to avoid the worst solution. The updated candidates ($X_{i,j,k}^{1}$) and the previous candidate ($X_{i,j,k}$) are given as inputs to the '*Comparison Phase*'.

2.4.3 Comparison Phase

For each candidate(X) in the solution set, its fitness value is evaluated. Fitness value resembles how close the given solution is to the optimal value. A higher fitness solution is more closer to the optimal solution and vice-versa. The objective functions addressed in this research work are of minimization type, thus the fitness value of each candidate solution is evaluated using Equation-(2.10).

Upon completion of *Updation phase*, compute the fitness values of $X_{i,j,k}$ and the updated candidate $X_{i,j,k}^{1}$. The fitness value of the candidate solution is evaluated as per Equation-(2.10).

$$fitness(X) = \frac{1}{1 + objective\ function\ value} \tag{2.10}$$

If the fitness of the updated candidate $X_{i,j,k}^{1}$ is better than the fitness of $X_{i,j,k}$, then replace the candidate $X_{i,j,k}$ with $X_{i,j,k}^{1}$ for the next generation, otherwise retain $X_{i,j,k}$ for the next generation and discard the updated candidate. This comparison has to be performed for all the candidates of the population.

With the above, one iteration of the Jaya Algorithm gets completed. All the fittest candidates in the '*Comparison phase*' at the end of iteration are saved in the memory and these values become the input to the next iteration. Repeat the above process until convergence criterion is satisfied. Thus, the algorithm tries to get closer to the global optimal.

Flowchart for Jaya Algorithm is presented in Fig-2.3. The algorithm for the optimal scheduling of Micro-Sources is as follows.

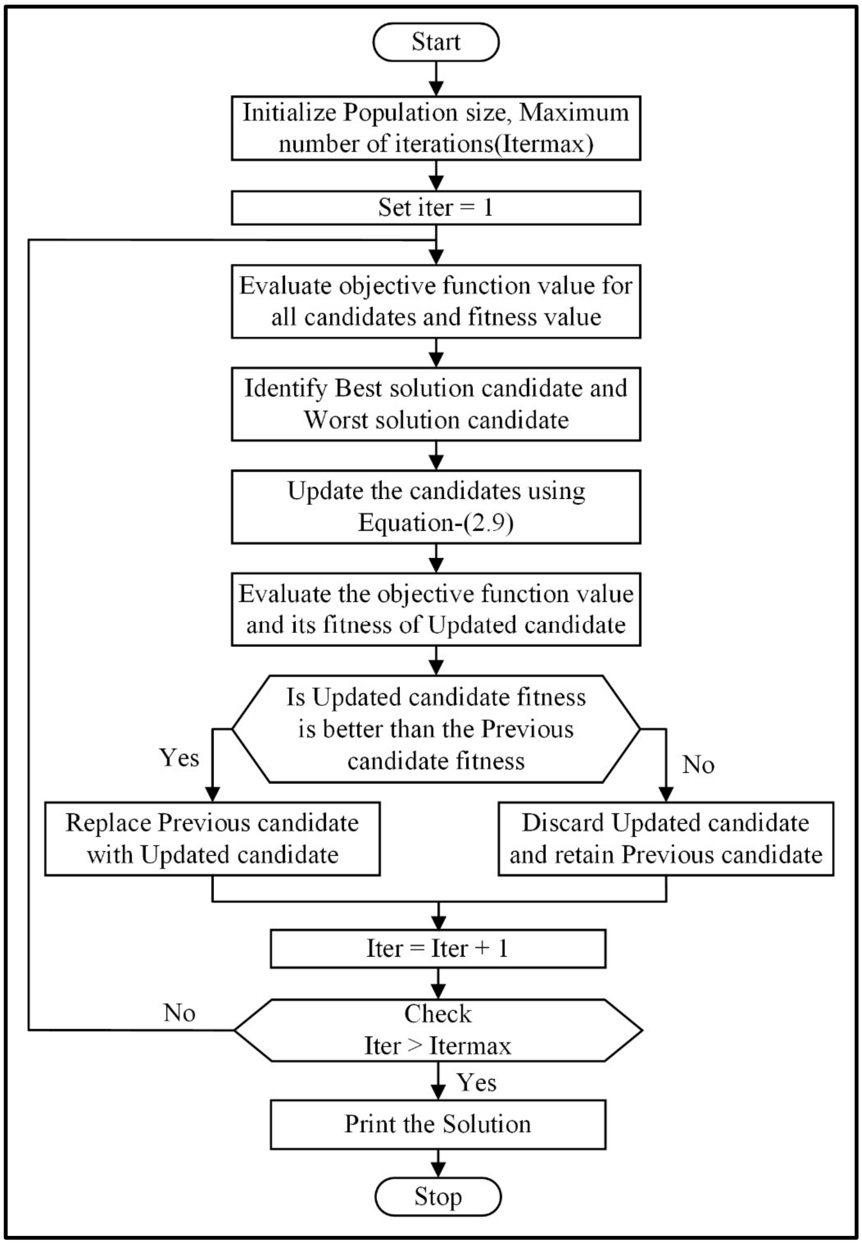

Fig-2.3: Flowchart for Jaya Algorithm

2.5 Algorithm for Optimal Scheduling of Micro-Sources using Jaya Algorithm

1. Read input data of the Multi-Microgrid System: number of Micro-Sources in each Microgrid, Micro-Sources location in each Microgrid, Initial Bus voltage magnitudes, fuel cost coefficients of generators, Active power limits of all generator, Line data of the system, Bus data of the system.
2. Read Jaya Algorithm parameters: population size (P_{size}) and maximum number of iterations(*iter_max*).
3. Select the Microgrid(s) (MG-1, MG-2, and MG-3) which are active.
4. Select the scenario based on the objective function to be optimized, i.e., Scenario-1(Operating *cost minimization*), Scenario-2 (*Active power losses minimization*) and Scenario-3(*Voltage Deviation minimization*).
5. Initialize population ($X_{i,j,k}$) within their limits of generators output power.

$$X_{i,j,k} = \{P_{i,j,1}\, P_{i,j,2} \dots \dots . P_{i,j,\mathrm{k}})$$
$$where\ i \in \{1,2, ..\, iter_{max}\}, j \in \{1,2,3 \dots P_{size}\}\ and\ k \in \{1,2,3 \dots N_{gen}\}$$

6. Set iteration count (*iter*) = 1.
7. Run Current Injection based Load flow (presented in Appendix-IV) to evaluate the voltage magnitude at each bus and losses in each line of the system.
8. Calculate the total cost of generation using Equation-(2.1), total loss in the system using Equation-(2.2), Voltage Deviation using Equation-(2.4) and evaluate the fitness function based on objective function.
9. Evaluate the Best fitness candidate and the Worst fitness candidate in the population.
10. Update the candidate using *Updation phase* as indicated in Equation-(2.9)
11. Go to *Comparison phase* and based on updated candidate fitness value either replace the candidate or retain the candidate.
12. Increment iteration count (*iter*=*iter*+1) and repeat above steps (Step-(7) to Step-(11)) until a convergence criterion is met.
13. Stop the program and print the optimal scheduled values of Micro-Sources and the objective function value for the selected scenario.

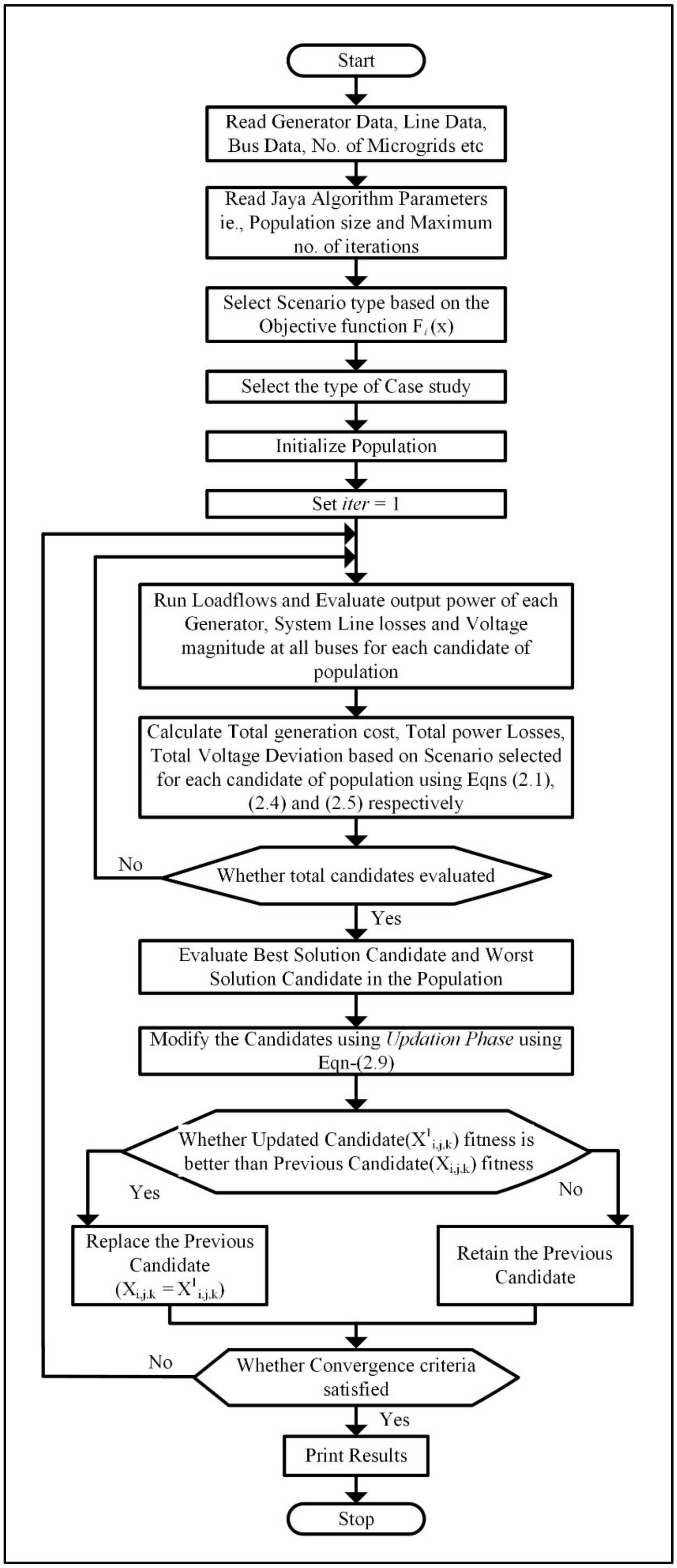

Fig-2.4: Flow chart for optimal scheduling of Micro-Sources using Jaya Algorithm for various Scenarios and Case studies.

2.6 Results and Discussions

The flowchart for the optimal scheduling of Micro-Sources for the problem considered in this chapter has been presented in Fig-2.4. The test Distribution Systems considered in this research work are the standard 33 Bus Distribution System and Practical Indian 85 Bus Distribution System. The IEEE 33 Bus Distribution System data[62] and the Practical Indian 85 Bus Distribution System data [63][64] have been presented in Appendix-1 and Appendix-2 respectively. The Distribution Systems are sectionalized into three self-adequate Microgrids, as a test case and the radiality of the system has been preserved. The sectionalisation has been performed considering the topology of the network, size & location of DGs and the load demand.

Table-2.1: Area wise Active and Reactive power load percentage of 33 Bus Distribution System and 85 Bus Distribution System

	33 Bus Distribution System		85 Bus Distribution System	
MICROGRIDS	**Area wise Active power(P) in percentage**	**Area wise Reactive power(Q) in percentage**	**Area wise Active power(P) in percentage**	**Area wise Reactive power(Q) in percentage**
MG1	12.38	9.57	22.69	22.69
MG2	37.82	29.57	35.55	35.55
MG3	49.80	60.87	41.76	41.76
MG1 & MG2	50.20	39.13	58.24	58.24
MG2 & MG3	87.62	90.43	64.45	64.45
MG1 & MG3	62.18	70.43	77.31	77.31
MG1, MG2 & MG3	100.00	100.00	100.00	100.00

While making the Multi-Microgrid System, the existing 33 Bus Distribution System and 85 Bus Distribution System are modified for certain cases as explained below. The modified 33 Bus and modified 85 Bus Distribution Systems are having a total active power load of 3.715MW & 2.57 MW and the reactive power demand of 2.30MVAr & 2.62MVAr respectively as that of the original system. The area-wise, meeting the percentage of the active power load and reactive power load are presented in Table-2.1 and Table-2.2 below.

2.6.1 Modified 33 Bus Distribution System and modified 85 Bus Distribution System and formation of Multi-Microgrid System:

The 33 Bus Distribution System and 85 Bus Distribution System are sectionalized into three self-adequate Microgrids and named as Microgrid-1(MG1), Microgrid-2(MG2) and Microgrid-3(MG3). The following modifications are made in the 33 Bus Distribution System and 85 Bus Distribution System, for sectionalizing the system into Multi-Microgrid

Systems. The modified 33 Bus Distribution System and 85 Bus Distribution System are shown in Fig-2.5 and Fig-2.6 respectively indicating locations of DGs and tie-lines. The details of the line status are provided in Table-2.2 and Table 2.3 for various case studies of 33 Bus and 85 Bus Distribution System respectively.

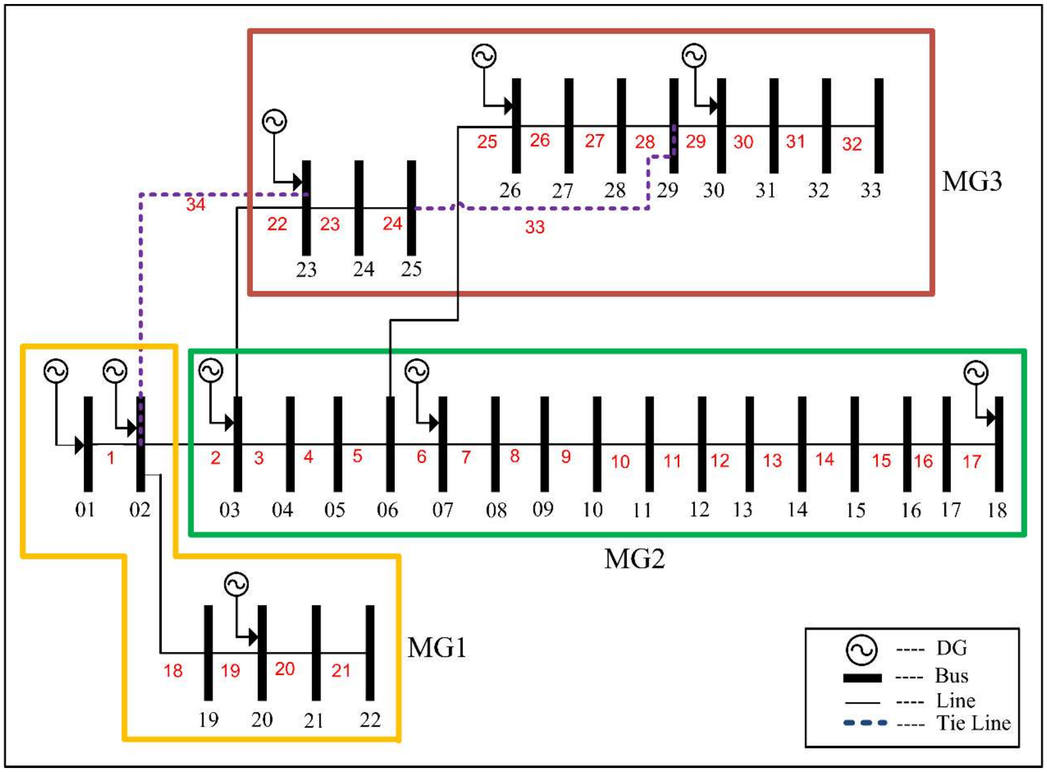

Fig-2.5: Modified IEEE 33 Bus Distribution System with DG locations and Tie-line connections

2.6.1.1 Line status of modified IEEE 33 Bus Distribution System for formulation of Multi-Microgrid System

The following are the details of modifications in the line status for the formulation of Multi-Microgrid System of 33 Bus Distribution System.

a) Microgrid-1 alone is active: The lines (no.2 and 34) between Bus no.2 & Bus no.3 and Bus no.2 & Bus no.23 are opened.

b) Microgrid-2 alone is active: Three lines (no.2, 22 and 25) between Bus no.2 & Bus no.3, Bus no.3 & Bus no.23 and Bus no.6 & Bus no.26 are opened.

c) Microgrid-3 alone is active: The line (no.33) is closed between Bus no.25 & Bus no.29 and the lines (no.22, 25 and 34) between Bus no.3 & Bus no.23, Bus no.6 & Bus no.26 and Bus no.2 and Bus no.23 are opened. The details of line (no.33) resistance and reactance are presented in Table-2.2.

Table-2.2: Line parameters of closed/opened lines for 33 Bus Distribution System for various Case studies

Microgrids Active	**Line no.**	**From Bus**	**To Bus**	**R (P.U)**	**X (P.U)**
Microgrid-1	2	2	3	Line open	Line open
	34	2	23	Line open	Line open
Microgrid-2	2	2	3	Line open	Line open
	22	3	23	Line open	Line open
	25	6	26	Line open	Line open
Microgrid-3	33	25	29	0.001264	0.000644
	22	3	23	Line open	Line open
	25	6	26	Line open	Line open
	34	2	23	Line open	Line open
Microgrid-1 & Microgrid-2	22	3	23	Line open	Line open
	25	6	26	Line open	Line open
	34	2	23	Line open	Line open
Microgrid-2 & Microgrid-3	2	2	3	Line open	Line open
	34	2	23	Line open	Line open
Microgrid-1 & Microgrid-3	33	25	29	0.001264	0.000644
	34	2	23	0.002809	0.001920
	2	2	3	Line open	Line open
	22	3	23	Line open	Line open
	25	6	26	Line open	Line open
Microgrid-1, Microgrid-2 & Microgrid-3	33	25	29	Line open	Line open
	34	2	23	Line open	Line open

d) Microgrid-1 and Microgrid-2 are working together: Three lines (no.22, 25 & 34) are opened between Bus no.3 & Bus no.23, Bus no.6 & Bus no.26 and Bus no.2 & Bus no.23.

e) Microgrid-2 and Microgrid-3 are working together: The lines (no.2 & 34) between Bus no.2 & Bus no.3 and Bus no.2 & Bus no.23 are opened.

f) Microgrid-1 and Microgrid-3 are working together: Two lines (no.33 and 34) are closed between Bus no.25 & Bus no.29 and Bus no.2 & Bus no.23 and the lines (no.2, 22 and 25) between Bus no.2 & Bus no.3, Bus no.3 & Bus no.23 and Bus no.6 & Bus no.26 are opened.

g) All the Microgrids are working together: The line (no.33 and 34) between the Bus no.2 & Bus no.23 and Bus no. 25 & Bus no.29 are opened.

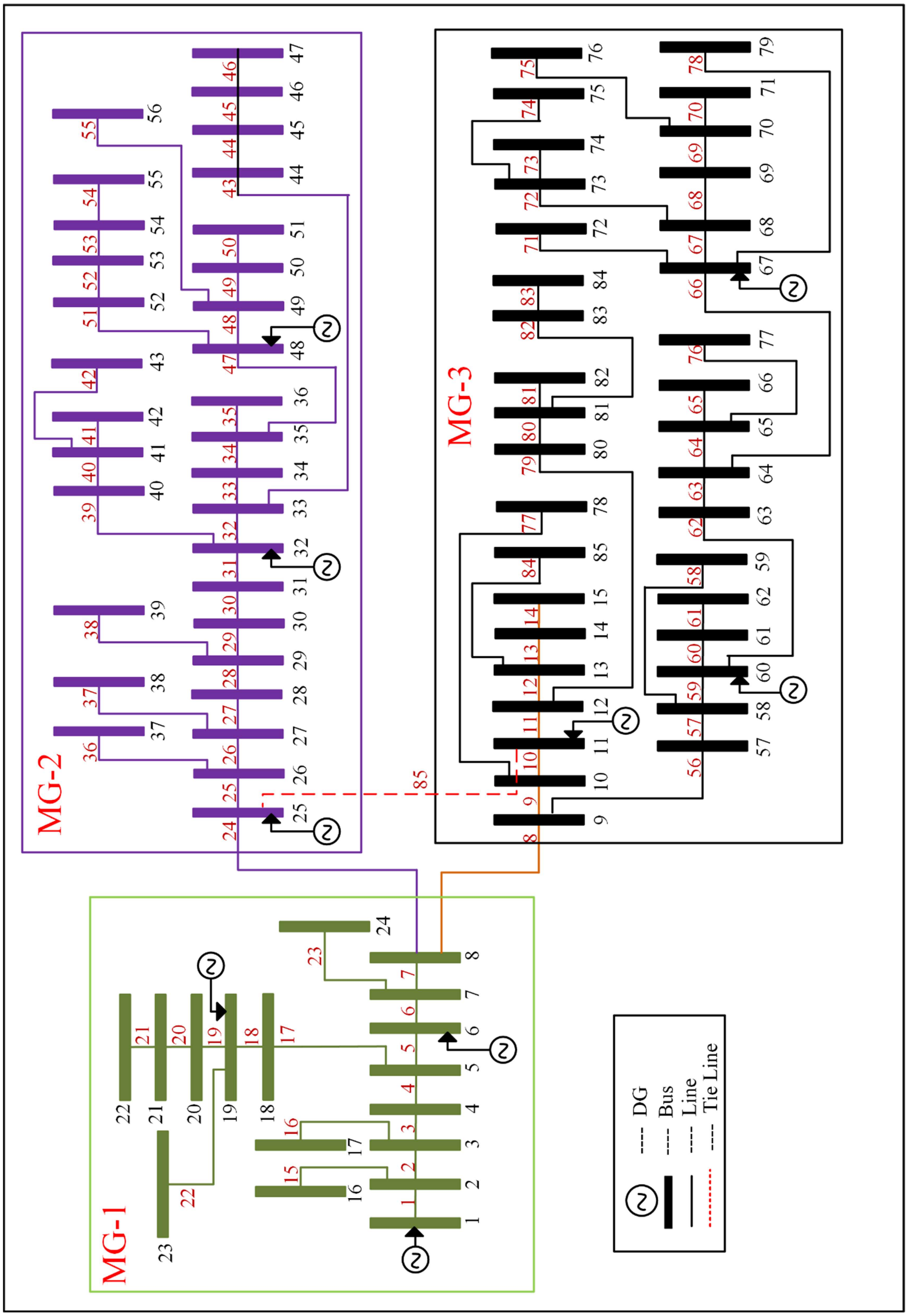

Fig-2.6: Modified Indian Practical 85 Bus Distribution System with DG locations and Tie-line connections

2.6.1.2 Line status of modified Practical Indian 85 Bus Distribution System for formulation of Multi-Microgrid System

The modified line details of 85 Bus Distribution System for formulation of Multi-Microgrid System are as follows.

a) Microgrid-1 alone is active: The lines (no.8 and 24) between Bus no.8 & Bus no.9 and Bus no.7 & Bus no.25 are opened.

b) Microgrid-2 alone is active: The two lines (no.24 and 85) between Bus no.7 & Bus no.25 and Bus no.11 & Bus no.25 are opened.

c) Microgrid-3 alone is active: The two lines (no.8 and 85) between Bus no.8 & Bus no.9 and Bus no.11 & Bus no.25 are opened.

d) Microgrid-1 and Microgrid-2 are working together: The two lines (no.8 and 85) between Bus no.8 & Bus no.9 and Bus no.11 & Bus no.25 are opened.

e) Microgrid-2 and Microgrid-3 are working together: The Tie-line (no.85) is closed between Bus no.11 & Bus no.25 and the lines (no.8 and 24) between Bus no.8 & Bus no.9 and Bus no.7 and Bus no.25 are opened. The details of line (no.85) resistance and reactance are presented in Table-2.3.

Table-2.3: Line parameters of closed/opened lines for 85 Bus Distribution System for various Case studies

Microgrids Active	Line no.	From Bus	To Bus	R (P.U)	X (P.U)
Microgrid-1	8	8	9	Line open	Line open
	24	7	25	Line open	Line open
Microgrid-2	24	7	25	Line open	Line open
	85	11	25	Line open	Line open
Microgrid-3	8	8	9	Line open	Line open
	85	11	25	Line open	Line open
Microgrid-1 & Microgrid-2	8	8	9	Line open	Line open
	85	11	25	Line open	Line open
Microgrid-2 & Microgrid-3	85	11	25	0.089256	0.061983
	8	8	9	Line open	Line open
	24	7	25	Line open	Line open
Microgrid-1 & Microgrid-3	24	7	25	Line open	Line open
	85	11	25	Line open	Line open
Microgrid-1, Microgrid-2 & Microgrid-3	85	11	25	Line open	Line open

f) Microgrid-1 and Microgrid-3 are working together: Two lines (no.24 and 85) between Bus no.7 & Bus no.25 and Bus no.11 & Bus no.25 are opened.

g) All the Microgrids are working together: The line (no.85) between the Bus no.11 & Bus no.25 is opened.

For testing the proposed algorithm, the following assumptions are made:

1. The DGs considered in this work are dispatchable and their locations are fixed by considering the topology of the network and the load demand in the respective Microgrid. The DG locations of the 33 Bus and 85 Bus Distribution Systems are presented in Table-2.4.
2. Isolation and tie-line connections are possible through a static switch.

Table-2.4: Location of DGs in 33 Bus and 85 Bus Distribution Systems

Sl.No	Bus System	Generator location at Bus no.		
		Microgrid-1	Microgrid-2	Microgrid-3
1.	33 Bus Distribution System	1, 2, 20	3, 7, 18	23, 26, 30
2.	85 Bus Distribution System	1, 6, 19	25, 32, 48	11, 60, 67

The Jaya algorithm parameters considered in this work are: *Population size* = 80; *Maximum iterations* = 200; Based on the optimization parameters, three scenarios are formulated to optimize for single-objective optimization. The details of the scenarios are as follows

Scenario-1 : Operating cost minimization

Scenario-2 : Active power loss minimization

Scenario-3 : Voltage Deviation minimization

Further, based on the operation of the Multi-Microgrid Systems, various case studies are formulated as presented in Table 2.5. The faulty Microgrid(s) which are not functioning are isolated from the rest of the active system.

Table-2.5: Case Studies in each Scenario

Case study	**Operating MG(s)**	**Fault Type***	**Faulty MG(s)**
Case-1	MG-1	MMGF	MG-2 and MG-3
Case-II	MG-2	MMGF	MG-1 and MG-3
Case-III	MG-3	MMGF	MG-2 and MG-3
Case-IV	MG-1 and MG-2	SMGF	MG-3
Case-V	MG-2 and MG-3	SMGF	MG-1
Case-VI	MG-1 and MG-3	SMGF	MG-2
Case-VII	All MGs	NF	-

*SMGF – Single MG fault MMGF – Multi MG fault NF – No fault

2.6.2 33 Bus Distribution System

2.6.2.1 Scenario-1 (Cost minimization)

In this scenario, the objective function considered is only operating cost minimization. The fuel cost coefficients of each DG [27] for 33 Bus Distribution System are presented in Appendix-I.

Table-2.6: Optimal values for various Case Studies with Scenario-1 for 33 Bus system with Jaya Algorithm

	Case-I	Case-II	Case-III	Case-IV	Case-V	Case-VI	Case-VII
$P_{G1}(kW)$	164.1906	-	-	264.2062	-	327.7459	321.8560
$P_{G2}(kW)$	198.4859	-	-	198.3882	-	199.9999	199.2185
$P_{G3}(kW)$	98.0219	-	-	99.2185	-	99.9999	99.2185
$P_{G4}(kW)$	-	272.3697	-	263.7362	335.2371	-	296.4591
$P_{G5}(kW)$	-	663.0524	-	613.6262	749.0109	-	717.1672
$P_{G6}(kW)$	-	479.2673	-	438.2416	542.4175	-	486.1538
$P_{G7}(kW)$	-	-	463.3698	-	434.5543	439.3162	439.6825
$P_{G8}(kW)$	-	-	642.0365	-	545.7875	578.7545	560.4395
$P_{G9}(kW)$	-	-	778.9009	-	703.8827	699.9755	667.9364
$P_{loss}(kW)$	0.6985	9.6894	34.3074	12.4172	55.8899	35.7920	73.1315
$Q_{loss}(kVAR)$	0.6625	7.6934	27.6696	9.1481	42.1789	26.6916	50.7329
Cost($/hr)	**19256.43**	**70902.88**	**97919.59**	**89446.93**	**168665.57**	**115067.73**	**187652.72**
VD (P.U)	8.1003E-6	2.8230E-4	1.9680E-4	2.8900E-4	7.9362E-4	4.3140E-4	1.0510E-3
$P_{demand}(kW)$	460	1405	1850	1865	3255	2310	3715
$Q_{demand}(kVAR)$	220	680	1400	900	2080	1620	2300

Table-2.6 and Table-2.7 show the scheduled power output of various DGs, total system losses, total cost of generation, system power demand in each case considering cost minimization as an objective function using Jaya Algorithm and Genetic Algorithm respectively. From the Table-2.6 and Table-2.7, it is observed that Jaya Algorithm is offering better cost of 19256.43$/hr, 70902.88$/hr, 97919.59$/hr, 89446.93$/hr, 168665.57$/hr, 115067.73$/hr and 187652.72$/hr as against Genetic Algorithm of 19256.44$/hr, 70902.99$/hr, 97919.86$/hr, 89480.97$/hr, 168996.73$/hr, 115367.94$/hr and 188885.73$/hr from Case-I to Case-VII respectively. From the test results of Case-VII, it is clear that as the size of the system increases, the effectiveness of Jaya Algorithm is significant in minimization of operating cost.

The convergence characteristics of Jaya Algorithm and Genetic Algorithm are plotted in Fig-2.7 for Case-VII. From the convergence characteristics, it is perceived that Jaya Algorithm converged in 30 iterations. The voltage profile at various buses for Case-I to Case-VII is plotted on Fig-2.8 using Jaya Algorithm. From the Fig-2.8, it is assessed that the voltage profile at various buses is within the limits of ±5% in all the case studies.

Table-2.7: Optimal values for various Case Studies with Scenario-1 for 33 Bus system using Genetic Algorithm.

	Case-I	Case-II	Case-III	Case-IV	Case-V	Case-VI	Case-VII
$P_{G1}(kW)$	164.1402	-	-	259.7259	-	297.3819	293.9110
$P_{G2}(kW)$	198.0952	-	-	199.1697	-	198.7301	149.6458
$P_{G3}(kW)$	98.4615	-	-	99.9756	-	99.7802	99.1697
$P_{G4}(kW)$	-	272.5549	-	281.8070	322.1065	-	300.8546
$P_{G5}(kW)$	-	664.6153	-	604.2489	760.1464	-	697.8265
$P_{G6}(kW)$	-	477.5091	-	432.5274	539.0475	-	552.2343
$P_{G7}(kW)$	-	-	464.9572	-	372.7716	405.8607	404.3955
$P_{G8}(kW)$	-	-	640.2331	-	628.8155	555.5554	626.3735
$P_{G9}(kW)$	-	-	779.0963	-	688.8399	787.8875	665.2013
$P_{loss}(kW)$	0.6969	9.6793	34.2866	12.4546	56.7276	35.1960	74.6125
$Q_{loss}(kVAR)$	0.6610	7.6759	27.6529	9.1438	42.7519	26.1826	52.2449
Cost($/hr)	**19256.44**	**70902.99**	**97919.86**	**89480.97**	**168996.73**	**115367.94**	**188885.73**
VD (P.U)	8.0959E-6	2.8224E-4	1.9683E-4	2.9162E-4	7.9180E-4	4.3243E-4	1.0780E-3
$P_{demand}(kW)$	460	1405	1850	1865	3255	2310	3715
$Q_{demand}(kVAR)$	220	680	1400	900	2080	1620	2300

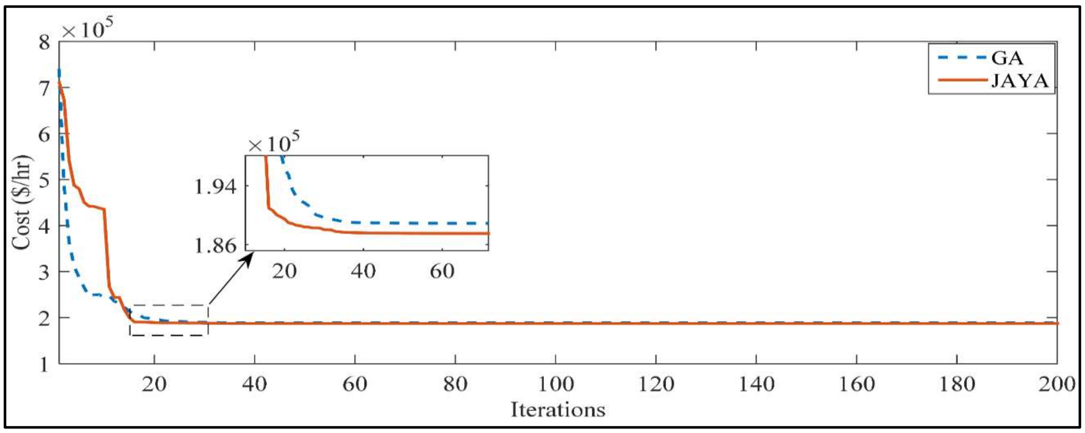

Fig-2.7: Convergence characteristics of Jaya algorithm vs GA for Cost minimization as objective function for 33 Bus system Scenario-1 Case-VII

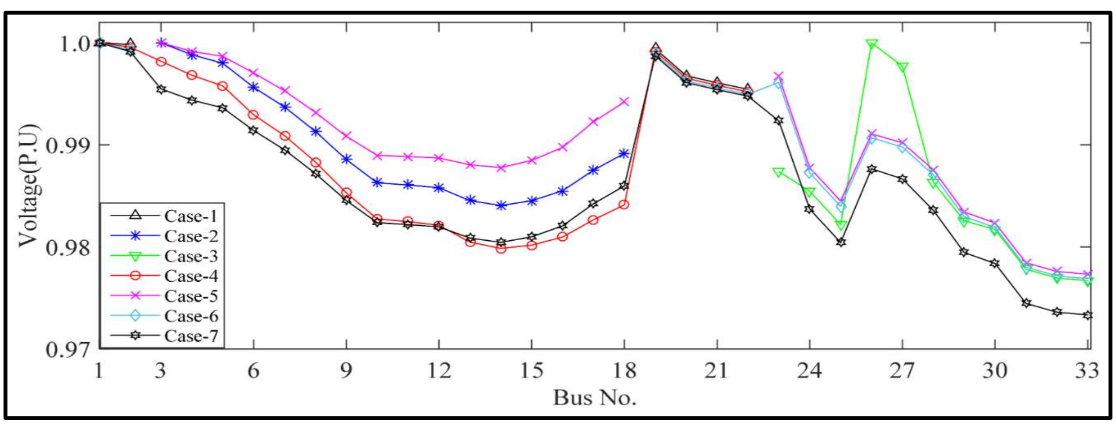

Fig-2.8: Voltage(P.U) profile of 33 Bus system for different case studies with Scenario-1 using Jaya Algorithm

2.6.2.2 Scenario-2 (Loss minimization)

In this scenario, only Active power loss minimization is considered as the objective function. The Active power loss obtained for various case studies is presented in Table-2.8 and Table-2.9 for Jaya Algorithm and Genetic Algorithm respectively for 33 Bus Distribution System.

Table-2.8: Optimal values for various case studies with Scenario-2 for 33 Bus system using Jaya Algorithm

	Case-I	Case-II	Case-III	Case-IV	Case-V	Case-VI	Case-VII
$P_{G1}(kW)$	160.6905	-	-	126.1091	-	338.7745	130.7375
$P_{G2}(kW)$	199.9999	-	-	199.3162	-	174.4077	68.5226
$P_{G3}(kW)$	99.9999	-	-	98.4127	-	99.9755	99.0232
$P_{G4}(kW)$	-	221.5814	-	265.6898	640.1225	-	849.8167
$P_{G5}(kW)$	-	767.5701	-	761.5139	751.3552	-	666.3735
$P_{G6}(kW)$	-	425.3479	-	426.0805	424.7618	-	415.2380
$P_{G7}(kW)$	-	-	499.9999	-	498.5347	499.3894	483.3943
$P_{G8}(kW)$	-	-	583.6733	-	221.0011	798.6324	758.5835
$P_{G9}(kW)$	-	-	799.9999	-	772.6495	433.4554	315.0183
$\boldsymbol{P_{loss}(kW)}$	**0.6905**	**9.4994**	**33.6732**	**12.1222**	**53.4249**	**34.6351**	**71.7077**
$Q_{loss}(kVAR)$	0.6553	7.2989	27.1512	8.9479	39.6031	25.7239	49.2475
Cost($/hr)	19257.57	71409.28	98125.16	91347.5	177748.39	116787.91	208990.64
VD (P.U)	7.9987E-06	2.8901E-04	1.9666E-04	2.9148E-04	7.6903E-04	4.3278E-04	1.0280E-03
$P_{demand}(kW)$	460	1405	1850	1865	3255	2310	3715
$Q_{demand}(kVAR)$	220	680	1400	900	2080	1620	2300

The scheduled output power of each DG, active and reactive power losses of system, the total operating cost for various case studies are encapsulated in Table-2.8 and Table-2.9. From these tables, it is noticed that Jaya Algorithm is scheduling the DGs optimally for attaining the desired objective function of minimum losses of the system. The active power losses obtained are 690.474watts, 9499.427watts, 33673.17watts, 12122.236watts, 53424.97watts, 34635.059watts and 71707.68watts as against Genetic Algorithm of 690.496watts, 9520.185watts, 33708.979watts, 12150.093 watts, 53469.600watts, 34644.690watts and 71902.238watts from Case-I to Case-VII respectively.

It is analyzed from the test results that the power losses obtained by Jaya Algorithm in Case-VII of Scenario-2 is 71707.68watts, which is lesser than 73131.50watts attained in Case-VII of Scenario-1 by 1423.82watts. Thus, the proposed Jaya Algorithm is scheduling the DGs optimally to realize the desired objective function.

From the convergence characteristics shown in Fig-2.9, it can be noticed that Jaya Algorithm offers minimum power losses as compared to Genetic Algorithm. The voltage profile at various buses from Case-I to Case-VII is plotted on Fig-2.10 using Jaya algorithm. From this figure, it is clear that on sectionalizing the Distribution System into Multi-

Table-2.9: Optimal values for various case studies with Scenario-2 for 33 Bus system using Genetic Algorithm

	Case-I	Case-II	Case-III	Case-IV	Case-V	Case-VI	Case-VII
$P_{G1}(kW)$	160.6905	-	-	187.6509	-	334.0467	119.6744
$P_{G2}(kW)$	199.9999	-	-	124.2002	-	199.5604	154.5787
$P_{G3}(kW)$	99.9999	-	-	95.3113	-	98.7789	99.8535
$P_{G4}(kW)$	-	221.4068	-	271.0622	628.8851	-	780.4638
$P_{G5}(kW)$	-	767.7655	-	775.7752	599.9511	-	393.4554
$P_{G6}(kW)$	-	425.3479	-	423.1501	426.6666	-	427.1062
$P_{G7}(kW)$	-	-	499.9999	-	498.7789	483.8828	495.7264
$P_{G8}(kW)$	-	-	586.8349	-	390.7203	428.5714	559.2185
$P_{G9}(kW)$	-	-	796.8741	-	763.4675	799.8045	756.8253
$\boldsymbol{P_{loss}(kW)}$	**0.6904**	**9.5202**	**33.7089**	**12.1501**	**53.4696**	**34.6447**	**71.9022**
$Q_{loss}(kVAR)$	0.6553	7.2991	27.1816	8.9616	39.6179	25.7300	49.6359
Cost($/hr)	19257.57	71412.58	98111.21	91807.97	175424.45	116155.69	205233.28
VD (P.U)	8.0137E-06	2.8905E-04	1.9668E-04	2.9020E-04	7.6860E-04	4.3220E-04	1.0405E-03
$P_{demand}(kW)$	460	1405	1850	1865	3255	2310	3715
$Q_{demand}(kVAR)$	220	680	1400	900	2080	1620	2300

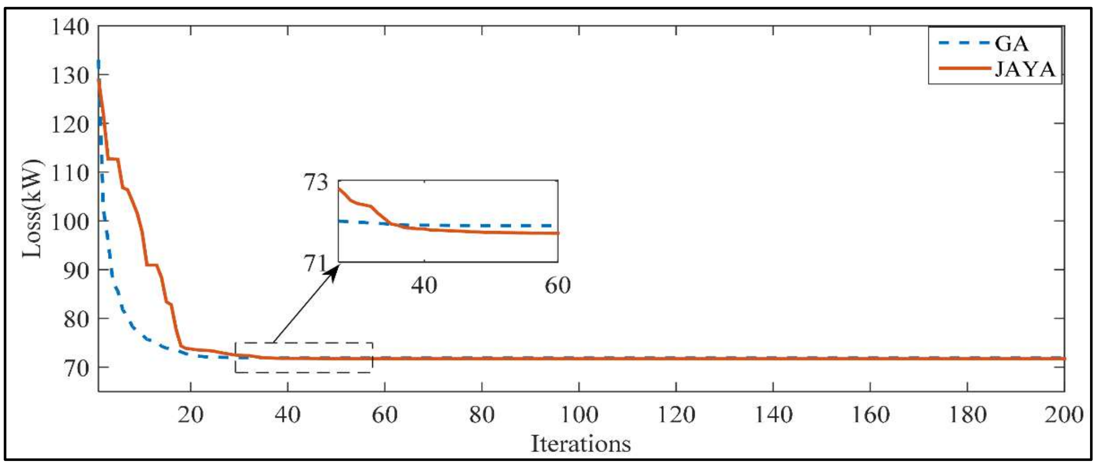

Fig-2.9: Convergence characteristics of Jaya algorithm vs GA for Loss minimization as objective function for 33 Bus system Scenario-2 Case-VII

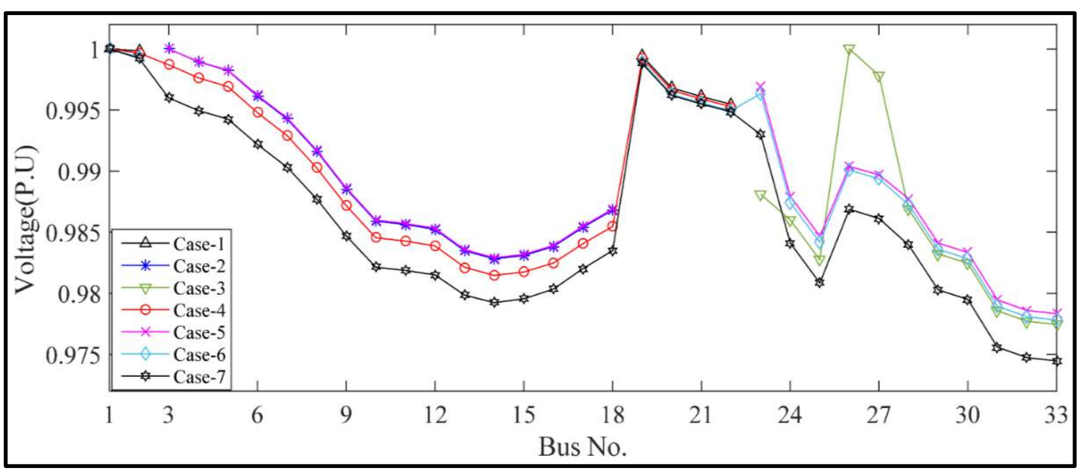

Fig-2.10: Voltage(P.U) profile of 33 Bus system for different case studies with Scenario-2 using Jaya Algorithm

Microgrid system, the minimum P.U voltage value in sectionalized Microgrids is improved than the combined operation of Microgrids and is maintained within the permissible limits of ±5% for all the cases.

2.6.2.3 Scenario-3 (Voltage Deviation minimization)

In this scenario, Voltage Deviation minimization is considered as the objective function. The Voltage Deviation minimization values for various case studies described above are presented in Table-2.10 and Table-2.11 for 33 Bus system using Jaya Algorithm and Genetic Algorithm.

Table-2.10: Optimal values for various Case Studies with Scenario-3 for 33 Bus system using Jaya Algorithm

	Case-I	Case-II	Case-III	Case-IV	Case-V	Case-VI	Case-VII
$P_{G1}(kW)$	160.6905	-	-	0.3273	-	178.2768	12.7326
$P_{G2}(kW)$	199.9999	-	-	40.8303	-	198.3882	8.4493
$P_{G3}(kW)$	99.9999	-	-	71.8437	-	99.8779	70.3052
$P_{G4}(kW)$	-	492.1649	-	989.0108	65.2201	-	709.6458
$P_{G5}(kW)$	-	348.7179	-	186.9597	0.7814	-	15.0427
$P_{G6}(kW)$	-	575.6776	-	592.0878	350.0366	-	290.5494
$P_{G7}(kW)$	-	-	499.9999	-	457.9975	486.3247	117.5824
$P_{G8}(kW)$	-	-	583.6733	-	2018.3147	582.4175	2485.9581
$P_{G9}(kW)$	-	-	799.9999	-	425.8852	799.9999	96.5079
$P_{loss}(kW)$	0.6905	11.5604	33.6732	16.0596	63.2356	35.2851	91.7735
$Q_{loss}(kVAR)$	0.6554	9.6482	27.1512	12.8562	47.4622	26.2615	64.6140
Cost($/hr)	19257.57	76157.67	98125.16	129300.31	251389.09	116995.68	347147.63
VD (P.U)	**7.9987E-06**	**2.7652E-04**	**1.9666E-04**	**2.6924E-04**	**7.0616E-04**	**4.2488E-04**	**9.7410E-04**
$P_{demand}(kW)$	460	1405	1850	1865	3255	2310	3715
$Q_{demand}(kVAR)$	220	680	1400	900	2080	1620	2300

Table-2.10 and Table-2.11 show the scheduled power output of various DGs, Total system losses, Total cost of generation, Voltage Deviation in each case considering Voltage Deviation minimization as objective using Jaya Algorithm and Genetic Algorithm respectively. From the Table-2.10 and Table-2.11, it is observed that Jaya algorithm is giving minimum Voltage Deviation in P.U of 7.9987E-06, 2.76524E-04, 1.96663E-03, 2.69284E-04, 7.06163E-04, 4.24881E-04, and 9.74101E-04 as against Genetic Algorithm of 7.99898E-06, 2.76533E-04, 1.96671E-02, 2.70032E-04, 7.07138E-04, 4.25313E-04 and 9.80675E-04 from Case-I to Case-VII respectively.

The convergence characteristics of Jaya Algorithm and Genetic Algorithm are presented in Fig-2.11. Though both the algorithms converge for the same number of iterations, Jaya Algorithm provides minimum Voltage Deviation compared to Genetic Algorithm. It is noticed from the Fig-2.12 that the voltage profile is improved with the formulation of Multi-Microgrid System compared to the operation of the entire Distribution System as a single network.

Table-2.11: Optimal values for various case studies with Scenario-3 for 33 Bus system using Genetic Algorithm

	Case-I	**Case-II**	**Case-III**	**Case-IV**	**Case-V**	**Case-VI**	**Case-VII**
$P_{G1}(kW)$	160.7882	-	-	2.1878	-	121.7831	18.4760
$P_{G2}(kW)$	199.9023	-	-	51.0867	-	199.0720	37.2649
$P_{G3}(kW)$	99.9999	-	-	10.8181	-	99.9023	38.7789
$P_{G4}(kW)$	-	482.2716	-	1005.1281	134.7699	-	1185.8362
$P_{G5}(kW)$	-	362.5884	-	260.8058	0.1954	-	9.37729
$P_{G6}(kW)$	-	571.5750	-	550.4761	384.7618	-	403.2234
$P_{G7}(kW)$	-	-	497.5579	-	491.0866	499.9999	116.7277
$P_{G8}(kW)$	-	-	586.5325	-	1747.2525	625.1525	1246.6421
$P_{G9}(kW)$	-	-	799.6092	-	556.7765	799.8045	734.7496
$P_{loss}(kW)$	0.6905	11.4351	33.6996	15.5026	59.8427	35.7145	76.0762
$Q_{loss}(kVAR)$	0.6554	9.5244	27.1725	12.1646	45.0715	26.6051	53.3733
Cost($/hr)	19257.51	75701.58	98103.03	129402.15	227514.85	118538.95	269585.36
VD (P.U)	**7.9989E-06**	**2.7653E-04**	**1.9667E-04**	**2.7002E-04**	**7.0714E-04**	**4.2531E-04**	**9.8067E-04**
$P_{demand}(kW)$	460	1405	1850	1865	3255	2310	3715
$Q_{demand}(kVAR)$	220	680	1400	900	2080	1620	2300

Further, it is analyzed from the test results that the Voltage Deviation values obtained in this Scenario-3 are minimum in comparison to various case studies executed in Scenario-1 and Scenario-2 above. As the DGs in this scenario are scheduled to provide minimum Voltage Deviation, the other objective function values (Operating cost and Active power losses) are found to be more in comparison to other scenarios. It is evident from these test results that the Jaya Algorithm has scheduled the DGs optimally for Voltage Deviation minimization problem.

Fig-2.13 depicts the voltage profile at various buses for different Scenarios of Case-VII. The Scenarios include a Base case (Source of power generation is at Bus no.1), individual cases of Cost minimization, Loss minimization and Voltage Deviation minimization. From the Fig-2.13, it is perspicuous that the Voltage Deviation in the Base-case is beyond the permissible limits of ±5%, with a minimum voltage of 0.9133P.U at Bus no.18. The minimum voltage magnitudes for the case of Voltage Deviation minimization objective is found to be 0.9695P.U whereas in case of Cost minimization and Loss minimization objectives, it is found to be 0.9691P.U at 33 Bus no. for all the objective functions. These values are above 0.9133P.U and well within the ±5% voltage deviation limits.

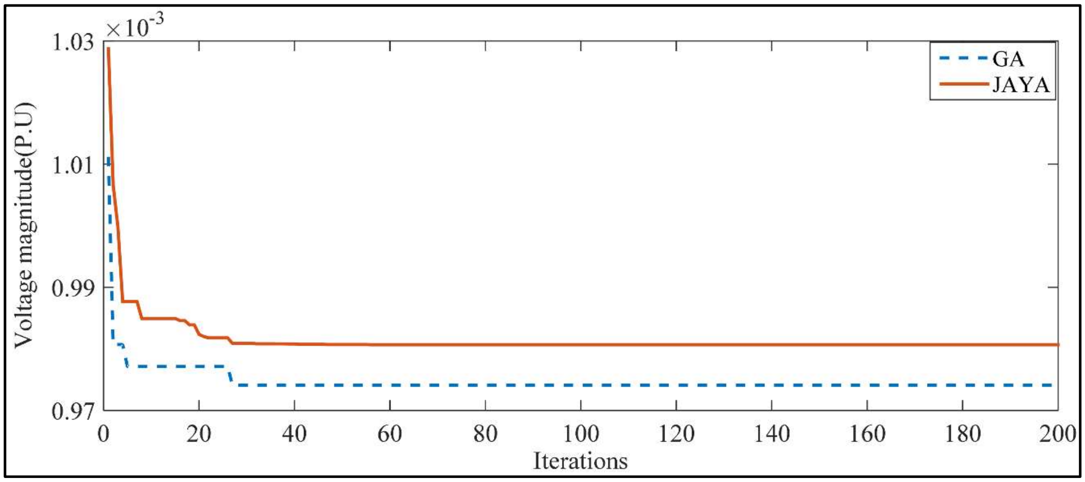

Fig-2.11: Convergence characteristics of Jaya Algorithm vs GA for Voltage Deviation minimization as objective function for 33 Bus system Scenario-3 Case-VII

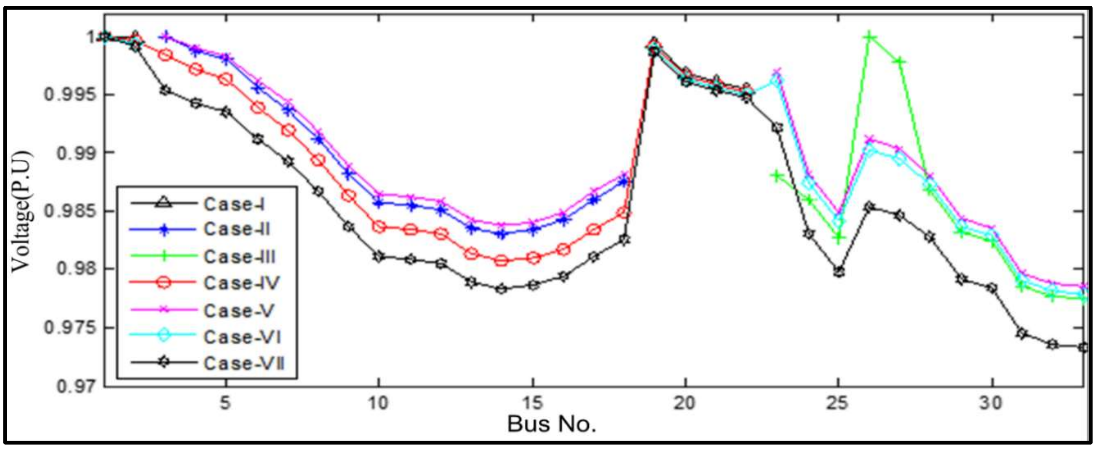

Fig-2.12: Voltage(P.U) profile of 33 Bus system for different case studies with Scenario-3 using Jaya Algorithm

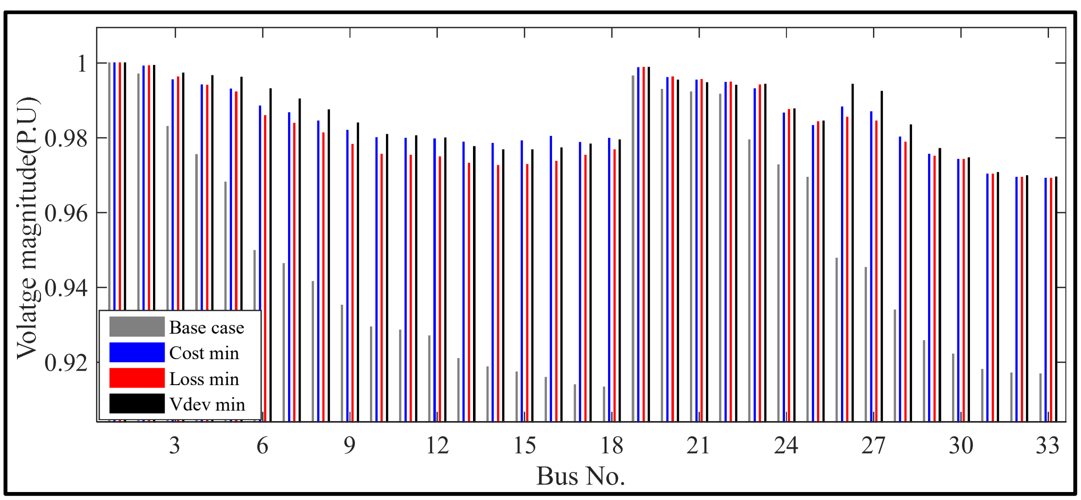

Fig-2.13: Voltage(P.U) profile of 33 Bus Distribution System for different Scenarios using Jaya Algorithm and Base case Load flows

2.6.3 85 Bus Distribution System:

2.6.3.1 Scenario-1 (Cost minimization)

In this scenario, Operating Cost minimization is regarded as the objective function. The fuel cost coefficients of each DG [27] for Indian 85 Bus Distribution System are presented in Appendix-II.

Table-2.12: Optimal values for various case studies with Scenario-1 for 85 Bus system with Jaya Algorithm

	Case-I	Case-II	Case-III	Case-IV	Case-V	Case-VI	Case-VII
$P_{G1}(kW)$	227.3001	-	-	233.2695	-	317.3417	306.4235
$P_{G2}(kW)$	72.9134	-	-	76.3804	-	100.0000	100.0000
$P_{G3}(kW)$	285.3294	-	-	291.0507	-	367.8978	358.9201
$P_{G4}(kW)$	-	368.1779	-	385.0844	489.1914	-	453.3466
$P_{G5}(kW)$	-	251.1934	-	258.6239	302.1059	-	287.2758
$P_{G6}(kW)$	-	300.0000	-	300.0000	300.0000	-	300.0000
$P_{G7}(kW)$	-	-	492.8121	-	405.8350	377.9075	367.9179
$P_{G8}(kW)$	-	-	189.3617	-	155.5133	143.8066	139.8869
$P_{G9}(kW)$	-	-	400.0000	-	400.0000	400.0000	400.0000
$P_{loss}(kW)$	2.5828	6.0113	9.2138	48.0889	66.3256	51.0337	144.4908
$Q_{loss}(kVAR)$	1.4636	2.4910	4.4277	27.2133	32.5269	31.8287	90.2311
Cost($/hr)	**23840.38**	**30627.02**	**43449.32**	**56323.14**	**75924.69**	**68248.23**	**103099.16**
VD (P.U)	7.8652E-06	1.0890E-05	2.2000E-05	5.9200E-04	3.2400E-04	6.3500E-04	1.6660E-03
$P_{demand}(kW)$	582.96	913.36	1072.96	1496.32	1986.32	1655.92	2569.28
$Q_{demand}(kVAR)$	594.74	931.81	1094.64	1526.55	2026.45	1689.37	2621.19

The optimal scheduled power output of various DGs for attaining minimum cost considering Cost minimization as the objective, for different case studies using Jaya Algorithm and Genetic Algorithm are emphasized in Table 2.12 and Table 2.13 respectively. The total Generation cost obtained with optimal scheduling of DGs along with active power loss, Voltage Deviation values are presented in Table 2.12 and Table 2.13. It is noticeable from the above results that Jaya Algorithm is yielding better cost of 23840.38$/hr, 30627.02$/hr, 43449.32$/hr, 56323.14$/hr, 75924.69$/hr, 68248.23$/hr and 103099.16$/hr as against Genetic Algorithm of 23849.92$/hr, 30627.49$/hr, 43450.85$/hr, 56323.68$/hr, 75929.71$/hr, 73297.60$/hr and 103395.19$/hr from Case-I to Case-VII respectively. Thus, it is evident from the results that as the loading level increases, the cost saving is significant.

Fig-2.14 outlined below represents the convergence characteristics of Jaya Algorithm and Genetic Algorithm for Case-VII with Operating cost minimization as the objective function. It is perceptible from the Fig-2.14 that Jaya Algorithm converges in 25 iterations as against 55 iterations by the Genetic Algorithm. It is noticeable that the proposed Jaya Algorithm converges faster than Genetic Algorithm on a Practical Distribution System.

Table-2.13: Optimal values for various case studies with Scenario-1 for 85 Bus system with Genetic Algorithm

	Case-I	Case-II	Case-III	Case-IV	Case-V	Case-VI	Case-VII
$P_{G1}(kW)$	218.0677	-	-	233.5952	-	338.2800	281.3239
$P_{G2}(kW)$	67.3828	-	-	76.5625	-	99.9756	99.9756
$P_{G3}(kW)$	300.0977	-	-	291.3086	-	293.6523	350.0000
$P_{G4}(kW)$	-	367.6758	-	384.2285	488.6719	-	430.3711
$P_{G5}(kW)$	-	251.7658	-	258.7891	296.7529	-	277.2217
$P_{G6}(kW)$	-	299.9268	-	299.9268	299.9268	-	299.9268
$P_{G7}(kW)$	-	-	492.0654	-	412.1094	374.8779	375.0000
$P_{G8}(kW)$	-	-	190.2032	-	155.3084	350.0000	200.1953
$P_{G9}(kW)$	-	-	399.9023	-	399.9023	249.8047	399.9023
$P_{loss}(kW)$	2.5882	6.0083	9.2110	48.0906	66.3517	50.6706	144.6367
$Q_{loss}(kVAR)$	1.4632	2.4897	4.4260	27.2144	32.5376	31.5962	90.3331
Cost(*$/hr*)	**23849.92**	**30627.49**	**43450.85**	**56323.68**	**75929.71**	**73297.60**	**103395.19**
VD $(P.U)$	7.8499E-06	1.0897E-05	2.1638E-05	5.9274E-04	3.2665E-04	6.1449E-04	1.5857E-03
$P_{demand}(kW)$	582.96	913.36	1072.96	1496.32	1986.32	1655.92	2569.28
$Q_{demand}(kVAR)$	594.74	931.81	1094.64	1526.55	2026.45	1689.37	2621.19

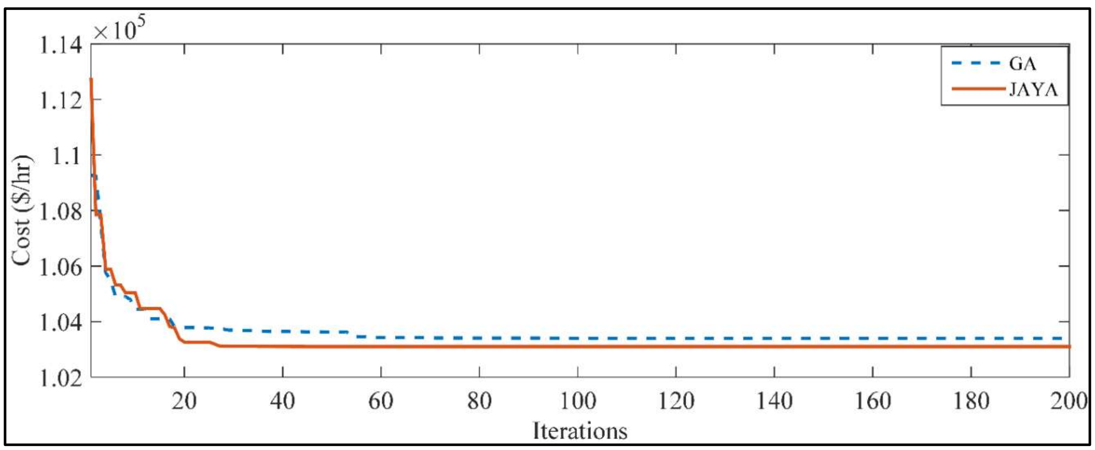

Fig-2.14: Convergence characteristics of Jaya Algorithm vs GA for Cost minimization as objective function for 85 Bus system Scenario-1 Case-VII

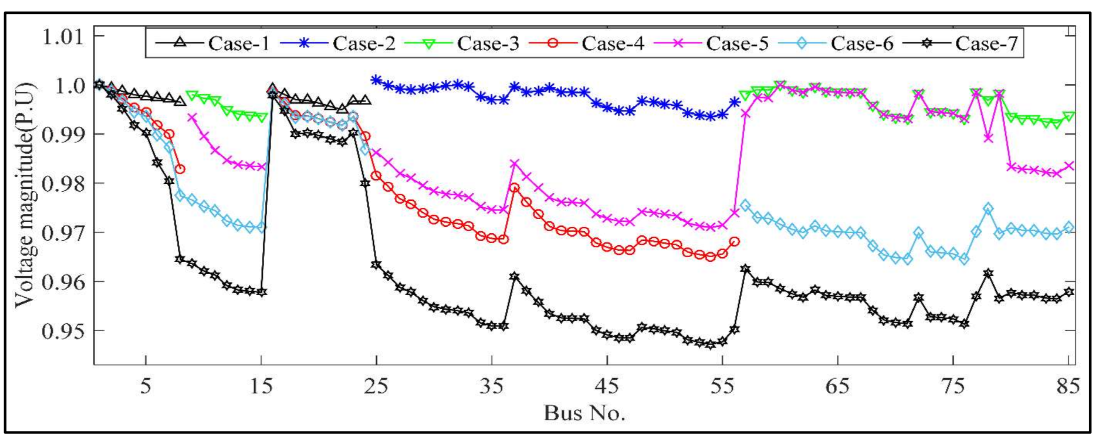

Fig-2.15: Voltage(P.U) profile of 85 Bus system for different case studies with Scenario-1 using Jaya Algorithm

Fig-2.15 depicts the voltage profile at various buses from Case-I to Case-VII using Jaya algorithm. It is assessed from this plot that the Voltage Deviation is within the limits of ±5% in all the case studies except Case-VII, where all Microgrids are active. Thus, it is evident that the individual operation of Microgrids has improved the voltage profile of the system for the given locations of DGs.

2.6.3.2 Scenario-2 (Loss minimization)

In this scenario, the objective function addressed is only active power loss minimization. The Active power losses for various case studies are encapsulated in Table-2.14 and Table-2.15 for Jaya Algorithm and Genetic Algorithm respectively, for 85 Bus Distribution System.

Table-2.14: Optimal values for various case studies with Scenario-2 for 85 Bus system with Jaya Algorithm

	Case-I	**Case-II**	**Case-III**	**Case-IV**	**Case-V**	**Case-VI**	**Case-VII**
$P_{G1}(kW)$	195.8020	-	-	152.5054	-	178.9979	155.1976
$P_{G2}(kW)$	100.0000	-	-	100.0000	-	100.0000	100.0000
$P_{G3}(kW)$	289.7060	-	-	284.1365	-	294.7551	306.9213
$P_{G4}(kW)$	-	231.2381	-	309.0028	244.0640	-	372.0580
$P_{G5}(kW)$	-	387.7115	-	398.1423	397.9214	-	397.2527
$P_{G6}(kW)$	-	300.0000	-	300.0000	300.0000	-	300.0000
$P_{G7}(kW)$	-	-	412.2778	-	448.7059	435.5996	405.3178
$P_{G8}(kW)$	-	-	286.6343	-	278.3296	313.5037	292.3253
$P_{G9}(kW)$	-	-	383.1086	-	383.1090	382.7774	382.5820
$\boldsymbol{P_{loss}(kW)}$	**2.5480**	**5.5896**	**9.0607**	**47.4669**	**65.8098**	**49.7136**	**142.3745**
$Q_{loss}(kVAR)$	1.4386	2.3161	4.3252	26.9268	32.2380	31.0103	89.0266
Cost(*$/hr*)	23900.20	32455.84	44538.12	58033.52	79568.28	71145.24	106598.08
VD (*P.U*)	7.4787E-06	1.3000E-05	3.1218E-05	4.2800E-04	3.5700E-04	4.2200E-04	1.2680E-03
$P_{demand}(kW)$	582.96	913.36	1072.96	1496.32	1986.32	1655.92	2569.28
$Q_{demand}(kVAR)$	594.74	931.81	1094.64	1526.55	2026.45	1689.37	2621.19

Table-2.14 and Table-2.15 unveil the optimal scheduled output power of each DG, total Generation cost, Voltage Deviation values for various case studies. From the above test results, it is apparent that Jaya Algorithm is scheduling the DGs optimally for attaining the desired objective function of minimizing active power losses of the system. The active power losses obtained are 2.54802kW, 5.58956kW, 9.060678kW, 47.46691kW, 65.809831kW, 49.713619kW and 142.374521kW as against Genetic Algorithm of 2.548044kW, 5.590582kW, 9.060680kW, 47.467299kW, 65.81596kW, 49.800818kW and 143.640221kW from Case-I to Case-VII respectively.

From the convergence characteristics shown in Fig-2.16, it is discernible that the Jaya Algorithm provides minimum power losses as compared to the Genetic Algorithm. Both the

Table-2.15: Optimal values for various Case Studies with Scenario-2 for 85 Bus system with Genetic Algorithm

	Case-I	Case-II	Case-III	Case-IV	Case-V	Case-VI	Case-VII
$P_{G1}(kW)$	195.7864	-	-	149.9152	-	171.6144	150.6155
$P_{G2}(kW)$	99.9756	-	-	99.9756	-	99.9756	99.9756
$P_{G3}(kW)$	289.7461	-	-	287.5000	-	300.0000	305.4688
$P_{G4}(kW)$	-	224.8535	-	310.1074	301.1719	-	375.0000
$P_{G5}(kW)$	-	394.1703	-	396.3623	406.2500	-	406.2500
$P_{G6}(kW)$	-	299.9268	-	299.9268	299.9268	-	299.9268
$P_{G7}(kW)$	-	-	411.9873	-	383.3008	427.9785	406.2500
$P_{G8}(kW)$	-	-	286.8303	-	273.9865	406.2500	369.5313
$P_{G9}(kW)$	-	-	383.2031	-	387.5000	299.9023	299.9023
$\boldsymbol{P_{loss}(kW)}$	**2.5480**	**5.5906**	**9.0607**	**47.4673**	**65.8160**	**49.8008**	**143.6402**
$Q_{loss}(kVAR)$	1.4386	2.3166	4.3252	26.9264	32.2421	31.0419	89.7885
Cost($/hr)	23900.17	32632.62	44540.53	58004.54	78815.15	74903.60	109759.28
VD (P.U)	7.4773E-06	1.2680E-05	3.1252E-05	4.9834E-04	3.5138E-04	4.3032E-04	1.2443E-03
$P_{demand}(kW)$	582.96	913.36	1072.96	1496.32	1986.32	1655.92	2569.28
$Q_{demand}(kVAR)$	594.74	931.81	1094.64	1526.55	2026.45	1689.37	2621.19

algorithms converged in 33 iterations. The voltage profile in P.U at various Buses from Case-I to Case-VII obtained by Jaya Algorithm is plotted on Fig-2.17. From this figure, it is clear that on sectionalizing the Distribution System into Multi-Microgrid system, the minimum P.U voltage value in sectionalized Microgrids is better than the combined operation of Microgrids and is maintained within the permissible limits of ±5% for all the cases.

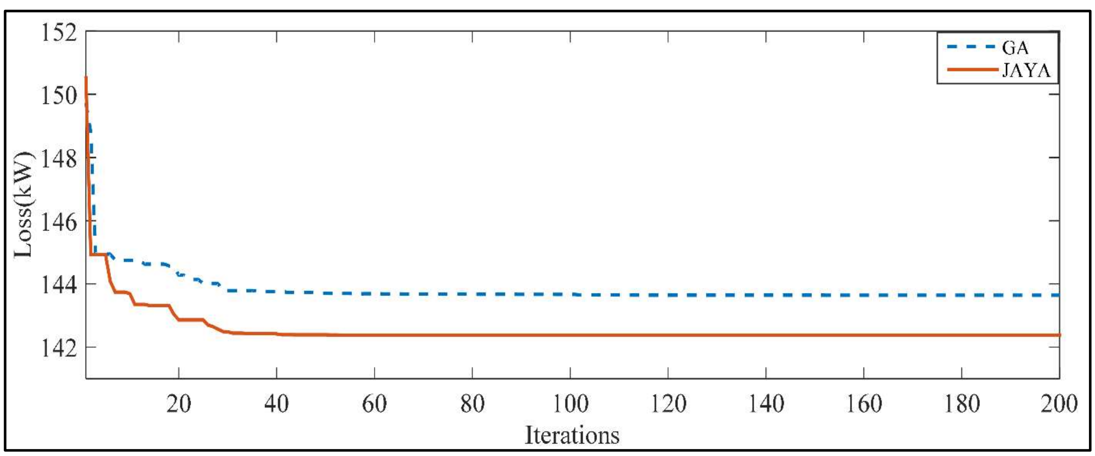

Fig-2.16: Convergence characteristics of Jaya algorithm vs GA for Loss minimization as objective function for 85 Bus system Scenario-2 Case-VII

From the test results, it is investigated that the power losses obtained by Jaya Algorithm in Scenario-2 for various case studies is much lesser than that of Scenario-1. The reduction in power losses for Case-VII is identified as 2116.30watts. From the above test results, the proposed Jaya Algorithm's optimal scheduling of DGs for various scenarios is promising.

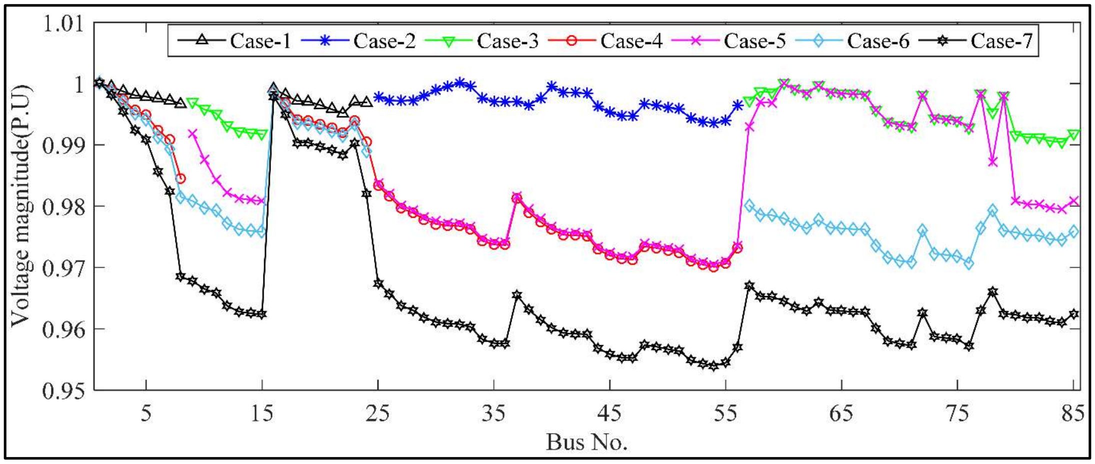

Fig-2.17: Voltage(P.U) profile of 85 Bus system for different case studies with Scenario-2 using Jaya Algorithm

2.6.3.3 Scenario-3 (Voltage Deviation minimization)

In this scenario, Voltage Deviation minimization is considered as the objective function. The Voltage Deviation minimization values for various case studies described above are presented in Table-2.16 and Table-2.17 for 85 Bus Distribution System using Jaya Algorithm and Genetic Algorithm respectively.

Table-2.16: Optimal values for various Case Studies with Scenario-3 for 85 Bus system with Jaya Algorithm

	Case-I	Case-II	Case-III	Case-IV	Case-V	Case-VI	Case-VII
$P_{G1}(kW)$	85.7148	-	-	0.2728	-	0.0547	4.1948
$P_{G2}(kW)$	100.0000	-	-	100.0000	-	15.4684	6.8153
$P_{G3}(kW)$	400.0000	-	-	47.3080	-	0.3588	0.0000
$P_{G4}(kW)$	-	394.6044	-	600.0000	600.0000	-	275.4859
$P_{G5}(kW)$	-	224.9447	-	500.0000	500.0000	-	500.0000
$P_{G6}(kW)$	-	300.0000	-	300.0000	300.0000	-	300.0000
$P_{G7}(kW)$	-	-	500.0000	-	500.0000	500.0000	473.8153
$P_{G8}(kW)$	-	-	182.2017	-	0.7193	799.7360	761.4577
$P_{G9}(kW)$	-	-	400.0000	-	158.0648	400.0000	400.0000
$P_{loss}(kW)$	2.7548	6.1891	9.2417	51.2609	72.4641	59.6980	152.4891
$Q_{loss}(kVAR)$	1.5123	2.5646	4.4444	29.2316	35.8715	36.5468	94.8147
Cost($/hr)	24736.48	30694.78	43454.27	64899.08	85300.10	105524.93	140895.01
VD (*P.U*)	**3.1245E-06**	**1.0846E-05**	**2.0877E-05**	**1.5709E-04**	**7.3850E-05**	**9.0958E-05**	**5.9473E-04**
$P_{demand}(kW)$	582.96	913.36	1072.96	1496.32	1986.32	1655.92	2569.28
$Q_{demand}(kVAR)$	594.74	931.81	1094.64	1526.55	2026.45	1689.37	2621.19

The optimal scheduled power output of various DGs considering Voltage Deviation minimization as the objective for each case study using Jaya Algorithm and Genetic

Algorithm are illustrated in Table-2.16 and Table-2.17 respectively. These tables also present the total system losses and the total cost of generation in each case. From these test results, it is observed that Jaya Algorithm is offering minimum Voltage Deviation in P.U of 3.1245E-06, 1.0846E-05, 2.0877E-05, 1.5709E-04, 7.3850E-05, 9.0958E-05 and 5.9473E-04 as against Genetic Algorithm of 3.1277E-06, 1.0851E-05, 2.0892E-05, 1.6503E-04, 7.4015E-05, 9.9281E-05 and 6.1097E-04 from Case-I to Case-VII respectively.

Table-2.17: Optimal values for various Case Studies with Scenario-3 for 85 Bus system with Genetic Algorithm

	Case-I	**Case-II**	**Case-III**	**Case-IV**	**Case-V**	**Case-VI**	**Case-VII**
$P_{G1}(kW)$	85.8365	-	-	0.0017	-	0.0456	0.0029
$P_{G2}(kW)$	99.9756	-	-	68.2129	-	22.2412	20.3857
$P_{G3}(kW)$	399.9023	-	-	100.0977	-	28.4180	0.9766
$P_{G4}(kW)$	-	394.6289	-	581.1035	599.5605	-	580.0781
$P_{G5}(kW)$	-	224.9937	-	497.9248	499.8779	-	495.3613
$P_{G6}(kW)$	-	299.9268	-	299.9268	299.6338	-	290.2588
$P_{G7}(kW)$	-	-	499.8779	-	499.8779	466.1865	290.1611
$P_{G8}(kW)$	-	-	182.4209	-	0.1247	799.6094	693.1641
$P_{G9}(kW)$	-	-	399.9023	-	160.0586	398.3398	351.4648
$P_{loss}(kW)$	2.7544	6.1894	9.2411	50.9473	72.8135	58.9206	152.5735
$Q_{loss}(kVAR)$	1.5122	2.5647	4.4441	29.0512	36.0446	36.0626	95.0140
Cost($\$/hr$)	24734.95	30695.08	43455.47	63940.02	85268.54	104679.55	135151.63
VD ($P.U$)	**3.1277E-06**	**1.0851E-05**	**2.0892E-05**	**1.6503E-04**	**7.4015E-05**	**9.9281E-05**	**6.1097E-04**
$P_{demand}(kW)$	582.96	913.36	1072.96	1496.32	1986.32	1655.92	2569.28
$Q_{demand}(kVAR)$	594.74	931.81	1094.64	1526.55	2026.45	1689.37	2621.19

The convergence characteristics of Jaya Algorithm and Genetic Algorithm are depicted in Fig-2.18. Though both the algorithms converge for the same number of iterations, Jaya Algorithm provides minimum Voltage Deviation value in P.U compared to Genetic Algorithm. It is noticed from the Fig-2.19 that the voltage profile is improved with the formulation of Multi-Microgrid System compared to the operation of entire Distribution System as a single Distribution Network.

On scrutiny, it is analyzed that the voltage deviation values in P.U obtained by the proposed Jaya Algorithm for Case-VII of Scenario-3 is 6.0959E-04, which is superior to that of 1.6660E-03 and 1.2680E-03 attained in Scenario-1 and Scenario-2 respectively. Thus, the optimal scheduling of DGs by the Jaya algorithm for Scenario-3 is encouraging.

The voltage profile in P.U for Case-VII of Cost minimization, Loss minimization, Voltage Deviation minimization and Base case is depicted in Fig-2.20. From the Fig-2.20, it is perspicuous that the Voltage Deviation in the Base-case is beyond the acceptable limits of ±5%, with a minimum voltage magnitude of 0.873309P.U at Bus no.54. The minimum voltage magnitudes noticed in Voltage Deviation minimization objective is found to be 0.96725P.U at Bus no.54 whereas in case of Cost minimization and Loss minimization objectives, the values of voltage magnitude are found to be 0.95397P.U and 0.95142P.U at Bus no.54. These are much improved values compared to 0.873309P.U and this promises healthy voltage profile at all the buses.

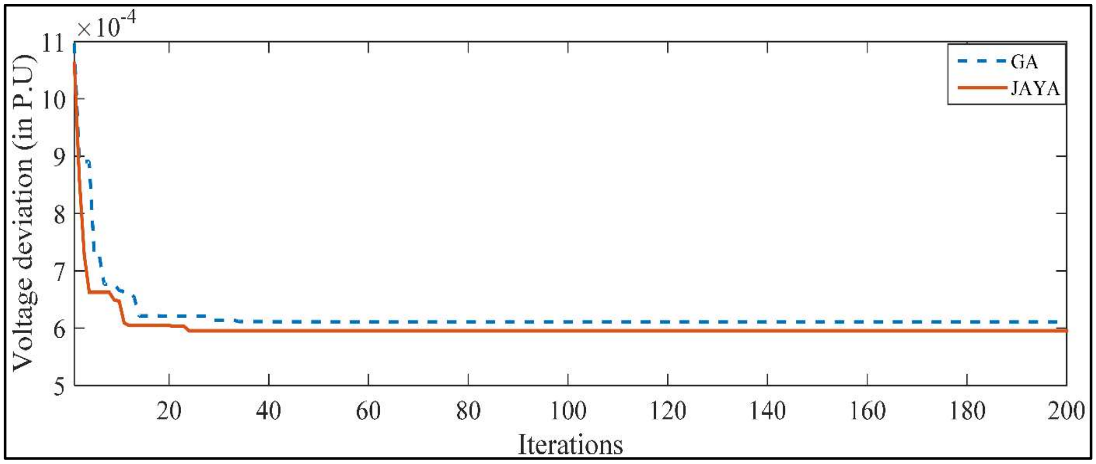

Fig-2.18: Convergence characteristics of Jaya Algorithm vs GA for Voltage Deviation minimization as objective function for 85 Bus system Scenario-3 Case-VII

Based on the above studies, it may be concluded that, whenever a fault is noticed in an active islanded Distribution System, a part of the total load can be fed with the individual operation of Microgrid or group operation of Microgrids by isolating the faulty portion, such that the number of consumers being affected by power interruption will be minimum. Based on the importance of objectives, the Microgrid Central Controller (MGCC) has to take a decision to operate the Microgrids in Scenario-1 or Scenario-2 or Scenario-3.

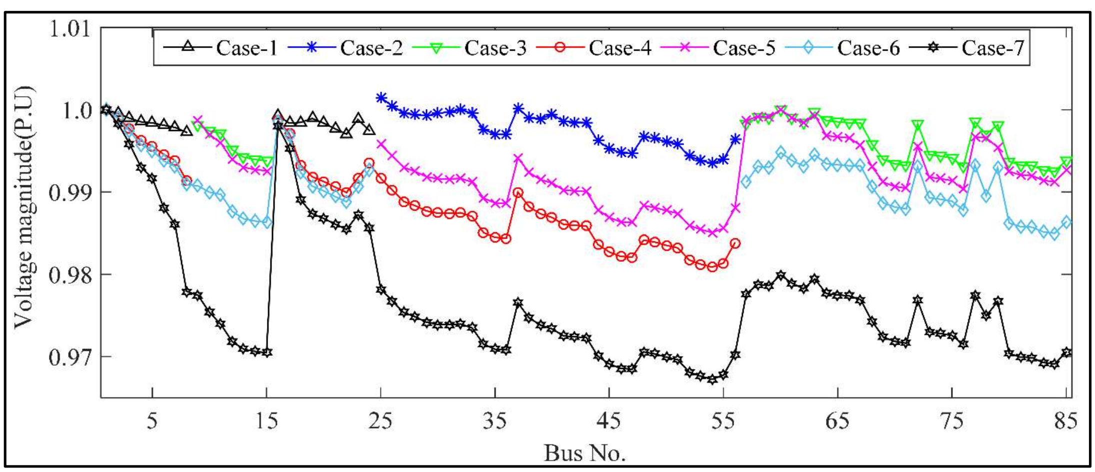

Fig-2.19: Voltage(P.U) profile of 85 Bus system for different case studies with Scenario-3 using Jaya Algorithm

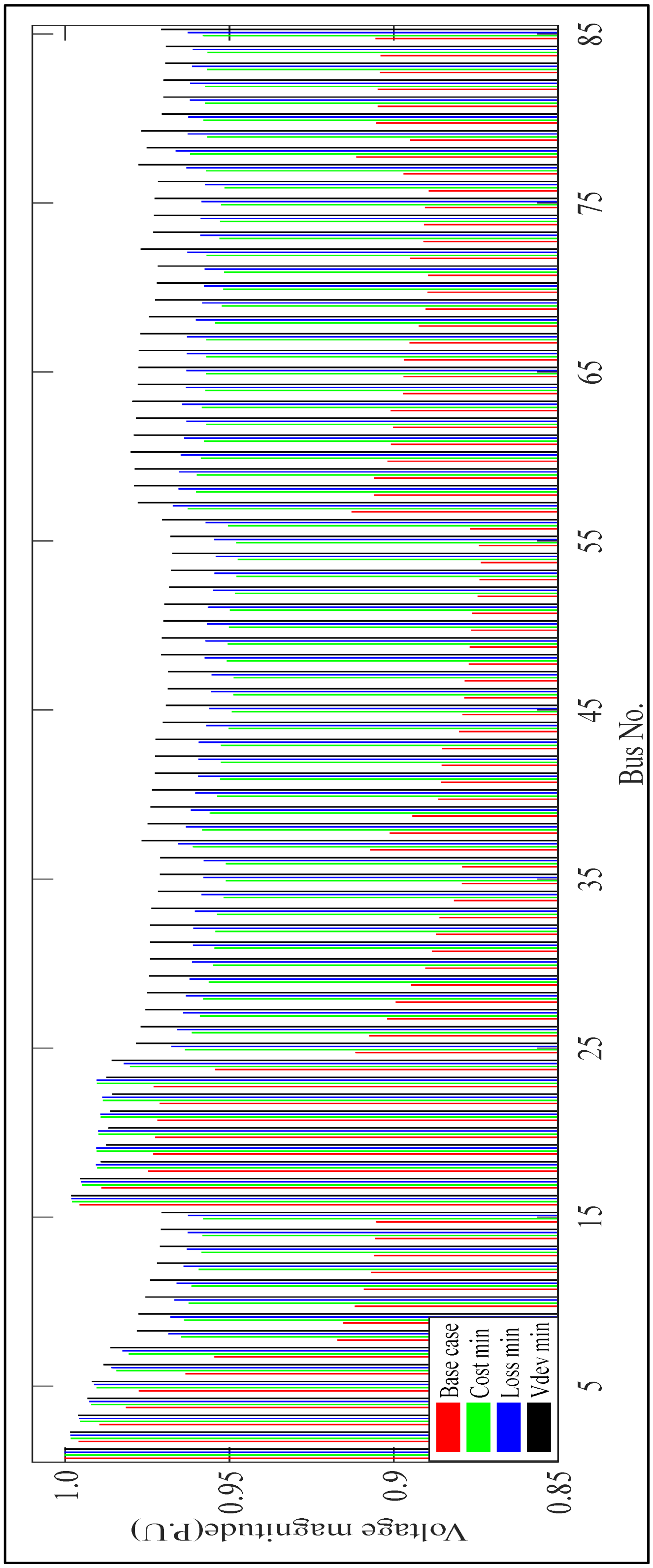

Fig-2.20: Voltage(P.U) profile of 85 Bus Distribution System for different Scenarios using Jaya Algorithm and Base case Load flows

2.7 Summary

In summary, this chapter has considered the optimal operation of Multi-Microgrid System by sectionalizing the existing islanded active Distribution System into several self-sufficient Microgrids. The optimal operation of the Multi-Microgrid System has been achieved by optimal scheduling of controllable DGs. These Microgrids are proposed to operate individually or united with other Microgrids so as to attain the desired objective. Single objective optimization has been addressed in this chapter for optimal scheduling of controllable DGs either in the individual mode of operation of Microgrid or combined mode of operation of Microgrids. The objective functions attempted in this work are *minimizing the total Operating cost of DGs, system Active power losses and Voltage Deviation*. Jaya Algorithm, which is a novel meta-heuristic optimization algorithm, has been exercised for optimizing the objective functions on modified 33 Bus Distribution System and modified Indian 85 Bus Distribution Systems. The obtained results are compared with the Genetic Algorithm, which is a well-known algorithm in the literature. The supremacy of the Jaya Algorithm is evident from the test results in terms of minimum *Operating Cost*, minimum *System Losses* and minimum *Voltage Deviation*.

A part of the work is published in "*IEEE International Conference on Sustainable Energy, Electronics and Computing Systems (SEEMS), I.T.S Engineering College, Greater Noida, India, 2018, DOI: 10.1109/SEEMS.2018.8687370.*

Though, to increase the customer satisfaction, sectionalisation of islanded Distribution System and optimal scheduling of controllable DGs have been performed, the Forced Outage Rate (FOR) of the DGs has not been considered in this chapter. Thus, to improve the reliability of customer service, in the next chapter, FOR of DGs has been considered for optimal scheduling to achieve the desired objectives.

CHAPTER-3

Reliability Constraint Optimal Scheduling of Micro-Sources in Multi-Microgrid system

3.1 Introduction

As a well-known fact that supplying electricity in an economical and reliable way is the aim of the power system. To achieve continuous power supply, proper planning and operation of Generating stations, Transmission & Distribution System and all other power supplying infrastructure is essential. Though planning of generation capacity, transmission & distribution network capacity, operating capacity are evaluated deterministically, it is also essential to have the knowledge of reliability parameters of the various power system components, for reliable operation of the system. The major power system components are generators, transformers and transmission lines. Out of all major components, it is apparent that generators fail more frequently.

Reliability is the probability of a device or system performing its function adequately, for the period intended, under the specified operating conditions. The reliability of a power system pertains to its ability to satisfy its load demand under the specified operating conditions and supporting policies [65]. Thus, in this chapter, optimal scheduling of controllable DGs has been attempted considering Forced Outage Rate (FOR) of generators.

3.2 Problem Formulation

Identifying the best solution from an exponentially large set of feasible solutions is defined as the optimization problem. The aim of the optimization problem considered in this chapter is the minimization of the objective function value. In this chapter, at a time, only one of the objective functions described below is treated for minimization by optimally scheduling the controllable DGs output which are considered as control variables, such that Energy Index of Reliability (EIR) denoted as τ is maintained as $\tau \geq 0.97$. The EIR, which depends on Forced Outage Rate (FOR) of the controllable DGs has been explained in the section-3.2.4.4 of this chapter and the EIR value is evaluated as per Equation-(3.8) of this chapter.

3.2.1 Minimization of Generation cost

Minimization of total Operating cost or Generating cost in an isolated Microgrid or Multi-Microgrid System by optimally scheduling the controllable DGs output is considered as an objective function, defined in the chapter-2. The objective function is presented again for the ready reference as per Equation-(3.1).

$$F_1(X) = \sum_{q=1}^{m} \sum_{k=1}^{N_{gen}} (a_{qk}P_{qk}^2 + b_{qk}P_{qk} + c_{qk}) \frac{\$}{hr} \tag{3.1}$$

where m is the total number of Microgrids in the system, N_{gen} is the total number of generators in each Microgrid-q. The a_{qk}, b_{qk} and c_{qk} are the fuel cost coefficients of k^{th}generator in q^{th} Microgrid, P_{qki} is active power generation value of k^{th}generator in q^{th} Microgrid at i^{th} iteration, X is a control variable relating any P_{qk}. However, while optimizing the generation cost, equality constraint i.e., power balance constraints, as well as inequality constraint i.e., generators capacity constraints and bus voltage constraints are need to be satisfied.

3.2.2 Minimization of Active Power Loss

As defined in chapter-2, the Active power loss minimization objective function is achieved by optimally scheduling the controllable DGs, which is expressed in Equation-(3.2) and Equation-(3.3).

$$F_2\,(X) = Minimize(P_{loss}) \tag{3.2}$$

$$P_{loss} = \sum_{q=1}^{m} P_{q,loss} = \sum_{q=1}^{m} \left[\sum_{k=1}^{N_{gen}} P_{qk} - P_{q\,demand} \right] \tag{3.3}$$

where P_{qk} is power output of k^{th} DG in q^{th} Microgrid, $P_{q\,demand}$ is active power demand in q^{th} Microgrid, $P_{q,loss}$ is the total active power loss in q^{th} Microgrid, P_{loss} is total active power loss in m-active Microgrids, and X is a control variable relating any P_{qk}.

3.2.3 Minimization of Voltage Deviation

Third objective function considered in this chapter is the minimization of Voltage Deviation, which is elucidated in chapter-2 above. The mathematical representation for Voltage Deviation minimization is defined in Equation-(3.4).

$$F_3(X) = Minimize\left[\frac{1}{n_{bus}} \sum_{q=1}^{m} \sum_{k=1}^{nbus_q} \left(|V_{qk}| - |V_{qk}^{sp}|\right)^2 \right] \tag{3.4}$$

where V_{qk} and V_{qk}^{sp} are the absolute voltage value and the specified voltage value at k^{th} bus of q^{th} Microgrid respectively, $nbus_q$ is total number of buses in q^{th} Microgrid and n_{bus} is total number of buses in all active Microgrids, m represents the total number of active Microgrids.

3.2.4 System Constraints

3.2.4.1 Power balance constraint

The mathematical representation for power balance in the Multi-Microgrid System is presented in Equation-(3.5) below, which is same as that defined in the chapter-2.

$$\sum_{q=1}^{m}\left[\sum_{k=1}^{N_{gen}} P_{qk}\right] = \sum_{q=1}^{m}\left[P_{q\,demand} + P_{q\,loss}\right] \tag{3.5}$$

3.2.4.2 Generator capacity constraints

The active power generation boundaries of a DG, which are inequality constraints as defined below.

$$P_{ij}^{min} \le P_{ij} \le P_{ij}^{max} \tag{3.6}$$

where P_{ij}^{min} *and* P_{ij}^{max} are the lower and upper bound of active power generation limits of j^{th} DG in i^{th} Microgrid, respectively.

3.2.4.3 Bus voltage constraints

The boundaries of the bus voltages magnitude, which also act as inequality constraints as defined in Equation-(3.7).

$$V_{ij}^{min} \le V_{ij} \le V_{ij}^{max} \tag{3.7}$$

where V_{ij}- Voltage magnitude of j^{th} bus in i^{th}Microgrid. V_{ij}^{max} and V_{ij}^{min} are the upper and lower boundaries of voltage magnitude of j^{th}bus in i^{th}Microgrid respectively.

3.2.4.4 Energy Index of Reliability (EIR)

In this chapter, the Energy Index of Reliability (EIR) denoted as τ, has been considered as a constraint, which reflects the no. of customers being affected by an erratic power supply. This index quantifies the reliability of loads being power supplied in the system by the group of generators. Higher the value of the index, lower is the chance of customers being affected. The EIR value is influenced by Forced Outage Rate (FOR) of the i^{th} generator (λ_i) and its output power (P_i). Forced Outage Rate represents the chances of failure of a generator to supply the load adequately. The mathematical expression for evaluation of EIR[38][66] is expressed below in Equation-(3.8).

$$EIR(\tau) = 1 - \frac{\sum_{i=1}^{N_{gen}} \lambda_i P_i}{\sum_{i=1}^{N_{gen}} P_i} \tag{3.8}$$

Where λ_i and P_i are the forced outage rate and power output of i^{th}generator respectively.

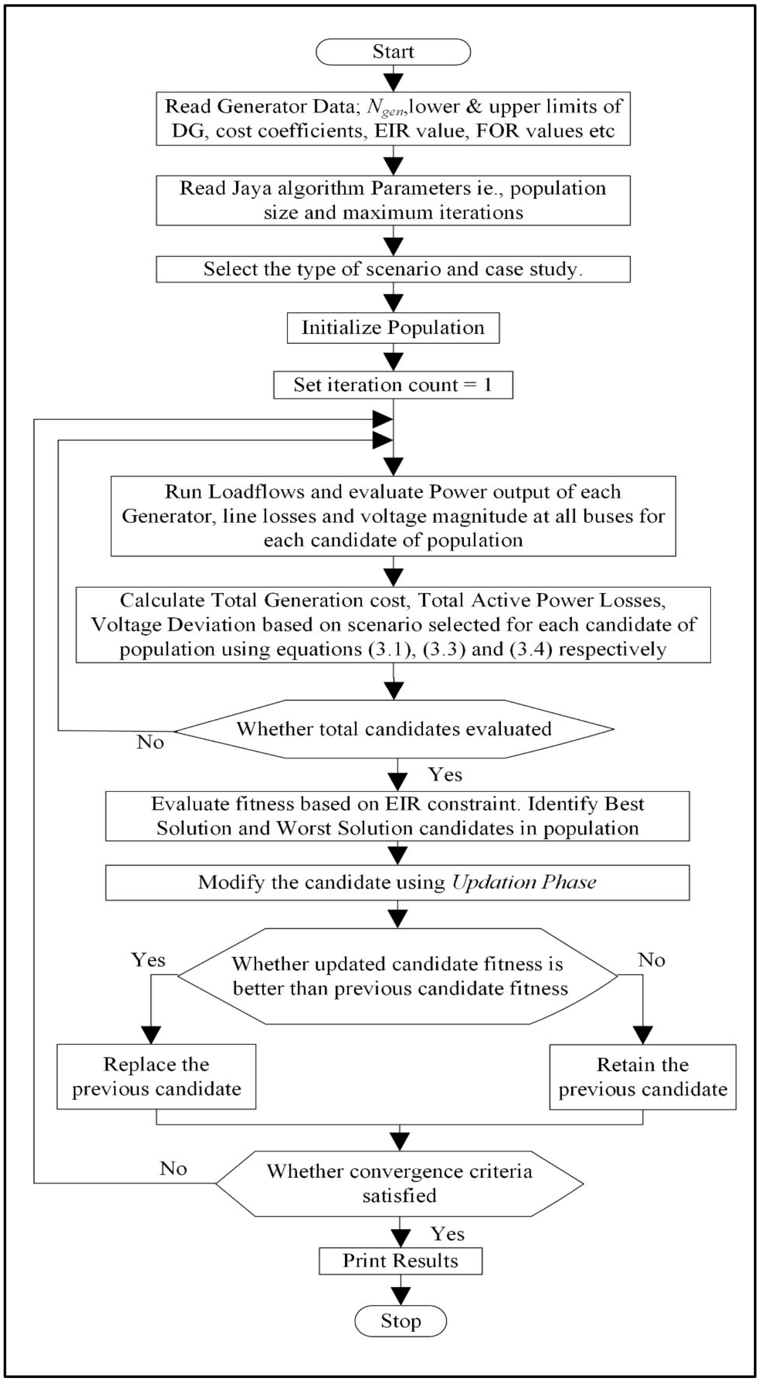

Fig-3.1: Flow chart of scheduling of DGs optimally using Jaya Algorithm considering single objective with EIR.

3.3 Results and Analysis

As stated earlier, considering the advantages associated with the Multi-Microgrid concept, the concept of sectionalizing the active Distribution System into Multi-Microgrid System has been experimented. The modified 33 Bus and modified Indian 85 Bus Distribution Systems, which are similar to the previous chapter-2, are considered for testing the proposed methodology. The generators location and their Forced outage rate (FOR) are presented in Table-3.1.

Table-3.1: Location and Forced Outage Rate (FOR) of DGs in Each Microgrid

Sl.No	MICROGRID		MG-1			MG-2			MG-3		
1	33 Bus Distribution System	DG Location at Bus No.	1	2	20	3	7	18	23	30	26
		FOR value	0.03	0.02	0.05	0.02	0.04	0.05	0.04	0.02	0.05
2	85 Bus Distribution System	DG Location at Bus No.	1	6	19	25	32	48	11	60	67
		FOR value	0.03	0.02	0.04	0.02	0.04	0.03	0.03	0.01	0.05

Jaya Algorithm, due to its advantage of independent of algorithm-specific parameters, has been used in this chapter to tackle the single-objective optimization problems as described above. The common parameters considered are population size as 80 and maximum generations as 200. Different Scenarios addressed in this chapter are described below. For each scenario, various case studies are considered similar to that of chapter-2. Based on the literature [38][67], the EIR(τ) value has been considered as greater than or equal to 0.97. Lower the value of EIR, greater the chance of power interruption. Thus, for reliable power supply to the customer, the EIR value can be maintained as high as possible. For an ideal case, the EIR value must be 1.0.

Scenarios of Single objective optimization

Scenario-1 : Operating cost minimization with EIR(τ) $\geq$ 0.97

Scenario-2 : Active power loss minimization with EIR(τ) $\geq$ 0.97

Scenario-3 : Voltage Deviation minimization with EIR(τ) $\geq$ 0.97

3.3.1 33 Bus Distribution System

3.3.1.1 Scenario-1 (Cost minimization with EIR)

Minimization of the total operating cost of DGs in Multi-Microgrid System by maintaining EIR(τ) $\geq$ 0.97 is taken as an objective function in this scenario. The Jaya

Algorithm and Genetic Algorithm have been used to obtain the optimal value of generators output after making an exhaustive number of trails and the obtained optimal values are presented in Table-3.2 and Table-3.3 respectively for various case studies. The actual details of Case-I to Case-VII are reported in Table-2.5. The EIR values for attained for various case studies using Jaya Algorithm and Genetic Algorithm are reported in Table-3.2 and Table-3.3 respectively.

Table-3.2: Optimal DG values for various Case Studies in Scenario-1 using Jaya Algorithm.

	Case-I	**Case-II**	**Case-III**	**Case-IV**	**Case-V**	**Case-VI**	**Case-VII**
$P_{G1}(kW)$	164.2694	-	-	378.8381	-	382.0899	347.7172
$P_{G2}(kW)$	198.3091	-	-	200.0000	-	200.0000	200.0000
$P_{G3}(kW)$	98.1198	-	-	0.0000	-	95.6945	27.5713
$P_{G4}(kW)$	-	748.6270	-	613.2056	687.7958	-	665.6593
$P_{G5}(kW)$	-	604.0570	-	575.0256	627.4096	-	586.0960
$P_{G6}(kW)$	-	72.2632	-	119.0799	169.5833	-	183.1205
$P_{G7}(kW)$	-	-	414.7686	-	402.2046	376.0187	390.4862
$P_{G8}(kW)$	-	-	1124.7363	-	1181.0390	989.0050	1109.1515
$P_{G9}(kW)$	-	-	354.9377	-	249.8010	310.7821	285.8432
$P_{loss}(kW)$	0.6982	19.9472	44.4426	21.1492	62.8333	43.5902	80.6452
$Q_{loss}(kVAR)$	0.6622	13.9437	35.9451	14.6668	45.8679	32.9790	55.3394
Cost($/hr)	**19256.43**	**87175.14**	**110298.17**	**102015.60**	**196723.42**	**125377.53**	**213372.95**
VD (P.U)	7.7973E-6	7.0421E-4	7.7595E-4	5.2575E-4	5.7848E-4	2.1707E-4	6.6321E-4
EIR	0.9700	0.9700	0.9700	0.9700	0.9700	0.9700	0.9700
$P_{demand}(kW)$	460	1405	1850	1865	3255	2310	3715
$Q_{demand}(kVAR)$	220	680	1400	900	2080	1620	2300

From these test results, it is apparent that Jaya Algorithm has scheduled the DGs optimally such that the operating cost obtained are 19256.431$/hr, 87175.14$/hr, 110298.17$/hr, 102015.60$/hr, 196723.42$/hr, 125377.53$/hr and 213372.95$/hr from Case-I to Case-VII are minimum in contrast to 19256.432$/hr, 87183.16$/hr, 110310.67$/hr, 106368.98$/hr, 196737.00$/hr, 126040.65$/hr and 228486.69$/hr from Case-I to Case-VII respectively of Genetic Algorithm.

It is conspicuous from the test results that as the loading increases, the cost saving is monumental. The convergence characteristics of Case-VII for Genetic Algorithm and Jaya Algorithm are depicted in Fig-3.3. From the convergence characteristics, it is apparent that Jaya algorithm offers minimum cost than that of Genetic Algorithm. It is noticed that the Genetic Algorithm converged prematurely with a higher operating cost.

Fig-3.2 depicts the voltage magnitude in P.U at each bus of modified 33 Bus Distribution System for various case studies using Jaya Algorithm. It is evident from this figure that the voltage profile is improved by independent operation of Microgrids than the operation of entire Distribution System as a single network.

Table-3.3: Optimal DG values for various Case Studies in Scenario-1 using Genetic Algorithm

	Case-I	Case-II	Case-III	Case-IV	Case-V	Case-VI	Case-VII
$P_{G1}(kW)$	164.2884	-	-	292.4169	-	416.1006	46.7550
$P_{G2}(kW)$	198.3883	-	-	147.4969	-	187.4481	177.7778
$P_{G3}(kW)$	98.0220	-	-	71.2576	-	74.4811	88.4005
$P_{G4}(kW)$	-	749.9876	-	750.1830	691.5291	-	624.6641
$P_{G5}(kW)$	-	599.9511	-	497.3870	658.9498	-	429.4016
$P_{G6}(kW)$	-	74.8718	-	127.4725	136.8498	-	287.6190
$P_{G7}(kW)$	-	-	403.5408	-	405.8607	381.9291	393.0402
$P_{G8}(kW)$	-	-	1128.4969		1166.0560	976.8008	1432.2342
$P_{G9}(kW)$	-	-	362.3931	-	259.4383	316.6788	313.7484
$P_{loss}(kW)$	0.6986	19.8104	44.4309	21.2139	63.6838	43.4385	78.6409
$Q_{loss}(kVAR)$	0.6625	13.8516	35.9367	14.8242	46.3965	32.8609	54.1817
Cost($/hr)	**19256.43**	**87183.16**	**110310.67**	**106368.98**	**196737.00**	**126040.65**	**228486.69**
VD (P.U)	7.8014E-6	7.0107E-4	7.7919E-4	5.3310E-4	6.0566E-4	2.1959E-4	4.3886E-4
EIR	0.9701	0.9700	0.9700	0.9700	0.9700	0.9700	0.9701
$P_{demand}(kW)$	460	1405	1850	1865	3255	2310	3715
$Q_{demand}(kVAR)$	220	680	1400	900	2080	1620	2300

It is noticeable from the test results that the DGs with higher values of Forced Outage Rate (FOR) are contributing minimum power output for meeting the load economically to satisfy the EIR criterion value as against economic scheduling of DGs without EIR criterion presented in chapter-2. For illustration, the DGs (P_{G3}, P_{G6}, P_{G9}) with a higher value of FOR, of magnitude 0.05 have contributed less output power of 27.5713kW, 183.1205kW and 285.8432kW in Case-VII of this Scenario with Jaya Algorithm as against 99.2185kW, 483.1538kW and 667.9364kW output power in optimal scheduling of DGs with Jaya Algorithm considering minimization of operating cost without EIR constraint in Case-VII (i.e., Chapter-2, Table-2.6). Similarly, DGs (P_{G2}, P_{G4}, P_{G8}) having a lower value of FOR, of 0.02 have supplied higher value of output power of 200.00kW, 665.6593kW and 1109.1515kW in this scenario with Jaya Algorithm as against 199.2184kW, 296.4591kW and 560.4395kW output power produced in economic scheduling without EIR criterion (i.e., Table-2.6 of Chapter-2,). Upon comparison of the test results, it is apparent that the Jaya Algorithm has scheduled the DGs optimally for operating cost minimization objective, by enforcing the EIR criterion of $\tau \geq 0.97$ along with equality and inequality constraints.

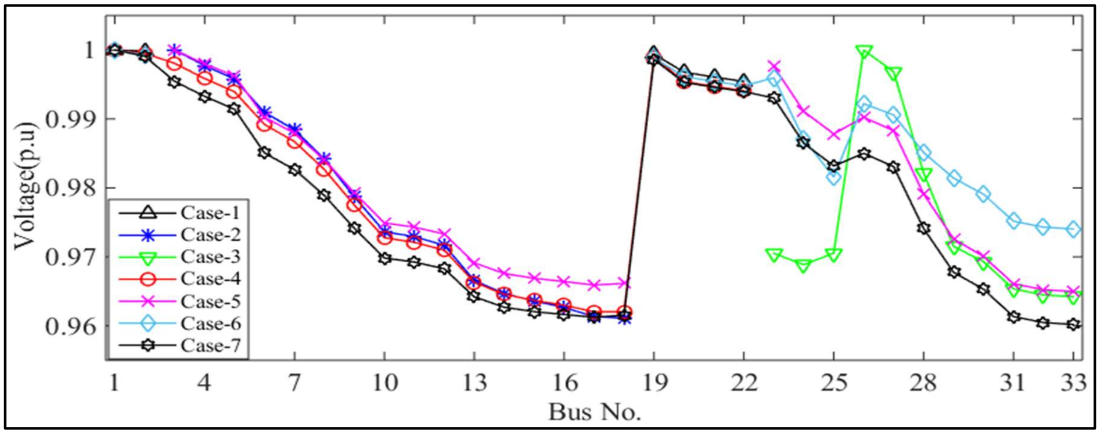

Fig-3.2: Voltage Magnitude(P.U) of 33 Bus System for various cases of Scenario-1 using Jaya Algorithm with EIR

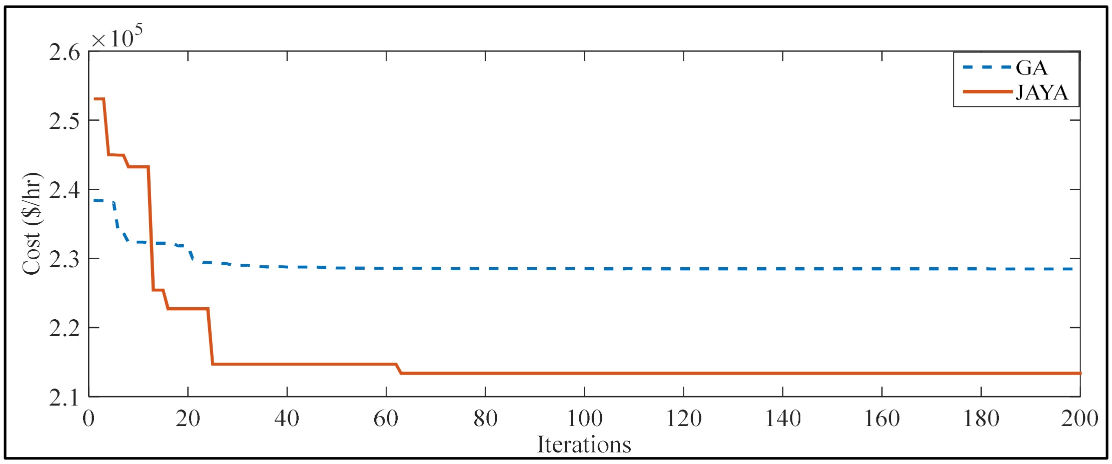

Fig-3.3: Convergence characteristics of Jaya algorithm vs GA for Cost minimization as objective function for 33 Bus system Scenario-1 Case-VII with EIR

3.3.1.2 Scenario-2 (Loss minimization with EIR)

Power loss minimization in MG(s) by maintaining EIR(τ) $\geq$ 0.97 is considered as an objective function in this scenario. Abundant trails are made using Jaya Algorithm and Genetic Algorithm to determine the optimal output values of DGs for power losses minimization and the test results are presented in Table-3.4 and Table-3.5. Figure-3.4 illustrates the voltage magnitude in P.U at each bus of 33 Bus Distribution System under Scenario-2 for various case studies considered in the chapter.

It is clear from the results that the Jaya Algorithm has scheduled the DGs optimally such that the active power loss obtained from Case-I to Case-VII are 0.690kW, 14.694kW, 43.912kW, 15.114kW, 56.574kW, 41.867kW and 75.364kW are minimum as compared to Genetic Algorithm active power losses of 0.697kW, 14.716kW, 43.913kW, 15.849kW, 57.338kW, 42.489kW and 75.414kW from Case-I to Case-VII respectively. It is noticeable that as the size of the Microgrid(s) system increases, the reduction in the losses also increases. The EIR values obtained by Jaya Algorithm and Genetic Algorithm are illustrated in Tables 3.4 and Table-3.5, respectively. In all the attempted cases, the $\tau \geq 0.97$ is well maintained. Fig-3.5 exhibits the convergence characteristics of Jaya Algorithm and Genetic Algorithm. It is apparent from the convergence characteristics that Jaya Algorithm provides minimum losses than Genetic Algorithm.

Table-3.4: Optimal DG values for various Case Studies in Scenario-2 using Jaya Algorithm.

	Case-I	**Case-II**	**Case-III**	**Case-IV**	**Case-V**	**Case-VI**	**Case-VII**
$P_{G1}(kW)$	160.6905	-	-	1.4583	-	599.7113	27.2177
$P_{G2}(kW)$	200.0000	-	-	200.0000	-	200.0000	200.0000
$P_{G3}(kW)$	100.0000	-	-	0.0000	-	0.0000	100.0000
$P_{G4}(kW)$	-	890.7633	-	928.9985	1052.1086		1311.1442
$P_{G5}(kW)$	-	167.1226	-	370.4980	0.0000	-	224.7097
$P_{G6}(kW)$	-	361.8090	-	379.1598	400.3185	-	319.0740
$P_{G7}(kW)$	-	-	500.0000	-	180.7945	254.1024	6.6882
$P_{G8}(kW)$	-	-	1095.9411	-	1095.3425	883.8379	928.3502
$P_{G9}(kW)$	-	-	297.9705		583.0095	414.2154	673.1805
$\boldsymbol{P_{loss}(kW)}$	**0.6905**	**14.6949**	**43.9116**	**15.1146**	**56.5737**	**41.8670**	**75.3645**
$Q_{loss}(kVAR)$	0.6554	11.3859	35.4963	11.0792	43.0113	31.5940	52.1657
Cost($/hr)	19257.57	96128.73	110930.25	119781.09	221848.93	130618.13	263911.99
VD (P.U)	7.7117E-6	4.1048E-4	7.5031E-4	2.4297E-4	4.1498E-4	2.2884E-4	4.7110E-4
EIR	0.9700	0.9700	0.9700	0.9700	0.9700	0.9700	0.9701
$P_{demand}(kW)$	460	1405	1850	1865	3255	2310	3715
$Q_{demand}(kVAR)$	220	680	1400	900	2080	1620	2300

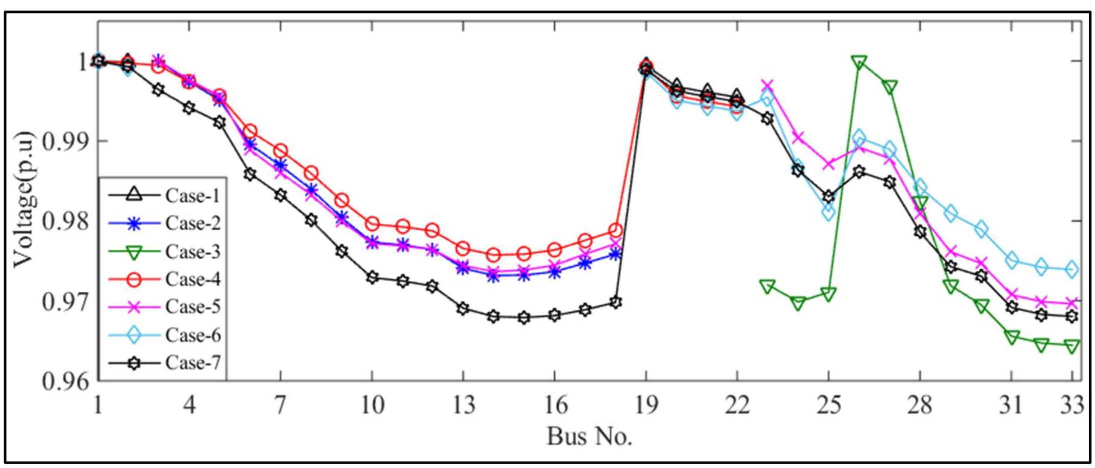

Fig-3.4: Voltage Magnitude(P.U) of 33 Bus System for various cases of Scenario-2 using Jaya Algorithm with EIR

Table-3.5: Optimal DG values for various case studies in Scenario-2 using Genetic Algorithm.

	Case-I	Case-II	Case-III	Case-IV	Case-V	Case-VI	Case-VII
$P_{G1}(kW)$	162.3084	-	-	12.7909	-	575.5903	204.8227
$P_{G2}(kW)$	199.9511	-	-	177.6801	-	195.3113	82.8816
$P_{G3}(kW)$	98.4371	-	-	24.9328	-	37.2894	8.1807
$P_{G4}(kW)$	-	878.2263	-	1001.7093	914.3653	-	1044.2001
$P_{G5}(kW)$	-	204.9328	-	199.8535	17.3871	-	82.2466
$P_{G6}(kW)$	-	336.5567	-	463.8827	299.4871	-	425.3479
$P_{G7}(kW)$	-	-	499.9999	-	359.3406	390.1098	145.1770
$P_{G8}(kW)$	-	-	1095.9888	-	1168.4980	859.5847	1192.9180
$P_{G9}(kW)$	-	-	297.9243	-	553.2600	294.6031	604.6397
$\boldsymbol{P_{loss}(kW)}$	**0.6967**	**14.7158**	**43.9130**	**15.8492**	**57.3381**	**42.4887**	**75.4144**
$Q_{loss}(kVAR)$	0.6609	11.2520	35.4973	12.1870	43.4980	32.0155	52.8884
Cost($/hr)	19256.78	94646.04	110932.85	127046.87	212795.65	128778.48	247274.32
VD (P.U)	7.7797E-6	4.3136E-4	7.5220E-4	2.1288E-4	5.0057E-4	2.7404E-4	3.7278E-4
EIR	0.9701	0.9700	0.9700	0.9700	0.9700	0.9700	0.9700
$P_{demand}(kW)$	460	1405	1850	1865	3255	2310	3715
$Q_{demand}(kVAR)$	220	680	1400	900	2080	1620	2300

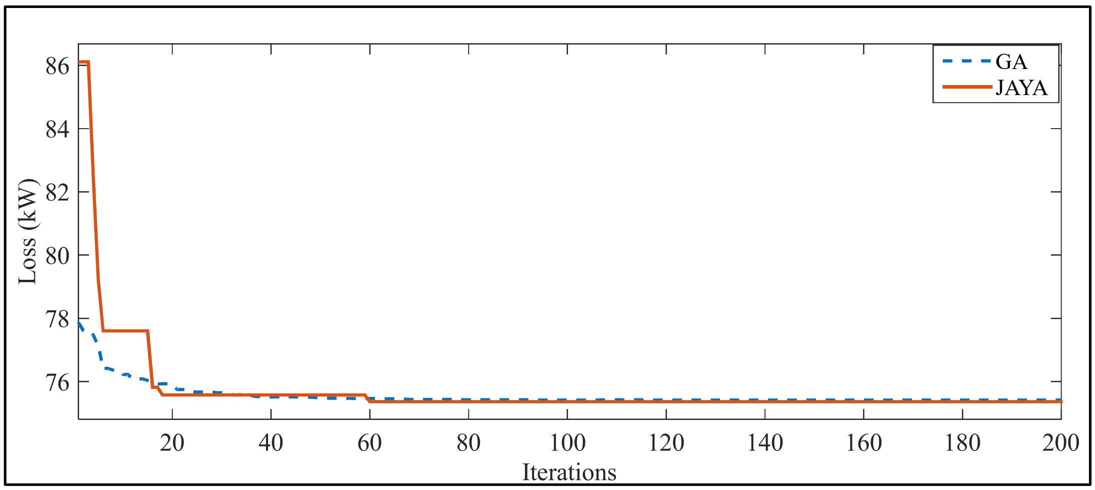

Fig-3.5: Convergence characteristics of Jaya Algorithm vs GA for Loss minimization as objective function for 33 Bus system Scenario-2 Case-VII with EIR

It is evident from the test results that the DGs with lower values of FOR are scheduled to maximum power output in this scenario for maintaining τ ≥ 0.97, compared to that of optimal scheduling of DGs for loss minimization without EIR criterion of Chapter-2. For illustration, the DGs (P_{G2}, P_{G4}, P_{G8}) with lower values of FOR (i.e.,0.02) have contributed more output power of 200.00kW, 1311.1442kW and 928.3502 in Case-VII of this scenario with Jaya Algorithm as against 68.5226kW, 849.8167kW and 758.5835kW output power produced in optimal scheduling of DGs without EIR criterion by Jaya Algorithm in Scenario-2 (Table-2.8) of Chapter-2. However, the DGs (P_{G3}, P_{G6}, P_{G9}) with higher FOR of 0.05 have supplied power outputs of 100.00kW, 319.0740kW and 673.1805kW as against 99.0232kW, 415.2380kW and 315.0183kW output power produced in optimal scheduling of DGs without EIR in Scenario-2 (Table-2.8) of Chapter-2. It is noticed that the resistance offered by the lines (line no.25 and line no.26) connected to Bus-26, where P_{G9} is located, are having lower resistance values compared to other lines in the system. Thus, the DG has scheduled to produce more power output of 673.1805kW to reduce the system losses, even though its FOR is higher. From the above, it is evident that the Jaya Algorithm has scheduled the DGs optimally to achieve minimum losses along with satisfying EIR criterion.

3.3.1.3 Scenario-3 (Voltage Deviation minimization with EIR)

In this scenario, Voltage Deviation minimization has been considered as an objective function by maintaining EIR(τ) greater than or equal to 0.97. Optimal DGs outputs are determined using Jaya Algorithm and Genetic Algorithm with numerous trails for minimizing the Voltage Deviation. The results obtained with the above algorithms are presented in Table-3.6 and Table-3.7.

Table-3.6: Optimal DG values for various Case Studies in Scenario-3 using Jaya Algorithm.

	Case-I	Case-II	Case-III	Case-IV	Case-V	Case-VI	Case-VII
$P_{G1}(kW)$	160.6905	-	-	10.6255	-	2.3921	3.6756
$P_{G2}(kW)$	200.0000	-	-	13.3205	-	36.3917	131.7079
$P_{G3}(kW)$	100.0000	-	-	0.0000	-	0.0000	0.7079
$P_{G4}(kW)$	-	947.8756	-	1225.1674	30.4193	-	297.1440
$P_{G5}(kW)$	-	0.0937	-	34.2735	11.1328	-	381.7197
$P_{G6}(kW)$	-	472.4963	-	600.0000	541.8457	-	570.2480
$P_{G7}(kW)$	-	-	500.0000	-	59.0820	1.0477	3.6072
$P_{G8}(kW)$	-	-	1095.9411	-	2164.3066	1547.8144	1988.5000
$P_{G9}(kW)$	-	-	297.9705	-	520.1172	790.4542	431.9197
$P_{loss}(kW)$	0.6905	15.4656	43.9116	18.3869	71.9037	68.1001	94.2302
$Q_{loss}(kVAR)$	0.6554	12.6866	35.4963	14.8820	53.5168	52.3174	65.7511
Cost($/hr)	19257.57	104387.06	110930.25	154364.23	271849.22	171216.10	275639.92
VD (P.U)	**7.7117E-6**	**3.2841E-4**	**7.5031E-4**	**1.3985E-4**	**8.8056E-5**	**4.5110E-5**	**1.0492E-4**
EIR	0.9700	0.9700	0.9700	0.9700	0.9700	0.9700	0.9701
$P_{demand}(kW)$	460	1405	1850	1865	3255	2310	3715
$Q_{demand}(kVAR)$	220	680	1400	900	2080	1620	2300

From the results, it is noticeable that the Jaya Algorithm is providing minimum Voltage Deviation of 7.7117E-06P.U, 3.2841E-04P.U, 7.5031E-04P.U, 1.3985E-04P.U, 8.8056E-05P.U, 4.5110E-05P.U, 1.0492E-04P.U for Case-I to Case-VII as against 7.7302E-06 P.U, 3.4366E-04P.U, 7.5058E-04P.U, 2.2715E-04P.U, 8.9228E-05P.U, 4.8739E-05P.U, 1.0917E-04P.U Genetic Algorithm results. It is evident from the test results that the DG(P_{G3}) having higher value of FOR is contributing minimum power output, i.e., in Case-IV, Case-

VI and Case-VII, the power outputs are almost equal to zero as its FOR is 0.05. Similarly, the DGs(P_{G4} and P_{G8}) with FOR of 0.02 are scheduled with higher power outputs.

The convergence characteristics of Case-VII for Jaya Algorithm and Genetic Algorithm are depicted in Fig-3.6. It is apparent from this figure that the Jaya Algorithm provides minimum Voltage Deviation value compared to Genetic Algorithm.

Table-3.7: Optimal DG values for various Case Studies in Scenario-3 using Genetic Algorithm.

	Case-I	**Case-II**	**Case-III**	**Case-IV**	**Case-V**	**Case-VI**	**Case-VII**
$P_{G1}(kW)$	86.2049	-	-	0.1551	-	8.0308	3.3735
$P_{G2}(kW)$	199.7559	-	-	14.7949	-	21.8262	39.7461
$P_{G3}(kW)$	99.5850	-	-	24.5361	-	47.0703	60.8398
$P_{G4}(kW)$	-	935.4933	-	1215.3320	2.6490	-	283.6914
$P_{G5}(kW)$	-	34.9609	-	193.1641	92.7734	-	44.3359
$P_{G6}(kW)$	-	449.7070	-	433.5938	570.8496	-	579.9316
$P_{G7}(kW)$	-	-	499.3896	-	26.2451	46.2646	56.3965
$P_{G8}(kW)$	-	-	1096.2861	-	2239.9902	1553.9551	2381.5918
$P_{G9}(kW)$	-	-	298.2422	-	397.2656	699.2188	361.3281
$P_{loss}(kW)$	0.6922	15.1612	43.9180	16.5760	74.7731	66.3657	96.2349
$Q_{loss}(kVAR)$	0.6569	12.2989	35.5015	12.5486	55.5525	51.0440	67.5517
Cost($/hr)	19257.19	102419.63	110928.91	148183.14	280238.09	167582.33	321447.43
VD (P.U)	**7.7302E-6**	**3.4366E-4**	**7.5058E-4**	**2.2715E-4**	**8.9228E-5**	**4.8739E-5**	**1.0917E-4**
EIR	0.9700	0.9700	0.9700	0.9706	0.9706	0.9702	0.9716
$P_{demand}(kW)$	460	1405	1850	1865	3255	2310	3715
$Q_{demand}(kVAR)$	220	680	1400	900	2080	1620	2300

The Fig-3.7 illustrates the voltage magnitude at each bus of 33 Bus Distribution System under Scenario-3 for various case studies formulated. The voltage magnitudes in P.U at different buses for Case-VII of Scenario-1, Scenario-2, Scenario-3 and Base case load flow study are compared and depicted in Fig-3.8. From the voltage magnitude comparison plot, it is conspicuous that the voltage magnitudes are improved at all the buses of Multi-Microgrid System for Voltage Deviation minimization scenario as against other scenarios. The minimum value of voltage magnitudes noticed in the Base case, Scenario-1, Scenario-2 and Scenario-3 are 0.913P.U at Bus 18, 0.960P.U at Bus 33, 0.967P.U at Bus 15 and 0.977P.U at Bus 33 respectively. The minimum voltage magnitude in P.U noticed in the Base case load flow study is below the Voltage Deviation limits of ±5%. Thus, it is necessary to operate the Multi-Microgrid System in other scenarios rather than Base case, where the source of power is at Bus no.1.

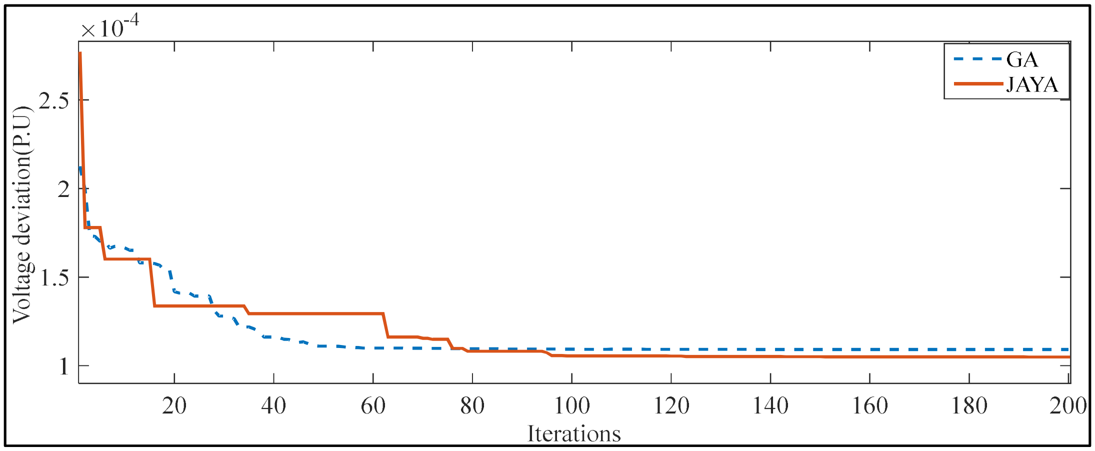

Fig-3.6: Convergence characteristics of Jaya algorithm vs GA for Voltage Deviation minimization as objective function for 33 Bus system Scenario-3 Case-VII with EIR

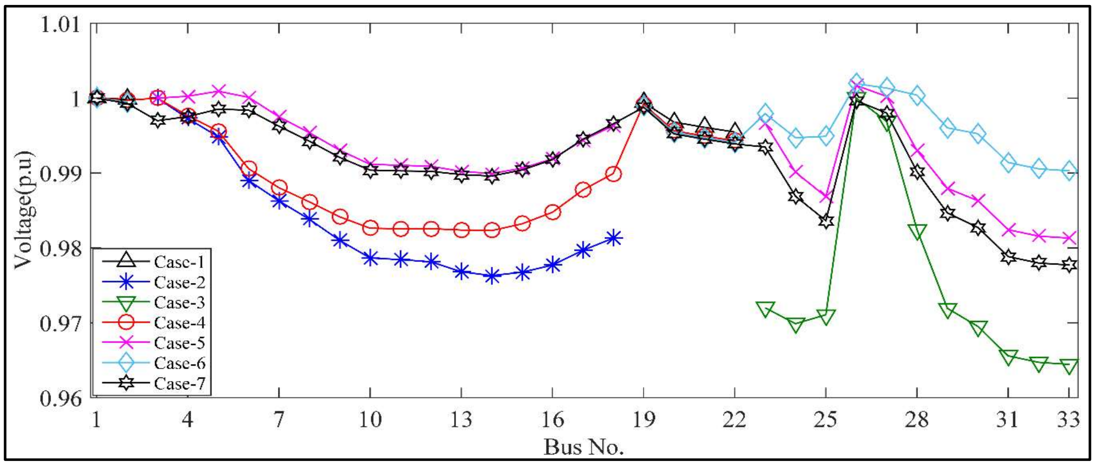

Fig-3.7: Voltage Magnitude(P.U) of 33 Bus system for various Cases of Scenario-3 using Jaya Algorithm with EIR

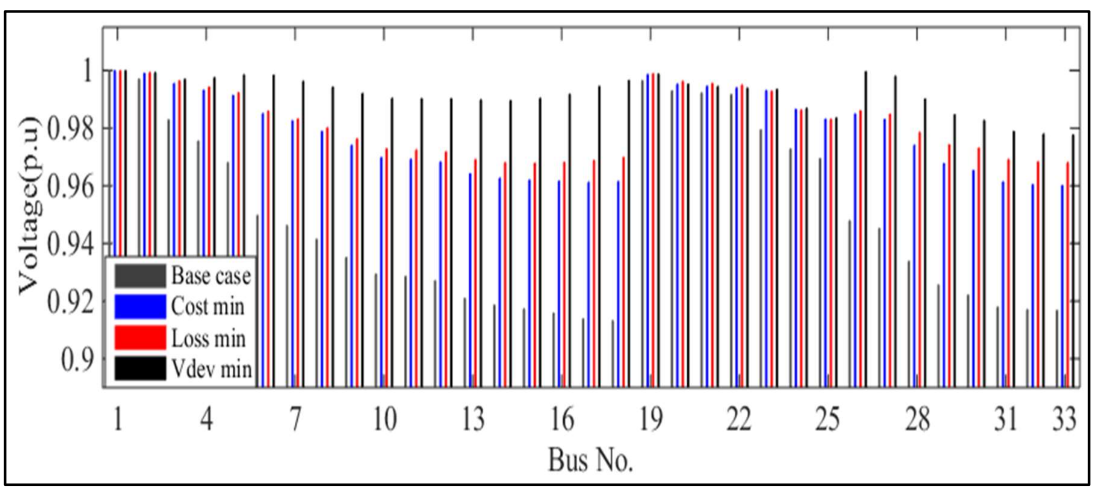

Fig-3.8: Voltage Magnitude (P.U) of 33 Bus Distribution System for different Scenarios using Jaya Algorithm with EIR and Base case Load flows

Table-3.8: Comparison of the EIR values for Optimal Scheduling of DGs with and without Reliability Criterion for various Scenarios

	Optimal Scheduling without EIR						Optimal Scheduling with EIR ($\tau \geq 0.97$)					
	Cost minimization		Loss minimization		Voltage Deviation minimization		Cost minimization		Loss minimization		Voltage Deviation minimization	
	EIR values											
Case Studies	**GA**	**Jaya**	**GA**	**Jaya**	**GA**	**Jaya**	**GA**	**Jaya**	**GA**	**Jaya**	**GA**	**Jaya**
Case-I	0.9700	0.9701	0.9700	0.9700	0.9700	0.9700	0.9701	0.9700	0.9701	0.9700	0.9700	0.9700
Case-II	0.9605	0.9605	0.9601	0.9601	0.9628	0.9629	0.9700	0.9700	0.9700	0.9700	0.9700	0.9700
Case-III	0.9627	0.9627	0.9620	0.9620	0.9620	0.9620	0.9700	0.9700	0.9700	0.9700	0.9700	0.9700
Case-IV	0.9637	0.9635	0.9624	0.9628	0.9683	0.9674	0.9700	0.9700	0.9700	0.9700	0.9706	0.9700
Case-V	0.9620	0.9616	0.9626	0.9616	0.9685	0.9702	0.9700	0.9700	0.9700	0.9700	0.9706	0.9700
Case-VI	0.9639	0.9646	0.9675	0.9630	0.9637	0.9636	0.9700	0.9700	0.9700	0.9700	0.9702	0.9700
Case-VII	0.9630	0.9631	0.9670	0.9648	0.9669	0.9657	0.9701	0.9700	0.9700	0.9701	0.9716	0.9701

Table-3.8 illustrates the EIR value for optimal scheduling of DGs for Cost minimization, Active power loss minimization and Voltage Deviation minimization as objectives with and without consideration of EIR as a criterion. The EIR(τ) values have been evaluated for various case studies under different scenarios of Chapter-2 by taking scheduled power outputs by DGs into consideration. It is analyzed from this table that, in all the case studies except Case-I of optimal scheduling without EIR criterion, the EIR values attained are less than 0.97. In Case-I, it is noticed that P_{G3} (connected at Bus-20) is having a higher value of FOR and also offers higher cost than DGs $P_{G1}$and P_{G2}. Further, the lines connected to Bus-20 are having higher value of resistance. Thus, P_{G3} is contributing a lower percentage of power w.r.t its capacity value, with and without EIR criterion. In view of this, the EIR value in Case-I, with and without EIR criterion is maintained greater than or equal to 0.97.

From the Table-3.9, it is identified that the Operating cost, System Active power losses and Voltage Deviation values increased minimally with the consideration of EIR criterion because the DGs are not scheduled for minimization of the objective function alone, but to meet the EIR criterion also. Thus, with the EIR criterion, the probability of a customer being affected by DGs failure has been reduced.

Table-3.9: Comparison of Operating Cost, Active Power Loss and Voltage Deviation with and without EIR criterion for various Case Studies

			Case-I	Case-II	Case-III	Case-IV	Case-V	Case-VI	Case-VII
Cost ($/hr)									
Economic scheduling	Cost minimization	Jaya	19256.43	70902.88	97919.59	89446.93	168665.57	115067.73	187652.72
		GA	19256.44	70902.99	97919.86	89480.97	168996.73	115367.93	188885.73
Reliability scheduling		Jaya	19256.43	87175.14	110298.17	102015.60	196723.42	125377.53	213372.95
		GA	19256.44	87183.16	110310.67	106368.97	196736.99	126040.65	228486.67
Active Power Loss (kW)									
Economic scheduling	Loss minimization	Jaya	0.6905	9.4994	33.6732	12.1222	53.4250	34.6447	71.7077
		GA	0.6905	9.5202	33.7090	12.1501	53.4696	34.6351	71.9022
Reliability scheduling		Jaya	0.6905	14.6949	43.9116	15.1146	56.5737	41.8670	75.3645
		GA	0.6967	14.7158	43.9130	15.8492	57.3381	42.4887	75.4144
Voltage Deviation (P.U)									
Economic scheduling	Voltage Deviation Minimization	Jaya	7.9987E-6	2.7652E-4	1.9666E-2	2.6928E-4	7.0616E-4	4.2488E-4	9.7410E-4
		GA	7.9990E-6	2.7653E-4	1.9667E-2	2.7003E-4	7.0714E-4	4.2531E-4	9.8068E-4
Reliability scheduling		Jaya	7.7117E-6	3.2841E-4	7.5031E-4	1.3985E-4	8.8056E-5	4.5110E-5	1.0492E-4
		GA	7.7302E-6	3.4366E-4	7.5058E-4	2.2715E-4	8.9228E-5	4.8739E-5	1.0917E-4

where EIR means Energy Index of Reliability

3.3.2 85 Bus Distribution System

3.2.1.1 Scenario-1 (Cost minimization with EIR)

In this scenario, the objective function attempted is the minimization of the total operating cost of DGs in Multi-Microgrid System by maintaining EIR(τ) $\geq$ 0.97. The optimal scheduling of controllable DGs has been performed using Jaya Algorithm and Genetic Algorithm. The best solution of these algorithms is taken after making an exhaustive number of trails, and the obtained results are presented in Table-3.10 and Table-3.11. The voltage magnitude in P.U at each bus of modified 85 Bus Distribution System for various case studies using Jaya algorithm is depicted in Fig-3.9.

Table-3.10: Optimal DG values for various Case Studies in Scenario-1 using Jaya Algorithm for 85 Bus System considering Reliability criterion.

	Case-I	**Case-II**	**Case-III**	**Case-IV**	**Case-V**	**Case-VI**	**Case-VII**
$P_{G1}(kW)$	386.1260	-	-	232.1250	-	376.2050	319.4418
$P_{G2}(kW)$	100.0000	-	-	93.5108	-	100.0000	100.0000
$P_{G3}(kW)$	100.0000	-	-	260.2371	-	235.1577	251.0074
$P_{G4}(kW)$	-	368.1779	-	412.5637	541.0594	-	569.3347
$P_{G5}(kW)$	-	251.1934	-	245.8281	252.9407	-	243.1950
$P_{G6}(kW)$	-	300.0000	-	300.0000	299.9811	-	300.0000
$P_{G7}(kW)$	-	-	460.3552	-	371.6891	433.4469	370.8318
$P_{G8}(kW)$	-	-	310.8891	-	221.3820	314.7324	236.4167
$P_{G9}(kW)$	-	-	310.8878	-	365.5374	247.0919	323.9172
$P_{loss}(kW)$	3.1660	6.0113	9.1721	47.9449	66.2696	50.7138	144.8645
$Q_{loss}(kVAR)$	1.7933	2.4910	4.3905	27.1215	32.4606	31.6170	90.4103
Cost($/hr)	**25446.43**	**30627.02**	**46056.16**	**56396.32**	**76893.48**	**72932.33**	**105388.85**
VD (P.U)	2.1000E-5	1.0890E-5	2.8448E-5	5.9200E-4	3.7147E-4	6.1900E-4	1.5730E-3
EIR	0.9700	0.9713	0.9700	0.9700	0.9700	0.9700	0.9700
$P_{demand}(kW)$	582.96	913.36	1072.96	1496.32	1986.32	1655.92	2569.28
$Q_{demand}(kVAR)$	594.74	931.81	1094.64	1526.55	2026.45	1689.37	2621.19

It is clear from the test results that Jaya Algorithm has scheduled the DGs optimally such that the operating cost from Case-1 to Case-VII are 25446.43$/hr, 30627.02$/hr, 46056.16$/hr, 56396.32$/hr, 76893.48$/hr, 72932.33$/hr and 105388.85$/hr are minimum in contrast to 25457.58$/hr, 30627.46$/hr, 46075.99$/hr, 56417.12$/hr, 76901.19$/hr, 73056.51$/hr and 105484.55$/hr from Case-I to Case-VII respectively of Genetic Algorithm. Fig-3.9 outlines the convergence characteristics of Case-VII for Genetic Algorithm and Jaya Algorithm. It is clear from the convergence characteristics that Jaya Algorithm gives minimum cost than that of Genetic Algorithm.

The test results reveal that the DGs with lower values of Forced Outage Rate (FOR) are contributing more power output for meeting the load economically and vice-versa to satisfy the EIR criterion as against economic scheduling of DGs without EIR criterion presented in chapter-2. For illustration, the DGs (P_{G3}, P_{G5}, P_{G9}) with a higher value of FOR, have contributed less output power of 251.0074kW, 243.1950kW and 323.9172kW in Case-VII of this Scenario with Jaya algorithm as against 358.9201kW, 287.2758kW and 400.00kW output power in optimal scheduling of DGs without EIR criterion with Jaya Algorithm in Case-VII of Scenario-1 of Chapter-2 (i.e., Table-2.12 of Chapter-2). Similarly, DGs (P_{G2}, P_{G4}, P_{G8}) having a lower value of FOR have committed higher value of output power of 100.00kW, 569.3347kW and 236.4167kW in this scenario with Jaya Algorithm as against 100.00kW, 453.3466kW and 139.8869kW output power produced in economic scheduling without EIR criterion(i.e.,Table-2.12 of Chapter-2). Further, it is noticed that the operating cost for various case studies in this scenario is found to be on the higher side than that of operating cost obtained in Scenario-1 of Chapter-2. Even though, operating cost increased, this promises improved system operation even under the outage of a DG with higher FOR as its role is properly accounted in arriving at the optimal value of its output.

Table-3.11: Optimal DG values for various Case Studies in Scenario-1 using Genetic Algorithm for 85 Bus System considering Reliability criterion.

	Case-I	**Case-II**	**Case-III**	**Case-IV**	**Case-V**	**Case-VI**	**Case-VII**
$P_{G1}(kW)$	386.2732	-	-	227.3224	-	350.9605	304.7739
$P_{G2}(kW)$	99.9512	-	-	87.5000	-	99.9756	99.9756
$P_{G3}(kW)$	99.9023	-	-	249.9023	-	287.4023	274.0234
$P_{G4}(kW)$	-	368.1152	-	421.8750	540.0879	-	549.7559
$P_{G5}(kW)$	-	251.3290	-	257.8125	260.8643	-	266.4795
$P_{G6}(kW)$	-	299.9268	-	299.9268	299.9268	-	299.9268
$P_{G7}(kW)$	-	-	477.9053	-	374.5117	437.5000	375.0000
$P_{G8}(kW)$	-	-	302.2387	-	218.9031	312.5000	244.5313
$P_{G9}(kW)$	-	-	302.0508	-	358.4961	218.6523	299.1211
$P_{loss}(kW)$	3.1704	6.0110	9.2348	48.0190	66.4698	51.0707	144.3074
$Q_{loss}(kVAR)$	1.7958	2.4909	4.4267	27.1746	32.5694	31.8007	90.0787
Cost($/hr)	**25457.58**	**30627.46**	**46075.99**	**56417.12**	**76901.19**	**73056.51**	**105484.55**
VD (P.U)	2.0913E-5	1.0895E-5	2.6976E-5	5.6299E-4	3.5897E-4	6.4435E-4	1.5642E-3
EIR	0.9700	0.9713	0.9700	0.9700	0.9700	0.9700	0.9700
$P_{demand}(kW)$	582.96	913.36	1072.96	1496.32	1986.32	1655.92	2569.28
$Q_{demand}(kVAR)$	594.74	931.81	1094.6369	1526.55	2026.45	1689.3742	2621.19

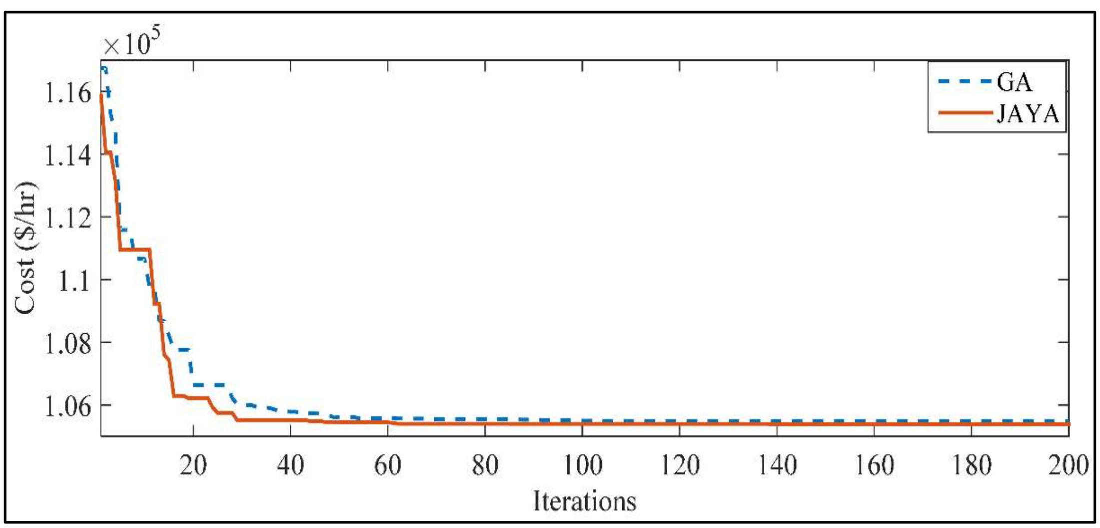

Fig-3.9: Convergence characteristics of Jaya Algorithm vs GA for Cost minimization as objective function for 85 Bus system Scenario-1 Case-VII with EIR

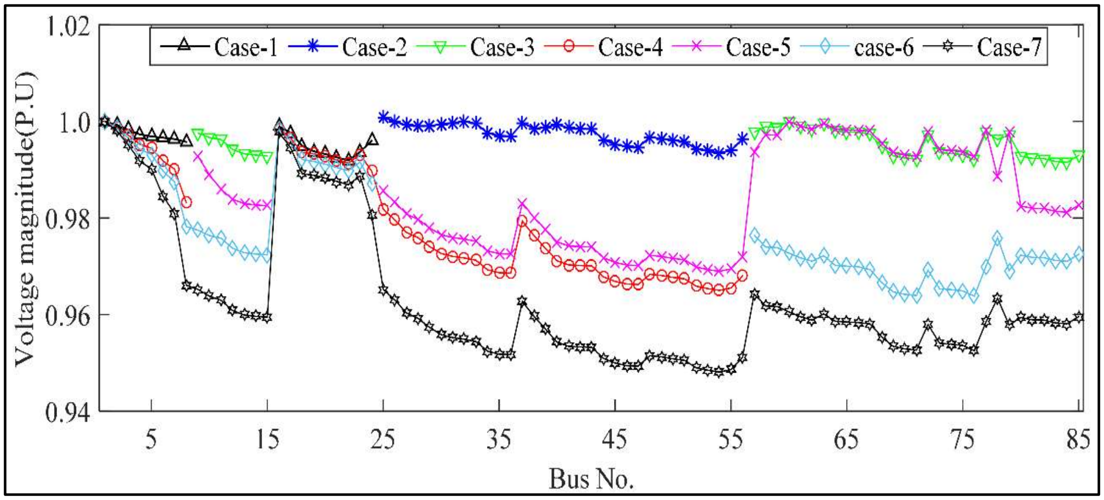

Fig-3.10: Voltage Magnitude(P.U) of 85 Bus system for various Cases of Scenario-1 using Jaya Algorithm with EIR

3.2.1.2 Scenario-2 (Loss minimization with EIR)

In this Scenario, power loss minimization in the system by maintaining $\tau \geq 0.97$ is considered as an objective function. Copious trails are attempted using Jaya Algorithm and Genetic Algorithm to determine the optimal output values of DGs for power losses minimization, and the obtained results are presented in Table-3.12 and Table-3.13. The Fig-3.11 illustrates the voltage magnitude at each bus of 33 Bus Distribution System under Scenario-2 for various case studies considered in the chapter.

Table-3.12: Optimal DG values for various Case Studies in Scenario-2 using Jaya Algorithm for 85 Bus System considering Reliability criterion.

	Case-I	**Case-II**	**Case-III**	**Case-IV**	**Case-V**	**Case-VI**	**Case-VII**
$P_{G1}(kW)$	386.1260	-	-	170.3709	-	185.0179	159.9057
$P_{G2}(kW)$	100.0000	-	-	100.0000	-	100.0000	100.0000
$P_{G3}(kW)$	100.0000	-	-	215.8563	-	279.7178	290.2189
$P_{G4}(kW)$	-	309.5439	-	436.8372	390.6778	-	398.0805
$P_{G5}(kW)$	-	309.5434	-	320.9764	388.2391	-	380.1173
$P_{G6}(kW)$	-	300.0000	-	300.0000	300.0000	-	300.0000
$P_{G7}(kW)$	-	-	401.8068	-	299.4523	423.7025	388.3179
$P_{G8}(kW)$	-	-	340.1189	-	336.1419	403.5649	391.2681
$P_{G9}(kW)$	-	-	340.1186	-	337.4713	313.7020	305.0239
$\boldsymbol{P_{loss}(kW)}$	**3.1660**	**5.7274**	**9.0843**	**47.7209**	**65.6623**	**49.7851**	**143.6522**
$Q_{loss}(kVAR)$	1.7933	2.3733	4.3322	27.0597	32.1633	31.0373	89.7943
Cost($/hr)	25446.43	30961.47	46234.53	56963.30	80032.12	74598.63	109885.60
VD (P.U)	2.1000E-5	1.1305E-5	3.4348E-5	4.5102E-4	3.7000E-4	4.2481E-4	1.2640E-3
EIR	0.9700	0.9700	0.9700	0.9700	0.9700	0.9700	0.9700
$P_{demand}(kW)$	582.96	913.36	1072.96	1496.32	1986.32	1655.92	2569.28
$Q_{demand}(kVAR)$	594.74	931.81	1094.64	1526.55	2026.45	1689.37	2621.19

It is apparent from the results that the DGs are more optimally scheduled with Jaya Algorithm than that of Genetic Algorithm. The active power losses obtained with Jaya Algorithm from Case-I to Case-VII are 3.165969kW, 5.727355kW, 9.084284kW, 47.720877kW, 65.662304kW, 49.785108kW and 143.652219kW which are minimum as compared to Genetic Algorithm active power losses of 3.170367kW, 5.728881kW, 9.085226kW, 47.778067kW, 65.892948kW, 49.787056kW and 143.919776kW from Case-I to Case-VII respectively.

The convergence characteristics exhibited by Jaya Algorithm and Genetic Algorithm are presented in Fig-3.11. It is evident from the convergence characteristics that the GA has resulted in premature convergence with higher values of Active power losses. The Jaya Algorithm has yielded a better optimal solution for Active power losses. The voltage magnitudes in P.U at each bus in Microgrid(s) System are depicted in Fig-3.12 and from this figure, it is detectable that the voltage magnitudes are within the permissible limits of regulation limits of ±5%. Moreover, by sectionalizing the system, voltage profile has been improved for the given locations of DGs.

Table-3.13: Optimal DG values for various Case Studies in Scenario-2 using Genetic Algorithm for 85 Bus System considering Reliability criterion.

	Case-I	Case-II	Case-III	Case-IV	Case-V	Case-VI	Case-VII
$P_{G1}(kW)$	386.2732	-	-	118.9028	-	187.3233	152.0670
$P_{G2}(kW)$	99.9512	-	-	94.5313	-	99.5850	99.9756
$P_{G3}(kW)$	99.9023	-	-	249.9023	-	274.7070	299.9023
$P_{G4}(kW)$	-	309.8145	-	468.7500	300.0000	-	300.0000
$P_{G5}(kW)$	-	309.3477	-	312.3779	390.6250	-	437.5000
$P_{G6}(kW)$	-	299.9268	-	299.6338	299.9268	-	293.7012
$P_{G7}(kW)$	-	-	406.1279	-	406.2500	419.1895	380.2490
$P_{G8}(kW)$	-	-	338.5150	-	355.5088	406.2500	500.0000
$P_{G9}(kW)$	-	-	337.4023	-	299.9023	318.6523	249.8047
$\boldsymbol{P_{loss}(kW)}$	**3.1704**	**5.7289**	**9.0852**	**47.7781**	**65.8929**	**49.7871**	**143.9198**
$Q_{loss}(kVAR)$	1.7958	2.3740	4.3338	27.0935	32.2757	31.0372	89.9057
Cost($/hr)	25457.58	30959.41	46230.73	57135.85	81573.04	74629.27	116927.80
VD (P.U)	2.0913E-5	1.1305E-5	3.3807E-5	4.3043E-4	3.5644E-4	4.2077E-4	1.2210E-3
EIR	0.9700	0.9700	0.9700	0.9700	0.9701	0.9700	0.9706
$P_{demand}(kW)$	582.96	913.36	1072.96	1496.32	1986.32	1655.92	2569.28
$Q_{demand}(kVAR)$	594.74	931.81	1094.64	1526.55	2026.45	1689.37	2621.19

As the DGs are forced to schedule optimally by maintaining EIR criterion, it is apparent from the test results that the DGs with higher values of FOR are scheduled to minimum power output in this scenario and vice-versa. For illustration, the DGs (P_{G2}, P_{G4}, P_{G8}) with lower values of FOR have contributed more output power of 100.00kW, 398.0805kW and 391.2681kW in Case-VII of this scenario with Jaya Algorithm as against 100.00kW, 372.0580kW and 292.3253kW output power produced in optimal scheduling of DGs without EIR criterion by Jaya algorithm in Scenario-2 (Table-2.14) of Chapter-2. Similarly, the DGs (P_{G3}, P_{G5}, P_{G9}) with higher FOR have supplied lower power outputs of 290.2189kW, 380.1173kW and 305.0239kW as against 306.9213kW, 397.2527kW and 382.5820kW output power produced in optimal scheduling of DGs without EIR in Scenario-2 (Table-2.14) of Chapter-2. From this, it is clear that the Jaya Algorithm has scheduled the DGs optimally for loss minimization objective by enforcing EIR criterion.

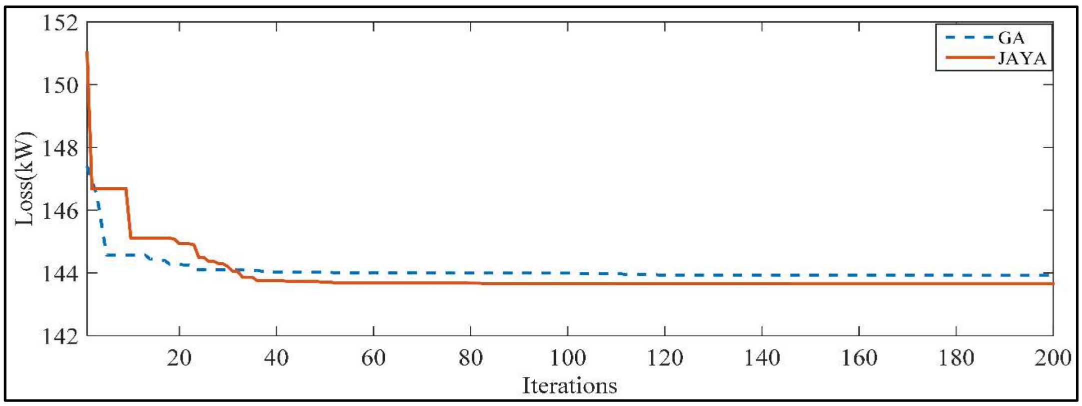

Fig-3.11: Convergence characteristics of Jaya Algorithm vs GA for Loss minimization as objective function for 85 Bus system Scenario-2 Case-VII with EIR

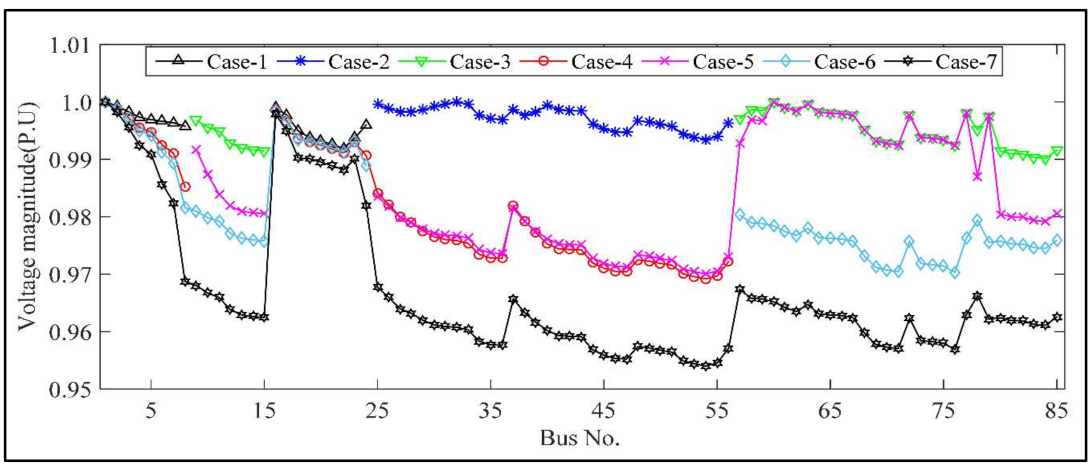

Fig-3.12: Voltage Magnitude(P.U) of 85 Bus system for various cases of Scenario-3 using Jaya Algorithm with EIR

3.2.1.3 Scenario-3 (Voltage Deviation minimization with EIR)

Voltage Deviation minimization has been contemplated in this scenario as an objective function by maintaining EIR greater than or equal to 0.97. The minimum Voltage Deviation values are obtained for various case studies by optimally scheduling the DGs outputs using Jaya Algorithm and Genetic Algorithm with numerous trails. The results obtained with the above algorithms are presented in Table-3.14 and Table-3.15.

Table-3.14: Optimal DG values for various Case Studies in Scenario-3 using Jaya Algorithm for 85 Bus System considering Reliability criterion.

	Case-I	Case-II	Case-III	Case-IV	Case-V	Case-VI	Case-VII
$P_{G1}(kW)$	386.3221	-	-	0.0328	-	0.0736	0.0302
$P_{G2}(kW)$	100.0000	-	-	43.7256	-	11.8896	1.5625
$P_{G3}(kW)$	99.8052	-	-	109.2773	-	12.7930	1.9531
$P_{G4}(kW)$	-	394.6044	-	594.5801	599.8535	-	306.8848
$P_{G5}(kW)$	-	224.9447	-	499.8779	497.9248	-	491.9434
$P_{G6}(kW)$	-	300.0000	-	299.9268	299.3408	-	293.9209
$P_{G7}(kW)$	-	-	500.0000	-	499.8779	497.4365	488.8916
$P_{G8}(kW)$	-	-	291.1472	-	75.5006	793.5547	747.4609
$P_{G9}(kW)$	-	-	291.1472	-	87.0117	399.6094	390.4297
$P_{loss}(kW)$	3.1673	6.1891	9.3344	51.1005	73.1894	59.4368	153.7971
$Q_{loss}(kVAR)$	1.7940	2.5646	4.4828	29.1500	36.1942	36.4148	95.7073
Cost($/hr)	25449.97	30694.78	46139.13	64124.40	85958.07	104733.68	139567.68
VD (P.U)	**2.0861E-5**	**1.0846E-5**	**2.5300E-5**	**1.5991E-4**	**7.7422E-5**	**9.2316E-5**	**5.8569E-4**
EIR	0.9700	0.9718	0.9700	0.9702	0.9704	0.9746	0.9719
$P_{demand}(kW)$	582.96	913.36	1072.96	1496.32	1986.32	1655.92	2569.28
$Q_{demand}(kVAR)$	594.74	931.81	1094.64	1526.55	2026.45	1689.37	2621.19

From the results, it is noticeable that the Jaya Algorithm is providing minimum Voltage Deviation of 2.0861E-05P.U, 1.0846E-05P.U, 2.5300E-05P.U, 1.5991E-04P.U, 7.7422E-05P.U, 9.2316E-05P.U, 5.8569E-04P.U from Case-I to Case-VII as against 2.0976E-05P.U, 1.0851E-05P.U, 2.5344E-05P.U, 3.5345E-04P.U, 3.6163E-04P.U, 1.9711E-04P.U and 8.8121E-04P.U from Case-I to Case-VII using Genetic Algorithm.

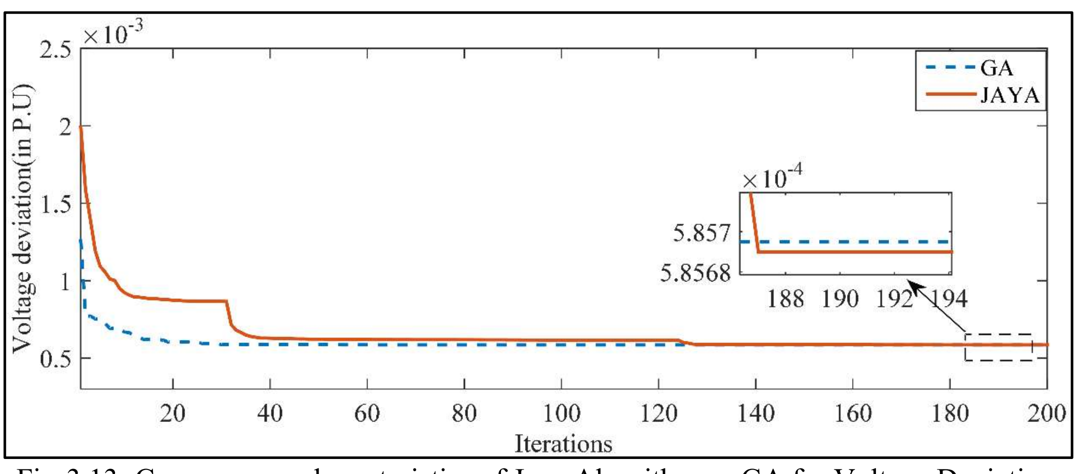

Fig-3.13: Convergence characteristics of Jaya Algorithm vs GA for Voltage Deviation minimization as objective function for 85 Bus system Scenario-3 Case-VII with EIR

The convergence characteristics of Case-VII for Jaya Algorithm and Genetic Algorithm are depicted in Fig-3.13. From the convergence characteristics, it is evident that

Jaya Algorithm provides minimum Voltage Deviation value than Genetic Algorithm, however, the order of comparison is in the range of 10^-4 P.U. Fig-3.14 illustrates the voltage magnitude at each bus of 85 Bus Distribution System under Scenario-3 for various case studies formulated. This figure reveals that operating of Distribution system as Multi-Microgrid System improves the voltage profile at all the Buses in the system.

Table-3.15: Optimal DG values for various Case Studies in Scenario-3 using Genetic Algorithm for 85 Bus System considering Reliability criterion.

	Case-I	**Case-II**	**Case-III**	**Case-IV**	**Case-V**	**Case-VI**	**Case-VII**
$P_{G1}(kW)$	386.2487	-	-	156.3411	-	47.5420	41.7762
$P_{G2}(kW)$	99.9756	-	-	38.2762	-	9.4309	81.6550
$P_{G3}(kW)$	99.9023	-	-	121.8358	-	214.2460	174.6274
$P_{G4}(kW)$	-	394.7754	-	582.3593	285.3838	-	343.5898
$P_{G5}(kW)$	-	224.8483	-	416.3399	452.0249	-	485.6642
$P_{G6}(kW)$	-	299.9268	-	230.0187	226.8101	-	280.5171
$P_{G7}(kW)$	-	-	499.8779	-	462.9692	343.7834	269.0382
$P_{G8}(kW)$	-	-	291.9878	-	433.7144	741.5712	734.2474
$P_{G9}(kW)$	-	-	290.4297	-	191.5843	352.9490	304.4805
$P_{loss}(kW)$	3.1667	6.1904	9.3354	48.8512	66.1666	53.6026	146.3157
$Q_{loss}(kVAR)$	1.7936	2.5652	4.4831	27.7247	32.3780	32.9519	91.1088
Cost($/hr)	25448.33	30695.83	46166.17	60840.06	88569.86	96584.11	134890.90
VD (P.U)	**2.1000E-5**	**1.0851E-5**	**2.5344E-5**	**3.5345E-4**	**3.6163E-4**	**1.9711E-4**	**8.8121E-4**
EIR	0.9700	0.9718	0.9700	0.9705	0.9715	0.9733	0.9723
$P_{demand}(kW)$	582.96	913.36	1072.96	1496.32	1986.32	1655.92	2569.28
$Q_{demand}(kVAR)$	594.74	931.81	1094.64	1526.55	2026.45	1689.37	2621.19

The voltage magnitudes in P.U at different buses of 85 Bus System for Case-VII of Scenario-1, Scenario-2, Scenario-3 and Base Case study are compared and depicted in Fig-3.15. From the voltage magnitude comparison plot, it is apparent that the voltage magnitudes are improved at all the buses of Multi-Microgrid System for Voltage Deviation minimization scenario as against other scenarios. The minimum value of voltage magnitudes noticed in Base case, Scenario-1, Scenario-2 and Scenario-3 are 0.873309P.U, 0.95012P.U, 0.95401P.U and 0.96027P.U respectively at Bus 54. The minimum voltage magnitude in P.U, noticed in the Base case, is below the Voltage Deviation limits of ±5%. Thus, it is necessary to operate the Multi-Microgrid System in other scenarios rather than Base case.

Table-3.16 illustrates the EIR value for optimal scheduling of DGs for cost minimization, loss minimization and Voltage Deviation minimization as objectives with and without consideration of EIR as a criterion. The EIR values for optimal scheduling of DGs without EIR criterion (test results presented in Table-2.12 to Table-2.16 of chapter-2) have

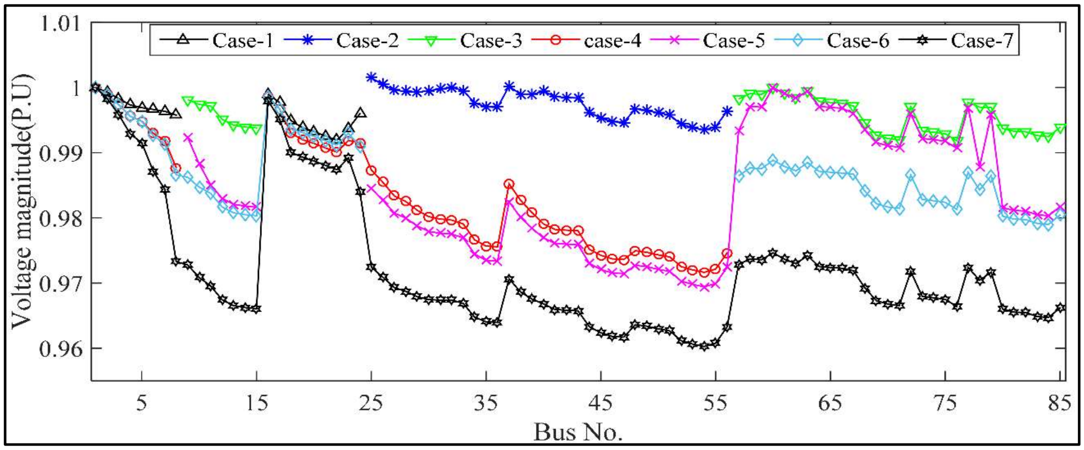

Fig-3.14: Voltage Magnitude(P.U) of 85 Bus system for various cases of Scenario-3 using Jaya Algorithm with EIR

been evaluated by considering the DGs power output. It can be noticed from the above table that by incorporating EIR criterion, the DGs have been scheduled optimally so as to satisfy the EIR criterion along with minimization of the desired objective function. It has been analyzed from the Table-3.17 that, with the consideration of reliability criterion, the Operating cost, System Active power losses and Voltage Deviation values have been increased. However, improved system operation has been promised even under the outage of a DG with higher FOR as its role is promptly accounted in arriving at the optimal value of its output.

Table-3.16: Comparison of EIR values for Optimal Scheduling of DGs with and without Reliability criterion for various scenarios for 85 Bus System

Case Studies	**Optimal Scheduling without EIR**						**Optimal Scheduling with EIR (τ ≥0.97)**					
	Cost minimization		Loss minimization		Voltage Deviation minimization		Cost minimization		Loss minimization		Voltage Deviation minimization	
	EIR values											
	GA	**Jaya**	**GA**	**Jaya**	**GA**	**Jaya**	**GA**	**Jaya**	**GA**	**Jaya**	**GA**	**Jaya**
Case-I	0.9660	0.9664	0.9668	0.9668	0.9649	0.9649	0.9700	0.9700	0.9700	0.9700	0.9700	0.9700
Case-II	0.9713	0.9713	0.9682	0.9683	0.9718	0.9718	0.9713	0.9713	0.9700	0.9700	0.9718	0.9718
Case-III	0.9661	0.9661	0.9682	0.9682	0.9660	0.9660	0.9700	0.9700	0.9700	0.9700	0.9700	0.9700
Case-IV	0.9694	0.9694	0.9682	0.9682	0.9703	0.9710	0.9700	0.9700	0.9700	0.9700	0.9705	0.9702
Case-V	0.9686	0.9685	0.9684	0.9682	0.9689	0.9690	0.9700	0.9700	0.9700	0.9701	0.9715	0.9704
Case-VI	0.9700	0.9654	0.9701	0.9680	0.9746	0.9746	0.9700	0.9700	0.9700	0.9700	0.9733	0.9746
Case-VII	0.9682	0.9677	0.9685	0.9696	0.9729	0.9719	0.9700	0.9700	0.9700	0.9706	0.9723	0.9719
EIR = Energy Index of Reliability												

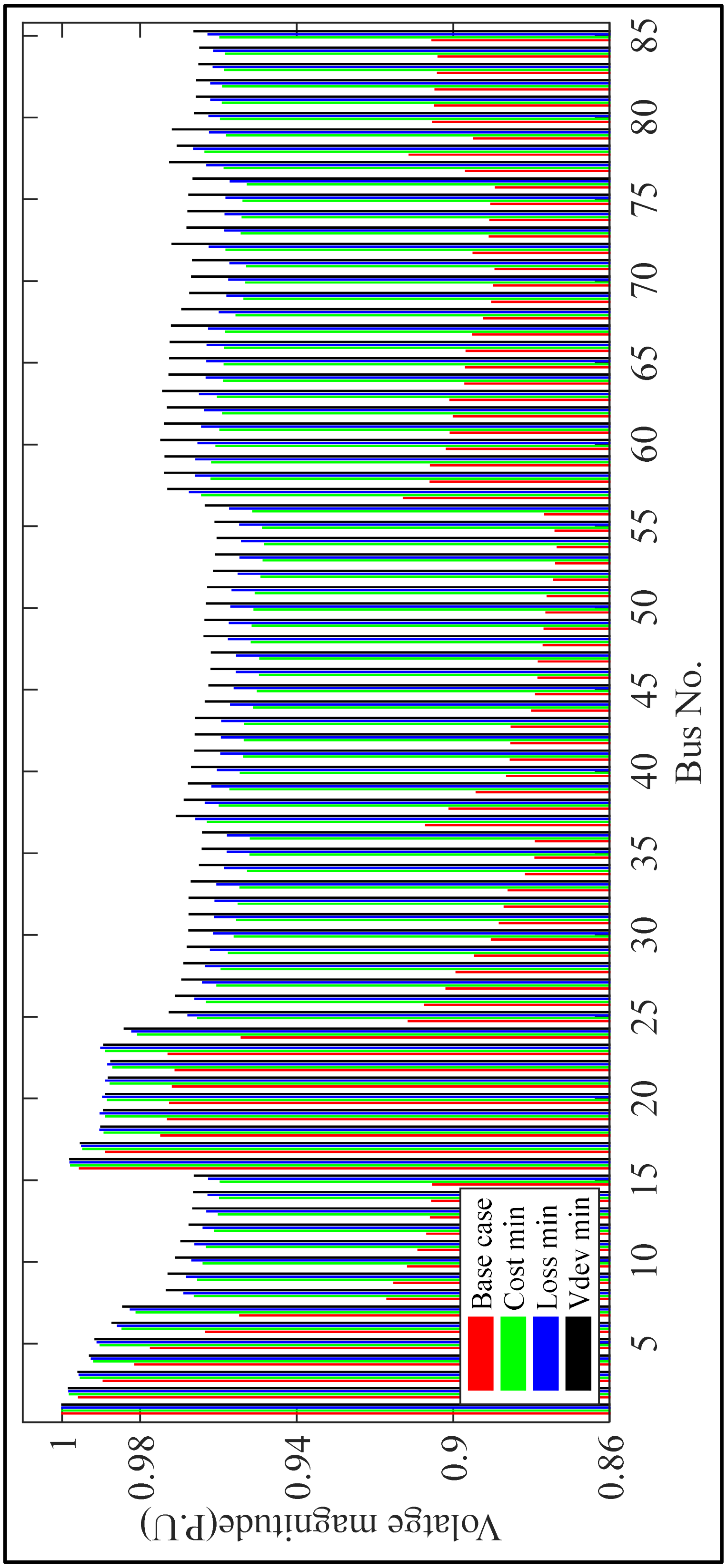

Fig-3.15: Voltage Magnitude(P.U) of 85 Bus Distribution System for different Scenarios using Jaya Algorithm with EIR and Base case Load flows

Table-3.17: Comparison of Cost, Loss and Voltage Deviation with and without Reliability criterion for various Case Studies for 85 Bus System

			Case-I	Case-II	Case-III	Case-IV	Case-V	Case-VI	Case-VII
Cost ($/hr)									
Economic scheduling	**Cost minimization**	**Jaya**	23840.38	30627.02	43449.32	56323.14	75924.69	68248.23	103099.16
		GA	23849.92	30627.49	43450.85	56323.68	75929.71	73297.60	103395.19
Reliability scheduling		**Jaya**	25446.43	30627.02	46056.16	56396.32	76893.48	72932.33	105388.85
		GA	25457.58	30627.46	46075.99	56417.12	76901.19	73056.51	105484.55
Active Power Loss (kW)									
Economic scheduling	**Loss minimization**	**Jaya**	2.5480	5.5896	9.0607	47.4669	65.8098	49.7136	142.3745
		GA	2.5480	5.5906	9.0607	47.4673	65.8160	49.8008	143.6402
Reliability scheduling		**Jaya**	3.1660	5.7274	9.0843	47.7209	65.6623	49.7851	143.6522
		GA	3.1704	5.7289	9.0852	47.7781	65.8929	49.7871	143.9198
Voltage Deviation (P.U)									
Economic scheduling	**VD minimization**	**Jaya**	3.1245E-6	1.0846E-5	2.0877E-5	1.5709E-4	7.3850E-5	9.0958E-5	5.9473E-04
		GA	3.1277E-6	1.0851E-5	2.0892E-5	1.6503E-4	7.4015E-5	9.9281E-5	6.1097E-4
Reliability scheduling		**Jaya**	2.0861E-5	1.0846E-5	2.5300E-5	1.5991E-4	7.7422E-5	9.2316E-5	5.8569E-4
		GA	2.1000E-5	1.0851E-5	2.5344E-5	3.5345E-4	3.6163E-4	1.9711E-4	8.8121E-4

3.4 Summary

In summary, in this chapter, similar to the previous chapter, the independent Distribution System is sectionalized into self-adequate Microgrids. On sectionalization, the DGs are optimally scheduled to accomplish the desired objectives. Single objective optimization problem has been focused in this chapter. The objectives tackled in this research work are: a) Minimization of Operating cost of DGs, b) Minimization of Active power losses and c) Minimization of system Voltage Deviation. Among the three objective functions, only one of the objective functions is attempted to optimize at a time. Energy Index of Reliability (EIR) has been incorporated as a criterion while optimally scheduling the DGs in all the cases of objective functions along with the enforcement of equality and inequality constraints.

Jaya Algorithm, which is free from algorithm-specific parameters, has been used for optimal scheduling of Micro-sources. The superiority of Jaya Algorithm has been assessed by validating the obtained results for various case studies of Scenario-1, Scenario-2 and Scenario-3 of single-objective optimization by comparing with the Genetic Algorithm. It is evident from the test results of Scenario-1, Case-VIII that the operating cost obtained by Jaya Algorithm is 213372.95$/hr, which is optimum in comparison to that of 228486.69$/hr attained with GA for 33 Bus Distribution System. Also, it is noticeable from the Table-3.2 and Table-3.3 that the EIR value is maintained as $\tau \geq 0.97$ in both the cases. In case of 85 Bus Distribution System, the operating cost achieved by Jaya Algorithm and GA are 105388.85$/hr and 105484.55$/hr respectively. It is perceptible from these test results that Jaya Algorithm produces optimum results.

The Active power losses attained with Jaya Algorithm and GA are 75.3645kW and 75.4144kW respectively for Case-VII of Scenario-2 for 33 Bus Distribution System whereas for 85 Bus Distribution system, the Active power losses are identifies as 143.6522kW and 143.9188kW using Jaya Algorithm and GA respectively for Scenario-2 and Case-VII. It is apparent from these test results that Jaya Algorithm provides optimum values.

In all the case studies of various scenarios, it is noticed that the proposed Jaya Algorithm has outperformed. Further, it is observed that the objective function values for various scenarios and case studies obtained with incorporation of EIR criterion have increased slightly from that of economic scheduling of Micro-Sources without EIR criterion which have been addressed in the Chapter-2 above(Reference Table-3.17). Though the objective function values have raised, but with EIR criterion, the chance of erratic power supply to customer has been minimizes. *A part of the work is published in "9th National Power Electronics Conference (NPEC), National Institute of Technology Tiruchirappalli, Tamilnadu, India, 2019.*

In the above chapters, preference is given to only one of the objective functions at a time. It is observed that a better solution for the selected single objective function requires a compromise in other objectives. What degree of compromise is to be allowed may not be known to the System Operator. An analytical approach would go as a supporting tool to address this aspect. Considering this as a driving source, a Multi-Objective Optimization problem has been formulated in the next chapter to get the best trade-off solution among various objectives, which is essential in a real-world scenario.

CHAPTER-4

Multi-Objective Optimization for Optimal Scheduling of Micro-Sources in Multi-Microgrid System with and without Reliability Constraint

4.1 Introduction

In the previous chapters of this thesis, optimal scheduling of controllable DGs have been performed considering any one of the objective functions among Cost minimization, Loss minimization and Voltage Deviation minimization at a time, which is called single objective optimization problem. When an optimization problem involves more than one objective function, the task of finding one or more optimal solutions is called Multi-Objective Optimization (MOO). In this chapter, two objective functions among the three objectives defined above are considered at a time to obtain the solution. Since more than one objective function is considered at a time, an unique solution for MOO is not possible. A set of solutions for MOO is named as Pareto optimal solution set. Among the Pareto optimal solution set, based on the priority of the objective function, one solution shall be considered as the best solution, which is called as Best Compromised Solution (BCS) among the Pareto front.

4.2 Multi-Objective Optimization

Mr.Vilfredo Pareto[68] has introduced the concept of Multi-Objective Optimization (MOO). MOO alludes to determining the optimal solution set for two or more conflicting objectives. The advantage of using MOO is that it does not require to solve complicated equations, thus simplifies the problem [66]. Making decision on MOO allows for compromise on other contradictory objectives. Assume a Decision-maker wants to optimize *n* objectives which are non-commensurable and with no preference of objective concerning other objectives. Considering that there are *n* objectives of minimization category, the MOO is then expressed as per Equation-(4.1) subjected to equality and inequality constraints as defined in Equation-(4.2) and Equation-(4.3) respectively [68].

$$Minimize\ F(x) \tag{4.1}$$

$$\text{Subjected to:}\ \ g_j(x) \le 0 \qquad j = 1,2,3 \dots .J \tag{4.2}$$

$$h_k(x) = 0 \qquad k = 1,2,3 \dots .K \tag{4.3}$$

$$F(x) = \{\, f_1(x), f_2(x), \dots f_i(x) \dots\ f_n(x)\} \tag{4.4}$$

$$x = \left\{x_1, x_2, x_3, \dots . x_p\right\} \tag{4.5}$$

where $F(x)$ is the set of objective functions of *n*-dimensions as per Equation-(4.4), $g_j(x)$ is j^{th} inequality constraint evaluated at x ; $h_k(x)$ is k^{th} equality constraint evaluated at x ; $f_i(x)$ is i^{th} objective function evaluated at x; *n* represents the number of objective functions;

x, as expressed in Equation-(4.5), is the control variable vector of p-dimension; The control vector $\hat{x} \epsilon \boldsymbol{X}$ must be in the feasible region of the search space bounded by the equality and the inequality constraints. There will be situations in seldom that an optimum solution $\hat{x}$ is common to all the objective functions such that $\hat{x} \epsilon \boldsymbol{X}$. Thus, the solutions of Multi-Objective Optimization problems in the absence of precedence to any particular objective are compared with the notion of Pareto dominance.

In general, for an optimization problem of minimizing all the objectives, a solution $\hat{x} \epsilon \boldsymbol{X}$ is Pareto-optimal if it satisfies two conditions [69]:

(i) These is no other x ϵ $\boldsymbol{X}$ such that $f_i(x) \leq f_i(\hat{x})\ \forall\, i \in \{1,2, \dots n\}$ and

(ii) $\hat{x}$ is strictly better than x for at least any $i \in \{1,2, \dots n\} \ni\ f_i(\hat{x}) < f_i(x)$.

The set of solutions for a MOO is referred to as Pareto-optimal solution set or Pareto-front. In this chapter, MOO problem has been formulated as: (a) Simultaneous minimization of Operating cost of DGs generation and Active power losses in Microgrid(s), (b) Minimizing Active power losses and Voltage Deviation simultaneously and (c) Minimization of Operating cost of DGs and Voltage Deviation, concurrently the EIR is maintained as $\tau \geq 0.97$ for all the Multi-Objective Optimizations.

4.3 Implementation Procedure for Multi-Objective Optimization using Jaya Algorithm

Jaya Algorithm, which was described in the section-2.4 of the chapter-2, is suitable for solving single-objective optimization problems. However, for solving the Multi-Objective Optimization (MOO) problem using Jaya Algorithm, posterior version of the same, which is developed by Prof.R.Venkat Rao, known as Multi-Objective Jaya Algorithm (MOJA)[61] is exercised. Non-dominated Sorting approach and Crowding Distance evaluation methodology have been embedded in Multi-Objective Jaya Algorithm for effective and efficient handling of MOO problems. The Crowding Distance (CD), a popularly known operator, whose value of a solution provides an estimate of the density of solutions surrounding that solution. It is mostly used in solving MOO problem in the literature [70][71][72]. The advantage of calculation of Crowding Distance has been illustrated in [70].

In Multi-Objective-Jaya-Algorithm (MOJA), the Best solution and the Worst solution candidates will be evaluated based on the Non-dominance rank and the Crowding

Distance of the solution set. The candidate with the highest rank (rank=1) and larger value of Crowding Distance is specified as the Best solution candidate. Similarly, the candidate with the lowest rank and least value of Crowding Distance is identified as the Worst solution candidate. Upon evaluation of the Best and the Worst solution candidates, the updation of the candidate is similar to that of the *Update Phase* as described in Section 2.4.2. Upon updating all the candidates, the updated candidates are pooled with the initial candidates, thus the total size of candidates becomes $2P_{size}$. Non-dominance ranking and Crowding Distance will be evaluated for $2P_{size}$ to select P_{size} good solutions for the next generation[61].

4.3.1 Non-dominated Sorting

The Non-dominant solution is a solution, which is not dominated by any solution in the P_{size} solution set. In the Non-dominated sorting approach, the population is sorted into several fronts based on dominance. The solution is said to be Non-dominance if and only if, it satisfies the two conditions (i) and (ii) stated in section-4.2 above. Rank one will be assigned to all such Non-dominated solutions identified in first sorting and designated as the first front. These solutions which are in the first front are deleted from P_{size} solution set and the remaining solutions are sorted again until all the solutions in P_{size} are assigned a rank and fronts will be formed [69][61]. The step by step procedure for Non-dominated sorting is as follows[70]:

1. Assume that the total number of solutions be P.
2. Initialize domination counter $n_p = 0$;   // where n_p indicates the number of solutions which dominate the solution $p \epsilon P$.
3. Initialize $S_p = \phi$;   // where S_p is a set of solutions dominated by p and ϕ is null set.
4. Check
   - (a) whether solution p dominates other solutions q,
   - (b) If p dominates q, add q to S_p
   - (c) If q dominates p, increment dominator counter (n_p) by one.
   - (d) Check the dominator counter value of p.
   - (e) $n_p = 0$ indicates no. of solutions dominated p is zero, thus assign its rank as 1.
   - (f) Add the solution p to the vector indicating Front with rank-1($\mathcal{F}_1$).

The above steps can be written as follows:

```
For each p ϵ P                 // solution p belongs to P
 S_p = ϕ                       // set S_p as null set
  n_p = 0;                     // initialize n_p to zero
   For each q ϵ P              // solution q belongs to P
     If ( p ≺ q )              // if p dominates q,
        S_p = S_p ∪ {q}        // then add q to S_p
     else if ( q ≺ p )         // if q dominates p,
        n_p = n_p + 1          // then increment domination counter n_p
   End                         // End of q loop
Check if n_p = 0               // indicates no. of solutions dominated p is zero
     p_rank = 1                // Assign rank of p as 1.
     F_1 = F_1 ∪ {p}           // Add p to the F_1
End                            // End of p loop
```

5. Evaluate the solutions in higher rank Fronts

   a) Set front counter $i = 1$.

   b) Initialize $Q = \phi$, where Q stores the set of solutions in $i + 1$ front

   c) For each p from $\mathcal{F}_i$, retrieve a solution q from S_p.

   d) Reduce the domination counter of solution q by one.

   e) If $n_q = 0$, store q in Q .

   f) Increment front counter $i = i + 1$;

   g) Move set of solution in Q to $\mathcal{F}_i$

   h) Goto Step-5(b) until $\mathcal{F}_i = \phi$;

   The above steps can be written as follows:

```
i = 1                          // i indicates front counter
while F_i ≠ ϕ                  // condition for loop counter
  Set Q = ϕ                    //Q is used for storing solutions in i + 1
                               // front, initialized as null set
 For each p ϵ F_i              // solution p belongs to F_i
     For each q ϵ S_p          // retrieving solution q
        n_q = n_q − 1          // decrement domination counter of q^th solution
        If n_q = 0             // checking domination counter
          q_rank = i + 1       // assign rank of q^th solution as i + 1
          Q = Q ∪ {q}          // add q to solution set Q
       End                     // End of if loop
```

End // End of q^{th} for loop
End // End of p^{th} for loop
$i = i + 1$ // increment front counter
$\mathcal{F}_i = Q$ // move solution set Q into Front $\mathcal{F}_i$

4.3.2 Crowding Distance calculation

Each and every solution in the P_{size} solution set is assigned with a Crowding Distance with an aim to determine the density of solutions around each solution. The average distance between two other solutions on either side of a solution for each objective function is called Crowding Distance. The procedure for evaluation of Crowding Distance for each solution in the front is as follows[61].

Step-1: Evaluate number of solutions l in each front $\tilde{F}$ and set initial Crowding Distance of solution p as $CD_p = 0$.

Step-2: Sort the solution set in ascending order of objective function $f_i(x)$ for each *i*, $i \in \{1,2, \dots n\}$.

Step-3: Assign Crowding Distance of boundary solutions as infinity i.e., $CD_1 = \infty \; and \; CD_l = \infty$ in each front and for all other solutions in the front i.e., j = 2 to (*l*-1), evaluate Crowding Distance using Equation-(4.6).

$$CD_j = CD_j + \frac{f_i^{j+1} - f_i^{j-1}}{f_i^{max} - f_i^{min}} \quad \forall \, i \in \{1,2,3, \dots n\} \tag{4.6}$$

where *j* is the solution in the sorted list, *n* is number of objective functions, f_i is the objective function value of the i^{th} objective, f_i^{max} and f_i^{min} are the maximum and minimum values of the i^{th} objective function respectively.

4.3.3 Fuzzy Decision-Making Method

The Pareto front generated using Non-dominated sorting and Crowding Distance method will have a large set of solutions. Mathematically, all the solutions in the Pareto optimal sets are of non-dominated and none of the solutions has precedence over other solution. From a specific point of view, all the solutions are optimal and no solution can be identified as an optimal in any perspective. Thus, the difficulty is emanated for the decision-maker to find the Best Compromised Solution (BCS) from the set of solutions. For this purpose, the Fuzzy-set based approach and Min-Max approach are the two common methods generally used in the literature [73]. In this paper, the Fuzzy-set based approach is opted for selecting the Best Compromise Solution. According to the Fuzzy-set theory, linear membership function is defined for each objective function. If the objective function is monotonically decreasing, the following membership function[74] defined in the Equation-(4.7) is used.

$$\mu_i^{\eta} = \frac{f_i^{max} - f_i^{\eta}}{f_i^{max} - f_i^{\eta}} \tag{4.7}$$

where $f_i^{min}$and f_i^{max} are the minimum and maximum values of the i^{th} objective function respectively and f_i^{η} is objective function value of η^{th} non-dominated solution in i^{th} objective function. The normalized membership function of η^{th} non-dominated solution in the objective space is defined as per Equation-(4.8).

$$\mu^{\eta} = \frac{\sum_{i=1}^{N_f} \alpha_i \mu_i^{\eta}}{\sum_{\eta=1}^{N_p} \sum_{i=1}^{N_f} \alpha_i \mu_i^{\eta}} \tag{4.8}$$

Here α_i is weight coefficient of i^{th}objective function, N_f is the number of objective functions, N_p is the number of non-dominated solutions and μ^{η} is normalized membership value. The weight coefficient of a particular objective will be chosen by the Decision Maker based on his preference to that particular objective function. The maximum membership value of a particular solution is considered as the Best Compromised Solution (BCS) among the Pareto set as per the Fuzzy Decision-making theory.

The flowchart for optimal scheduling of DGs for MOO using MOJA is depicted in Fig-4.1. The implementation procedure of MOJA is explained as follows.

4.4 Algorithm for Implementation of Multi-Objective Optimization using Jaya Algorithm

1. Read input data i.e., number of Buses, number of lines, Bus Data, Line Data, number of generators (N_{gen}), locations of DGs, fuel cost coefficients of generators, lower and upper limits for generators output, EIR criterion value ($EIR_{criterion}$) etc.
2. Read Jaya algorithm data: population size (P_{size}), number of iterations/generations ($iter_{max}$).
3. Select the active Microgrid(s) among MG1, MG2 and MG3 based on case study.
4. Select the two objective functions among Operating cost minimization or Active power loss minimization or Voltage Deviation minimization considered for simultaneous minimization.

5. Initialize candidate solution ($X_{i,j,k}$). Check for lower and upper limits of each generator output of all candidate solutions.

$$X_{i,j,k} = \{P_{i,j,1}\, P_{i,j,2} \dots \dots .\, P_{i,j,\mathrm{k}})$$
$$where\ i \in \{1,2, ..\, iter_{max}\}, j \in \{1,2,3 \dots P_{size}\}\ and\ k \in \{1,2,3 \dots N_{gen}\}$$

6. Run Distribution System load flows. Evaluate voltage magnitude at each bus, line losses in the system satisfying equality, inequality constraints.
7. Evaluate total Operating cost of DGs, total Active power losses in the system and Voltage Deviation based on scenario opted.
8. Calculate for EIR (EIR_{calc}) value.
9. Calculate fitness for each candidate solution.

$$fitness = \frac{1}{1 + objective\ function\ value}$$

   if (EIR_{calc}<$EIR_{criterion}$), $fitness = 0$.
10. Apply Non-dominant Sorting and Crowding Distance approach as per Equation-(4.6) for evaluation of rank for each candidate solution.
11. Select the candidate with highest rank (rank=1) and larger value of Crowding Distance as Best Candidate Solution and lowest rank and least value of Crowding Distance as Worst Candidate Solution.
12. Set iteration count = 1.
13. Update the candidates mentioned in *Update Phase*, using Equation-(2.9)
14. Merge the updated solutions with initial solutions. With this, the total number of solutions becomes $2P_{size}$. Again, evaluate the fitness of all candidate solutions and apply Non-dominated sorting & Crowding Distance for selecting the P_{size} solutions among $2P_{size}$ for next generation based on higher rank and larger value of Crowding Distance.
15. Increment the iteration count. Repeat steps (13) and (14) until convergence criterion is satisfied.
16. Upon above steps, plot pareto-front of Non-dominated solution set.
17. Apply Fuzzy Decision-making method as per Equation-(4.7) and Equation-(4.8) for obtaining Best Compromised Solution among the set of solution in the front based on priority given by the Decision-maker to various objective functions (α_i).
18. Stop the program and print the Non-dominated solution front with Best Compromised Solution.

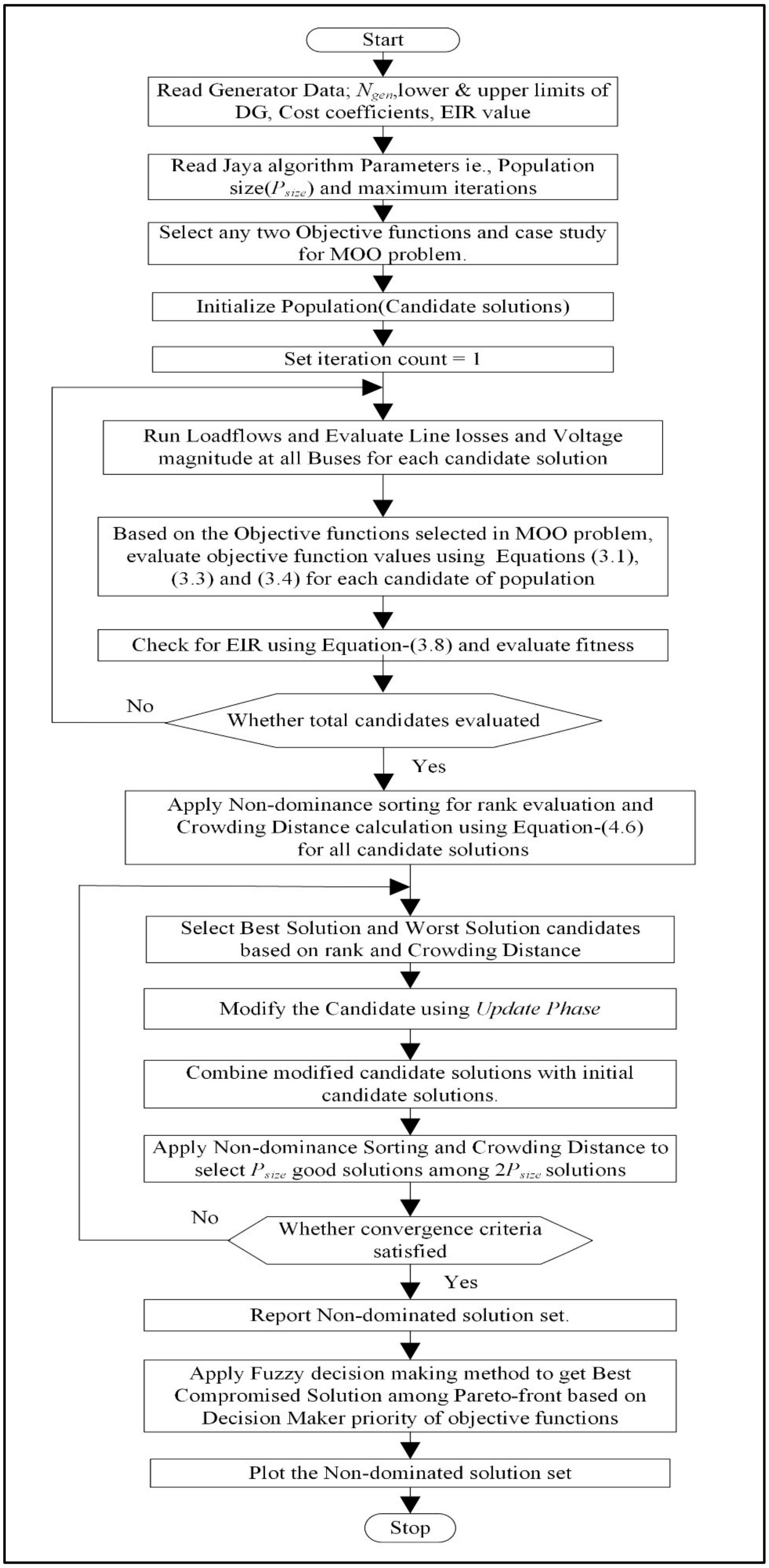

Fig-4.1: Flowchart of scheduling of DGs optimally using Jaya Algorithm considering Multi-Objective Optimization

4.5 Results and Discussion

In this section, the Pareto optimal fronts obtained by Multi-Objective Optimization (MOO) using Jaya Algorithm considering two objective functions at a time have been depicted. Non-dominated sorting and Crowding Distance concepts have been applied for evaluation of Pareto-front for the different case studies. Among the Pareto optimal, the Best Compromised Solution (BCS) has been evaluated using Fuzzy Decision-making approach described above, giving equal weightage to both the objective functions. The methodology of MOO has been tested on the modified IEEE 33 Bus Distribution System and Indian Practical 85 Bus Distribution System. It is evident from the test results reported in chapter-2 and chapter-3 that the Jaya Algorithm is superior in scheduling the controllable DGs optimally for attaining the desired objective function. Thus, in this chapter, only Jaya Algorithm has been used for optimal scheduling of controllable DGs for solving the MOO problem. Initially, MOO has been solved without considering EIR criterion and later-on, extended the MOO with EIR criterion maintaining $\tau \geq 0.97$. The following three Scenarios are formulated for both the test systems.

Scenario-A : Simultaneous minimization of Total Operating Cost and Active Power Losses

Scenario-B : Simultaneous minimization of Total Operating Cost and Voltage Deviation

Scenario-C : Simultaneous minimization of Active Power Losses and Voltage Deviation

4.5.1 Multi-Objective Optimization without considering EIR criterion on a modified 33 Bus Distribution System

In this section, as described in Section-2.2 of chapter-2, the modified 33 Bus Distribution System is sectionalized into Multi-Microgrid System. Different Scenarios are articulated as described above and under each Scenario, various case studies are formulated as presented in Table-2.5 of chapter-2. The optimal scheduling has been performed without considering EIR criterion in this section. The obtained results for various scenarios of the modified 33 Bus Distribution System upon the formulation of Multi-Microgrid System are as follows.

4.5.1.1 Scenario-A: Simultaneous minimization of Total Operating Cost and Active Power Losses

Simultaneous minimization of Total Operating cost of controllable DGs and Active Power losses of the system has been considered as an objective function in this scenario. Fig-4.2 presents the Pareto-optimal solution set for simultaneous minimization of operating cost of DGs and Active Power losses for various case studies by adopting Non-dominated sorting and Crowding Distance methodology.

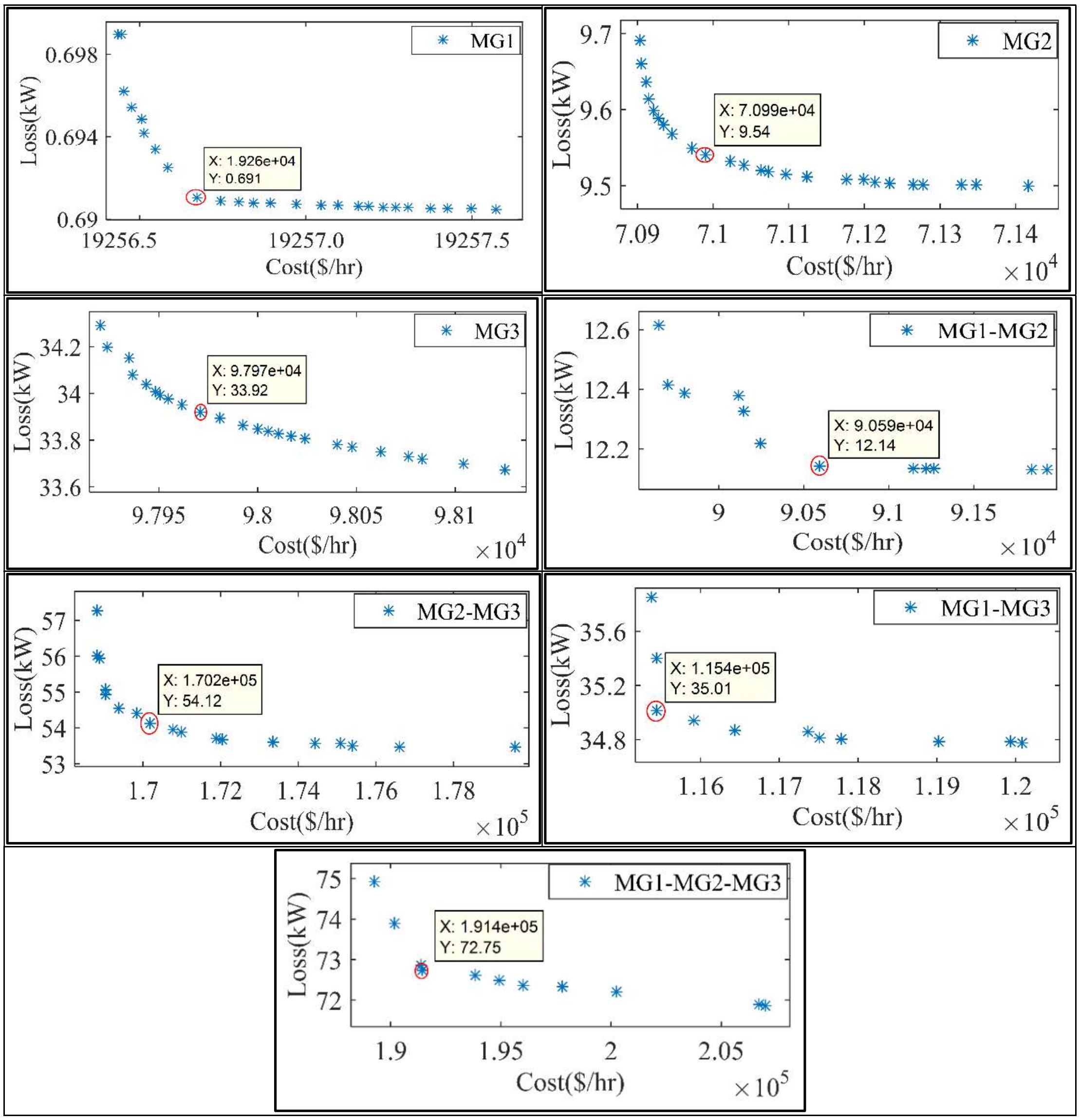

Fig-4.2: Simultaneous minimization of Operating Cost and Active Power Losses of 33 Bus system for different case studies using Jaya Algorithm

The weight coefficients (α_i) for both the objective functions considered are 0.5 (i.e., α_{cost}=0.5 and α_{loss}=0.5). Fuzzy Decision-making method has been applied in arriving the Best Compromised Solution among Pareto optimal solution set for various case studies. For Case-I to Case-VII, the Best Compromised Solutions are found to be (19256.67, 0.69103), (70990.62, 9.54004), (97970.68, 33.91906), (90594.72, 12.14005), (170186.97, 54.12403), (115441.36, 35.01063) and (191446.77, 72.74745) respectively. The red circle in the sub-plots of the Fig-4.2 indicate the Best Compromised Solution among the Pareto-front.

From the Pareto-optimal solution set, the Decision-maker, based on his preference, can opt the weights of the objective functions. By assigning different weights to the objective function other than equal weights, one of the objective function value decreases and the other objective function value increases. It is apparent from the Fig-4.2 that by giving less weightage to Operating cost and more weightage to Active power losses, the BCS moves towards increased operating cost direction. For illustration, by assigning α_{cost}=0.3 and α_{loss}=0.7, the Best Compromised Solutions for Case-VII would be (196022.63, 72.37076) signifies that the Active power loss decreases and Operating cost increases in comparison to BCS obtained with equal weights as presented above, i.e., (191446.77, 72.74745).

4.5.1.2 Scenario-B: Simultaneous minimization of Total Operating Cost and Voltage Deviation

The Total operating cost of controllable DGs and Voltage Deviation of the system have been considered as the Multi-Objective Optimization function in this scenario. Non-dominated sorting technique and Crowding Distance methodology have been applied to obtain the Pareto-optimal solution set for simultaneous minimization of operating cost of DGs and Voltage Deviation, as depicted in Fig-4.3.

The Best Compromised Solutions(BCS) obtained from the Pareto optimal set from Case-I to Case-VII are found to be (19256.68, 7.7184e-06), (71778.21, 6.1538e-05), (97993.26, 4.3436e-04), (93126.18, 4.8423e-05), (180645.40, 9.5186e-05), (128846.92, 8.2201e-05) and (204533.46, 1.0027e-04) respectively. The BCS among the Pareto-optimal front for various case studies has been indicated with a red circle in the sub-plots of the Fig-4.3.

It can be analyzed from the Fig-4.3 that the Decision-maker has a choice of selecting appropriate weights of the objective functions based on the Pareto optimal solution set. The BCS has been identified by assigning equal weightage to either of the objective functions i.e., α_{cost}=0.5 and α_{VD}=0.5. By assigning different weights to Operating cost minimization function and Voltage deviation minimization function, the BCS moves towards the higher weight objective function. The BCS arrived for Case-VII would be (221523.26 , 6.3949e-05) by selecting weights as α_{cost}=0.3 and α_{VD}=0.7 i.e., BCS move towards reduced Voltage Deviation value and increased Operating cost value.

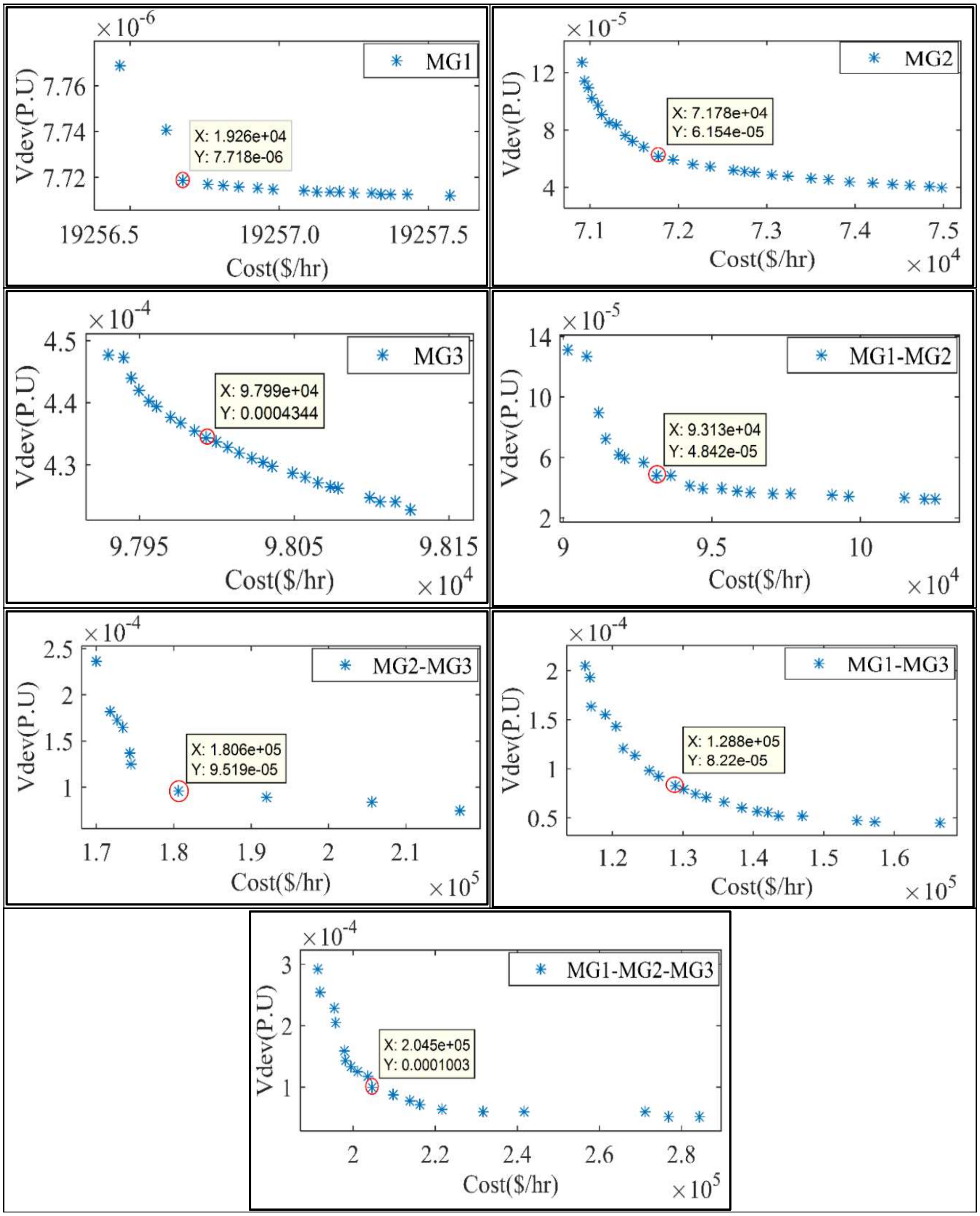

Fig-4.3: Simultaneous minimization of Operating Cost and Voltage Deviation of 33 Bus system for different case studies using Jaya Algorithm

4.5.1.3 Scenario-C: Simultaneous minimization of Active Power Losses and Voltage Deviation

In this scenario, minimization of Active power losses and Voltage Deviation of the system coincidently has been treated as an objective function. The Pareto-optimal solution set for different case studies is presented in the Fig-4.4.

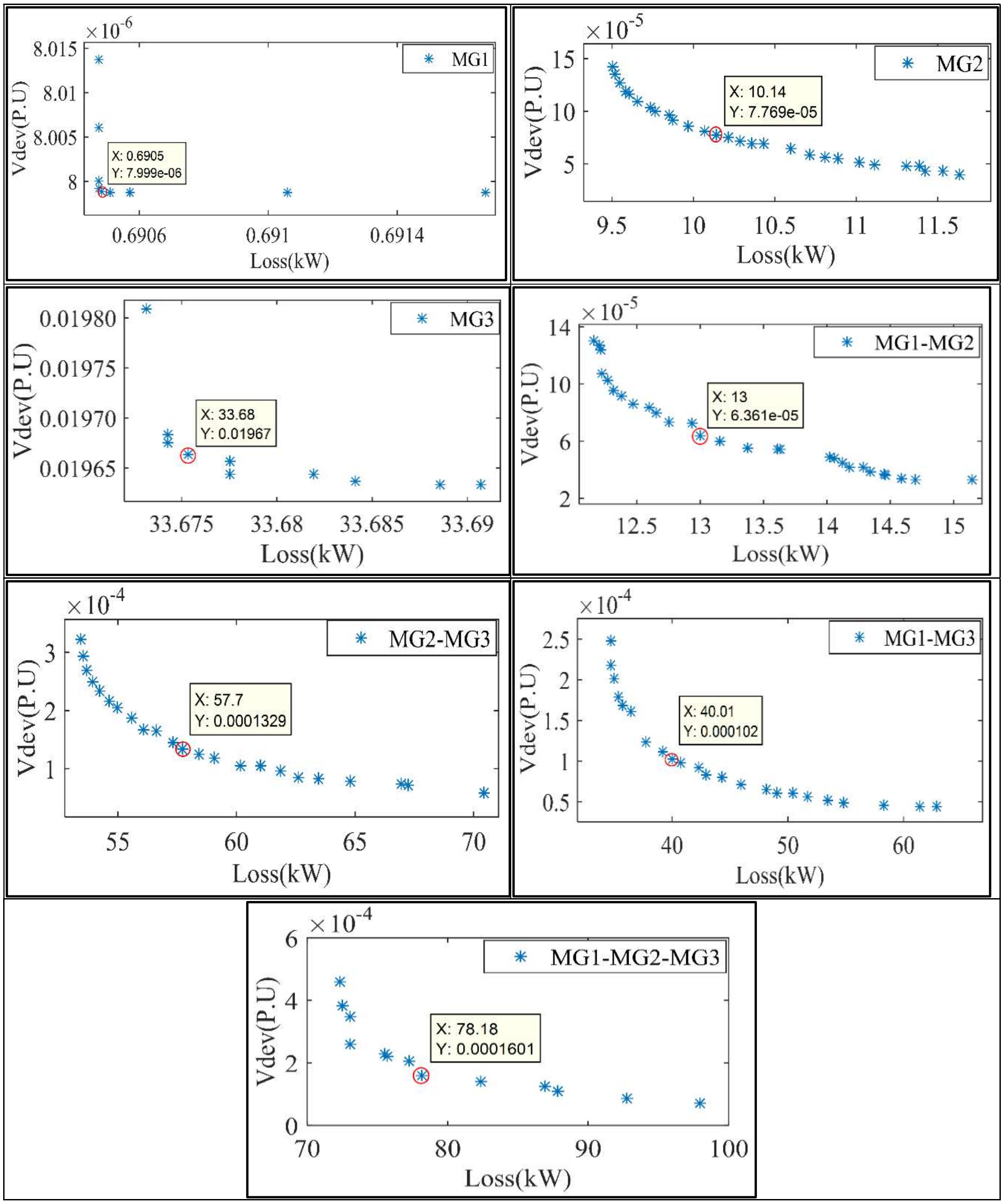

Fig-4.4: Simultaneous minimization of Active Power Losses and Voltage Deviation of 33 Bus system for different case studies using Jaya Algorithm

As a test case, the weightage allotted for Active power losses and Voltage Deviation objective functions are α_{loss}=0.5 and α_{VD}=0.5, thus the Best Compromised Solution for Case-I to Case-VII by applying Fuzzy Decision-making method, are found to be (0.69048, 7.9989e-06), (10.14166, 7.7688e-05), (33.67535, 1.96667e-02), (12.99658, 6.3614e-05), (57.7038, 1.3289e-04), (40.01138, 1.0184e-04) and (78.1787, 1.60104e-04) respectively. The red circle in the sub-plots of the Fig-4.4 indicate the Best Compromised Solution among the Pareto-front.

The BCS pointed out with equal priority to both the objectives in the Fig-4.4 gives an indication to the Decision-maker for opting the appropriate weights to the objective functions. The objectives are being minimization category, higher the weightage of an objective function, lower will be the corresponding objective function value. By earmarking α_{loss}=0.8 and α_{VD}=0.2 for Case-VII, the BCS obtained from the pareto optimal solution set shall be (73.0704, 2.5931e-04), which reveals that the Active power loss has decreased from 78.1787 to 73.0704 whereas Voltage Deviation value increased from 1.60104e-04 to 2.5931e-04. Thus, higher the weightage assigned, lower the corresponding objective function value. Based on the above, the System Operator has to select appropriate weights to the objective function values.

4.5.2 Multi-Objective Optimization without considering EIR criterion on a modified 85 Bus Distribution System

In previous section, case studies were carried out on 33 Bus system. The effectiveness of the proposed approach for Multi-Microgrid system is validated on bigger system. In this section, as described in Section-2.2 of chapter-2, the modified 85 Bus Distribution System is sectionalized into Multi-Microgrid System. As explained, different Scenarios are articulated and under each Scenario, various case studies are formulated as presented in Table-2.5 of chapter-2. The test results for various scenarios of modified 85 Bus Distribution System upon the formulation of Multi-Microgrid System are as follows.

4.5.2.1 Scenario-A: Simultaneous minimization of Total Operating Cost and Active Power Losses

Simultaneous minimization of Total operating cost of controllable DGs and System losses have been considered as an objective function in this scenario.

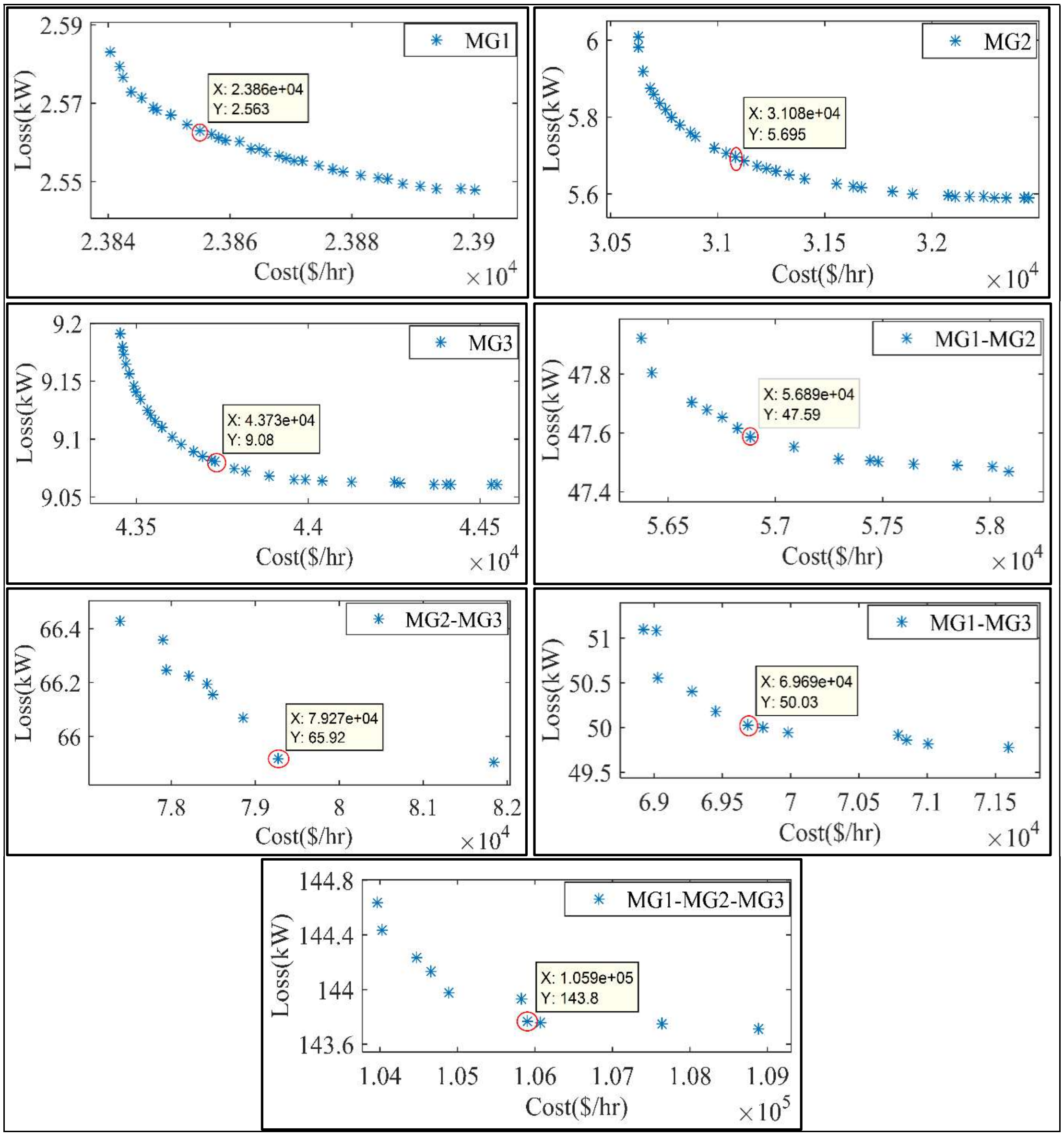

Fig-4.5: Operating Cost and Active Power Losses minimization simultaneously of 85 Bus system for different case studies using Jaya Algorithm

Pareto optimal solution set has been realized by applying Non-dominated sorting and Crowding Distance approach. From the Pareto optimal solution set, the Decision-maker can access Best Compromised Solution by assigning preferable weights of the objective functions using Fuzzy Decision-making method. As a test case, by assigning equal importance to both the objective functions (i.e., α_{cost} =0.5 and α_{loss} =0.5), the Best Compromised Solutions obtained from Case-I to Case-VII found to be (23855.11, 2.56290), (31083.97, 5.69515), (437299.23, 9.08018), (56885.33, 47.58645), (79273.89, 65.91769), (69686.81, 50.03271) and (105908.36, 143.77157) respectively. The BCS among the Pareto-optimal front for various case studies with equal weightage has been indicated with a red circle in the sub-plots of the Fig-4.5.

An objective with higher preference can be assigned with higher weightage such that the sum of the weights must be equal to unity. As the objective functions are of minimization category, higher the weightage, lower will be the corresponding objective function value. For illustration purpose, by assigning α_{cost}=0.8 and α_{loss}=0.2, the BCS for Case-VII would be (104022.75, 144.43331). It is evident from this illustration that as the α_{cost} has increases, its objective function value decreases. Thus, the System Operator has to choose the weights according to the preference of the objective function.

4.5.2.2 Scenario-B: Simultaneous minimization of Total Operating Cost and Voltage Deviation

The total operating cost of controllable DGs and Voltage Deviation of the system have been considered as a Multi-Objective Optimization function in this scenario.

The Pareto-optimal set for simultaneous minimization of operating cost of DGs and Voltage Deviation is depicted in Fig-4.6. By selecting equal weightage to both the objective functions, i.e., α_{cost}=0.5 and α_{VD}=0.5, the BCS has been arrived. The BCS obtained from the Pareto Optimal set from Case-I to Case-VII are found to be (24061.35, 5.3873e-06), (30644.27, 1.08567e-05), (43450.58, 2.12140e-05), (58198.60, 3.46325e-04), (82118.12, 1.11434e-04), (73071.39, 3.32162e-04) and (112110.39, 7.95643e-04) respectively. The circle in the sub-plots of the Fig-4.6 indicate the BCS among the Pareto-optimal front.

As an example, by changing the weights of the objective functions as α_{cost}=0.8 and α_{VD}=0.2, the BCS of Case-VII would be (107929.37, 9.82945e-04). From this, it is clear that by inclining towards the minimization of operating cost, the value of Voltage Deviation has increased from 7.95643e-04 to 9.82945e-04.

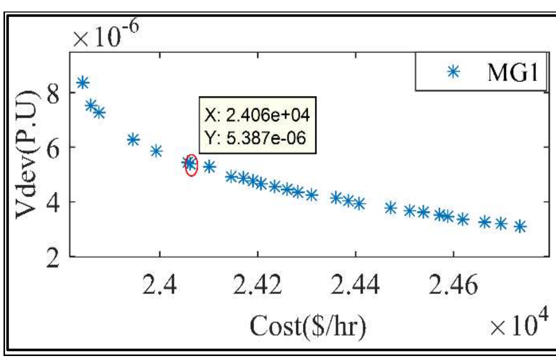

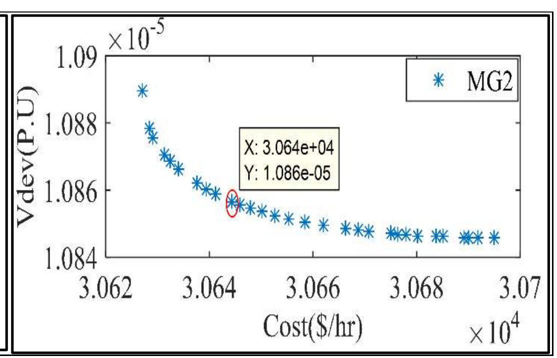

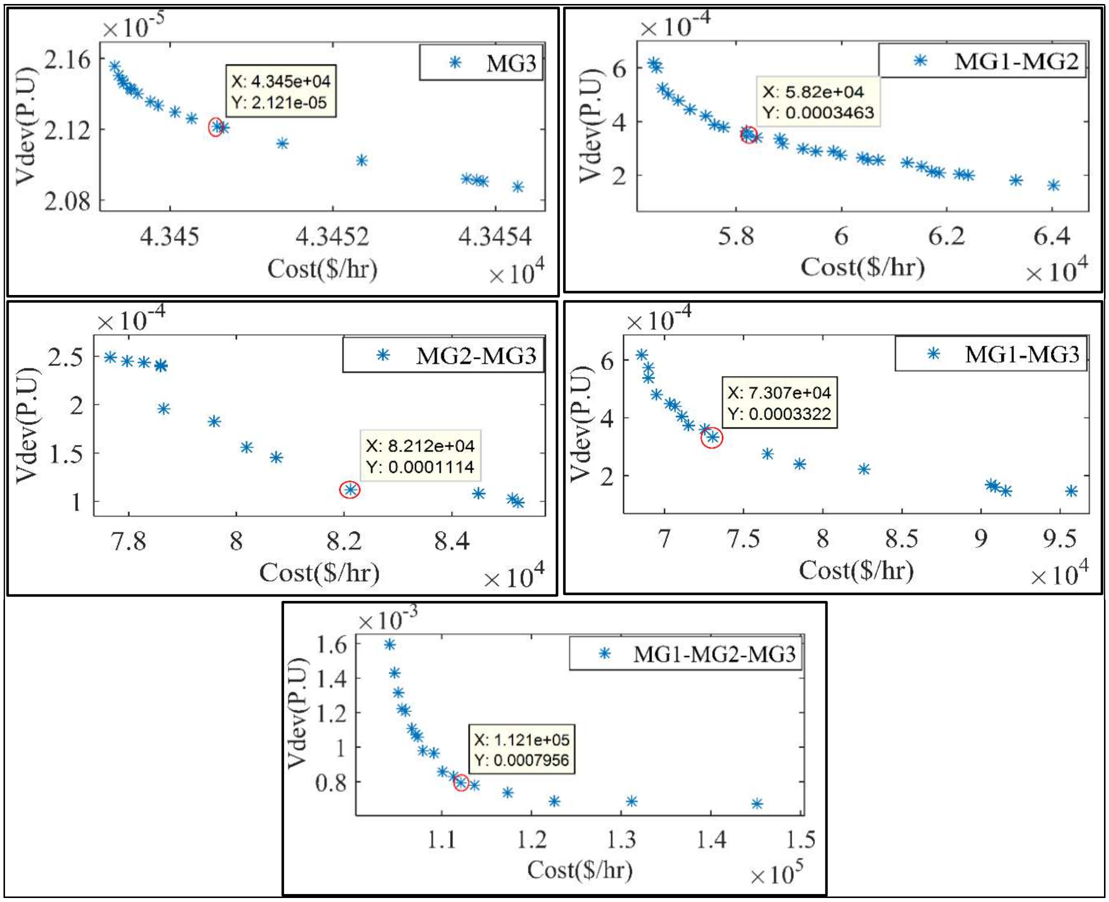

Fig-4.6: Operating Cost and Voltage Deviation minimization simultaneously of 85 Bus system for different case studies using Jaya Algorithm

4.5.2.3 Scenario-C: Simultaneous minimization of Active Power Losses and Voltage Deviation

In this scenario, minimization of Active power losses and Voltage Deviation of the system coincidently has been treated as an objective function. The Pareto-optimal solution set for different case studies has been presented in the Fig-4.7. For Case-I to Case-VII, the BCS are found to be (2.59945, 4.99767e-06), (5.73966, 1.12685e-05), (9.11835, 2.48557e-05), (47.95854, 2.97751e-04), (67.76408, 1.62226e-04), (52.50210, 1.94729e-04) and (147.10258, 7.86270e-04) respectively with equal weightage to both the objective functions. The Best Compromised Solution among the Pareto-front is pointed out with a red colour circle in the sub-plots of Fig-4.7.

From Fig-4.7, it is noticeable that a wide range of solutions is possible by selecting the weights of the objective function appropriately. Based on the preference of the objective function, the Decision Maker can choose the weights of the objective functions. Higher the weight of an objective function, lower will be its objective function value. If the weights are chosen as α_{loss} =0.8 and α_{VD} =0.2 for Case-VII, then the BCS would be (144.0108, 10.82689 e-04), where the loss has been decreased while the Voltage Deviation value has increased.

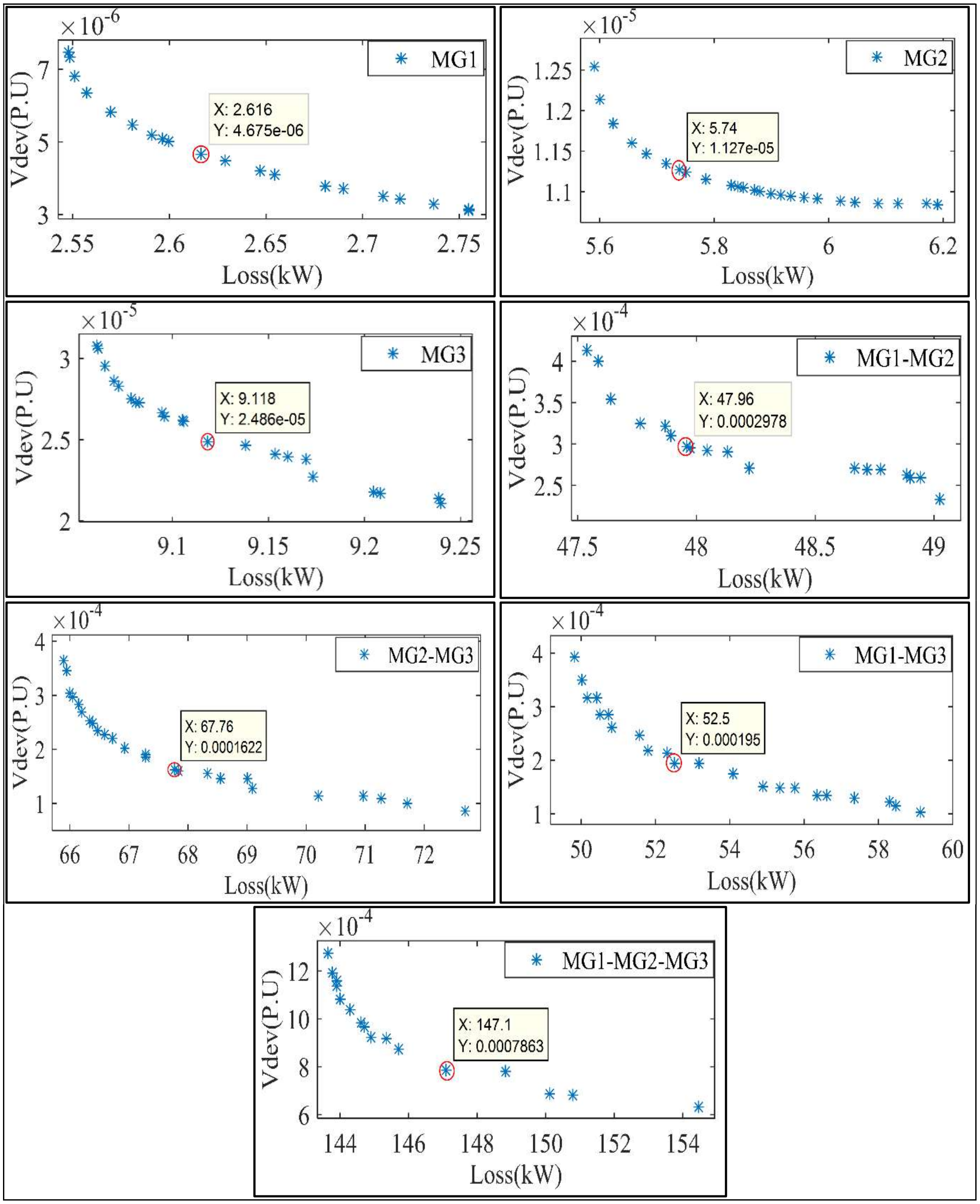

Fig-4.7: Active Power Losses and Voltage Deviation minimization simultaneously of 85 Bus system for different case studies using Jaya algorithm.

4.5.3 Multi-Objective Optimization with EIR criterion on a modified 33 Bus Distribution System

In the previous sections, the analysis has been carried out without considering EIR criterion, however, in this section, optimal scheduling of controllable DGs has been performed considering EIR criterion along with equality and inequality constraints. While optimizing, it is ensured that EIR(τ) ≥ 0.97 has been maintained. The test results for various scenarios of modified 33 Bus Distribution System upon the formulation of Multi-Microgrid System are as follows.

4.5.3.1 Scenario-A: Simultaneous minimization of Total Operating Cost and Active Power Losses

In this scenario, simultaneous minimization of operating cost of DGs and system Active power losses has been considered as an objective function, while maintaining EIR(τ) ≥ 0.97. The Pareto-optimal front obtained for various case studies is presented in Fig-4.8.

Pareto optimal solutions for various case studies have been accomplished by enforcing the Non-dominated sorting and Crowding Distance methodology. The investigation has been carried out by assigning equal weightage (i.e., α_{cost}=0.5 and α_{loss}=0.5) for both the objective functions, in the Fuzzy Decision-making method, to achieve the Best Compromised Solution for various case studies. The Best Compromised Solution for Case-I to Case-VII are found to be (19256.65, 0.69382), (89412.07, 15.98204), (110411.04, 44.14713), (106546.16, 17.79089), (201912.72, 58.55761), (127374.03, 42.73342) and (227690.37, 76.27862) respectively. The BCS among the set of solutions for all the case studies is depicted with a red circle in the sub-plots of the Fig-4.8.

It can be analyzed from the test results that by enforcing the EIR criterion, the Pareto optimal solution set has been changed from that of a normal case where EIR is not a criterion, i.e., Fig-4.2. The BCS realized for Case-VII with equal weightage to both objectives without EIR constraint was found to be (191446.77, 72.74745), whereas, with EIR constraint, it is found to be (227690.37, 76.27862). However, the BCS values have been increased by enforcing the EIR criterion, it promises improved system operation.

The BCS has been identified with equal weightage to both the objectives given an indication to the System Operator for choosing the appropriate weight coefficient of the objective function values. For illustration, by choosing α_{cost}=0.7 and α_{loss}=0.3, the BCS for

Case-VII would be (224846.28, 76.8279), where the operating cost value has been decreased whereas the system losses have been increased in comparison to equal weightage. Thus, it is evident that by increasing importance to one objective function, the other objective function value increases.

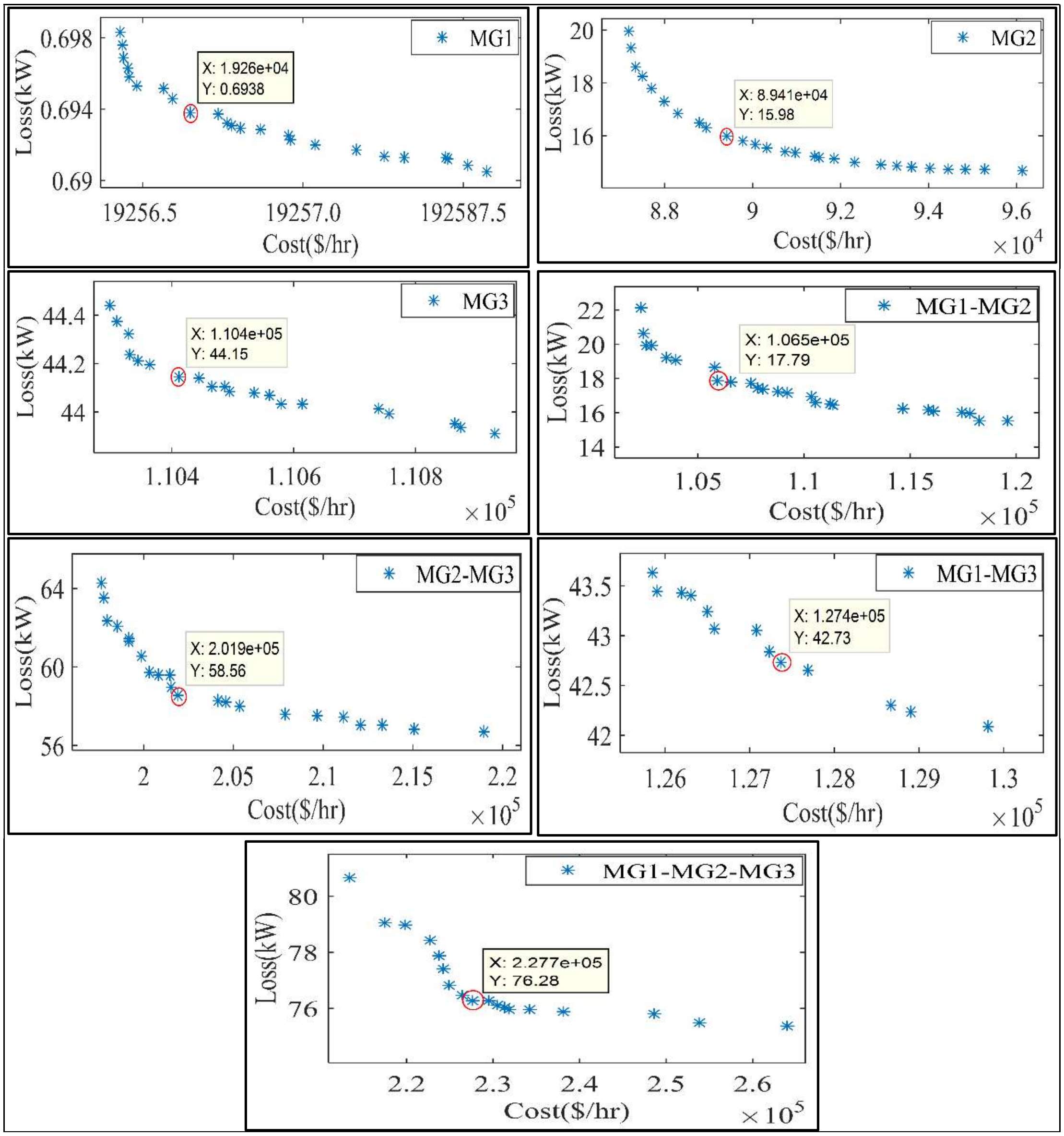

Fig-4.8: Simultaneous minimization of Operating Cost and Active Power Losses of 33 Bus system for different case studies using Jaya Algorithm with EIR

4.5.3.2 Scenario-B Simultaneous minimization of Total Operating Cost and Voltage Deviation

Concomitantly minimization of operating cost of DGs and Voltage Deviation of the system has been considered as an objective function in this Scenario. Fig-4.9 presents the

Pareto-optimal set for simultaneous minimization of operating cost of DGs and Voltage Deviation.

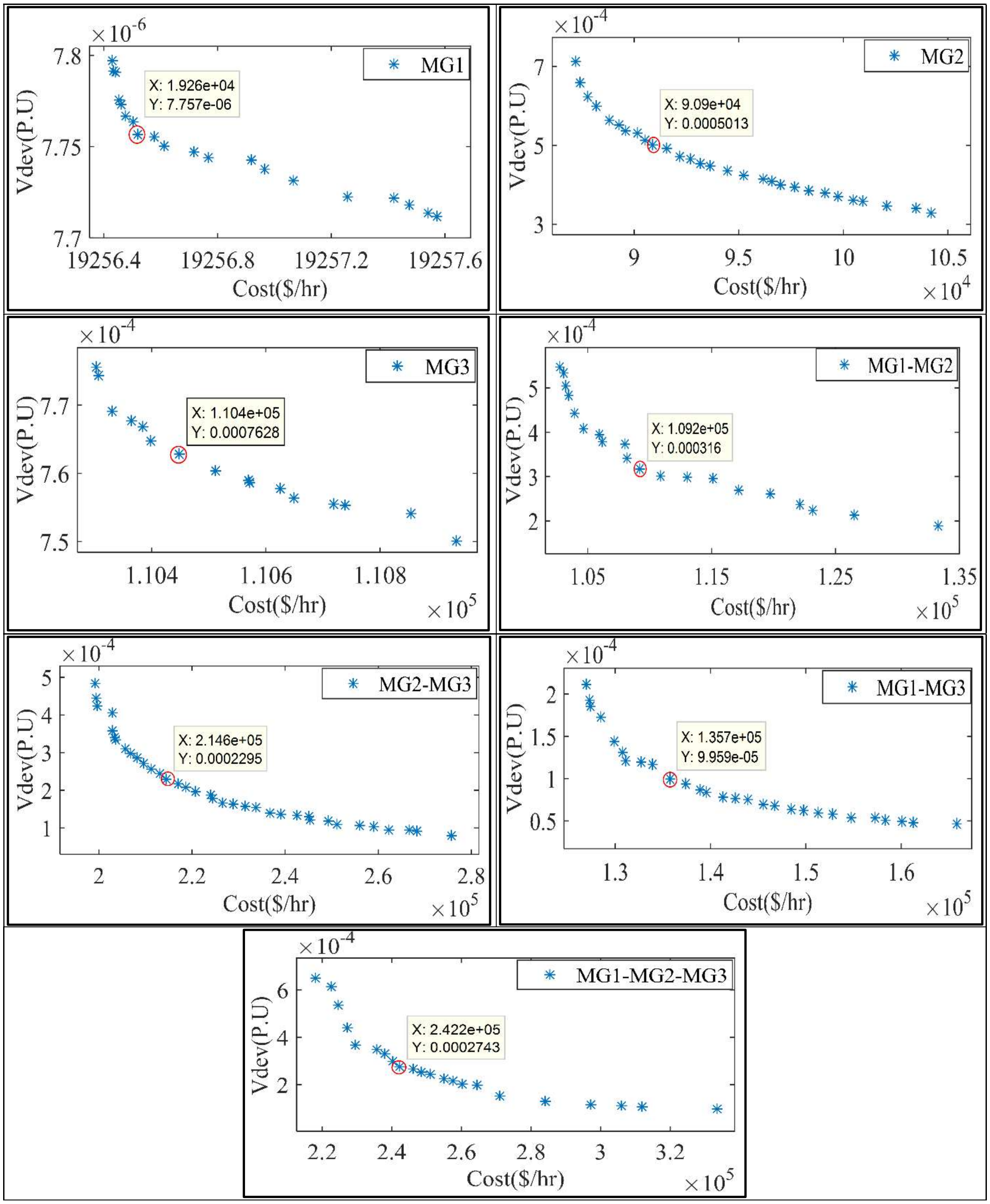

Fig-4.9: Simultaneous minimization of Operating Cost and Voltage Deviation of 33 Bus system for different case studies using Jaya algorithm with EIR

By assigning equal weightage to both the objective functions and enforcing EIR criterion, the Best Compromised Solution (BCS) for Case-I to Case-VII are found to (19256.52, 7.7565e-06), (90895.88, 5.0128e-04), (110448.41, 7.6283e-04), (109196.79, 3.1649e-04), (214565.45, 2.2953e-04), (135730.98, 9.9594e-05) and (242225.65, 2.7428e-04) respectively. The circle in the sub-plots of the Fig-4.9 indicate the BCS among the Pareto-front.

The BCS found in Case-VII without consideration of EIR criterion, but with equal weights, to both the objective functions is (204533.46, 1.0027e-04), whereas with EIR criterion, the BCS is found to be (242225.65, 2.7428e-04). It can be analyzed from the test results that by imposing the EIR criterion, the objective function values of BCS have been increased. However, the reliability of the system operation improves by EIR.

It can be seen from Fig-4.9, the Decision-maker has a wide range of operating region from the pareto optimal solution set. By assigning α_{cost}=0.7 and α_{loss}=0.3, the BCS would be (229483.68, 3.6487e-04) thereby, the operating cost has been decreased monumentally whereas the Voltage Deviation value has increased.

4.5.3.3 Scenario-C: Simultaneous minimization of Active Power Losses and Voltage Deviation

In this scenario, minimization of Active Power Losses and Voltage Deviation of the system coincidently has been considered as an objective function. The Pareto-optimal solution set for different case studies enforcing the EIR criterion has been presented in Fig-4.10. Choosing equal weights to both the objective functions, i.e., α_{loss}=0.5 and α_{VD}=0.5, the Best Compromised Solutions found for Case-I to Case-VII are found to be (0.69047, 7.7117e-06), (14.85772, 3.68383e-04), (44.39137, 7.69321e-04), (16.38885, 2.02511e-04), (64.10693, 1.58169e-04), (48.71869, 9.17636e-05) and (83.55429, 1.92712e-04) respectively. The BCS among the Pareto-optimal front is pointed out with a red colour circle in the sub-plots.

It is noticed that, after making an exhaustive number of trails by enforcing the Non-dominated sorting technique, there is only one solution with Rank-1 for Case-I and Case-III, with satisfies equality, inequality constraints and also EIR criterion. Thus, the BCS in Case-I and Case-III would be the single solution, which has been depicted in Fig-4.10. However, for other case studies, the Pareto-optimal front exists.

Based on the above, the Decision-maker, depending on the priority of the objective function, the weight can be selected appropriately for all case studies except Case-I and Case-III. The BCS identified by choosing α_{loss}=0.7 and α_{VD}=0.3 for Case-VII would be (77.04, 2.9852e-04), where the Active power loss decreased substantially.

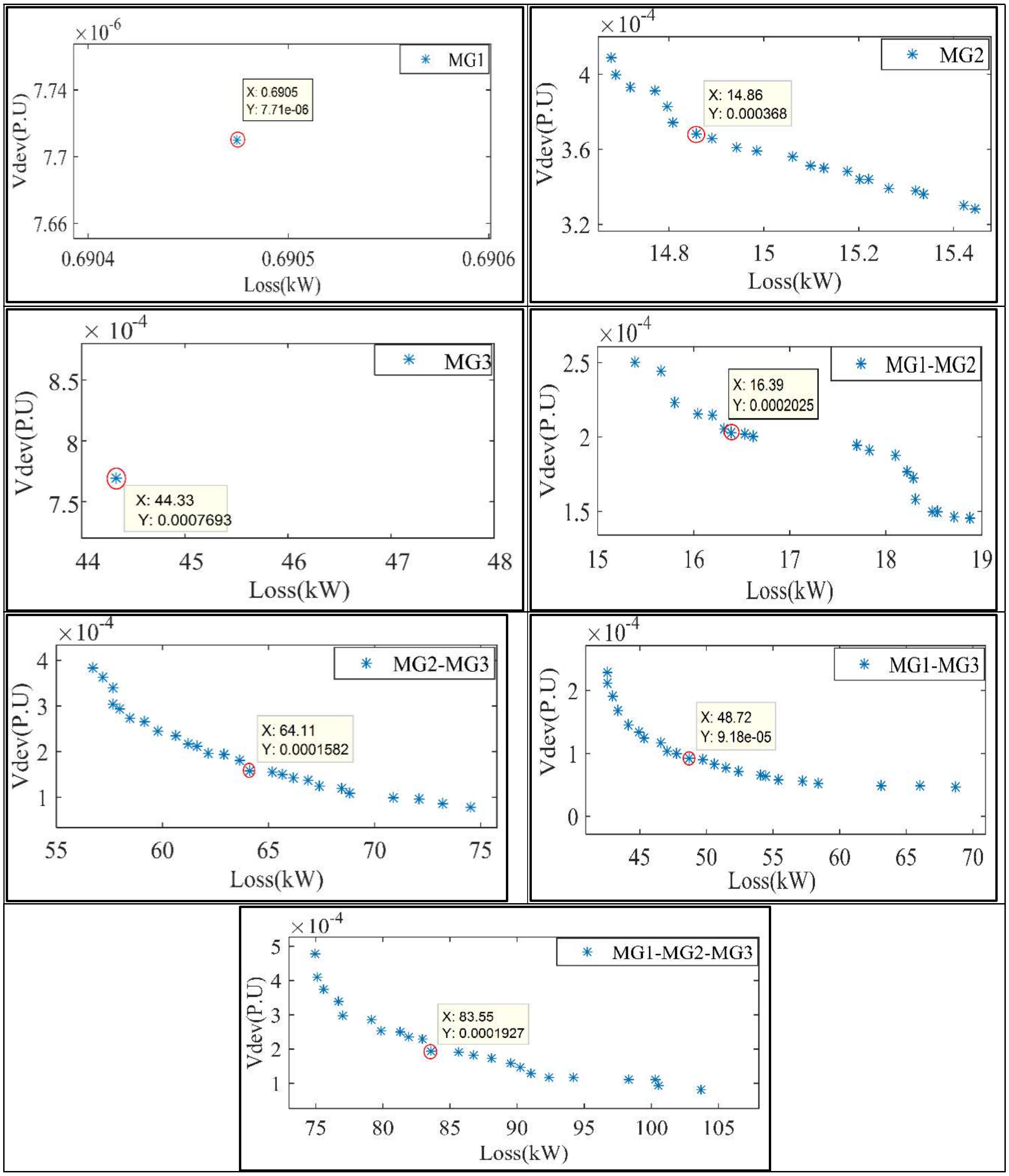

Fig-4.10: Simultaneous minimization of Active Power Losses and Voltage Deviation of 33 Bus system for different case studies using Jaya Algorithm with EIR

4.5.4 Multi-Objective Optimization with EIR criterion on a modified 85 Bus Distribution System

The above section presents the test results of 33 Bus Distribution system with EIR criterion. However, in this section, to test the effectiveness of the proposed approach, a bigger size system has been considered. In this section, optimal scheduling of controllable DGs has been performed considering EIR criterion in addition to equality and inequality constraints. While optimizing, it is ensured that EIR(τ) ≥ 0.97 has been maintained. The test results for various scenarios of modified 85 Bus Distribution System upon formulation of Multi-Microgrid System are as follows.

4.5.4.1 Scenario-A: Simultaneous minimization of Total Operating Cost and Active Power Losses

Minimization of Operating Cost of DGs and System Losses in unison has been considered as an objective function in this scenario.

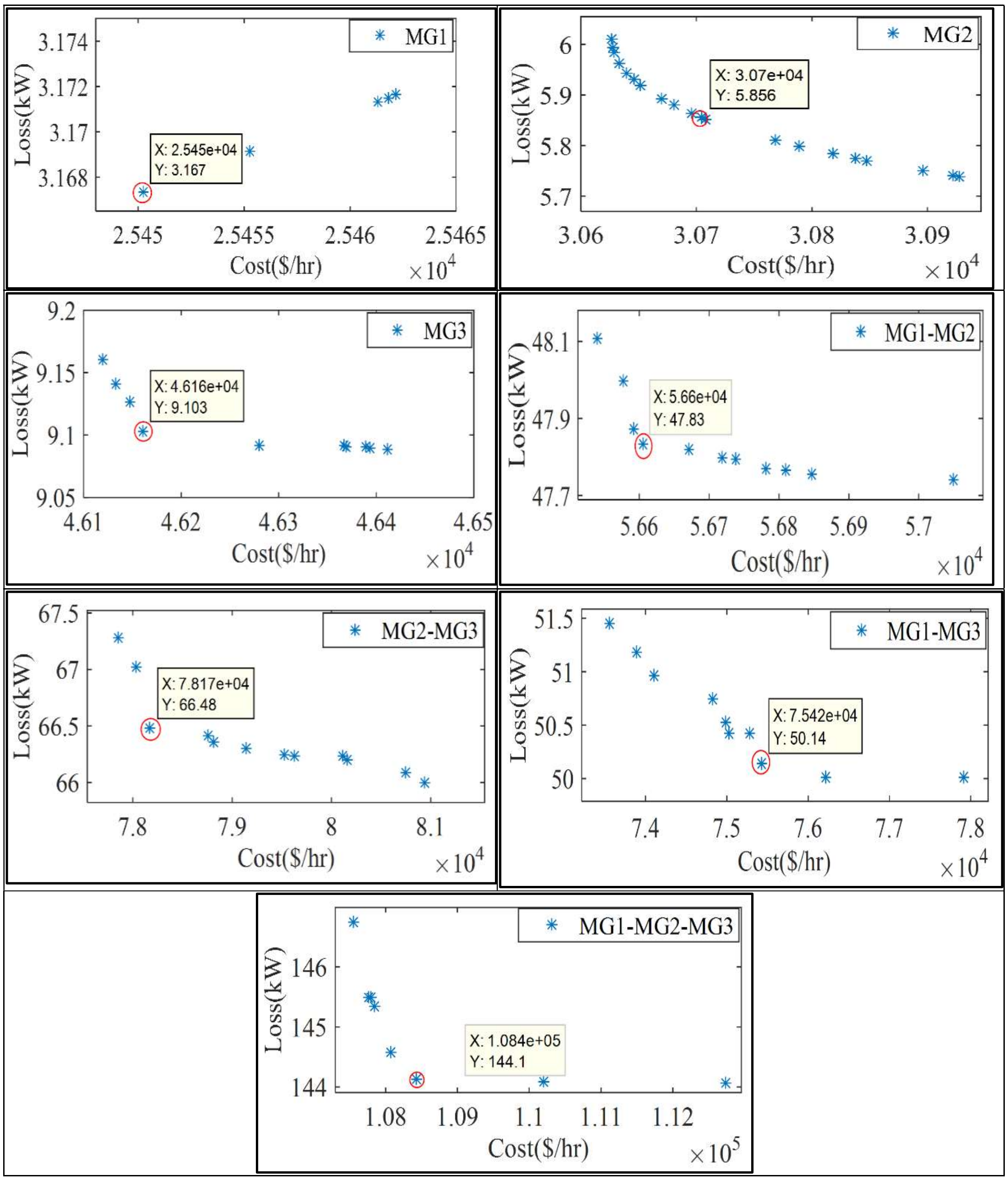

Fig-4.11: Operating Cost and Active Power Losses minimization simultaneously of 85 Bus system for different case studies using Jaya Algorithm with EIR

The Non-dominated sorting technique has been applied to obtain the Pareto optimal solutions for various case studies by enforcing the EIR criterion in addition to equality and inequality constraints. The investigation has been carried out by assigning equal weightage (i.e., α_{cost} =0.5 and α_{loss} =0.5) for both the objective functions to achieve the Best Compromised Solution for various case studies using Fuzzy Decision-making approach, as presented in Fig-4.11. The Best Compromised Solutions for Case-I to Case-VII are found to be (25450.24, 3.16734), (30704.60, 5.85557), (46160.89, 9.10334), (56604.71, 47.8321), (78174.34, 66.4826), (75423.99, 50.1437) and (108433.84, 144.1268) respectively. The Best Compromised Solution among the set of solutions for all the case studies is depicted with a red circle in the sub-plots.

Nevertheless, the Decision-maker, based on the preference of the objective functions, can choose the BCS by varying the weights of the objective functions for other case studies except for Case-I. It can be noticed that by making exhaustive trails, only a single solution is feasible with Rank-1 in pareto optimal solution set for Case-I, by enforcing EIR criterion along with equality and inequality constraints, which is considered to be BCS. Fig-4.11 depicts the other solutions with lower ranks (rank-2, rank-3 etc) for Case-I, wherein the objective function values of these solutions are more than that of BCS. Thus, the BCS for Case-I would be a unique solution irrespective of the weightage assigned to the objective functions.

4.5.4.2 Scenario-B: Simultaneous minimization of Total Operating Cost and Voltage Deviation

Minimization of Operating cost of DGs and Voltage Deviation of the system at a time has been considered as an objective function in this Scenario while satisfying EIR criterion $\tau \geq 0.97$. Fig-4.12 presents the Pareto-optimal solution set for this Scenario for various case studies with Non-dominated sorting of Rank-1. For Case-I to Case-VII, the Best Compromised Solution with equal weightage to both the objectives (i.e., α_{cost}=0.5 and α_{VD}=0.5) are found to be (25447.62, 2.0857e-05), (30644.13, 1.0856e-05), (46096.26, 2.6234e-05), (58736.06, 3.1514e-04), (80509.74, 2.3397e-04), (79734.51, 2.5452e-04) and (117323.75, 7.4501e-04) respectively and are encircled with red colour in the subplots of Fig-4.12.

For Case-I, a unique solution has been identified in the Pareto-front with rank-1 after extensive runs of optimization, which is considered to be BCS. However, solutions with lower Rank (rank-2, rank-3 etc) has been evaluated and depicted in the Fig-4.12. It can be analyzed from this figure that the corresponding objective function values of lower rank solutions will be more than that of the BCS identified.

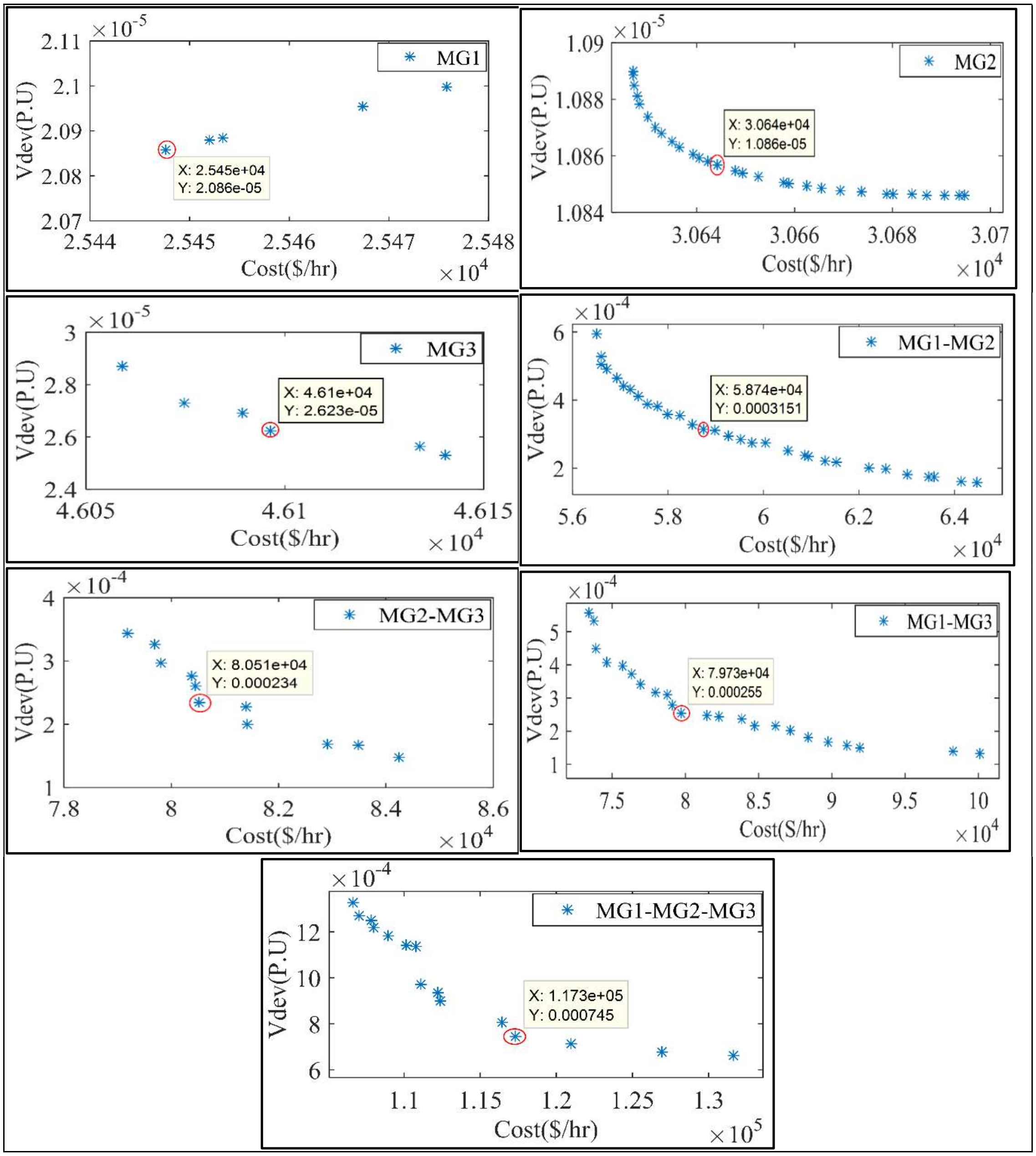

Fig-4.12: Operating Cost and Voltage Deviation minimization simultaneously of 85 Bus system for different case studies using Jaya Algorithm with EIR

The Decision Maker, based on the preference of the objective function, can identify BCS using Fuzzy Decision-making approach, among the Pareto optimal solution set exists for other case studies. For illustration purpose, considering α_{cost}=0.7 and α_{VD}=0.3, the BCS for Case-VII would be (111103.14, 9.7358e-04), where significant operating cost reduction has been noticed than that of equal weightage to either of the objectives. However, the other objective function value has increased.

4.5.4.3 Scenario-C: Simultaneous minimization of Active Power Losses and Voltage Deviation

In this scenario, minimization of Active power losses and Voltage Deviation of the system coincidently has been treated as an objective function with EIR criterion. The Pareto-optimal solution set for different case studies is presented in Fig-4.13.

For Case-I to Case-VII, the BCS with equal weightage to both the objective functions (i.e., α_{loss}=0.5 and α_{VD}=0.5) are found to be (3.1672, 2.0868e-05), (5.9175, 1.0961e-05), (9.1587, 2.9115e-05), (49.2750, 2.3166e-04), (67.6840, 1.8472e-04), (52.0170, 2.0875e-04) and (145.8708, 8.8352e-04) respectively. The Best Compromised Solution among pareto-front is pointed out with a red colour circle in the sub-plots.

It can be noticed that in Case-I, only one solution is available in the Pareto-front with rank-1 after exhaustive trails with optimization, which is considered to be BCS. From these test results, the Decision Maker can identify the BCS among the Pareto-optimal solution set using Fuzzy Decision-making approach for all other case studies except case-I, by choosing the preference weights of the objective functions,

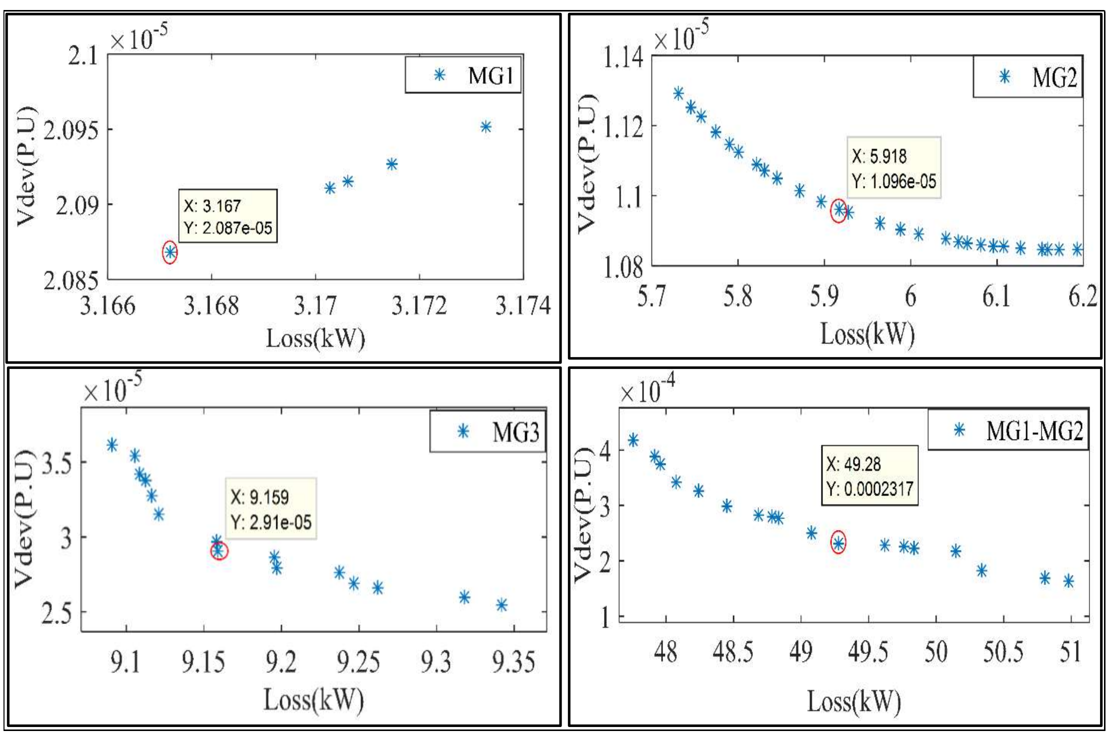

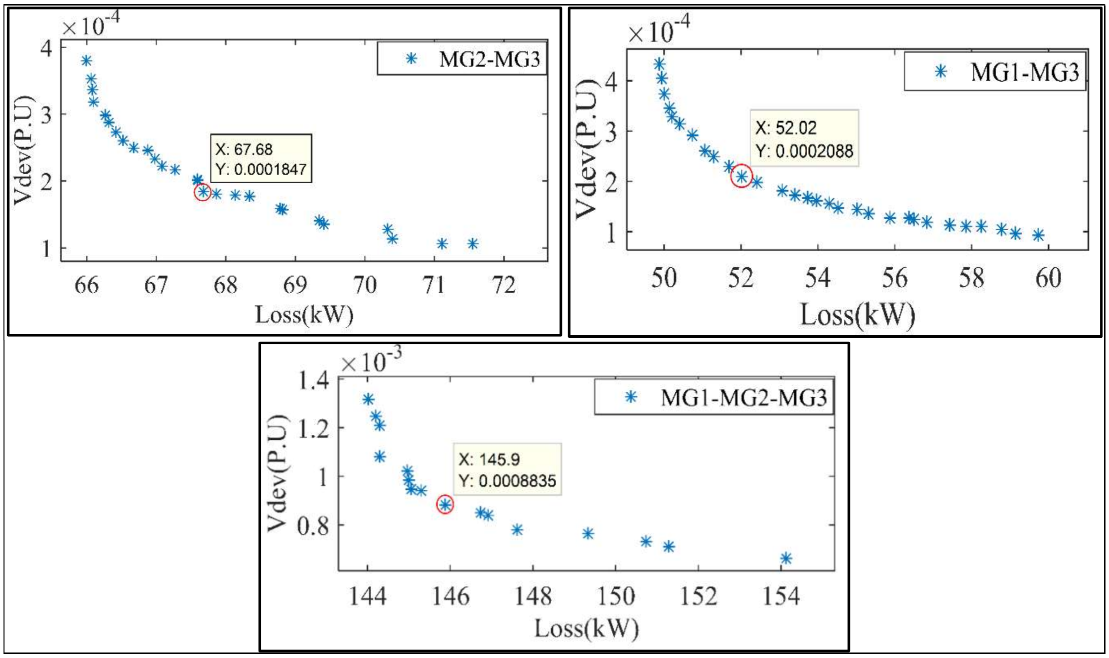

Fig-4.13: Active Power Losses and Voltage Deviation minimization simultaneously of 85 Bus system for different case studies using Jaya Algorithm with EIR

4.6 Summary

In summary, in this chapter, Multi-Objective Optimization (MOO) problem has been attempted on an islanded active Distribution System sectionalized into Multi-Microgrid System. The objectives addressed in this chapter are minimization of Total Operating Cost of DGs, minimization of Active Power Losses and minimization of system Voltage Deviation in Multi-Microgrid System. The MOO problem has been performed treating two objective functions simultaneously.

Initially, MOO problem is formulated enforcing equality and inequality constraints only without considering EIR criterion. Three Scenarios are formulated considering two objective functions at a time. Under Scenario-A, simultaneous minimization of total Operating cost & Active power losses has been attempted, where are in Scenario-B and Scenario-C, simultaneous minimization of Operating cost & Voltage Deviation, simultaneous minimization of Active power losses and Voltage Deviation have been attempted respectively. Under each scenario, different case studies are addressed, considered different combinations of Microgrids operation.

Jaya Algorithm, which is found to be the best in optimal scheduling problem in previous chapters, is used to solve the MOO problem. For solving MOO using Jaya Algorithm, Multi-Objective Jaya Algorithm (MOJA) has been formed by incorporating

Non-Dominated sorting and Crowding Distance (CD) methodology as described in the section-4.3.1 and section-4.3.2 above respectively, to the simple single objective Jaya Algorithm. Upon formation of MOJA, it is attempted for different scenarios as addressed above, to obtaining the Non-Dominated Pareto-front. On identification of Pareto-front, the Best Compromised Solution (BCS) is identified using Fuzzy Decision- making method which is presented in the section 4.3.3.

Considering the importance of reliability constraint in providing the continuous power supply, the MOO problem is attempted with EIR criterion along with equality and inequality constraints. This part of the work will act as a supporting tool to the practicing Engineer when they start attempting with EIR enforcement. The MOJA, which is developed, is used to solve this complex constrained optimization problem. The Non-dominated Pareto-front with rank-1 and BCS are identified in each case study of various scenarios. The above methods are tested on a modified 33 Bus Distribution System and the modified Indian 85 Bus Distribution System.

Initially, the MOJA has attempted on IEEE 33 Bus Distribution System without EIR criterion. The BCS obtained with equal weightage to both objectives have been found to be (19256.67, 0.69103), (70990.62, 9.54004), (97970.68, 33.91906), (90594.72, 12.14005), (170186.97, 54.12403), (115441.36, 35.01063) and (191446.77, 72.74745) for Case-I to Case-VII respectively for Scenario-A. With EIR criterion, the BCS has been identified with similar weightage to both objectives as (19256.65, 0.69382), (89412.07, 15.98204), (110411.04, 44.14713), (106546.16, 17.79089), (201912.72, 58.55761), (127374.03, 42.73342) and (227690.37, 76.27862) for Case-I to Case-VII respectively. It is evident from the test results that on enforcing EIR criterion, the operating cost and Active power losses for all the case studies has been increased in the BCS. Similar observation has been identified on all the scenarios of IEEE 33 Bus Distribution System. In all these case studies, the BCS attained are with alike weightage to both objectives, however, Decision-maker, based on their preference to the objective function, can obtain the BCS from the Pareto-front by applying Fuzzy Decision-making approach.

Similarly, the BCS for Practical 85 Bus Distribution System for Scenario-A without EIR criterion, for Case-I to Case-VII are (23855.11, 2.56290), (31083.97, 5.69515), (437299.23, 9.08018), (56885.33, 47.58645), (79273.89, 65.91769), (69686.81, 50.03271) and (105908.36, 143.77157) respectively, with identical weights to both objectives, whereas with EIR criterion, the BCS attained with similar constraints to both objectives are

(25450.24, 3.16734), (30704.60, 5.85557), (46160.89, 9.10334), (56604.71, 47.8321), (78174.34, 66.4826), (75423.99, 50.1437) and (108433.84, 144.1268) respectively. On comparison of both the test results, analogous observation as that of IEEE 33 Bus System has been identified for all the scenarios.

In the above chapters, controllable DGs are considered for optimal scheduling with various objective functions. However, the importance of Renewable Energy Sources (RES) is increasing day-by-day due to its abundant availability, non-depletable and eco-friendly nature of power generation. By nature, the RES are intermittent in nature and thus power output from these sources is highly irregular. These sources, when connected to Multi-Microgrid System, leads to frequency fluctuations and tie-line power flow deviations due to mismatch of demand generation imbalance. In view of this, the next chapter is dealt with Load Frequency Control of Multi-Microgrid System with the incorporation of RES.

CHAPTER-5

Load Frequency Control of Multi-Microgrid System considering Renewable Energy Sources using Meta-heuristic Techniques

5.1 Introduction

As stated, the per capita consumption of electrical energy is a reliable indicator of the development of any country in the World. Thus, the overall GDP of any country also depends on availability and consumption of electrical energy. However, a large percentage of electrical energy is generated from conventional fossil fuels such as coal, oil, natural gas. From the estimated data, it is clear that these fossil fuels will not last for more than another 200 years. In addition to this, due to the combustion of fossil fuels, the release of harmful gases such as CO_2, NO_x, SO_2, causing serious environment problem majorly acid rains and Global warming [75]. Considering these challenges, electrical power utilities around the World are integrating the Renewable Energy Sources (RES) based power generation technologies. Not only, power generation from RES relieved from the insecurity of energy sources but also can be used as a most useful resource of power generation for the places where central power grid power cannot be accessible considering geo-graphical issues[16] [76].

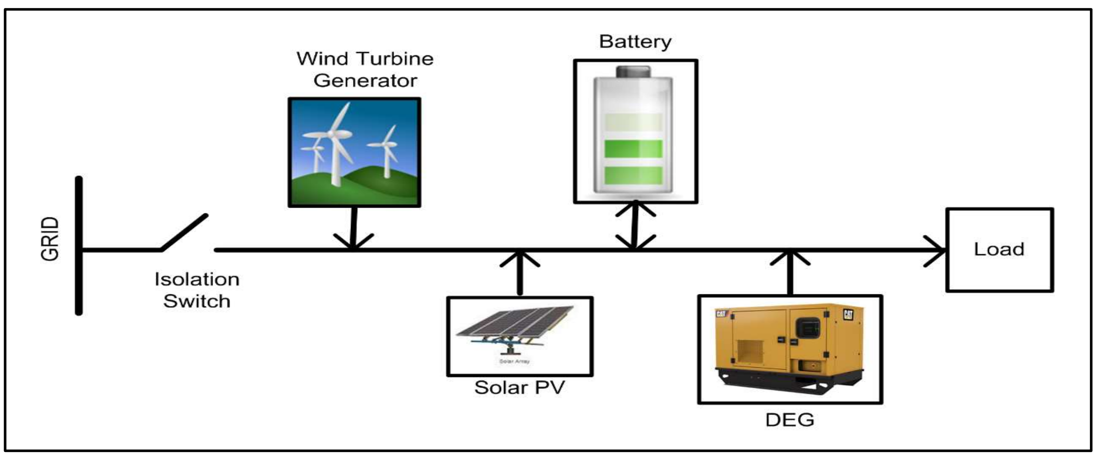

Fig-5.1: Schematic view of Microgrid System consisting of Various Sources

A Microgrid is a low voltage grid consists of Distributed generation (DG) Mcro-sources such as Micro-turbines, Diesel Engine Generators (DEG), Battery Energy Storage System (BESS), Wind Turbine Generators (WTG), Solar Photo-Voltaic (SPV) generators, Fuel Cells (FC) which are knitted together along with small loads through feeders. The schematic view of the Microgrid system consisting of various sources is shown in Fig-5.1.

Whenever demand and supply fluctuate in the Microgrid System, frequency controller restores the frequency to the nominal value. Traditionally frequency controller has been performed on the generation side. The primary frequency controller operates in the timescale of low tens of seconds[77] with decentralized governor mechanism and does not restore the frequency to the nominal value. However, the secondary frequency control restores the system frequency to nominal value but in the timescale of up to a minute or so with centralized governor mechanism [77]. In view of this, secondary frequency control is generally adopted for operating the system at nominal frequency.

However, an autonomous Microgrid may consists of RES such as Wind power, Solar power, which supply highly wiggling power to the Microgrid due to irregular Wind speed and Solar radiation aberration[78]. Penetration of high power by RES to fluctuating load will result in low power contribution by Diesel Engine Generator (capacity of DEG is less), which leads to low inertia of the system. Severe and consequential large oscillation can be observed due to the low inertia system [79]. Therefore, Microgrid faces a serious problem of frequency deviations and voltage fluctuations due to the inconsistent power supply from RES to Microgrid [52][80]. Since the RES are nature dependent, these cannot be used for frequency control. A Diesel generator is used for demand response, but it cannot handle the sudden change in power demand of a Microgrid because of its inertia. Hence, Battery Energy Storage System(BESS) is used for quick balancing[81]. In order to regulate the frequency deviation of the Microgrid for any change in supply or load, a controller is needed to ensure that the setpoints of the Microgrid are at optimal requirement [82].

Further, the design of a simplified model of the realistic system is created to model uncertainties. In addition to this, model uncertainty is introduced due to lack of sufficient knowledge and difficulties in precision measurement of parameters [83]. Thus, if the real Microgrid parameters and the assumed model differs by some extent, then the secondary frequency controller should able to tackle the parametric uncertainty and stabilize the system [84].

In view of the above, there is a need of robust Load Frequency Controller (LFC) to mitigate the oscillation and to ensure that the dynamic performance of the autonomous Microgrid and Multi-Microgrid Systems is within the satisfactory limits even with parametric uncertainty and irregular power supply from RES. Considering the above facts, an efficient and appropriate LFC technique is required for stable operation of system.

As logically proved by the No Free Lunch (NFL) Theorem, no meta-heuristic technique is best suitable for solving all optimization problems[85] [86]. A meta-heuristic technique providing a promising solution to a set of the problem may fail to identify the global solution to a different set of problems. Thus, various meta-heuristic techniques are addressed in this chapter, for tuning the gains of the PID controllers.

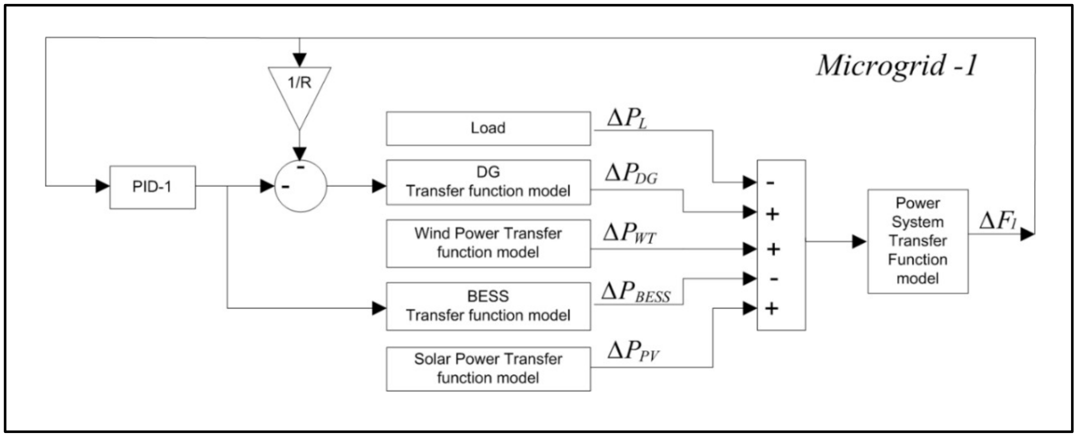

Fig-5.2: Block diagram of stand-alone Microgrid

It is noticed that Grey Wolf Optimization (GWO) has been attempted in various disciplines such as Engineering, Networking, Environmental modelling applications, Machine learning, Image processing, Medical and Bioinformatics due to its impressive nature of exploration and exploitation ability in locating the optimal solution [87]. In view of this, the GWO algorithm has been attempted for fine-tuning the gains of PID controller for dynamic stability of the considered test systems with step load changes, incorporating RES and parametric variation.

5.2 Modelling of Multi-Microgrid System

The Block diagram of stand-alone single Microgrid and Multi-Microgrid Systems are shown in Fig-5.2 and Fig-5.3 respectively. Both the system consists of a Diesel Engine Generator, Wind Turbine Generator, Solar Photo-Voltaic system and Battery Energy Storage System. The load demand is mainly being supplied by the RES.

The proposed systems are very reliable because whenever RES sources fail to feed the desired load demand due to the intermittent nature of Wind and Solar irradiance, the Diesel Generator will act cushion to deliver the balance load demand. BESS is used for backup supply for short time duration to account dynamic stability of the system. The excess energy generated by the RES will be used by the Battery for its charging. Further, Microgrid Systems can be expanded in case the load demand is enhanced.

PID controller output is connected to Diesel Engine Generator (DEG) and BESS in each individual microgrid to mitigate the frequency deviation in both the Microgrids and also variation in tie-line power flow by varying the active power support, so as to make zero steady-state error in frequency response and tie-line power flow and also for obtaining a quicker steady-state response.

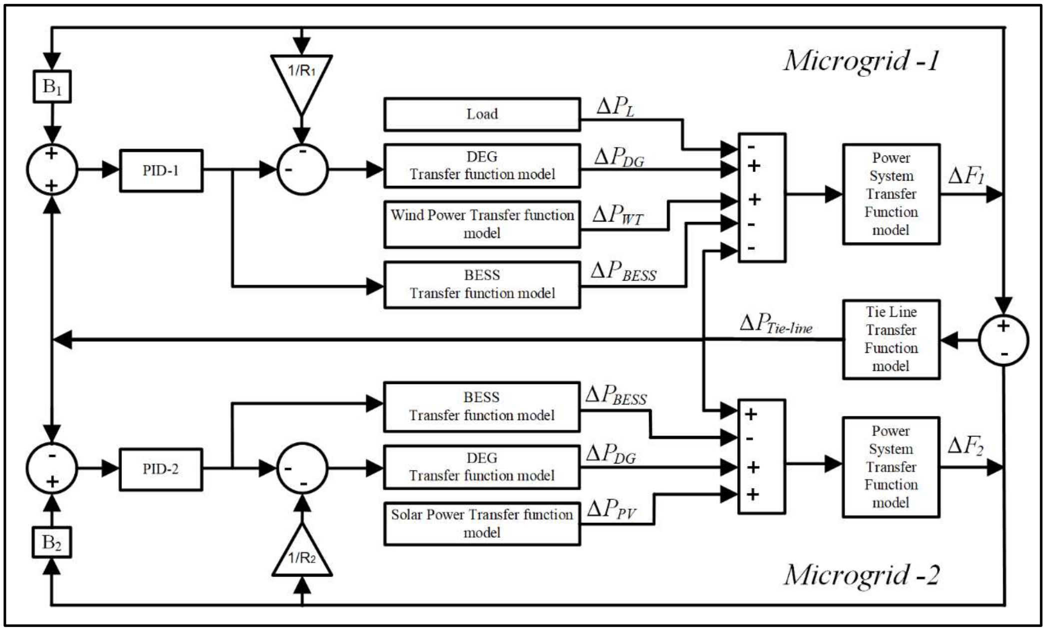

Fig-5.3: Block diagram of Multi-Microgrid System connected with Tie-line

5.2.1 Diesel Engine Generator

The block diagram of the first-order transfer function model of DEG [79] has shown in the Fig-5.4. The equilibrium between power demand and its generation in an autonomous Microgrid due to variation in Solar power and Wind power maintained by DEG with Speed Governor control action.

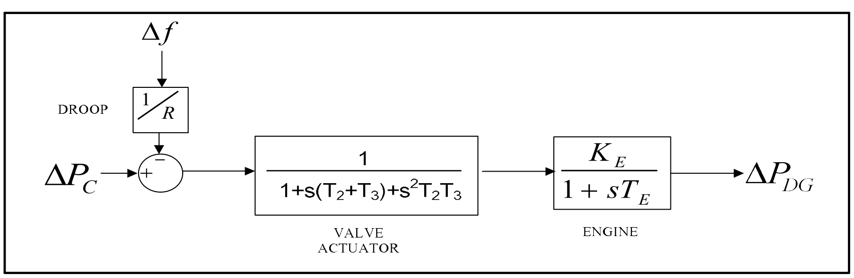

Fig-5.4: Block Diagram of Diesel Engine Generator Transfer Function model

5.2.2 Wind Turbine model

The Wind turbine is used to exploit the kinetic energy from wind energy and it is converted as mechanical energy (P_{mech}). This mechanical energy is then transferred to the rotor of the generator. The Wind turbine consists of a turbine-generator shaft mechanism, which is used to convert the rotor rotation into electrical energy [77].

$$P_{wt} = \left\{ \begin{array}{cc} 0, & V_w < V_{cut-in} \\ 0, & V_w > V_{cut-o} \\ P_{rated}, & V_{rated} \leq V_w \leq V_{cut-out} \\ \begin{array}{c} 0.001312V_w^6 - 0.04603V_w^5 + 0.3314V_w^4 + \\ 3.687V_w^3 - 51.1V_w^2 + 2.33V_w + 366 \end{array} & else \end{array} \right\} \tag{5.1}$$

$$\Delta P_{wt} = \left\{ \begin{array}{cc} 0, & V_w < V_{cut-i} \\ 0, & V_w > V_{cut-out} \\ 0, & V_{rated} \leq V_w \leq V_{cut-out} \\ \begin{array}{c} [0.007872V_w^5 - 0.23015V_w^4 + 1.3256V_w^3 + \\ 11.061V_w^2 - 102.2V_w + 2.33].\Delta V_w \end{array} & else \end{array} \right\} \tag{5.2}$$

The power output from the wind turbine has been formulated as the sixth order polynomial by a curve fitting technique [52] as given in Equation-(5.1). For small-signal stability of the system, the rate of change of Wind Power output[88] is governed by Equation-(5.2). It has been considered for assessing the stability of the proposed systems. Fig-5.5 represents the block diagram of the first-order transfer function model of WTG.

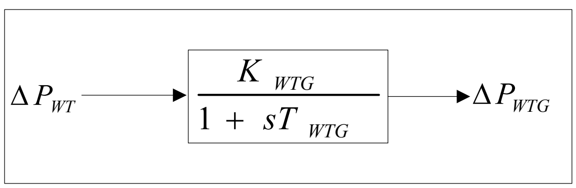

Fig-5.5: Wind Turbine First Order Transfer Function model

5.2.3 Battery Energy Storage System

Due to the high inertia of the rotating mass of conventional frequency regulating device like DEG, it is not suitable for frequency regulation for dynamic load variations [79]. In view of this, there is a need to introduce a fast and dynamic frequency regulating device which is Battery Energy Storage System (BESS) considering sudden load variations[89]. The first-order transfer function model of BESS is given in the Fig-5.6.

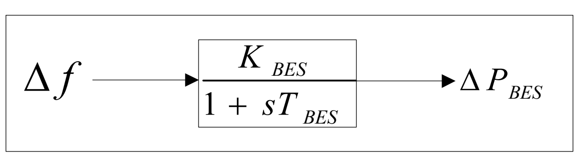

Fig-5.6: BESS First Order Transfer Function model

The BESS can be either in charging mode or discharging mode based on the system frequency as shown in the Table-5.1.

Table-5.1: Battery charging status based on system frequency

Δf	**BESS status**
Positive	Charging
Negative	Discharging

5.2.4 Solar Power

Practical Solar irradiance data has been obtained from the National Renewable Energy Laboratory (NREL) for a specific duration and the profile of Solar PV Power is presented in Section-5.9.3. The first-order transfer function model [79] of Solar PV Power is given in the Fig-5.7, where $\Delta\Psi$ represents the change in Solar irradiance.

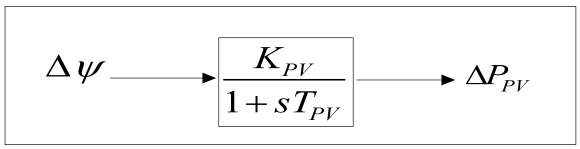

Fig-5.7: Solar Power First Order Transfer Function model

5.3 Problem Formulation

Frequency deviation of Microgrid and Multi-Microgrid System and tie-line power flow deviation (only in case of Multi-Microgrid System) are considered as the reference for optimal tuning of PID controller gains. Integral Time multiplied Absolute Error (ITAE) has been considered as fitness function which is the performance index in fine-tuning the PID controllers gains due to its advantages of smaller overshoots/undershoots and oscillations compared to other performance indices (i) Integral Squared Error (ISE) which gives minimum overshoot but more settling time, (ii) Integral Absolute Error (IAE) which produces slower response than ISE in LFC controller design, (iii) Integral Time-weighted Squared Error (ITSE) wherein for a sudden change in input, produces larger controller output as stated in reference [52]. The fitness function ITAE[90] is governed by Equation-(5.3) and the boundaries for gains of the PID controller are defined in Equation-(5.4).

$$Fitness = Minimize\{ITAE\} = Min\left\{\int_0^{T_{sim}} t.(|\Delta f_1| + |\Delta f_2| + |\Delta P_{tie-line}|).dt\right\} \quad (5.3)$$

Subjected to PID gain limits

$$\left.\begin{aligned} K_p^{min} \le K_p \le K_p^{max} \\ K_i^{min} \le K_i \le K_i^{max} \\ K_d^{min} \le K_d \le K_d^{max} \end{aligned}\right\} \quad (5.4)$$

Area Control Error (ACE) is given as input for the PID controller, which is defined as the difference between the error signal of tie-line flow $\Delta P_{tie-line}$ and Bias (B) times the change in i^{th} Microgrid System frequency. For stand-alone Microgrid system, the ACE is simply Bias times the change in frequency as there is no tie-line. The ACE_i for i^{th} Microgrid System is defined in Equation-(5.5). M

$$ACE_i = B_i \Delta f_i + \Delta P_{tie,ij} \tag{5.5}$$

It is noteworthy to highlight that for controlling the power system dynamic, these load frequency controllers are designed in the off-line mode as planning studies considering various scenarios before placing them into online action. Accordingly, the Grey Wolf Optimization (GWO) Controller can be used for tuning the PID gains during the off-line mode before incorporating in original system operation [52].

5.4 Optimization of PID Controller Gains

Load frequency controller problem exemplifies the need of PID controller. Designing and tuning a PID controller for LFC application that has multiple objectives i.e., minimum overshoot/undershoot and smaller settling time, is a difficult task for a Design Engineer. Poor control performance can be noticed with fixed parameters of the conventional PID controller. When system parameters i.e., gain and time constants change with operating conditions, conventional controllers result in sub-optimal corrective action and hence fine-tuning is required. This necessitates the development of tools that can assist Control Engineers to achieve the best PID control for the entire operating envelope of a given process. Thus, in this chapter, meta-heuristic techniques are used for tuning the PID controller gains of Multi-Microgrid System. The meta-heuristic techniques applied for tuning PID gains are as follows

a) Grey Wolf Optimization(GWO)
b) Teaching Learning Based Optimization(TLBO)
c) Jaya Algorithm
d) Particle Swarm Optimization(PSO)

The brief introduction of various optimization techniques is as follows

5.5 Grey Wolf Optimization

Grey Wolf Optimization (GWO) is a novel Swarm Intelligence technique. Grey Wolf belongs to the category of the canidae family. This algorithm has been developed from the behaviour of Grey wolves by Seyedali Mirjalili and et al. [86]. Grey Wolves are considered to be the best predators in finding the prey. A very strict dominant hierarchy of the pack, as shown in Fig-5.8, is an interesting behaviour in Grey Wolves.

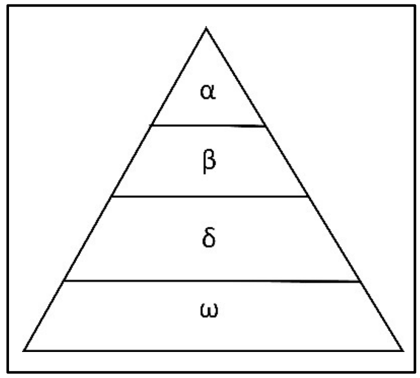

Fig-5.8: Hierarchy of Grey Wolves

Alpha(α) is the most powerful wolf in the pack and it can be either a male or a female. Decisions regarding hunting, migration, sleeping place, feeding are taken by the Alpha Wolf. An interesting aspect is that the Alpha Wolf is that it must be best in managing the pack but not essentially the strongest member of the pack, which means that organization and discipline are more important than strength.

The next level in the hierarchy is Beta(β) wolves. They assist the Alpha in decision-making. When the Alpha in the pack is ill or dead, then they lead the pack. They act as an advisor to the Alpha and discipliner for the pack.

Delta(δ) is the third category in the hierarchy. They should report to the Alpha and the Beta but dominate the Omega. Scouts, caretakers and hunters belong to the Delta category.

Omega(ω) is the last in the ranking and plays the role of scapegoat. They are the last wolves allowed to eat. The importance of these wolves is that due to the non-presence of these wolves' leads to internal fighting and problems among the pack.

5.5.1 Mathematical modelling of GWO Algorithm

In this section, the social hierarchy of Grey Wolves, tracking, encircling and attacking the prey are mathematically modelled in [53].

5.5.1.1 Social Hierarchy

In this optimization technique Alpha (α), Beta(β) and Delta(δ) are considered as the first, second and third best solutions respectively and the rest of the solutions of the pack are considered as Omega(ω). These Omega (ω) Wolves follow the best wolves in the pack.

5.5.1.2 Encircling

During the hunting process, the first step of the Grey Wolves is to encircle the prey. As the encircling depends on the position of the prey, the mathematical model of encircling [86] is as defined in the Equation-(5.6).

$$\bar{X}(t+1) = \bar{X}_P(t) - \bar{A}.\bar{D} \tag{5.6}$$

where, $\bar{X}(t+1)$ indicates the next location of the Grey Wolf, $\overline{X_p}(t)$ denotes current position of prey and t denotes current iteration.

$\bar{A}$ is a coefficient matrix and $\bar{D}$ is a vector that depends on the location of the prey which is computed as per the Equation-(5.7).

$$\bar{D} = |\bar{C}.\bar{X}_P(t) - \bar{X}(t)| \tag{5.7}$$

The Equation-(5.6) and Equation-(5.7) represents the movement of the Grey Wolf towards the prey. The random components A and C are computed using the Equation-(5.8) and Equation-(5.9) respectively. These random components simulate different step sizes and movement speeds of the Grey Wolves for encircling the prey.

$$\bar{A} = 2\bar{a}.\bar{r}_1 - \bar{a} \tag{5.8}$$

$$\bar{C} = 2.\bar{r}_2 \tag{5.9}$$

$\overline{r_1}$, $\overline{r_2}$ are the random vectors in [0, 1] and the components of $\bar{a}$ are linearly decreases from 2 to 0 as number of iterations progresses and is defined as per the Equation-(5.10)

$$\bar{a} = 2 - 2(\frac{iter}{itermax}) \tag{5.10}$$

Where *iter* – current iteration and *itermax* – maximum number of iterations, the limits of $\bar{A}$ = [-2$\bar{a}$ 2$\bar{a}$]

5.5.1.3 Hunting

Recognizing the prey location and encircling the prey is the ability of the Grey Wolves. With the equations presented in the Encircling phase, the Grey Wolves relocate their position to anywhere in the search space. However, this is not enough to simulate to social intelligence of Grey Wolves. As mentioned above, social hierarchy plays a key role in hunting and also for the survival of the pack. To simulate social hierarchy, three best solutions are considered to be Alpha(α), Beta(β) and Delta(δ). The mathematical model of the hunting strategy of the Grey Wolves has been described in [87][86][53]. For the sake of simplicity, it is considered that, there is only one solution belong to each class in GWO. Alpha Grey Wolf guides the hunting process. Even Beta and Delta Grey Wolves assist in the hunting process. To simulate the hunting process mathematically, as stated earlier, Alpha (the best solution), Beta and Delta Wolves are assumed to have knowledge of the potential location of prey as the global optimum of optimization problems is unknown. The above assumption is reasonable because they are the best solutions in the entire population. The first three best solutions (i.e., α, β and δ) obtained are saved and the rest of the population updates their position based on the position of the first three best solutions. The mathematical model for updating the position of other wolves is governed by Equation-(5.11).

$$\bar{X}(t+1) = \frac{\bar{X}_1 + \bar{X}_2 + \bar{X}_3}{3} \tag{5.11}$$

The values of $\bar{X}_1$, $\bar{X}_2$ and $\bar{X}_3$ are calculated as using to Equation-(5.12) to Equation-(5.14).

$$\bar{X}_1 = \bar{X}_\alpha - \bar{A}_1.\bar{D}_\alpha \tag{5.12}$$

where $\bar{D}_\alpha = |\bar{C}_1.\bar{X}_\alpha - \bar{X}|$

$$\bar{X}_2 = \bar{X}_\beta - \bar{A}_2.\bar{D}_\beta \tag{5.13}$$

where $\bar{D}_\beta = |\bar{C}_2.\bar{X}_\beta - \bar{X}|$

$$\bar{X}_3 = \bar{X}_\delta - \bar{A}_3.\bar{D}_\delta \tag{5.14}$$

where $\bar{D}_\delta = |\bar{C}_3.\bar{X}_\delta - \bar{X}|$

5.5.1.4 Attacking Prey

As stated above, the Grey Wolves encircle and hunt the prey. Once the prey stops moving, the hunting process gets finished by attacking the prey. The mathematical model of approaching the prey is modelled by decreasing the value of $\bar{a}$ which in turn decrease the fluctuating range of $\bar{A}$ in the random value interval of -2 to 2. The exploration of prey is emphasized when the value of A>1 or A<-1 and exploitation is emphasized when -1<A<1. The exploration and exploitation behaviour of the algorithm based on the value of A has been presented by running the program five times in the reference [87]. Though the agents update their position for attacking the prey, based on the location of α, β and δ Wolves and the values of parameters $\bar{A}$, $\bar{D}$ and $\bar{a}$, the algorithm may prone to stagnate at local optimum. Hence, there is a need for more parameters for exploration.

5.5.1.5 Search for Prey

In addition to the parameters defined above, there is another parameter favouring exploration of the algorithm is $\bar{C}$. The value of $\bar{C}$ varies randomly from 0 to 2 in contrast to $\bar{A}$, which decreases linearly from 2 to 0. The contribution of prey in defining the next position of wolves is decided by the value of $\bar{C}$. When the value of parameter $\bar{C} > 1$, the wolves are attracted more towards prey. Since the value of $\bar{C}$ is randomly generated in the algorithm, the emphasis is more towards exploration from starting to final iteration which avoids local optimum.

5.5.2 Algorithm for LFC problem using GWO-PID Controller

As mentioned above, the GWO controller has been implemented in this work for optimal tuning of PID gains for LFC of stand-alone Microgrid and Multi-Microgrid Systems. The algorithm implementation steps are enumerated as follows.

1. Initialize the population size (P_{size}) , number of control variable (n) ($ie., K_p, K_I$ $and\ K_D\ for\ each\ controller$), boundaries of PID controller gains ($K_P^{min}, K_P^{max}, K_I^{min}, K_I^{max}, K_D^{min}$ $and\ K_D^{max}$), itermax.
2. Generate the population (Pop) randomly with in their limits.
3. Run the Simulink Program and evaluate the fitness (ITAE) values for all the populations using Equation-(5.3).
4. Sort the population according to fitness. Assign Alpha(α), Beta(β), Delta(δ) and Omega(ω) Wolves based on fitness values.
5. Update the positions of α, β and δ Grey Wolves based on fitness value as follows

$$
\begin{aligned}
&For\ i = 1\ to\ P_{size}\\
&\quad if\ (fitness(pop(i)) > fitness(\alpha)\\
&\qquad\qquad \alpha = pop(i)\\
&\quad end\\
&\quad if\ (fitness(pop(i)) < fitness(\alpha)\ \ and\ \ fitness(pop(i)) > fitness(\beta)\\
&\qquad\qquad \beta = pop(i)\\
&\quad end\\
&\quad if\ (fitness(pop(i)) < fitness(\alpha)\ \ and\ \ fitness(pop(i))\\
&\qquad\qquad\qquad < fitness(\beta)\ and\ fitness(pop(i)) > fitness(\delta)\\
&\qquad\qquad \delta = pop(i)\\
&\quad end\\
&end
\end{aligned}
$$

6. Update the position of Grey Wolves using Equation-(5.11) to Equation-(5.14).
7. Check whether Grey Wolves are violating their limits. If violated, keep within their limits.
8. Repeat the above Steps from Step-3 to Step-7 until convergence criterion is satisfied.

9. Print the *α values (i.e., PID controllers Gain values), Time-domain specifications, ITAE value.*

5.5.3 Flowchart for LFC problem using GWO-PID Controller

The flowchart for the implementation of GWO-PID Controller for optimal tuning of PID gains is shown in the Fig-5.9.

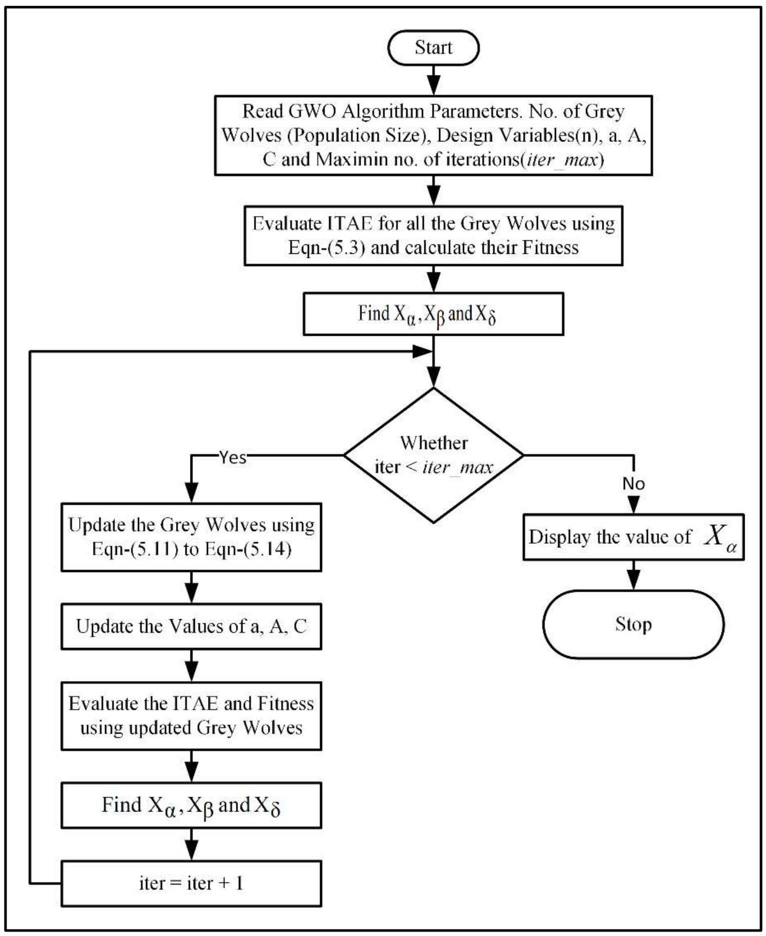

Fig-5.9: Flowchart of GWO-PID Controller for LFC in Multi-Microgrid System

5.6 Teaching Learning Based Optimization

Teaching Learning Based Optimization (TLBO) technique [91] is developed by Prof. R.Venkata Rao, and it is algorithm-specific parameter-free optimization technique. This algorithm is based on the output of the Learners in a class based on the influence of a Teacher. It mimics the Teaching-Learning ability of the Teacher and Learner in a classroom.

5.6.1 Mathematical modelling of the TLBO Algorithm

The mathematical modelling of the TLBO algorithm involves two phases (a) Teacher Phase (b) Learner Phase. The brief discussion of these phases is explained as below.

5.6.1.1 Teacher Phase

The initial phase of the TLBO algorithm is the Teacher Phase. In this phase, learners' acquire knowledge from the teacher. In this algorithm, the teacher is considered as the most knowledgeable among the class. The mean result of the class in a particular subject is reflected by the teacher capability. The teacher always tries to increase the mean result of the class in the subject dealt.

Similar to other Meta-heuristic techniques, the TLBO also starts with a set of initial solutions known as population. The objective function value and thus, the fitness value is evaluated for the population. As the teacher is more knowledgeable among all the population, the best fitness value solution among the population is treated as the teacher. As each student possess different knowledge level, it is impractical for the teacher to bring all the students to the same knowledge level. Thus, a teacher, after teaching, increases the mean knowledge of the class to better mean level. The mathematical representation of the Teacher phase is as follows.

Each solution in the TLBO algorithm is represented as $X_{j,k,i}$, where j represents design variable and it varies as $j=\{1,2,\ldots n\}$, k represent population member & it varies as $k=\{1,2,\ldots P_{size}\}$ and i represents iteration number and it varies as $i=\{1,2,\ldots iter\_max\}$.

The teacher is identified as the best fitness solution in the population and is represented as ($X_{j,best,i}$). As the teacher tries to enhance the mean result of the class, the increase in mean of the subject taught by the teacher is evaluated as per Equation-(5.15)

$$Difference\_Mean_{j,k,i} = r_{j,i}(X_{j,kbest,i} - T_F M_{j,i}) \tag{5.15}$$

where, $r_{j,i}$ is a random number varies between 0 to 1. T_F is the teaching factor which reflects the capability of the teacher. It is a random value with equal probability in the range of 1 to 2 and is evaluated as per Equation-(5.16).

$$T_F = round[1 + rand(0,1)\{2 - 1\}] \tag{5.16}$$

The existing solutions ($X_{j,k,i}$) are updated with the evaluate *Difference_Mean* as per Equation-(5.17).

$$X^1_{j,k,i} = X_{j,k,i} + Difference\_Mean_{j,k,i} \tag{5.17}$$

If the updated solution ($X^1_{j,k,i}$) fitness value is better than the previous solution ($X_{j,k,i}$), then retain the updated solution otherwise retain the previous solution. With this, the Teacher phase is completed. These updated solutions set is given as the inputs to the Learners phase.

5.6.1.2 Learner Phase

The next and the final part of this optimization technique is the Learner phase. In this phase, the students(solutions) by interaction among themselves, acquire knowledge. Each student interacts with any other student selected randomly. If the randomly selected student has more knowledge than the corresponding student, then the corresponding student enhances his knowledge by interaction. The mathematical expressions for the Learner phase is presented as follows.

From the updated population in the teacher phase, for each learner P, select any other learner Q in the population, such that $X^1_{j,P,i} \neq X^1_{j,Q,i}$. If the fitness of $X^1_{j,P,i}$ is better than the fitness of $X^1_{j,Q,i}$ then, the Equation-(5.18) is used for updation otherwise Equation-(5.19) is used.

$$X''_{j,P,i} = X'_{j,P,i} + rand_{j,i}(X'_{j,P,i} - X'_{j,Q,i}) \tag{5.18}$$

$$X''_{j,P,i} = X'_{j,P,i} + rand_{j,i}(X'_{j,Q,i} - X'_{j,P,i}) \tag{5.19}$$

Once updated, the present iteration of the TLBO algorithm is completed and this updated population becomes the input to the Teacher phase of the next iteration. This process is continued until termination criteria is satisfied.

5.6.2 Algorithm for LFC problem using the TLBO-PID Controller

1. Initialize the Population size (P_{size}), number of Control Variable (*n*), boundaries of PID Controller Gains, Maximum no. of iterations (*iter_max)*.
2. Randomly initialize the population ($X_{j,k,i}$) with in their lower and upper limits of each Control Variable.
3. Initialize the iteration counter, i.e., i =1.
4. Evaluate the Integral Time multiplied Absolute Error (ITAE), which is the performance index for all the particles using Equation-(5.3) using MATLAB Simulink program and their corresponding fitness value.
5. *Teacher Phase*: Identify the Best solution ($X_{j,best,i}$) among the population based on the fitness values in the i^{th} iteration. Assign it as the teacher ($X_{j,best,i}$)

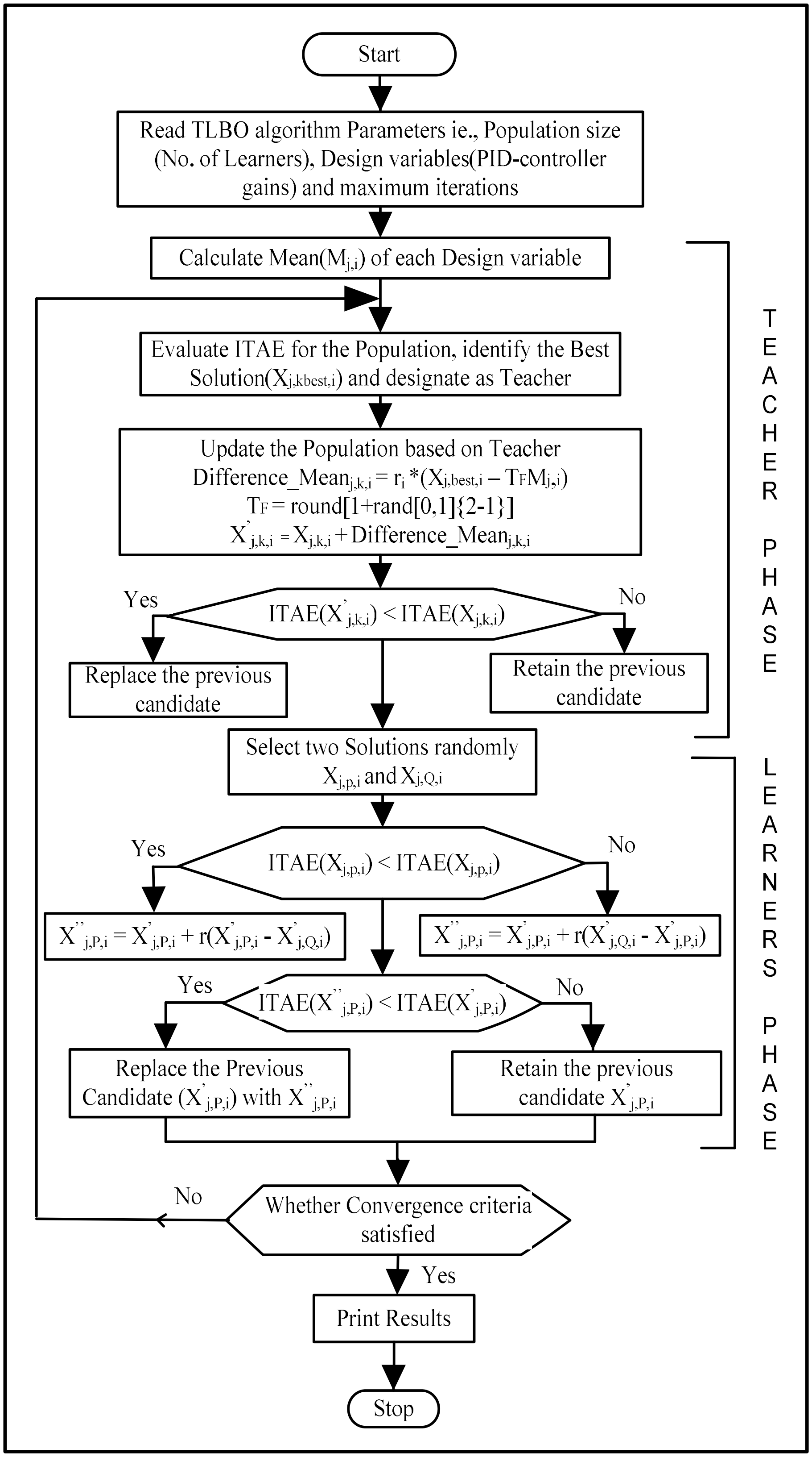

Fig-5.10: Flowchart of TLBO-PID controller for LFC in Multi-Microgrid System

6. Update the Learners ($X^1_{j,k,i}$) using the Equation-(5.15) to Equation-(5.17).
7. Check whether the updated Learner ($X^1_{j,k,i}$) fitness is better than the initial Learner ($X_{j,k,i}$) fitness. If Yes, replace the initial Learner ($X_{j,k,i}$) with updated Learner ($X^1_{j,k,i}$), otherwise, retain the initial Learner ($X_{j,k,i}$) and discard the updated Learner ($X^1_{j,k,i}$). i.e., $X^1_{j,k,i} = X_{j,k,i}$, with this step, Teacher Phase ends. The updated Learners in this Phase become the input for the Learner Phase.
8. Learners Phase: In this phase, for a learner P, select any other Learner Q such that $X^1_{j,P,i} \neq X^1_{j,Q,i}$. Update the Learner(P) based on fitness of Learner(Q) using Equation-(5.18) or Equation-(5.19).
9. Check the fitness of the updated Learner P.

   If *fitness* ($X''_{j,P,i}$) > *fitness* ($X^1_{j,P,i}$),

   replace $X^1_{j,P,i}$ with $X''_{j,P,i}$ in the population set

   else,

   discard the updated Particle $X''_{j,P,i}$.
10. Increment *iteration counter i=i+1.*
11. Repeat the above Steps (Step-4 to Step-10) until convergence criterion is satisfied.
12. Stop the program and display the *Optimal Gain values of PID Controllers*, *Time-domain specifications, ITAE value*.

5.6.3 Flowchart for LFC problem using TLBO-PID Controller

The flowchart of the TLBO Algorithm for implementing the LFC problem in the Multi-Microgrid System is depicted in the Fig-5.10.

5.7 Jaya Algorithm

Jaya Algorithm is a novel algorithm-specific parameter-free optimization technique. The steps involved in this optimization technique are explained in detail in the section-2.4 of the chapter-2. In view of this, only algorithm for solving the LFC problem of the Multi-Microgrid System is detailed as below.

5.7.1 Algorithm for LFC problem using JAYA-PID Controller

1. Initialize the Population size (P_{size}), number of Control Variable (n), Upper and Lower boundaries of PID Controller gains, maximum no. of iterations (*iter_max)*.

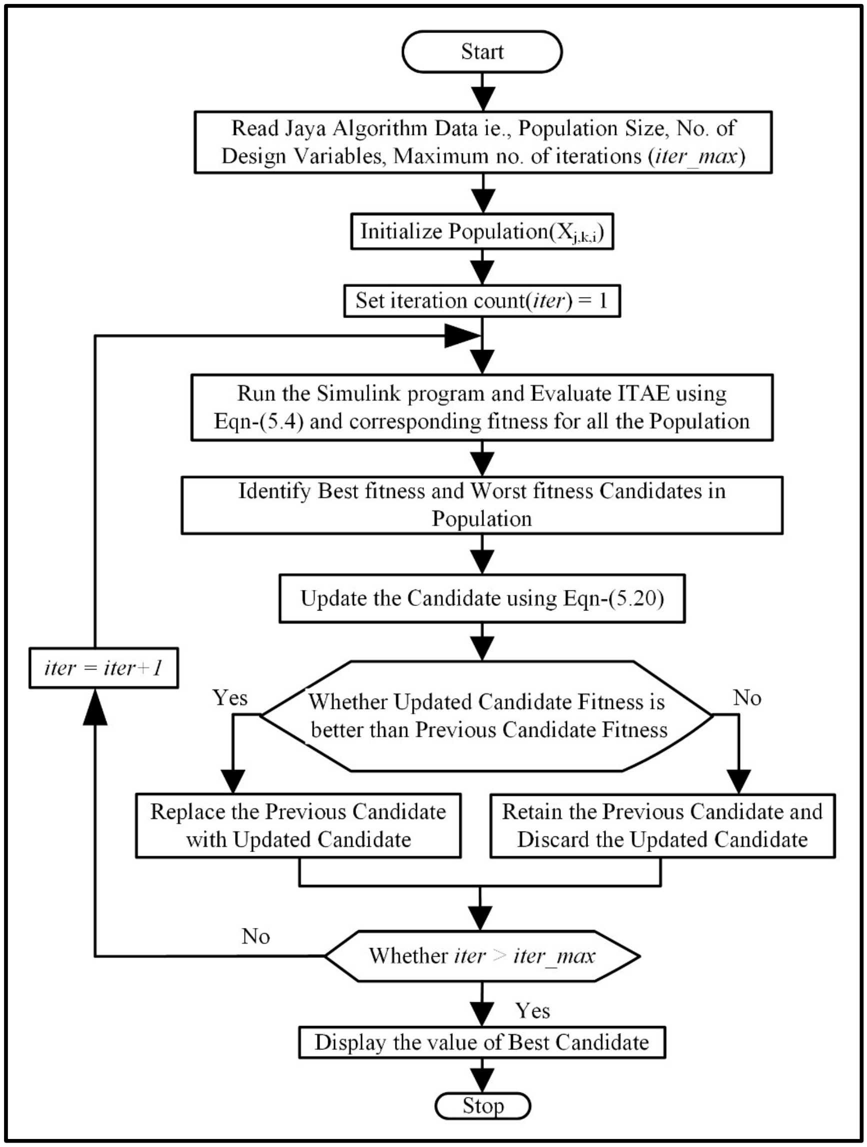

Fig-5.11: Flowchart of JAYA-PID Controller for LFC in Multi-Microgrid System

2. Randomly initialize the population ($X_{j,k,i}$) with in their lower and upper limits of each control variable, where j varies $\{1,2,\ldots n\}$, k varies $\{1,2,\ldots P_{size}\}$and i varies $\{1,2,\ldots iter\_max\}$.
3. Initialize the iteration counter, ie i =1.
4. Evaluate the performance index (ITAE) and calculate the fitness value, upon running the MATLAB Simulink program for all the particles using Equation-(5.3).
5. *Identification Phase*: Identify the Best solution ($X_{j,best,i}$) and the Worst solution ($X_{j,worst,i}$) among the population based on the fitness values in the i^{th} iteration.
6. Set *Particle counter k = 1*

7. *Updation Phase*: Update the particle using the following Equation-(5.20)

$$X_{j,k,i}^{1} = X_{j,k,i} + r_{1,j,i}\left(X_{j,best,i} - |X_{j,k,i}|\right) - r_{2,j,i}\left(X_{j,worst,i} - |X_{j,k,i}|\right) \quad (5.20)$$

8. Check whether the updated particle is violating their limits. If violated, keep within their limits.
9. *Comparision Phase*: Evaluate the fitness value for the updated particle ($X_{j,k,i}^{1}$).

   If *finess* ($X_{j,k,i}^{1}$) > *fitness* ($X_{j,k,i}$),

   Replace $X_{j,k,i}$ with $X_{j,k,i}^{1}$

   else, discard the updated particle ($X_{j,k,i}^{1}$)
10. Increment *particle counter k=k+1* and repeat above *Steps(7-9)* until *k*=P_{size}
11. Increment *iteration counter i=i+1.*
12. Repeat the above Steps (4 to 11) until convergence criterion are satisfied.
13. Stop the program and display the *Optimal Gain values of PID Controllers*, *Time-domain specifications, ITAE value*.

5.7.2 Flowchart for LFC problem using JAYA-PID Controller

The flowchart for solving the Load Frequency Control problem using Jaya algorithm for tuning the PID Controller gains in the MMG is presented in Fig-5.11.

5.8 Particle Swarm Optimization

Particle Swarm Optimization (PSO) was originally designed and introduced by Eberhart and Kennedy [92]. The PSO is a population-based search algorithm and its basic idea was originally inspired by simulation of the social behaviour of animals such as bird flocking, fish schooling. It is based on the natural process of group communication to share individual knowledge when a group of birds or insects search food or migrate and so forth in a searching space, although all birds or insects do not know where the best position is. But from the nature of the social behaviour, if any member can find out a desirable path to go, the rest of the members will follow quickly.

In PSO, each member of the population is called a *Particle* and the population is called a *Swarm*. Starting with a randomly initialized population and moving in randomly chosen directions, each particle goes through the searching space and remembers the best previous positions of itself and its neighbours. Particles of a swarm communicate their position to each other as well as dynamically adjust their position and velocity derived from the best position of all particles. The next step begins when all particles have been moved. Finally, all particles tend to fly towards better and better positions over the searching process until the swarm move close to an optimum of the fitness function. Since adjusting position depends on its own experience and that of its peers, the PSO algorithm is a member of Swarm Intelligence [93].

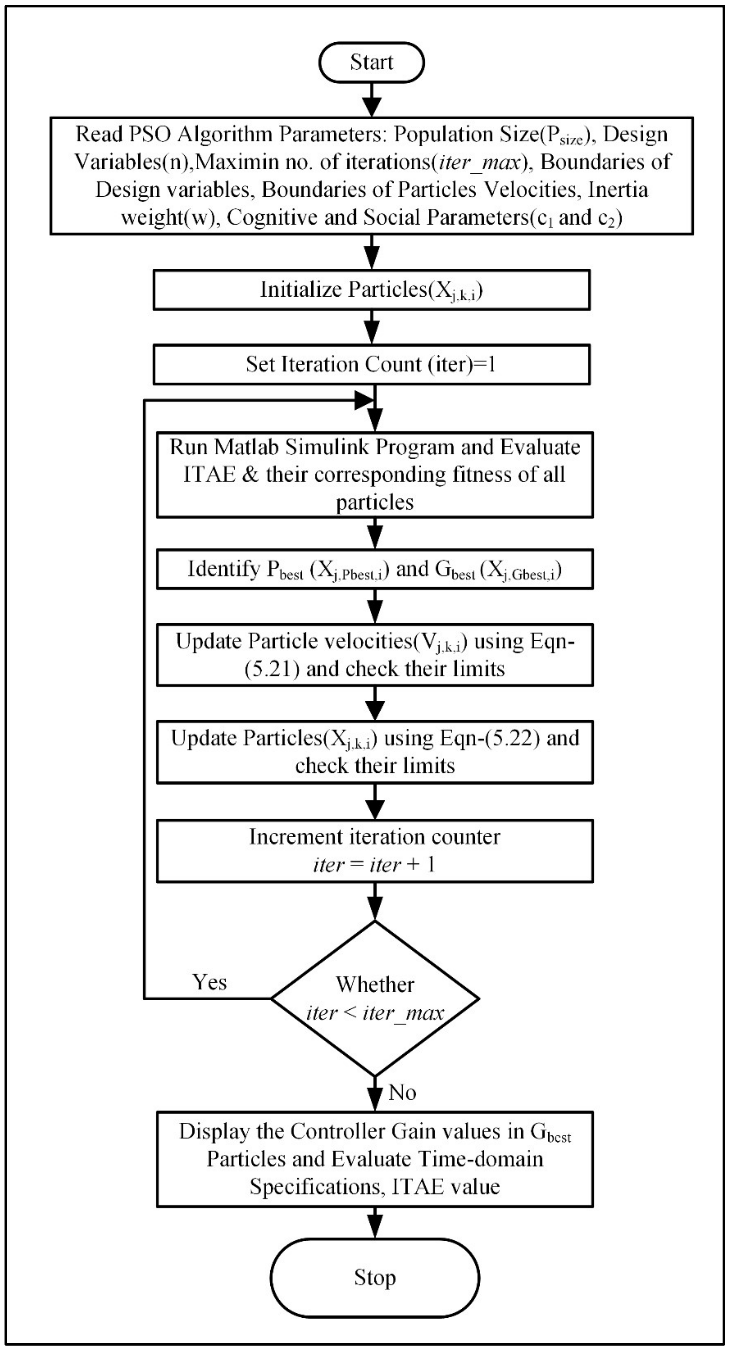

Fig-5.12: Flowchart of PSO-PID Controller for LFC in Multi-Microgrid System

The PSO method is becoming very popular because of its simplicity of implementation as well as the ability to swiftly converge to a good solution. It does not require any gradient information of the function to be optimized and uses only primitive mathematical operators.

As the PSO algorithm is well-known, the algorithm for implementation of LFC of Multi-Microgrid System is described as follows.

5.8.1 Algorithm for LFC problem using PSO-PID Controller

1. Initialize the Population size (P_{size}), Number of Control Variable (n), Boundaries of PID Controller Gains, maximum number of iterations (*iter_max)*, Boundaries of velocities (V_k^{max}), Inertia weight (w), Cognitive and Social parameters ($c_1$and c_2).
2. Initialize the particles in random positions within the boundaries of each control variable.
3. Initialize the particle velocity within their boundaries.
4. Initialize the iteration counter, ie i =1.
5. Running the MATLAB Simulink program and evaluate the performance index (ITAE) value for all the particles using Equation-(5.3).
6. Calculate the fitness value for all the particles.
7. Identification Present Population best particle (P_{best}) and Global Best Particle (G_{best}) among the iterations.
8. Set Particle counter k = 1.
9. Update the Particle Velocity

$$V_{j,k,i} = w_i V_{j,k,i} + c_1 r_1 \left(P_{best_{j,k,i}} - X_{j,k,i}\right) + c_2 r_2 (G_{best_{j,k,i}} - X_{j,k,i}) \tag{5.21}$$

10. Check for velocity limits.
11. Update the Particle

$$X_{j,k,i}^1 = X_{j,k,i} + V_{j,k,i} \tag{5.22}$$

12. Check whether the updated particle is violating their limits. If violated, keep within their limits.
13. Increment particle counter *k=k+1* and repeat Step-(8) to Step-(12) until k=P_{size}
14. Increment iteration counter *i=i+1*.
15. Repeat the above Step-(5) to Step-(14) until convergence criterion is satisfied.
16. Stop the program and display the *Optimal Gain values of PID Controllers*, evaluate *Time-domain specifications, ITAE value*.

5.8.2 Flowchart for the LFC problem using PSO-PID Controller

The flowchart for tuning the PID Controller gain values for the LFC problem of the Multi-Microgrid System is presented in Fig-5.12.

5.9 Simulation Results and Analysis

The desirable properties of any control system are quick response and stability. It is worth mentioning that higher relative stability and better time-domain specifications can be obtained with smaller performance indices. The acceptability of controller has been established after making a critical investigation of system dynamics i.e., transient response specifications, peak overshoot/undershoot and settling time. For identification of robustness of a closed-loop control system, the dynamic behaviour of the Microgrid System is to be evaluated with diverse loading conditions and parametric variation. Accordingly, the dynamic stability of the system has been investigated with Step load perturbation, with the incorporation of the intermittent nature of RES and also with parametric uncertainty of the system.

The performance of the proposed GWO-PID controller is investigated in finding the optimal gains of PID Controller on a stand-alone Microgrid and Multi-Microgrid Systems. The simulation work has been carried out using MATLAB/Simulink software on Intel Core i3 processor, 4GB RAM, for studying the performance of the proposed controller. Due to the stochastic nature of meta-heuristic algorithm, the input parameters presented in Table-5.2 are selected after an exhaustive number of trails. The boundaries for the PID gains are opted between 0 and 5 after making several trial and errors.

Table-5.2: Input Parameter values of Various Meta-Heuristic optimization techniques

Algorithm		PSO	TLBO	JAYA	GWO
Common Parameters	P_{size}	50	50	50	50
	$itermax$	300	300	300	300
Algorithm specific parameters		$C_1 = 2.0$ $C_2 = 2.0$ $W_{min} = 0.1$ $W_{max} = 0.9$	NIL	NIL	$\bar{a}, \bar{A}, \bar{C}$

To assess the dominance of the GWO-PID Controller, the simulations are carried out on (a) Stand-alone Microgrid System and (b) Multi-Microgrid System, consisting of Diesel Engine Generator, BESS, Solar Power Generation, Wind Power Generation and load variations respectively. To verify the superiority of the proposed GWO-PID Controller in

Table-5.3: PID Gains obtained for various Controllers

Sl.No	Controller	PID-1 Gains			PID-2 Gains		
		K_p	K_i	K_d	K_p	K_i	K_d
1.	Conventional PID	4.3718	1.6559	4.0041	4.4381	1.6995	4.2908
2.	PSO-PID	4.9047	0.9176	0.9826	4.9484	0.0034	4.8686
3.	JAYA-PID	2.9498	1.3145	1.0514	4.3062	0.4766	1.4603
3.	TLBO-PID	4.9827	0.9186	2.6694	4.9889	0.0076	4.3625
4.	GWO-PID	4.9970	0.9861	4.9485	4.9997	0.0097	4.9992

improving the dynamic response under various scenarios, a detailed comparison of the results with various controllers in the literature has been performed. The various parameters (Transfer function gains and Time constants) considered in the Multi-Microgrid System are presented in Appendix-3. The PID controller gain values obtained by various controllers are presented in Table-5.3.

Table-5.4: ITAE values obtained for different Scenarios using various Controllers

ITAE values	Conventional PID	PSO-PID	JAYA-PID	TLBO-PID	GWO-PID
Scenario-1	0.01898	0.01467	0.027259	0.01416	0.01394
Scenario-2	0.04954	0.03924	0.063882	0.03802	0.03750
Scenario-3	0.62851	0.53994	0.813233	0.51307	0.49770
Scenario-4	0.14361	0.12929	0.180076	0.12889	0.12649
Scenario-5	0.80508	0.57100	0.791131	0.55893	0.54620
Scenario-6	0.15065	0.13056	0.183949	0.13033	0.12690
Scenario-7	0.83459	0.57857	0.810969	0.56507	0.55401

5.9.1 Scenario-1: Single Microgrid - Step Load disturbance

In this scenario, a single Microgrid with Diesel Engine Generator and BESS system only have been considered. A single-step load deviation of 6% is applied to the system, as shown in Fig-5.13. The frequency response of the system is presented in the Fig-5.14.

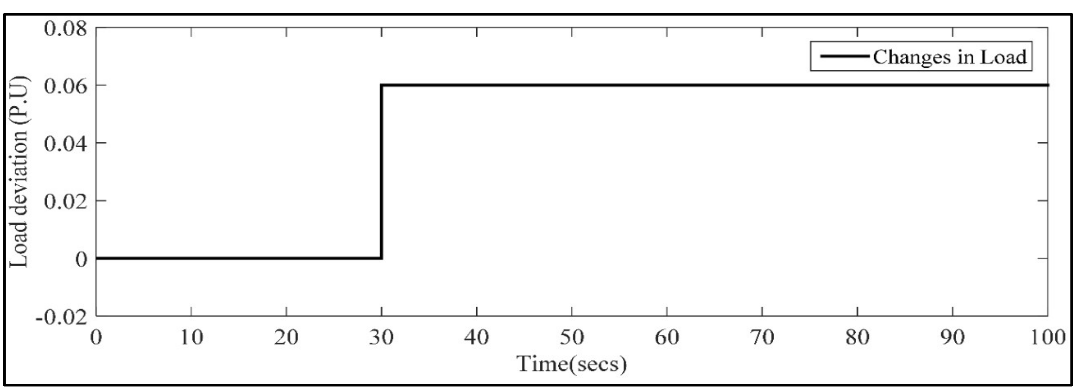

Fig-5.13: Step Load fluctuation

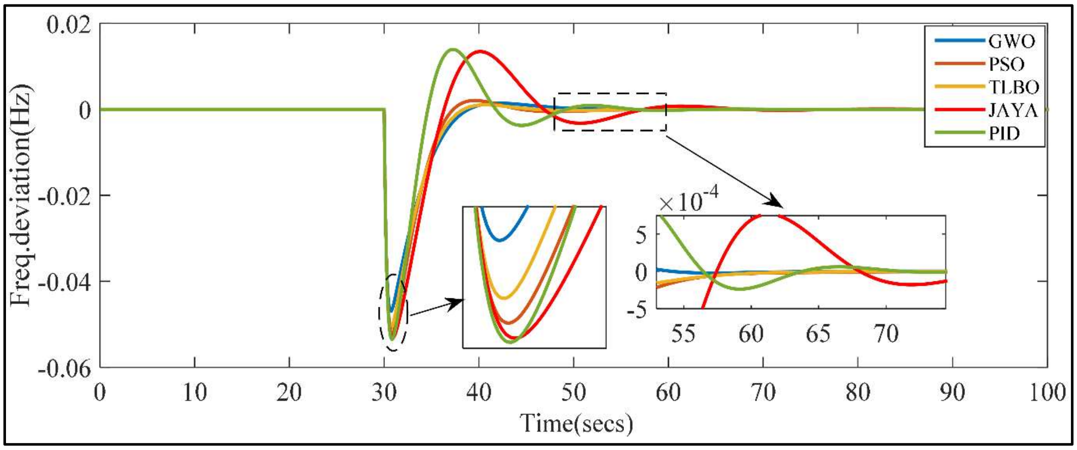

Fig-5.14: Comparison of Single MG frequency response of GWO-PID, PSO-PID,TLBO-PID, JAYA-PID and Conventional-PID Controllers

From the Table-5.5, it is noticeable that the proposed GWO-PID controller is having minimum overshoot of 0.047Hz and minimum settling time of 21secs (51-30=21) in comparison with other controllers. It is conspicuous from the Table-5.4 that the ITAE values obtained with GWO-PID Controller are minimum compared to that of other controllers. From the Table-5.4, it is clear that the peak overshoot/undershoot by GWO-PID controller is 9.62%, 6.00%, 11.32% and 14.55% smaller as against PSO-PID, TLBO-PID and conventional-PID Controllers respectively.

Table-5.5: Settling time and peak overshoot/undershoot of various Controllers for Scenario-1

Controller		**GWO-PID**	PSO-PID	TLBO-PID	JAYA-PID	Conventional PID
Disturbance occurred at t = 30secs	Settling time in secs	**21**	26	25	42	35
	Peak Overshoot / undershoot in Hz	**0.047**	0.052	0.050	0.053	0.055

5.9.2 Scenario-2: Single Microgrid - Multi-Step Load disturbance without RES

In this scenario, multi-step load deviation, as shown in the Fig-5.15, has been applied to the stand-alone Microgrid System consisting of DEG and BESS. The dynamic response of the system obtained for various controllers has been presented in Fig-5.16. It is apparent from the Fig-5.16 and Table-5.6 that, the magnitude of oscillations, peak overshoot/undershoot and settling time has been reduced considerably using the GWO-PID controller as against the other controllers. It is clear from the Table-5.6 that, the peak overshoot/undershoot by GWO-PID controller is 12.43%, 8.82%, 22.11% and 10.40%

smaller in comparison to PSO-PID, TLBO-PID and conventional-PID controllers respectively.

Table-5.6: Settling time and peak overshoot/undershoot of various Controllers for Scenario-2

Controller		**GWO-PID**	PSO-PID	TLBO-PID	JAYA-PID	Conventional PID
Disturbance occurred at t = 30Secs	Settling time (in Secs)	**20**	24.5	23.5	29	25
	Peak Overshoot/ undershoot in Hz	**0.0155**	0.0177	0.0170	0.0199	0.0173

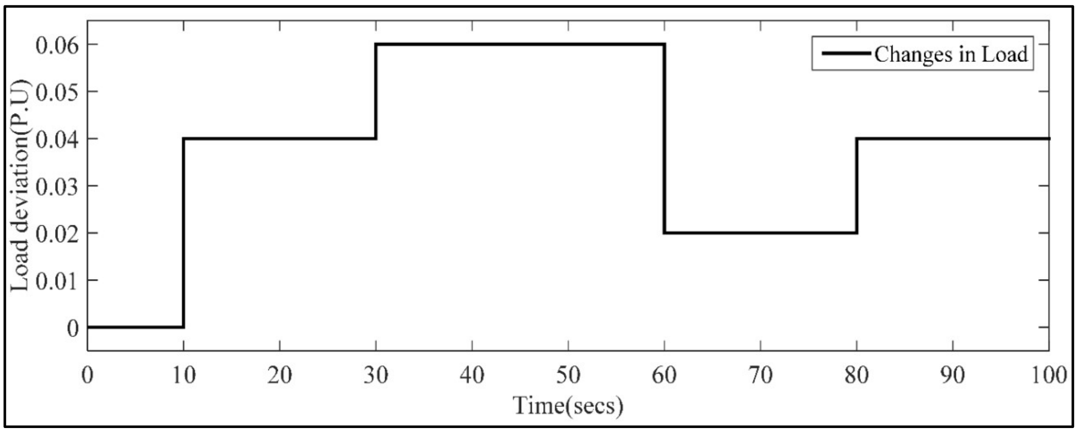

Fig-5.15: Multi-Step Load fluctuation

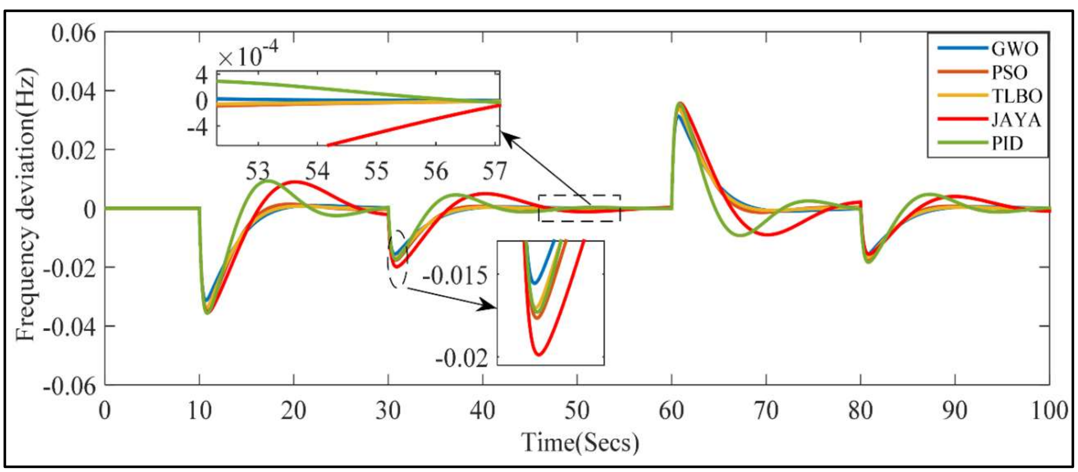

Fig-5.16: Comparison of Stand-alone MG frequency response of GWO-PID, PSO-PID, TLBO-PID, JAYA-PID and Conventional-PID Controllers

5.9.3 Scenario-3: Single Microgrid - Multi-Step Load disturbance with RES

In this scenario, isolated Microgrid with Multi-Step load perturbations, Wind Power Generation, Solar Power Generation and BESS has been considered. The plot for multiple

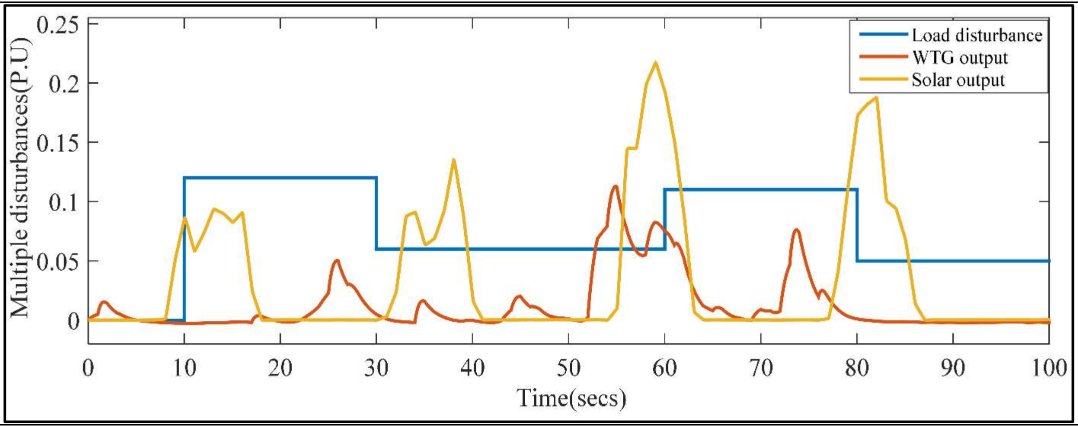

Fig-5.17: Multiple signal disturbances

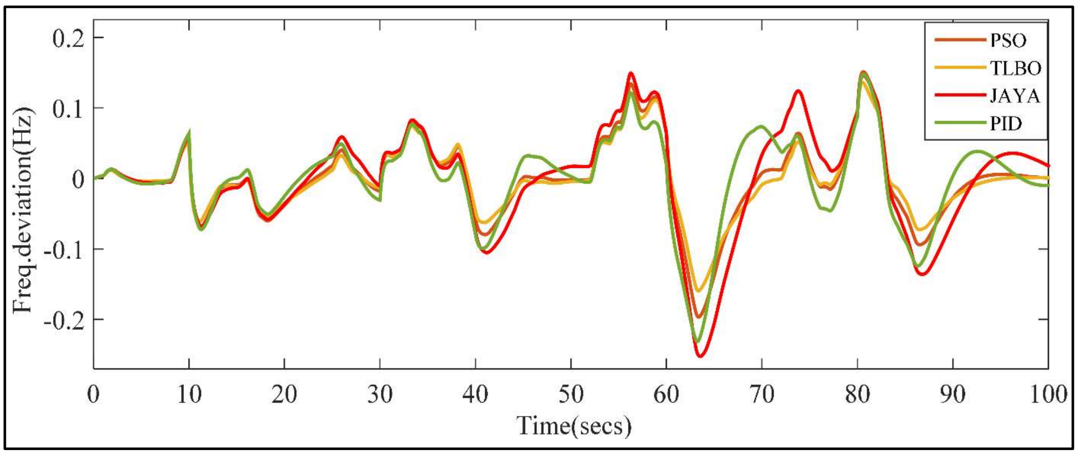

Fig-5.18: Comparison of Stand-alone MG frequency response of PSO-PID, TLBO-PID, JAYA-PID and Conventional-PID Controllers

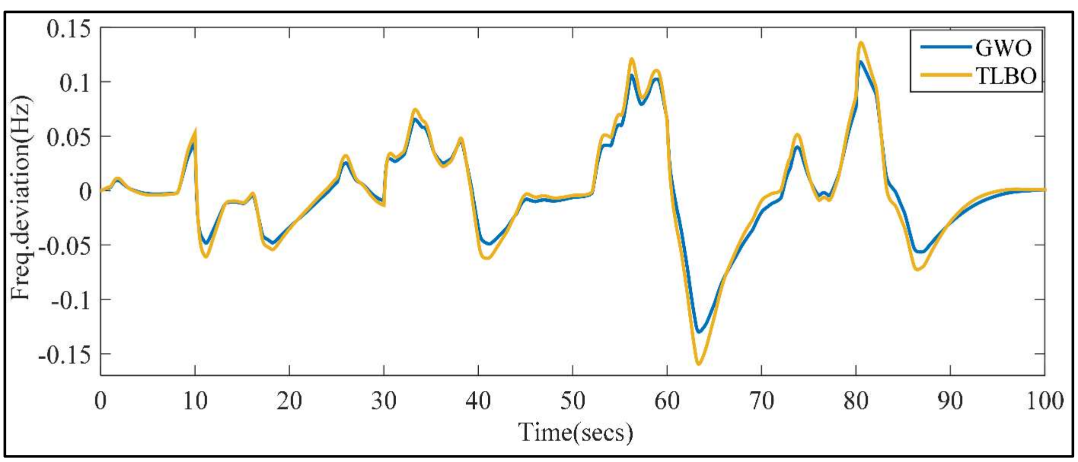

Fig-5.19: Comparison of Stand-alone MG frequency response of TLBO-PID and GWO-PID Controllers

perturbations has been shown in the Fig-5.17. To get better understandability of frequency response of various controllers, initially Conventional-PID, TLBO-PID, JAYA-PID and

PSO-PID Controllers are compared. From Fig-5.18, the better controller out of the above four controllers is found to be TLBO-PID controller and the same is used for comparison with the proposed GWO-PID controller as shown in Fig-5.19. It is manifested from the Fig-5.19 that the GWO-PID controller has lower peak overshoot/undershoot and settling time as against the TLBO-PID controller. Thus GWO-PID controller is found to be robust for Multi-step load disturbances with the integration of RES into the system.

5.9.4 Scenario-4: Multi-Microgrids - Multi-Step Load disturbance without RES

In this scenario, Multi-Microgrid System connected with tie-line has been considered. A multi-step load disturbance in Microgrid-1 has been initiated. The dynamic frequency response of both the Microgrids (MG-1 and MG-2) and tie-line flow deviation have been shown in Fig-5.20, Fig-5.21and Fig-5.22 respectively.

The supremacy of the proposed GWO-PID controller as against PSO-PID, TLBO-PID, JAYA-PID and Conventional-PID controllers is evident from the figures (Fig-5.20 to Fig-5.22) and Table-5.7, which has less peak overshoot and small settling time. Thus, the GWO-PID controller exhibits better controlling than other controllers.

Table-5.7: Settling time and peak overshoot/undershoot of various Controllers for Scenario-4

Controllers	Disturbance considered at t=10secs					
	ΔF_1		ΔF_2		$\Delta P_{tie-line}$	
	Settling Time (in Secs)	Peak Overshoot/ undershoot in Hz	Settling time (in Secs)	Peak Overshoot/ undershoot in Hz	Settling Time (in Secs)	Peak Overshoot/ Undershoot in Hz
GWO-PID	**20**	**0.07553**	**21**	**0.0496**	**24**	**0.02753**
PSO-PID	23	0.08082	24	0.05427	25.5	0.03063
TLBO-PID	21	0.07974	22	0.05385	26	0.02959
JAYA-PID	30	0.08075	34	0.05741	36	0.03108
Conventional-PID	28	0.08202	28	0.05844	27	0.03117

5.9.5 Scenario-5: Multi-Microgrids-Multi-Step Load disturbance with RES

In this scenario, Multi-Microgrids System having Wind Power Generation in Microgrid-1 and Solar Power Generation in Microgrid-2 is shown in Fig-5.2. The multi-step load deviation considered to arise in Microgrid-1. Due to the intermittent nature of Solar Power and Wind Power Generation, continuous oscillations can be observed in the frequency response of both the Microgrids and tie-line flow deviation.

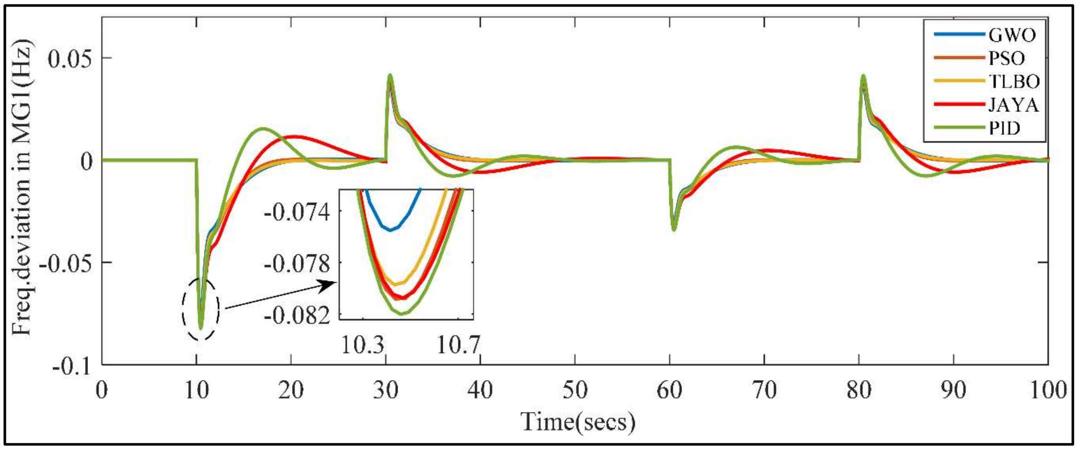

Fig-5.20: Comparison of MG-1 frequency response of GWO-PID, PSO-PID,TLBO-PID, JAYA-PID and Conventional-PID Controllers

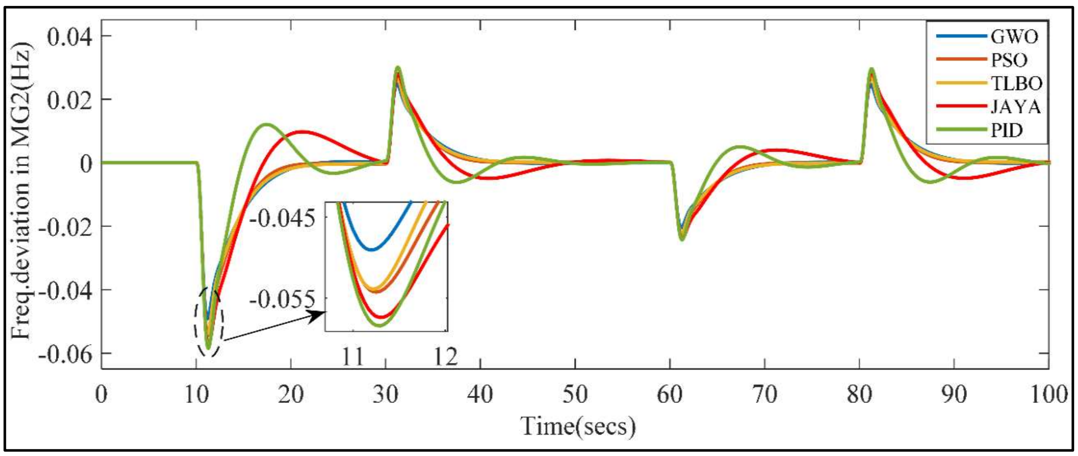

Fig-5.21: Comparison of MG-2 frequency response of GWO-PID, PSO-PID, TLBO-PID, JAYA-PID and Conventional-PID Controllers

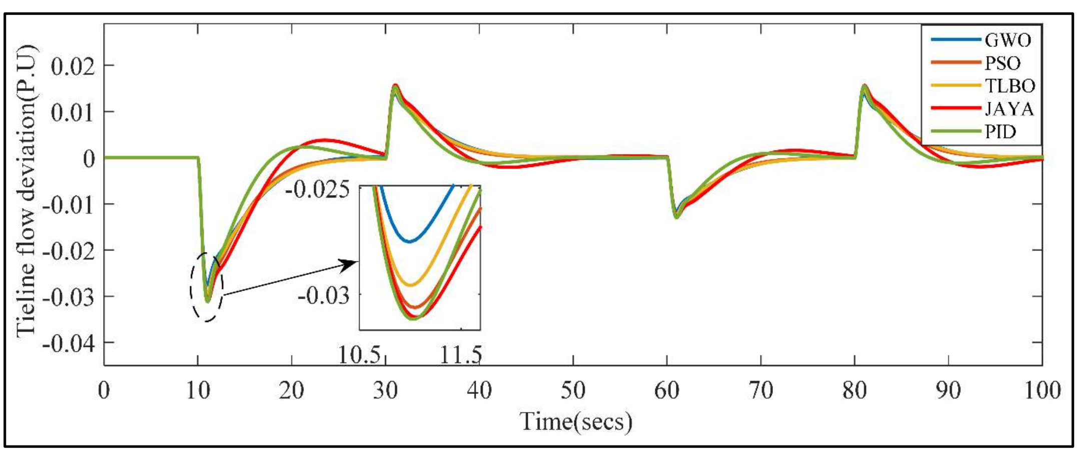

Fig-5.22: Comparison of Tielineflow Deviation in P.U between MG-1 and MG-2 of GWO-PID, PSO-PID, TLBO-PID, JAYA-PID and Conventional-PID Controllers for Multi-step load disturbance

To verify the superiority of proposed GWO-PID controller, initially, Conventional-PID, PSO-PID, JAYA-PID and TLBO-PID controllers are compared and the obtained frequency response of Microgrid-1, Microgrid-2 and deviation in tie-line flow are presented in Fig-5.23, Fig-5.25 and Fig-5.27 respectively. The comparative analysis proves that the TLBO-PID Controller is superior over the other controllers. Accordingly, TLBO-PID controller is considered to ascertain the ascendancy of the GWO-PID controller, as shown in Fig- 5.24, Fig-5.26 and Fig-5.28. From these figures (Fig- 5.24, Fig-5.26 and Fig-5.28), it is clear that the GWO-PID Controller system exhibits lesser overshoot and smaller setting time than that of the TLBO-PID controller.

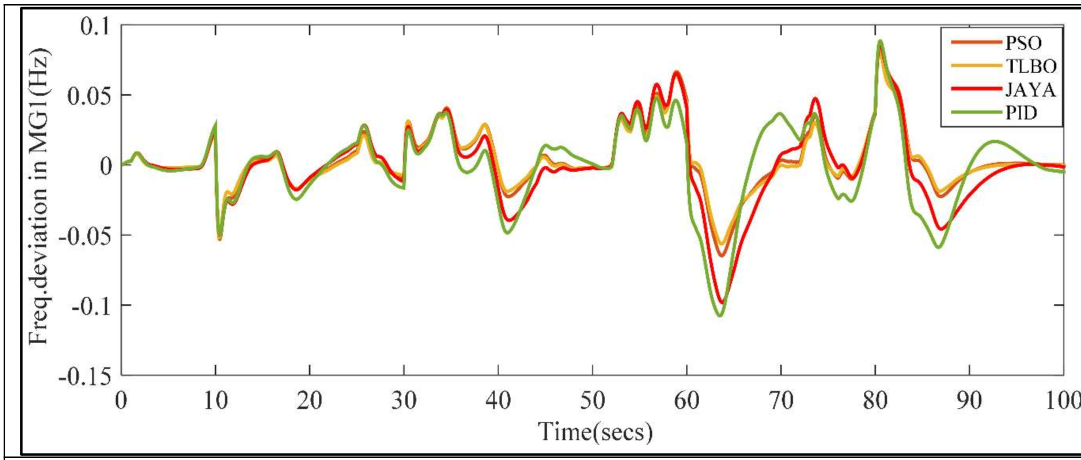

Fig-5.23: Comparison of MG-1 frequency response of PSO-PID,TLBO-PID, JAYA-PID and Conventional-PID Controllers for Multi-step load disturbance including RES

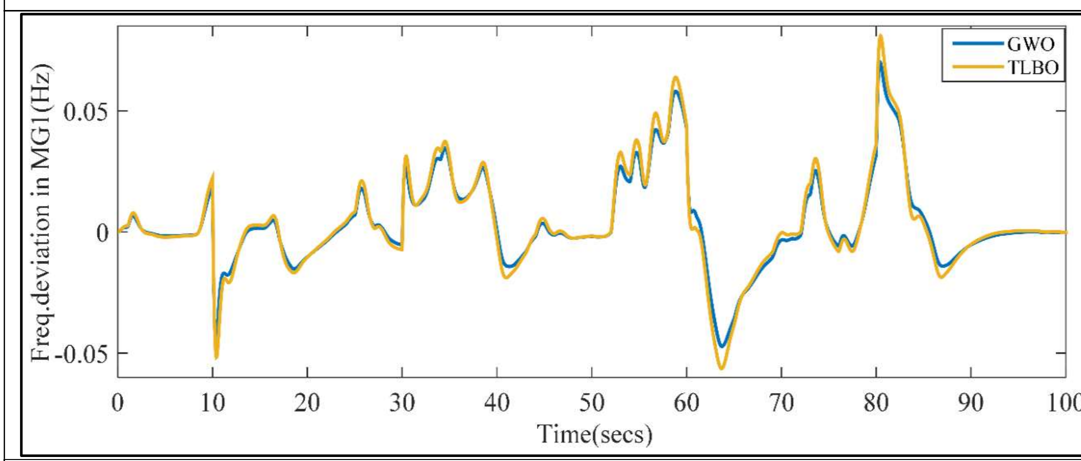

Fig-5.24: Comparison of MG-1 frequency response of TLBO-PID and GWO-PID Controllers for Multi-step load disturbance including RES

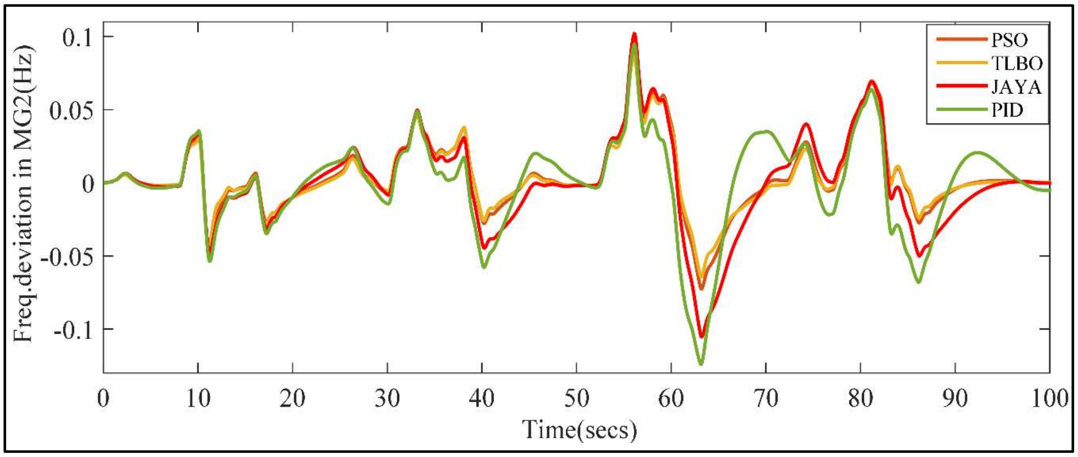

Fig-5.25: Comparison of MG-2 frequency response of PSO-PID, TLBO-PID, JAYA-PID and Conventional-PID Controllers for Multi-step load disturbance including RES

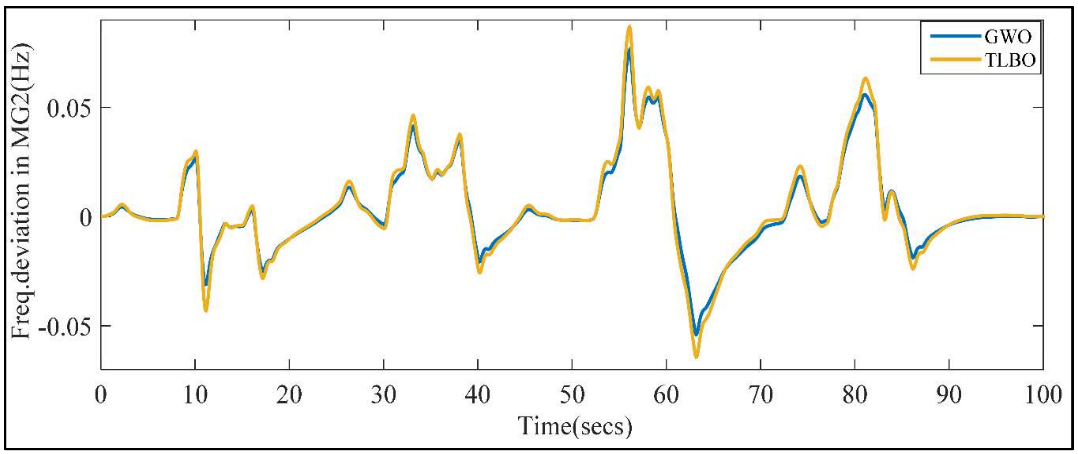

Fig-5.26: Comparison of MG-2 frequency response of TLBO-PID and GWO-PID Controllers for Multi-step load disturbance including RES

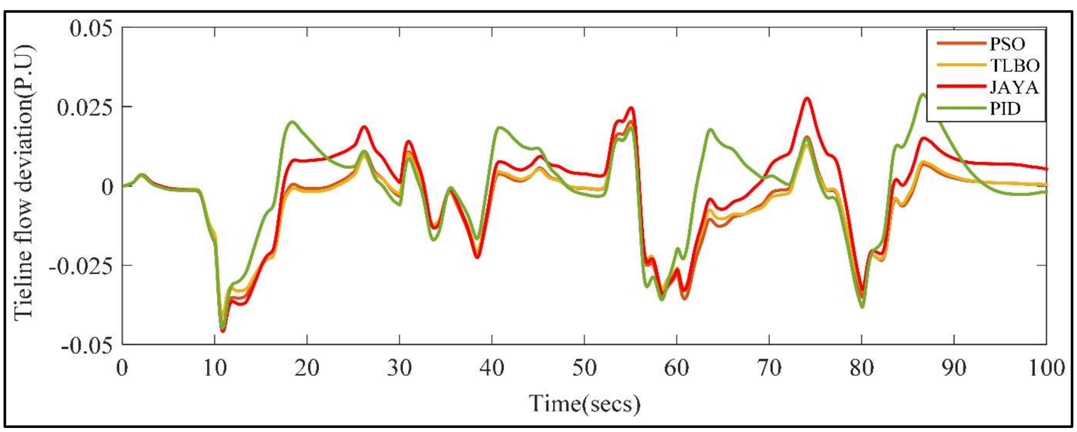

Fig-5.27: Comparison of Tielineflow deviation in P.U between MG-1 and MG-2 of PSO-PID, TLBO-PID, JAYA-PID and Conventional-PID Controllers for Multi-Step load disturbance including RES

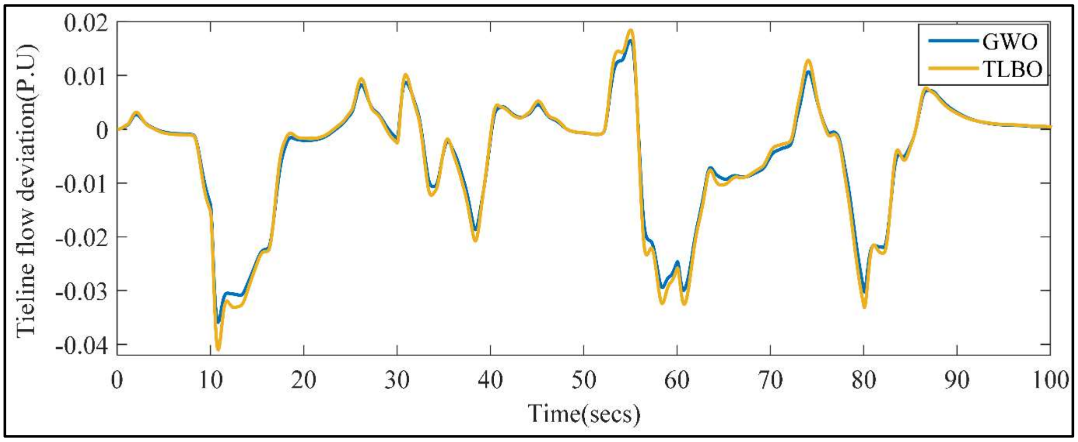

Fig-5.28: Comparison of Tielineflow deviation in P.U between MG-1 and MG-2 of TLBO-PID and GWO-PID Controllers for Multi-Step load disturbance including RES

5.9.6 Scenario-6: Multi-Microgrids - Multi-Step Load disturbance without RES including Parametric variation

As stated above, to verify the robustness of any controller, frequency response due to parametric uncertainty has to be gauged. According, in this scenario, dynamic responses of Multi-Microgrid System with load perturbation and parametric variation have been appraised. The variation in parameters is presented in Table-5.8.

Table-5.8: Details of Parameter variations

Sl.No	Parameter	% change
1	R	+5%
2	D	-25%
3	H	+30%

From the test results of Table-5.9, it is analysed that the GWO-PID Controller has reduced the overshoot/undershoot in Δf_1 by 7.19%, 5.78%, 7.35% and 8.75% with respect to PSO-PID, TLBO-PID, JAYA-PID and Convention-PID controllers respectively. With respect to Δf_2, the reduction in overshoot/undershoot in contrast to other controllers is found to 10.29%, 9.14%, 15.16% and 16.30% respectively. Also, the tie-line flow peak overshoot/undershoot fluctuations of GWO-PID controller improved by 10.27%, 7.35%, 11.86% and 12.10% as against PSO-PID, TLBO-PID, JAYA-PID and Convention-PID controllers respectively.

It is clear from the Fig-5.29, Fig-5.30 & Fig-5.31 and Table-5.9 that the proposed GWO-PID controller is producing minimum oscillations, smaller settling time and less peak

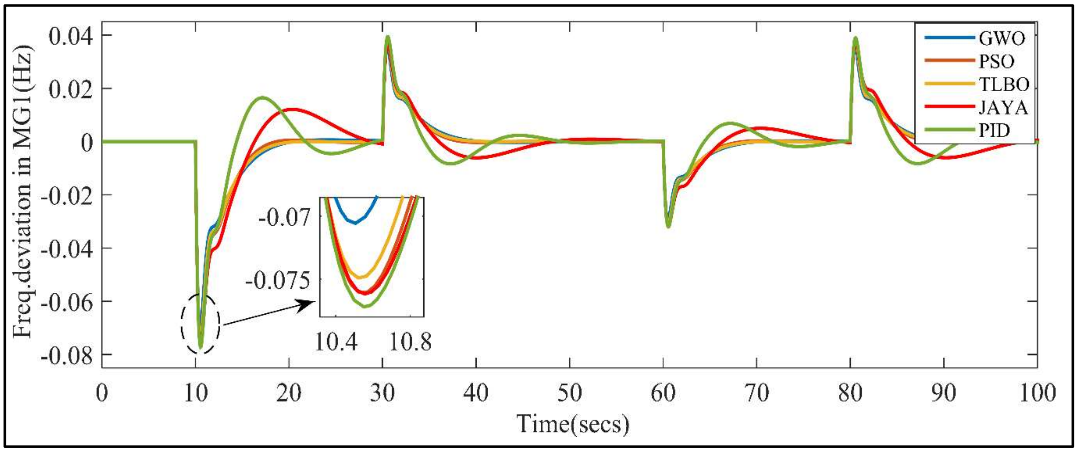

Fig-5.29: Comparison of MG-1 frequency response of GWO-PID, PSO-PID, TLBO-PID, JAYA-PID and Conventional-PID Controllers for Multi-step load disturbance and parametric variations

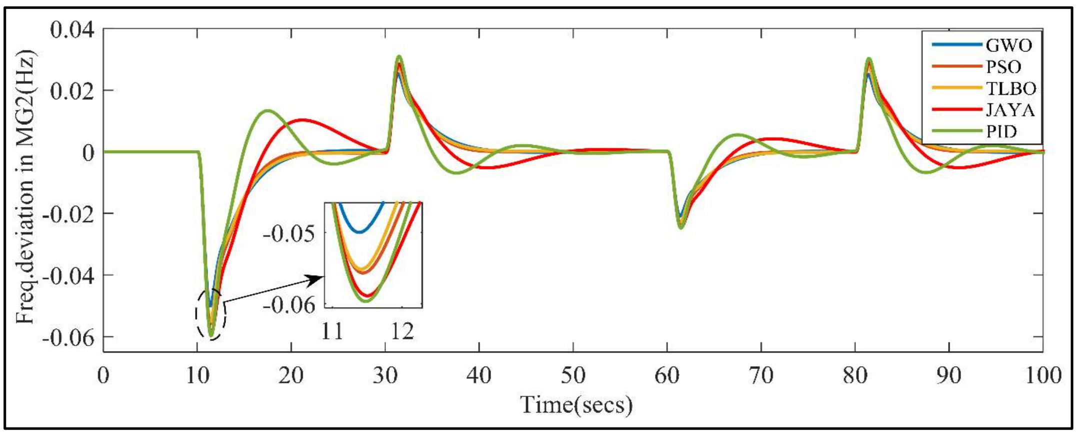

Fig-5.30: Comparison of MG-2 frequency response of GWO-PID, PSO-PID, TLBO-PID, JAYA-PID and Conventional-PID Controllers for Multi-step load disturbance and parametric variations

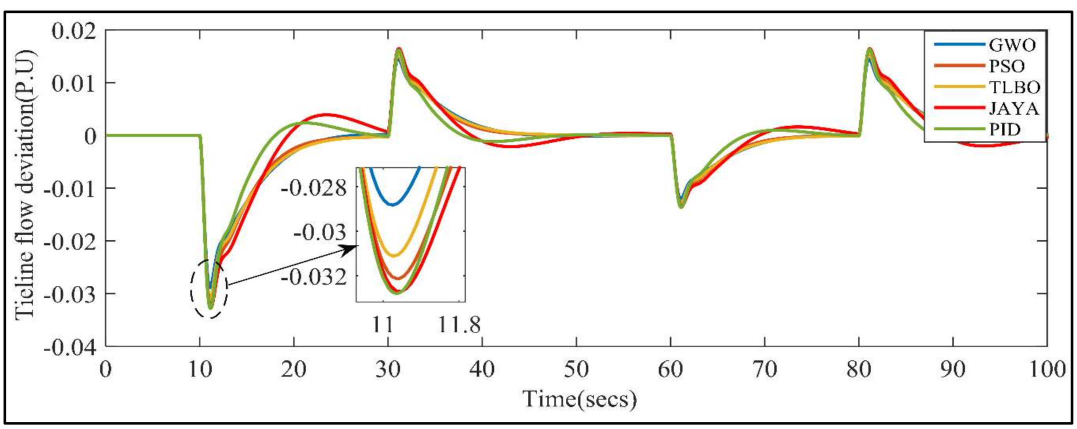

Fig-5.31: Comparison of Tielineflow deviation in P.U between MG-1 and MG-2 of PSO-PID, TLBO-PID, JAYA-PID and Conventional-PID Controllers for Multi-step load disturbance and parametric variations overshoot/undershoot than that of other controllers under parametric variation conditions also. Thus, GWO-PID Controller is robust than other controllers.

Table-5.9: Settling time and peak overshoot/undershoot of various Controllers for Scenario-6

Controllers	Disturbance considered at t=30secs					
	Δf_1		Δf_2		$\Delta P_{tie-line}$	
	Settling time (in Secs)	Peak Overshoot/ Undershoot in Hz	Settling time (in Secs)	Peak Overshoot/ Undershoot in Hz	Settling Time (in Secs)	Peak Overshoot/ Undershoot in Hz
GWO-PID	**24**	**0.07058**	**25**	**0.04995**	**24**	**0.02883**
PSO-PID	28	0.07605	28	0.05568	28.5	0.03213
TLBO-PID	27	0.07491	26	0.05514	28	0.03112
JAYA-PID	Not settling (under the given conditions)	0.07618	Not settling (under the given conditions)	0.05888	Not settling (under the given conditions)	0.03271
Conventional PID	Not settling (under the given conditions)	0.07720	Not settling (under the given conditions)	0.05968	Not settling (under the given conditions)	0.03280

5.9.7 Scenario-7: Multi-Microgrids - Multi-Step Load disturbance with RES including Parametric variation

In this scenario, Multi-Microgrids have been considered with load perturbations, RES integration and parametric variation. The frequency deviation ($\Delta f_1, \Delta f_2$) and ΔP_{tie} of different controllers have been presented in Fig-5.32 to Fig-5.37.

For better understandability of superiority of proposed controller, first Conventional-PID, PSO-PID, JAYA-PID and TLBO-PID controllers are compared and their frequency response of Microgrid-1, Microgrid-2 and Tie-line power flow deviations, are depicted in Fig-5.32, 5.34 and 5.36 respectively. It can be analyzed that the TLBO-PID controller gives better performance out of the above four controllers. Considering it, TLBO-PID and GWO-PID controllers are compared and their response is presented in Fig-5.33, 5.35 and 5.37. It is intelligible from these figures that the GWO-PID controller produces lesser oscillations and smaller settling time than TLBO-PID controller.

It is evident from the above case studies that the proposed GWO-PID controller is better in performance, such as minimum oscillations, smaller settling time, lesser peak overshoot/undershoot and minimum ITAE as presented in Table-5.3 in comparison with the other controllers available in the literate. The convergence plot obtained for Scenario-V (which includes multi-step load variations, integration of RES in Multi-Microgrids) with the proposed controller and other prior-art controllers is presented in Fig-5.38. It is clear from the convergence characteristics that, the proposed GWO-PID controller takes minimum number of iterations in comparison to other algorithms.

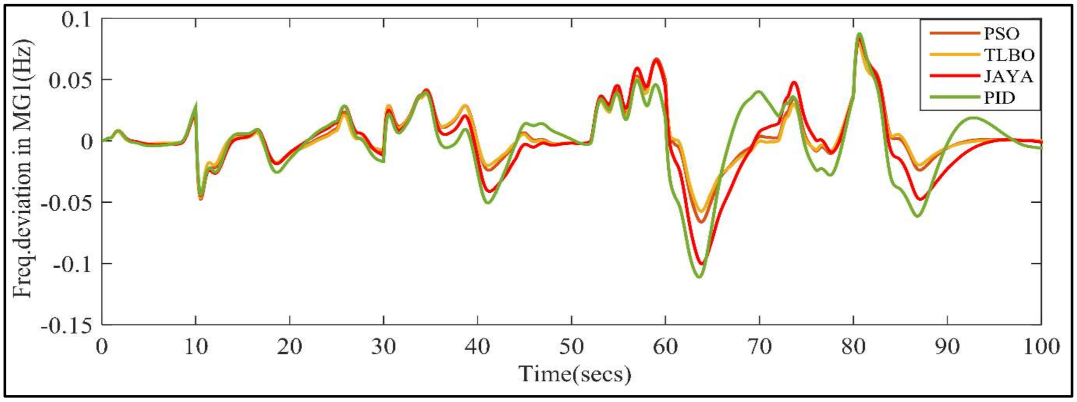

Fig-5.32: Comparison of MG-1 frequency response of PSO-PID, TLBO-PID, JAYA-PID and Conventional-PID Controllers for Multi-step load disturbance including RES and parametric variations.

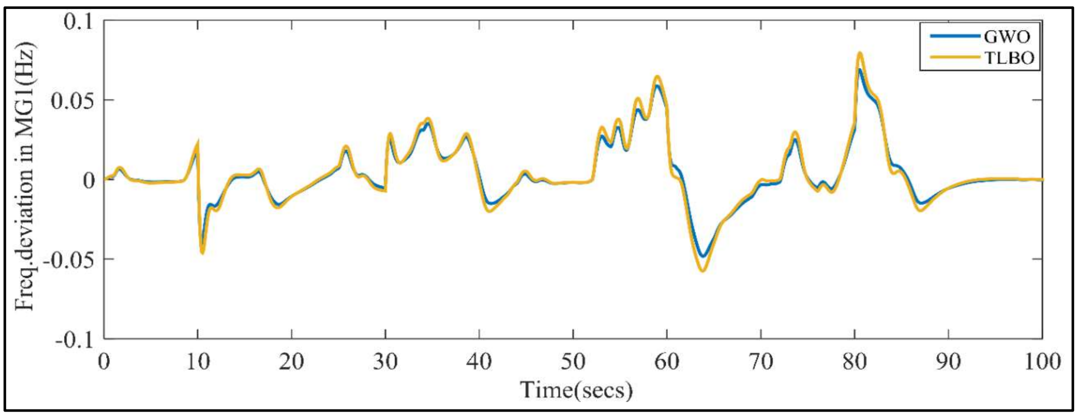

Fig-5.33: Comparison of MG-1 frequency response of TLBO-PID and GWO-PID Controllers for Multi-step load disturbance including RES and parametric variations

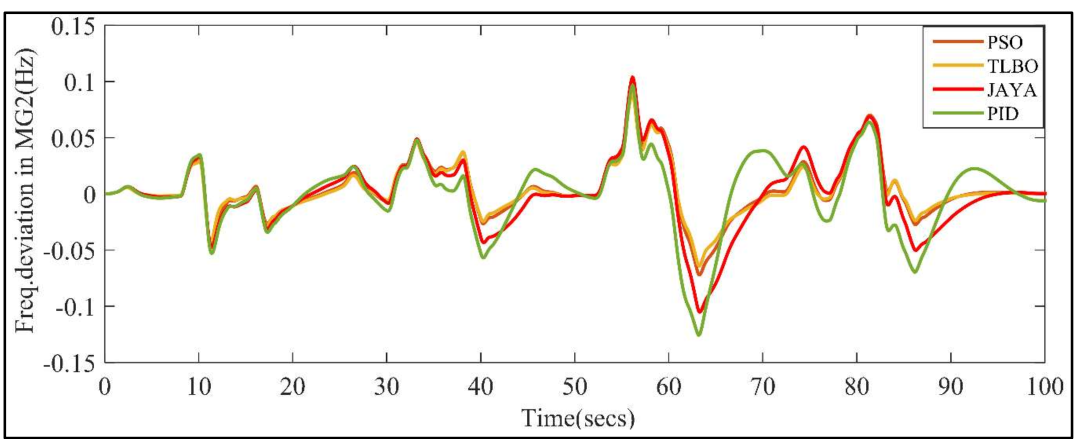

Fig-5.34: Comparison of MG-2 frequency response of PSO-PID, TLBO-PID, JAYA-PID and Conventional-PID Controllers for Multi-step load disturbance including RES and parametric variations.

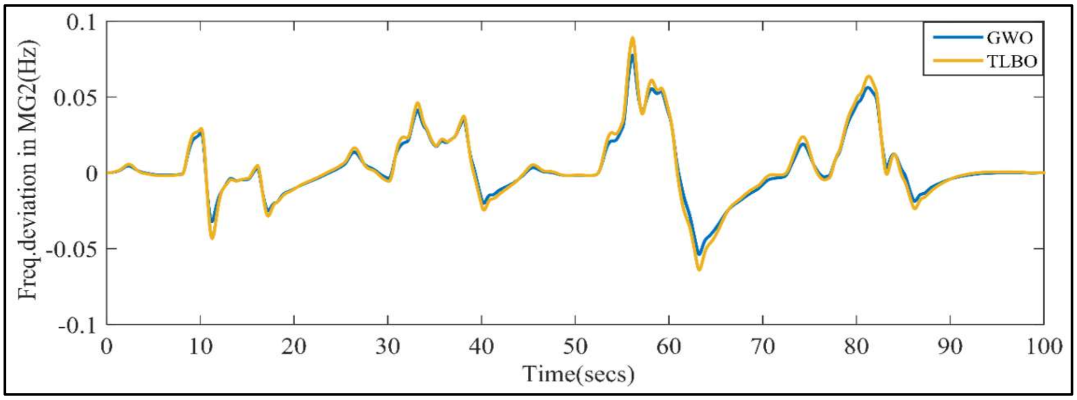

Fig-5.35: Comparison of MG-2 frequency response of TLBO-PID and GWO-PID Controllers for Multi-step load disturbance including RES and parametric variations.

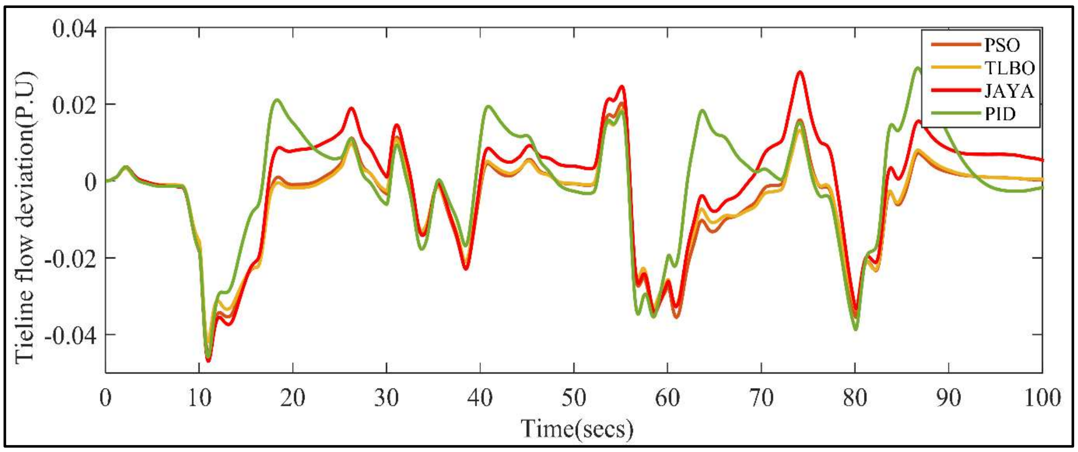

Fig-5.36: Comparison of Tielineflow deviation in P.U between MG-1 and MG-2 of PSO-PID, TLBO-PID, JAYA-PID and Conventional-PID Controllers for Multi-step load disturbance including RES and parametric variations

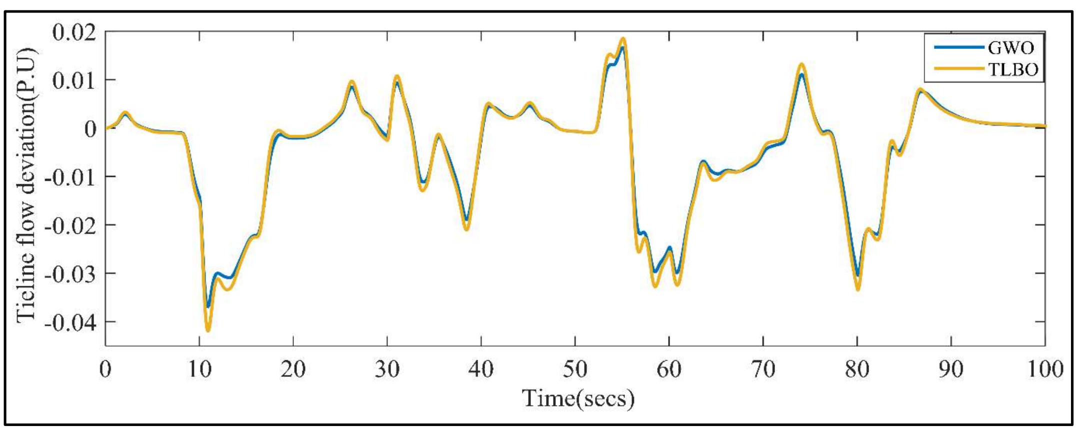

Fig-5.37: Comparison of Tielineflow deviation in P.U between MG-1 and MG-2 of TLBO-PID and GWO-PID Controllers for Multi-step load disturbance including RES and parametric variations

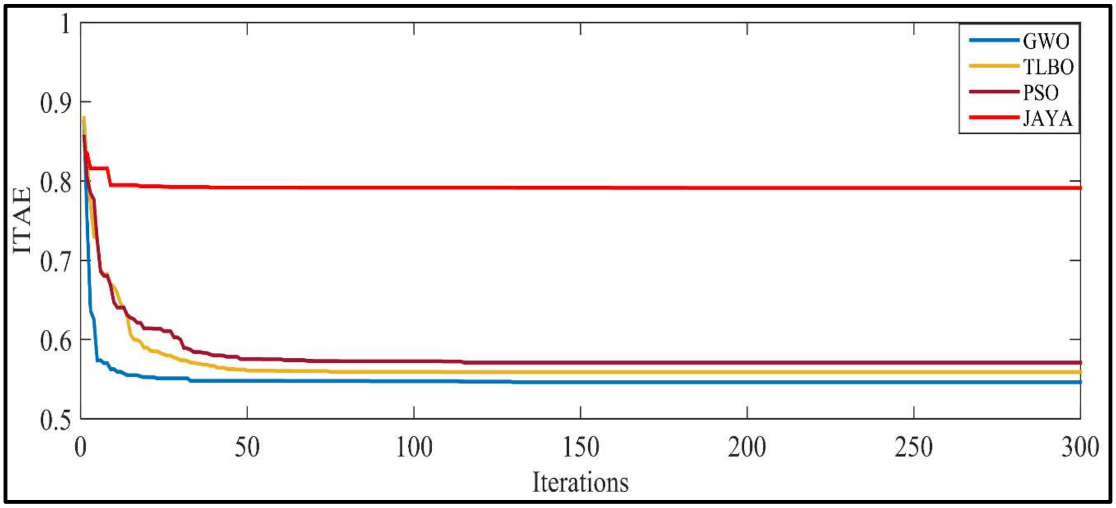

Fig-5.38: Comparision of Convergence characteristics of GWO-PID, TLBO-PID, PSO-PID and JAYA-PID Controllers

5.10 Summary

In Summary, in this chapter, load frequency control of Stand-alone Microgrid and Multi-Microgrids connected with tie-line by regulating the PID controller gains embedded in the individual Microgrid system has been addressed.

Initially, the PID gains are tuned with Conventional-PID, PSO-PID (being well-known optimization technique) and Jaya-PID controllers. It is noticed from the simulation results that the Jaya-PID controller performance is inferior in stabilizing the frequency deviations and tie-line power flow deviation of Multi-Microgrid System. As logically proved by the No Free Lunch (NFL) Theorem, no meta-heuristic optimization technique is best suitable for solving all optimization problems. Thus, an attempted has been made to analyse the performance of various other optimization techniques. As GWO and TLBO algorithms are being addressed by many researchers in the electrical domain, the same have been attempted in this chapter for tuning the gains of the PID controller.

Thus, conventional-PID, PSO-PID, JAYA-PID, TLBO-PID and GWO-PID controllers have been exercised for generating optimal gains of PID controller for dynamic stability of the system under various disturbances such as step load perturbations, sporadic nature of RES integration (Wind Power and Solar Power) and parametric uncertainty of the system. The efficacy and robustness of the proposed GWO-PID controller for stabilizing the system frequency deviations and tie-line flow deviation under various perturbations have been confirmed from the simulation results. Simulation results obtained using proposed GWO-PID controller have been compared with conventional-PID, PSO-PID, JAYA-PID and TLBO-PID controllers to corroborate the potential benefits of the proposed controller in terms of settling time, peak overshoot/undershoot and the obtained results are validated. *Part of this work is published in Smart Science – Taylor & Francis Group Publishers, Vol-7, Issue-3, pp. 198-217, 2018. DOI: 10.1080/23080477.2019.1630057 (ESCI Indexed)* and *remaining part of this work has been* published in *the 9th National Power Electronics Conference, NIT Tiruchirappalli, 13th -15th December 2019 with DOI: 10.1109/NPEC47332.2019.9034751.*

CHAPTER-6

Conclusions and Future Scope of Work

6.1 Conclusions

This chapter summarizes the following conclusions that have been arrived based on the investigation carried out at various stages of this Research work.

Power Systems are prone to faults very often due to many causes. A fault in a particular region in the Power System, may get cascaded, by overloading of other regions of the network causes a catastrophic effect, leads to a blackout. As proclaimed in *1547.4 - 2011 IEEE Guide for Design, Operation, and Integration of Distributed Resource Island Systems with Electric Power Systems*, the reliability of the Power Systems can be improved by islanding of the system into multiple networks.

For the inhabitation of human beings, electrical power is found to be essential in modern society. However, many places in the World are still found to be unelectrified. The percentage of World population being unelectrified is found to be around 11% as of 2017. The main reason for this problem is found to be non-feasibility or geographical issues of providing power supply.

Due to environmental concern, policies are made by the council of United Nations Framework Convention on Climate Change (UNFCCC) to reduce the carbon footprint and to adopt new technologies of power generation from Renewable Energy Sources (RES). Thus, the integration of RES to Power Systems is increasing significantly.

The problem of un-electrification, global warming has been solved by the initiation of Deregulation in Power Systems. Deregulation has given scope for installation of Distributed Generation Resources (DER) at suitable places in the systems. These DER are small scale power generation technologies located close to the load being served. The concept of DER feeding power to its local loads is termed as Microgrid System. Furthermore, islanded operation of the Microgrid System curbs the fault propagation and blackout of the vast region. Economics of the system, action towards improving the reliability, power quality issues, Environmental awareness, modifications in strategy to diversify the nature of energy sources has motivated the Microgrid Concept. These DER along with sophisticated metering in Distribution System, advanced communication technologies, modern control strategies have changed the conventional structure of Distribution System into Multi-Microgrid system over the past decade.

In Chapter-1 of this thesis, the advantages of the Microgrid System, its operating modes have been presented. A few existing Microgrids around the World which are in operation have been explained. Renewable Energy Sources are intermittent, unlike the conventional fossil-fuel power generation sources and causes deviation in system frequency and scheduled power flows in Tie-lines. To arrest the oscillations, Secondary Load Frequency Controller is being adopted. The role of secondary Load Frequency Controller in mitigating the system oscillation has been elaborated in this chapter.

Furthermore, in Chapter-1, Literature survey of optimal scheduling of Micro-Sources, reliability constraint optimal scheduling of Micro-Sources, Multi-objective optimal scheduling of Micro-Sources and Load Frequency Control in Multi-Microgrid System have been explained.

In Chapter-2, sectionalisation of the active Distribution System into Multi-Microgrids has been illustrated. As proposed, each test system is sectionalized into three Microgrid Systems as a case study based on the location of Micro-Sources and topology of the system. Seven case studies have been articulated based on possible operations of the Multi-Microgrid System i.e., Case-I (MG-1 alone is active), Case-II (MG-2 alone is active), Case-III (MG-3 alone is active), Case-IV (only MG-1 and MG-2 are active), Case-V (only MG-2 and MG-3 are active), Case-VI (only MG-1 and MG-3 are active), Case-VII (all MGs are active). Three objective functions have been formulated for optimization under each case study. The scenarios considered are Operating Cost minimization (Scenario-1), System Active Power Loss minimization (Scenario-2) and Voltage Deviation minimization (Scenario-3). Since the objective functions considered are of non-linear, complex, constrained optimization problem, Jaya Algorithm and Genetic Algorithm, which are meta-heuristic techniques have been exercised to solve the stated optimization problems. The proposed methodology and optimization of objective functions are examined on modified IEEE 33 Bus Distribution System and Practical Indian 85 Bus Distribution Systems. The results reveal that Jaya Algorithm is better in optimal scheduling of DGs for various objectives. Based on the results of Jaya Algorithm, the voltage magnitude at various Buses of the test systems are plotted. Based on the necessity of various objective functions, the Microgrid Central Controller operates the DGs with different scheduled values. *A part of the work is published in the IEEE International Conference on Sustainable Energy, Electronics and Computing Systems (SEEMS), I.T.S Engineering College, Greater Noida, India, 2018 with DOI: 10.1109/SEEMS.2018.8687370.* Though, to increase the customer satisfaction, sectionalisation of islanded Distribution System and optimal scheduling of controllable DGs have been performed, the Forced Outage Rate (FOR) of the DGs has not been considered in this chapter. Thus, to increase the reliability of power supply, these is a need to consider FOR of DGs for optimal scheduling to achieve the desired objectives.

In Chapter-3, to increase the reliability of power supply to the consumers with respect to DGs point of view, Forced Outage Rate (FOR) of DGs has been considered. In each sectionalized Microgrid System, optimal scheduling of DGs has been performed with criterion of the Energy Index of Reliability (EIR) greater than or equal to 0.97. The scenarios attempted are Operating Cost minimization (Scenario-1), System Active Power Loss minimization (Scenario-2) and Voltage Deviation minimization (Scenario-3). While scheduling of DGs, along with the EIR criterion, equality and inequality constraints of the system are taken into consideration. Further, the Energy Export Rate (EER) among interconnected Microgrids has been evaluated with the Energy Index of Reliability constraint and without the Energy Index of Reliability constraint. Similar to the previous chapter, these non-linear complex, constrained optimization problem has been solved using Jaya algorithm and Genetic algorithm. Modified IEEE 33 Bus Distribution System and Practical Indian 85 Bus Distribution Systems are considered for testing the proposed methodology. The convergence characteristics of the Jaya algorithm and the Genetic algorithm for various scenarios prove that the Jaya algorithm offers promising solutions. The DGs optimal scheduled values obtained with Jaya algorithm and Genetic algorithm are presented. However, it is noticed that, in each scenario with different case studies, the objective function value with the Energy Index of Reliability criterion is found to be more than that of optimal scheduling without the Energy Index of Reliability criterion. Based on the severity of the loads, the Microgrid Central Controller has to take the decision of operating the DGs either with Energy Index of Reliability criterion or without consideration of Energy Index of Reliability criterion. *A part of the work has been published in the 9th National Power Electronics Conference, NIT Tiruchirappalli, 13th-15th December 2019 with DOI:10.1109/NPEC47332.2019.9034703.* In this chapter, preference is given to only one of the objective functions at a time. It is observed that a better solution for the selected single objective function requires a compromise in other objectives. Thus, there is a need to address Multi-Objective Optimization (MOO) problem.

In the above two chapters, Single Objective Optimization of optimal scheduling of DGs has been attempted. Optimizing one objective function may lead to compromise on other objective functions. Thus, in Chapter-4, Multi-Objective Optimization (MOO) problem has been attempted for optimal scheduling of DGs in the Multi-Microgrid System. The concepts of Multi-Objective Optimization, Non-dominated sorting technique and Crowding Distance evaluation have been discussed in detail in this chapter. Three Scenarios are considered for solving the Multi-Objective Optimization (MOO) problem. In Scenario-1, Operating Cost & System Active Power Loss are considered for simultaneous minimization, in Scenario-2, simultaneous minimization of Operating Cost & Voltage Deviation and in Scenario-3, Operating Cost & System Active Power Loss are considered for simultaneous minimization. From the above two chapters (Chapter-2 and Chapter-3), it is noticed that the Jaya algorithm is best suitable for the optimal scheduling of DGs. In view of this, the MOO problem has been solved using Jaya algorithm. The Multi-Objective Jaya Algorithm (MOJA) has been described in detail, incorporating Non-dominated sorting technique and Crowding Distance methodology into Jaya algorithm. The Pareto-front for different scenarios is presented for modified IEEE 33 Bus Distribution System and Practical Indian 85 Bus Distribution Systems. The identification of Best Compromise Solution among the Pareto-front using Fuzzy Decision-making approach has been presented and the same is indicated in the Pareto-fronts. *Part of this work is published in Smart Science - Taylor & Francis Group Publishers, Vol-7, Issue-1, pp. 59-78, 2018. DOI:10.1080/23080477.2018. 1540381 (ESCI Indexed)* and *remaining part of this work is communicated to Electrical Power Components and Systems – Taylor & Francis Group Publishers (SCI Indexed) and it is under review.* In the above chapters, controllable DGs are attempted for optimal scheduling with various objective functions. However, due to advantages, more interest is being paid on RES day-by-day. As the RES are intermittent, these sources when connected to Multi-Microgrid System, leads to frequency fluctuations and tie-line power flow deviations. Thus, it is necessary to design a robust controller frequency.

Due to environmental concern, much interest is being paid throughout the World for production of electrical energy from non-conventional energy sources or Renewable Energy Sources. Out of various forms of Renewable Energy Sources, Solar energy and Wind energy have attracted much attention. In view of this, in Chapter-5, integration of Solar Power and Wind Power in Multi-Microgrid System has been considered. As the Renewable Energy Sources are intermittent in nature, leads to oscillations in the system frequency and power exchange through tie-lines. Thus, for immediate restoration of power balance, Battery Energy Storage System is incorporated in the System. The primary frequency controller, though balances the power generation and demand, it does not restore the frequency to the nominal value, thus arises a steady-state error. Thus, secondary load frequency controller (PID) is incorporated in the Multi-Microgrid System for restoring the frequency and tie-line flow to nominal values. The gains of the PID Controllers are tuned with Conventional-PID, PSO-PID, JAYA-PID, TLBO-PID and GWO-PID Controllers. Integral Time Multiplied Absolute Error (ITAE) and PID gains have been considered as Performance Index and control variables respectively for optimization. To verify the robustness of the controllers, various scenarios are formulated. In Scenario-1 and Scenario-2, the performance of the controllers is assessed with 'single-step load disturbance' and 'multi-step load disturbance' in isolated Microgrid System respectively. The frequency response (Δf) reveals that the GWO-PID Controller produces minimum overshoot/undershoot and less settling time than that of the other controllers. In Scenario-3, the system frequency response is analyzed with multi-step load disturbance with the integration of Renewable Energy Sources (RES) in isolated Microgrid System. The frequency response reveals that magnitude of overshoot/undershoot with the GWO-PID Controller is minimum. Scenario-4 details about response of various controllers for multi-step load disturbance in Multi-Microgrid System. It is noticed that the GWO-PID Controller has smaller magnitude of peak overshoots/undershoot and lesser settling time in frequency deviation $(\Delta f_1, \Delta f_2)$ of Microgrid-1, Microgrid-2 and tie-line power flow$(\Delta P_{Tie-line})$ compared with that of the other controllers. In Scenario-5, Renewable Energy Sources are integrated into Multi-Microgrid System and the frequency deviation in both the Microgrids and change in tie-line power flow have been analyzed. In Scenario-6 and Scenario-7, the performance of the controllers in Multi-Microgrid System has been analyzed with 'parametric variation with multi-step load change' and 'parametric variation with the integration of Renewable Energy Sources' respectively. System oscillations with GWO-PID Controller are found to be minimum in both the scenarios. The performance index (ITAE) of various controllers in different scenarios has been evaluated and it is noticed that the proposed GWO-PID Controller produced minimum ITAE values for all the scenarios. The convergence characteristics reveal that GWO-PID Controller converges faster than the other controllers with minimum ITAE value. Thus, it is concluded that the proposed GWO-PID Controller is better than the other controllers in stabilizing the response of Microgrid and Multi-Microgrid System. *Part of this work is published in Smart Science – Taylor & Francis Group Publishers, Vol-7, Issue-3, pp. 198-217, 2018. DOI: 10.1080/23080477.2019.1630057*

(ESCI Indexed) and *remaining part of this work has been* published in *the 9th National Power Electronics Conference, NIT Tiruchirappalli, 13th -15th December 2019 with DOI: 10.1109/NPEC47332.2019.9034751.* The proposed work on GWO-PID Controller will act as a good supporting tool to the real time System Operator.

6.2 Scope for future work

Further, Research work in the area of Multi-Microgrid System can be extended in the following directions.

1. Optimal scheduling approach for Multi-Microgrid System with integration of Electric Vehicles (EV) can be studied.
2. Cyber-attacks on optimal operation of Multi-Microgrid System can be analyzed.
3. Resiliency studies on Multi-Microgrid System operation can be investigated.

LIST OF PUBLICATIONS

JOURNALS PUBLISHED

1. C. Srinivasarathnam, Chandrasekhar Yammani & Sydulu Maheswarapu , "Multi-Objective Jaya Algorithm for Optimal Scheduling of DGs in Distribution System Sectionalized into Multi-Microgrids", *Smart Science, Taylor & Francis Group*, vol-7, issue-1, pp.59-78, DOI: 10.1080/23080477.2018.1540381(***Indexed in ESCI***).
2. C. Srinivasarathnam, Chandrasekhar Yammani & Sydulu Maheswarapu, "Load Frequency Control of Multi-microgrid System considering Renewable Energy Sources Using Grey Wolf Optimization", *Smart Science, Taylor & Francis Group*, vol-7, issue-3, pp.198-217, DOI: 10.1080/23080477.2019.1630057 (***Indexed in ESCI***).

JOURNAL COMMUNICATED

1. C. Srinivasarathnam, Chandrasekhar Yammani & Sydulu Maheswarapu, "A Reliability Constraint Optimal Scheduling of DGs in Multi-Microgrid System using Multi-Objective Optimization", submitted to *Electric Power Components and Systems, Taylor & Francis Group,* on 01st Dec,2019. Revision received on 8th March, 2020, revised manuscript submitted on 18th April, 2020– (***Indexed in SCI***)

CONFERENCE PUBLISHED

1. C. Srinivasarathnam, C. Yammani and S. Maheswarapu, "Multi-Objective Optimal Scheduling of Microsources in Distribution System based on Sectionalization into Microgrid," *IEEE International Conference on Sustainable Energy, Electronics, and Computing Systems (SEEMS)*, Greater Noida, India, 2018, pp. 1-5, DOI: 10.1109/SEEMS.2018.8687370.
2. C.Srinivasarathnam, C. Yammani and S. Maheswarapu, "Optimal Scheduling of Micro-sources in Multi-Microgrids for Reliability Improvement*", National Power Electronics Conference (NPEC), NIT Tiruchirappalli,* India, 2019, pp. 1-6, DOI: 10.1109/NPEC47332.2019.9034703(Published in IEEE Xplore).
3. C.Srinivasarathnam, C. Yammani and S. Maheswarapu, "Frequency control of Autonomous Hybrid Multi-Microgrid System", *National Power Electronics*

Conference (NPEC), NIT Tiruchirappalli, India, 2019, pp. 1-6, DOI: 10.1109/NPEC47332.2019.9034751.(Published in IEEE Xplore).

REFERENCES

[1] "Solar Schools," Types of Energy, 2019." [Online]. Available: https://www.solarschools.net/knowledge-bank/energy/types. [Accessed: 10-Jan-2020].

[2] D.P.Kothari and I.J.Nagrath, *Power Systems Engineering*, Second Edi. TMC, 2008.

[3] E. Crisostomi, M. Liu, M. Raugi, and R. Shorten, "Plug-and-play distributed algorithms for optimized power generation in a microgrid," *IEEE Trans. Smart Grid*, vol. 5, no. 4, pp. 2145–2154, 2014.

[4] "Press Information Bureau Government of India Ministry of Power," 2019. [Online]. Available: https://pib.gov.in/Pressreleaseshare.aspx?PRID=1592833. [Accessed: 08-Jul-2020].

[5] "Access to Electricity (% of Population)," *World Bank Open Data*, 2019. [Online]. Available: http://data.worldbank.org/indicator/EG.ELC.ACCS.ZS. [Accessed: 24-Feb-2020].

[6] "Government of India, Ministry of New and Renewable Energy. (2016, June), 'Draft national policy on renewable energy-based mini/microgrids,'" 2016.

[7] "Blackout : A Case Study of the 2003 North American Power Outage with Exercises," 2003.

[8] Union for the Coordination of the Transmission of Electricity (UCTE), "Final Report of the Investigation Committee on the 28th September 2003 Blackout in Italy," Italy, 2003.

[9] CERC, "Report on the Grid Disturbance on 30th July and Grid Disturbance on 31st July 2012," no. 167, p. 129, 2012.

[10] N. Voropai and T. Hammons, "Blackouts: Remedial measures and restoration practices; Asian and Australian experience," in *IEEE PES General Meeting, July 20-24 2008, Pittsburgh, PA, USA*, 2008, pp. 1–4.

[11] "Massachusetts Clean Energy Center." [Online]. Available: https://www.masscec.com/microgrids-0. [Accessed: 03-Nov-2019].

[12] "Microgrids – Benefits, Models, Barriers and Suggested Policy Initiatives for the Commonwealth of Massachusetts." [Online]. Available: https://files.masscec.com/research/Microgrids.pdf. [Accessed: 21-Mar-2019].

[13] P. Das, S. Chanda, and A. De, "Artificial Intelligence-Based Economic Control of Micro-grids: A Review of Application of IoT," in *Computational Advancement in*

Communication Circuits and Systems. Lecture Notes in Electrical Engineering, Springer, Singapore, 2020.

[14] S. A. Arefifar, M. Ordonez, and Y. A. R. I. Mohamed, “Energy Management in Multi-Microgrid Systems - Development and Assessment,” *IEEE Trans. Power Syst.*, vol. 32, no. 2, pp. 910–922, 2017.

[15] “Advanced Architectures and Control Concepts for More Microgrids, CORDIS EU research results.” [Online]. Available: https://cordis.europa.eu/project/rcn/75085/brief/en. [Accessed: 14-Nov-2019].

[16] C. 21 IEEE Standards Coordinating, “IEEE Guide for Design, Operation, and Integration of Distributed Resource Island Systems with Electric Power Systems,” *IEEE Std 1547.4-2011*, no. July, pp. 1–54, 2011.

[17] “GuideHouse Research. Microgrid deployment tracker-1q20.,” 2020. [Online]. Available: https://guidehouseinsights.com/reports/microgrid-deployment-tracker-1q20. [Accessed: 08-Jul-2020].

[18] “Microgrid Projects.” [Online]. Available: http://microgridprojects.com/india-microgrids/.

[19] Prabha Kundur, *Power Systems Stability and Control*. McGraw-Hill Inc, 2006.

[20] H. Bevrani, *Robust Power System Frequency Control*. Springer, 2009.

[21] H. Haes Alhelou, M. E. Hamedani-Golshan, R. Zamani, E. Heydarian-Forushani, and P. Siano, “Challenges and opportunities of load frequency control in conventional, modern and future smart power systems: A comprehensive review,” *Energies*, vol. 11, no. 10, 2018.

[22] P. Chilukuri *et al.*, “Introduction of Secondary Frequency Control in Indian Power System,” in *2018 20th National Power Systems Conference, NPSC 2018*, 2018, pp. 1–6.

[23] CERC, “Report of Expert Group to review and suggest measures for bringing power system operation closer to National Reference Frequency,” 2017.

[24] “Growth of Electricity Sector in India from 1947-2017,” *Central Electricity Authority, Ministry of Power, New Delhi*, 2011. .

[25] S. M. Dawoud, X. Lin, and M. I. Okba, “Hybrid renewable microgrid optimization techniques: A review,” *Renew. Sustain. Energy Rev.*, vol. 82, no. 3, pp. 2039–2052, Feb. 2018.

[26] R. T. Marler and J. S. Arora, “Survey of multi-objective optimization methods for engineering,” *Struct. Multidiscip. Optim.*, vol. 26, no. 6, pp. 369–395, 2004.

[27] Z. Wang, B. Chen, J. Wang, and C. Chen, “Networked microgrids for self-healing power systems,” *IEEE Trans. Smart Grid*, vol. 7, no. 1, pp. 310–319, 2016.

[28] C. A. Hernandez-Aramburo, T. C. Green, and N. Mugniot, "Fuel consumption minimization of a microgrid," *IEEE Trans. Ind. Appl.*, vol. 41, no. 3, pp. 673–681, 2005.

[29] D. Moga, D. Petreuş, V. Mureşan, N. Stroia, and G. Cosovici, "Optimal generation scheduling in islanded microgrids," *IFAC-PapersOnLine*, vol. 49, no. 27, pp. 135–139, 2016.

[30] Z. Wang and J. Wang, "Self-Healing Resilient Distribution Systems Based on Sectionalization into Microgrids," *IEEE Trans. Power Syst.*, vol. 30, no. 6, pp. 3139–3149, 2015.

[31] J. Matamoros, D. Gregoratti, and M. Dohler, "Microgrids energy trading in islanding mode," *2012 IEEE 3rd Int. Conf. Smart Grid Commun. SmartGridComm 2012*, pp. 49–54, 2012.

[32] J. Radosavljević, M. Jevtić, and D. Klimenta, "Energy and operation management of a microgrid using particle swarm optimization," *Eng. Optim.*, vol. 48, no. 5, pp. 811–830, 2016.

[33] N. Nikmehr and S. Najafi Ravadanegh, "A study on optimal power sharing in interconnected microgrids under uncertainty," *Int. Trans. Electr. Energy Syst.*, vol. 26, no. 1, pp. 208–232, Jan. 2016.

[34] S. Najafi Ravadanegh, T. Farhudi, N. Nikmehr, and M. R. Jannati Oskuee, "Statistical analysis on results of optimal power sharing between linked microgrids," *Int. J. Ambient Energy*, vol. 38, no. 7, pp. 710–718, 2017.

[35] S. Tan, J. X. Xu, and S. K. Panda, "Optimization of distribution network incorporating distributed generators: An integrated approach," *IEEE Trans. Power Syst.*, vol. 28, no. 3, pp. 2421–2432, 2013.

[36] M. R. Vallem, J. Mitra, and S. B. Patra, "Distributed generation placement for optimal microgrid architecture," in *Proceedings of the IEEE Power Engineering Society Transmission and Distribution Conference*, 2006, pp. 1191–1195.

[37] M. R. Vallem and J. Mitra, "Siting and sizing of distributed generation for optimal microgrid architecture," in *Proceedings of the 37th Annual North American Power Symposium, 2005*, 2005, pp. 611–616.

[38] C. Yammani and P. Prabhat, "Reliability improvement of future microgrid with mixed load models by optimal dispatch of DGs," *Int. Trans. Electr. Energy Syst.*, vol. 29, no. 4, p. e2816, Apr. 2019.

[39] T. Logenthiran, D. Srinivasan, and A. M. Khambadkone, "Multi-agent system for energy resource scheduling of integrated microgrids in a distributed system," *Electr. Power Syst. Res.*, vol. 81, no. 1, pp. 138–148, Jan. 2011.

[40] A. Kargarian, B. Falahati, Y. Fu, and M. Baradar, "Multiobjective optimal power flow algorithm to enhance multi-microgrids performance incorporating IPFC," *IEEE Power Energy Soc. Gen. Meet.*, pp. 1–6, 2012.

[41] G. Carpinelli, F. Mottola, D. Proto, and A. Russo, "A Multi-Objective Approach for Microgrid Scheduling," *IEEE Trans. Smart Grid*, vol. 8, no. 5, pp. 2109–2118, 2017.

[42] J. Chen, X. Yang, L. Zhu, and M. Zhang, "Study on Microgrid Multi-objective Economic Operation Optimization," *Int. J. Adv. Comput. Technol.*, vol. 5, no. 8, pp. 1218–1229, 2013.

[43] G. Aghajani and N. Yousefi, "Multi-objective optimal operation in a micro-grid considering economic and environmental goals," *Evol. Syst.*, vol. 10, no. 2, pp. 239–248, 2019.

[44] D. J. Lee and L. Wang, "Small-signal stability analysis of an autonomous hybrid renewable energy power generation/energy storage system part I: Time-domain simulations," *IEEE Trans. Energy Convers.*, vol. 23, no. 1, pp. 311–320, 2008.

[45] K. V. Vidyanandan and N. Senroy, "Frequency regulation in microgrid using wind Fuel cell Diesel generator," *IEEE Power Energy Soc. Gen. Meet.*, 2012.

[46] A. J. Veronica and N. S. Kumar, "Internal Model Based Load Frequency Controller Design for Hybrid Microgrid System," *Energy Procedia*, vol. 117, pp. 1032–1039, 2017.

[47] G. Mallesham, S. Mishra, and A. N. Jha, "Ziegler-Nichols based controller parameters tuning for load frequency control in a microgrid," *Proc. - 2011 Int. Conf. Energy, Autom. Signal, ICEAS - 2011*, pp. 335–342, 2011.

[48] K. V. Vidyanandan and N. Senroy, "Frequency regulation in a wind-diesel powered microgrid using flywheels and fuel cells," *IET Gener. Transm. Distrib.*, vol. 10, no. 3, pp. 780–788, 2016.

[49] H. Bevrani, M. R. Feizi, and S. Ataee, "Robust Frequency Control in an Islanded Microgrid: H∞ and μ-Synthesis Approaches," *IEEE Trans. Smart Grid*, vol. 7, no. 2, pp. 706–717, 2016.

[50] H. Li, X. Wang, and J. Xiao, "Differential evolution-based load frequency robust control for micro-grids with energy storage systems," *Energies*, vol. 11, no. 7, pp. 1–19, 2018.

[51] A. H. Chowdhury and M. Asaduz-Zaman, "Load frequency control of multi-microgrid using energy storage system," *8th Int. Conf. Electr. Comput. Eng. Adv. Technol. a Better Tomorrow, ICECE 2014*, pp. 548–551, 2015.

[52] A. A. El-Fergany and M. A. El-Hameed, "Efficient frequency controllers for autonomous two-area hybrid microgrid system using social-spider optimiser," *IET Gener. Transm. Distrib.*, vol. 11, no. 3, pp. 637–648, 2017.

[53] E. Gupta and A. Saxena, "Grey wolf optimizer based regulator design for automatic generation control of interconnected power system," *Cogent Eng.*, vol. 3, no. 1, 2016.

[54] M. Makandar, C. S. R. Atla, and S. Velamuri, "Reliability assessment of distribution system with renewable Distributed Generation," in *2016 Biennial International*

Conference on Power and Energy Systems: Towards Sustainable Energy (PESTSE), 2016, pp. 1–5.

[55] M. E. Khodayar, M. Barati, and M. Shahidehpour, “Integration of high reliability distribution system in microgrid operation,” *IEEE Trans. Smart Grid*, vol. 3, no. 4, pp. 1997–2006, 2012.

[56] A. Chaouachi, R. M. Kamel, R. Andoulsi, and K. Nagasaka, “Multiobjective intelligent energy management for a microgrid,” *IEEE Trans. Ind. Electron.*, vol. 60, no. 4, pp. 1688–1699, 2013.

[57] A. Zidan and E. F. El-Saadany, “A cooperative multiagent framework for self-healing mechanisms in distribution systems,” *IEEE Trans. Smart Grid*, vol. 3, no. 3, pp. 1525–1539, 2012.

[58] S. Surender Reddy and C. Srinivasa Rathnam, “Optimal Power Flow using Glowworm Swarm Optimization,” *Int. J. Electr. Power Energy Syst.*, vol. 80, pp. 128–139, 2016.

[59] Bruce Wollenberg and Allen J Wood., *Power Generation Operation and Control*, Second. Wiley, 2006.

[60] S. Xie, X. Wang, C. Qu, X. Wang, and J. Guo, “Parking lot allocation with maximum economic benefit in a distribution network,” *Int. Trans. Electr. energy Syst.*, vol. 20, pp. 1–6, 2013.

[61] R. V. Rao, D. P. Rai, and J. Balic, “A multi-objective algorithm for optimization of modern machining processes,” *Engineering Applications of Artificial Intelligence*, vol. 61. pp. 103–125, 2017.

[62] D. Singh, D. Singh, and K. S. Verma, “Multiobjective optimization for DG planning with load models,” *IEEE Trans. Power Syst.*, vol. 24, no. 1, pp. 427–436, 2009.

[63] D. Das, D. P. Kothari, and A. Kalam, “Simple and efficient method for load flow solution of radial distribution networks,” *Int. J. Electr. Power Energy Syst.*, vol. 17, no. 5, pp. 335–346, 1995.

[64] R. Sanjay, T. Jayabarathi, T. Raghunathan, V. Ramesh, and N. Mithulananthan, “Optimal allocation of distributed generation using hybrid grey Wolf optimizer,” *IEEE Access*, vol. 5, pp. 14807–14818, 2017.

[65] R. Preethi and C. Singh, “Monte Carlo and Analytical Methods for Forced Outage Rates Calculation of Peaking Units,” Texas A&M University, 2012.

[66] L. Wang and C. Singh, “Multicriteria design of hybrid power generation systems based on a modified particle swarm optimization algorithm,” *IEEE Trans. Energy Convers.*, vol. 24, no. 1, pp. 163–172, 2009.

[67] J. Mitra, S. B. Patra, and S. J. Ranade, “A Dynamic Programming Based Method for Developing Optimal Microgrid Architectures,” in *15th Power Systems Computational Conference*, 2005, pp. 1–7.

[68] N. Gunantara, “A review of multi-objective optimization: Methods and its applications,” *Cogent Eng.*, vol. 5, no. 1, pp. 1–16, 2018.

[69] K. Deb, *Multiobjective Optimization Using Evolutionary Algorithms*. John Wiley & Sons, Inc, 2010.

[70] K. Deb, A. Pratap, S. Agarwal, and T. Meyarivan, “A fast and elitist multiobjective genetic algorithm: NSGA-II,” *IEEE Trans. Evol. Comput.*, vol. 6, no. 2, pp. 182–197, 2002.

[71] N. C. Sahoo, S. Ganguly, and D. Das, “Simple heuristics-based selection of guides for multi-objective PSO with an application to electrical distribution system planning,” *Eng. Appl. Artif. Intell.*, vol. 24, no. 4, pp. 567–585, 2011.

[72] F. Zou, L. Wang, X. Hei, D. Chen, and B. Wang, “Multi-objective optimization using teaching-learning-based optimization algorithm,” *Eng. Appl. Artif. Intell.*, vol. 26, no. 4, pp. 1291–1300, Apr. 2013.

[73] A. Zangeneh and S. Jadid, “Fuzzy multiobjective model for distributed generation expansion planning in uncertain environment,” *Eur. Trans. Electr. Power*, vol. 21, no. 1, pp. 129–141, Jan. 2011.

[74] A. Ameli, M.-R. Farrokhifard, E. Davari-nejad, H. Oraee, and M.-R. Haghifam, “Profit-Based DG Planning Considering Environmental and Operational Issues: A Multiobjective Approach,” *IEEE Syst. J.*, vol. 11, no. 4, pp. 1959–1970, 2015.

[75] M. Dreidy, H. Mokhlis, and S. Mekhilef, “Inertia response and frequency control techniques for renewable energy sources: A review,” *Renewable and Sustainable Energy Reviews*, vol. 69. pp. 144–155, 2017.

[76] G. Shankar and V. Mukherjee, “Load frequency control of an autonomous hybrid power system by quasi-oppositional harmony search algorithm,” *International Journal of Electrical Power and Energy Systems*, vol. 78. pp. 715–734, 2016.

[77] E. Mallada, C. Zhao, and S. Low, “Optimal load-side control for frequency regulation in smart grids,” *IEEE Trans. Automat. Contr.*, vol. 62, no. 12, pp. 6294–6309, 2017.

[78] P. Das, S. Chanda, and A. De, *Artificial Intelligence-Based Economic Control of Micro-grids: A Review of Application of IoT*. Springer, Singapore, 2020.

[79] A. Annamraju and S. Nandiraju, “Robust Frequency Control in an Autonomous Microgrid: A Two-Stage Adaptive Fuzzy Approach,” *Electr. Power Components Syst.*, vol. 5008, pp. 1–12, 2018.

[80] M. Hajiakbari Fini and M. E. Hamedani Golshan, “Determining optimal virtual inertia and frequency control parameters to preserve the frequency stability in islanded microgrids with high penetration of renewables,” *Electric Power Systems Research*, vol. 154. pp. 13–22, 2018.

[81] K. M. Singh, S. Gope, and N. Pradhan, “Firefly Algorithm-Based Optimized Controller for Frequency Control of an Autonomous Multi-Microgrid,” in

International Conference on Innovative Computing and Communications, In:, J. A. Gupta D., Khanna A., Bhattacharyya S., Hassanien A., Anand S., and (eds), Eds. Springer, Singapore, 2021.

[82] S. A. Hassan Bevrani, Mohammad Ramin Feizi, "Robust Frequency Control in an Islanded Microgrid H ∞ and μ -Synthesis Approaches," *IEEE Trans. Smart Grid*, vol. 7, no. 2, pp. 706–717, 2016.

[83] L. Zhang, G. Chen, Z. Wang, Z. Dong, and D. Hill, "Robust H∞ load frequency control of future power grid with energy storage considering parametric uncertainty and time delay," *IEEE Power Energy Soc. Gen. Meet.*, vol. 2014-Octob, no. October, 2014.

[84] Y. Xu, C. Li, Z. Wang, N. Zhang, and B. Peng, "Load Frequency Control of a Novel Renewable Energy Integrated Micro-Grid Containing Pumped Hydropower Energy Storage," *IEEE Access*, vol. 6, pp. 29067–29077, 2018.

[85] D. H. Wolpert and W. G. Macready, "No free lunch theorems for optimization," *IEEE Trans. Evol. Comput.*, vol. 1, no. 1, pp. 67–82, 1997.

[86] S. Mirjalili, S. M. Mirjalili, and A. Lewis, "Grey Wolf Optimizer," *Adv. Eng. Softw.*, vol. 69, pp. 46–61, 2014.

[87] H. Faris, I. Aljarah, M. A. Al-Betar, and S. Mirjalili, "Grey wolf optimizer: a review of recent variants and applications," *Neural Comput. Appl.*, vol. 30, no. 2, pp. 413–435, 2018.

[88] A. Annamraju and S. Nandiraju, "Frequency Control in an Autonomous Two-area Hybrid Microgrid using Grasshopper Optimization based Robust PID Controller," in *8th IEEE India International Conference on Power Electronics, IICPE*, 2018, pp. 1–6.

[89] Y. Han, P. M. Young, A. Jain, and D. Zimmerle, "Robust control for microgrid frequency deviation reduction with attached storage system," *IEEE Trans. Smart Grid*, vol. 6, no. 2, pp. 557–565, 2015.

[90] R. K. Sahu, S. Panda, U. K. Rout, and D. K. Sahoo, "Teaching learning based optimization algorithm for automatic generation control of power system using 2-DOF PID controller," *Int. J. Electr. Power Energy Syst.*, vol. 77, pp. 287–301, 2016.

[91] D. P. V. R.V. Rao, V.J. Savsani, "Teaching–learning-based optimization: A novel method for constrained mechanical design optimization problems," *Comput. Des.*, vol. 43, no. 3, pp. 303–315, 2011.

[92] R. Eberhart and James Kennedy, "A New Optimizer Using Particle Swarm Theory," *Sixth Int. Symp. Micro Mach. Hum. Sci.*, vol. 0-7803–267, pp. 39–43.

[93] G. T. E.Bonabeau, M.Dorigo, *Swarm Intelligence: From Natural to Artificial System*. 1999.

Appendix-1

IEEE 33 BUS DISTRIBUTION SYSTEM DATA[62]

Number of Buses: 33

Number of lines: 32

Base voltage: 12.66kV

Base MVA: 100MVA

Total Active Power Load: 3.715MW

Total Reactive Power Load: 2.30MVAr

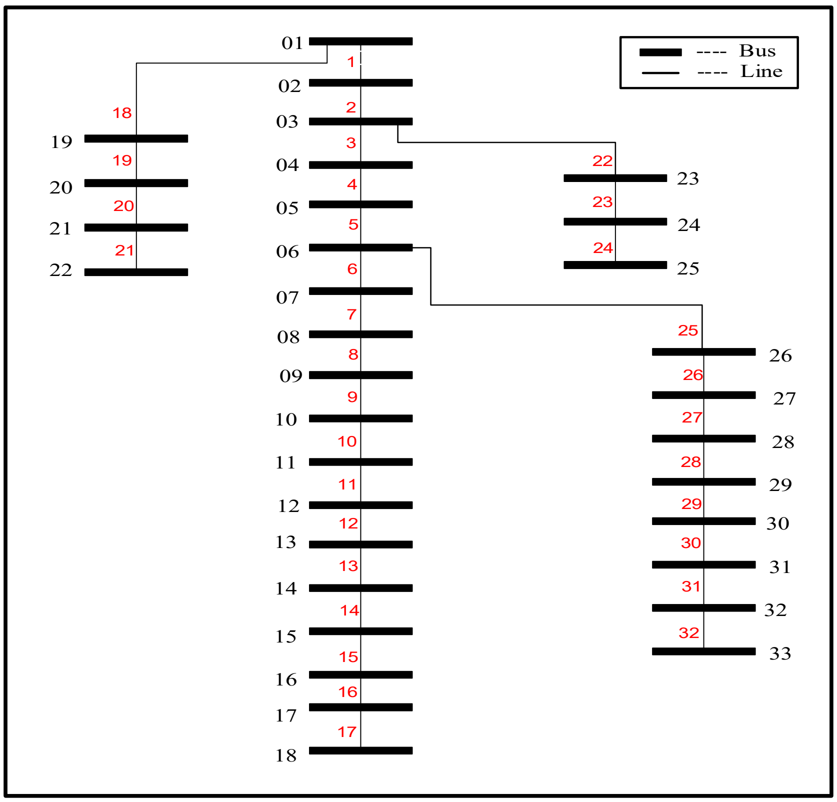

Fig-A1.1 33 Bus Distribution System

Table-A1.1 33 Bus Distribution System Line Data

Line No.	*From Bus*	*To Bus*	*R (P.U)*	*X (P.U)*	*Line No.*	*From Bus*	*To Bus*	*R (P.U)*	*X (P.U)*
1	1	2	0.000574	0.000293	17	17	18	0.004558	0.003574
2	2	3	0.003070	0.001564	18	2	19	0.001021	0.000974
3	3	4	0.002279	0.001161	19	19	20	0.009366	0.008440
4	4	5	0.002373	0.001209	20	20	21	0.002550	0.002979
5	5	6	0.005100	0.004402	21	21	22	0.004414	0.005836
6	6	7	0.001166	0.003853	22	3	23	0.002809	0.001920
7	7	8	0.004430	0.001464	23	23	24	0.005592	0.004415
8	8	9	0.006413	0.004608	24	24	25	0.005579	0.004366
9	9	10	0.006501	0.004608	25	6	26	0.001264	0.000644
10	10	11	0.001224	0.000405	26	26	27	0.001770	0.000901
11	11	12	0.002331	0.000771	27	27	28	0.006594	0.005814
12	12	13	0.009141	0.007192	28	28	29	0.005007	0.004362
13	13	14	0.003372	0.004439	29	29	30	0.003160	0.001610
14	14	15	0.003680	0.003275	30	30	31	0.006067	0.005996
15	15	16	0.004647	0.003394	31	31	32	0.001933	0.002253
16	16	17	0.008026	0.010716	32	32	33	0.002123	0.003301

Table-A1.2 33 Bus Distribution System Bus Data

Bus No	$\boldsymbol{P_{gen}}$ $(\boldsymbol{kW})$	$\boldsymbol{Q_{gen}}$ $(\boldsymbol{kVAR})$	$\boldsymbol{P_{load}}$ $(\boldsymbol{kW})$	$\boldsymbol{Q_{load}}$ $(\boldsymbol{kVAR})$	*Bus No*	$\boldsymbol{P_{gen}}$ $(\boldsymbol{kW})$	$\boldsymbol{Q_{gen}}$ $(\boldsymbol{kVAR})$	$\boldsymbol{P_{load}}$ $(\boldsymbol{kW})$	$\boldsymbol{Q_{load}}$ $(\boldsymbol{kVAR})$
1	0	0	0	0	18	0	0	60	20
2	0	0	0	0	19	0	0	90	40
3	0	0	100	60	20	0	0	90	40
4	0	0	90	40	21	0	0	90	40
5	0	0	120	80	22	0	0	90	40
6	0	0	60	30	23	0	0	90	40
7	0	0	60	20	24	0	0	90	50
8	0	0	200	100	25	0	0	420	200
9	0	0	200	100	26	0	0	420	200

10	0	0	60	20
11	0	0	60	20
12	0	0	45	30
13	0	0	60	35
14	0	0	60	35
15	0	0	120	80
16	0	0	60	10
17	0	0	60	20

27	0	0	60	25
28	0	0	60	25
29	0	0	60	20
30	0	0	120	70
31	0	0	200	600
32	0	0	150	70
33	0	0	210	100

Table-A1.3 Generator Cost coefficients for 33 Bus Distribution System

Bus No	***Gen***	***a ($/kW²)***	***b ($/kW)***	***C ($)***	P_{min} (kW)	P_{max} (kW)
1	G1	0.0696	26.244	31.67	0.0	600
2	G2	0.0288	37.697	17.95	0.0	200
20	G3	0.0468	40.122	22.02	0.0	100
3	G4	0.0468	40.122	22.02	0.0	2000
7	G5	0.0268	30.122	22.02	0.0	800
18	G6	0.0288	37.697	21.95	0.0	600
23	G7	0.0681	12.441	32.01	0.0	500
30	G8	0.0288	37.697	21.95	0.0	5000
26	G9	0.0288	30.697	21.95	0.0	800

Appendix-2

INDIAN 85 BUS DISTRIBUTION SYSTEM DATA[63]

Number of Buses: 85

Number of Lines: 84

Base Voltage: 11kV

Base MVA: 100MVA

Total Active Power Load: 2.57MW

Total Reactive Power Load: 2.62MVAr

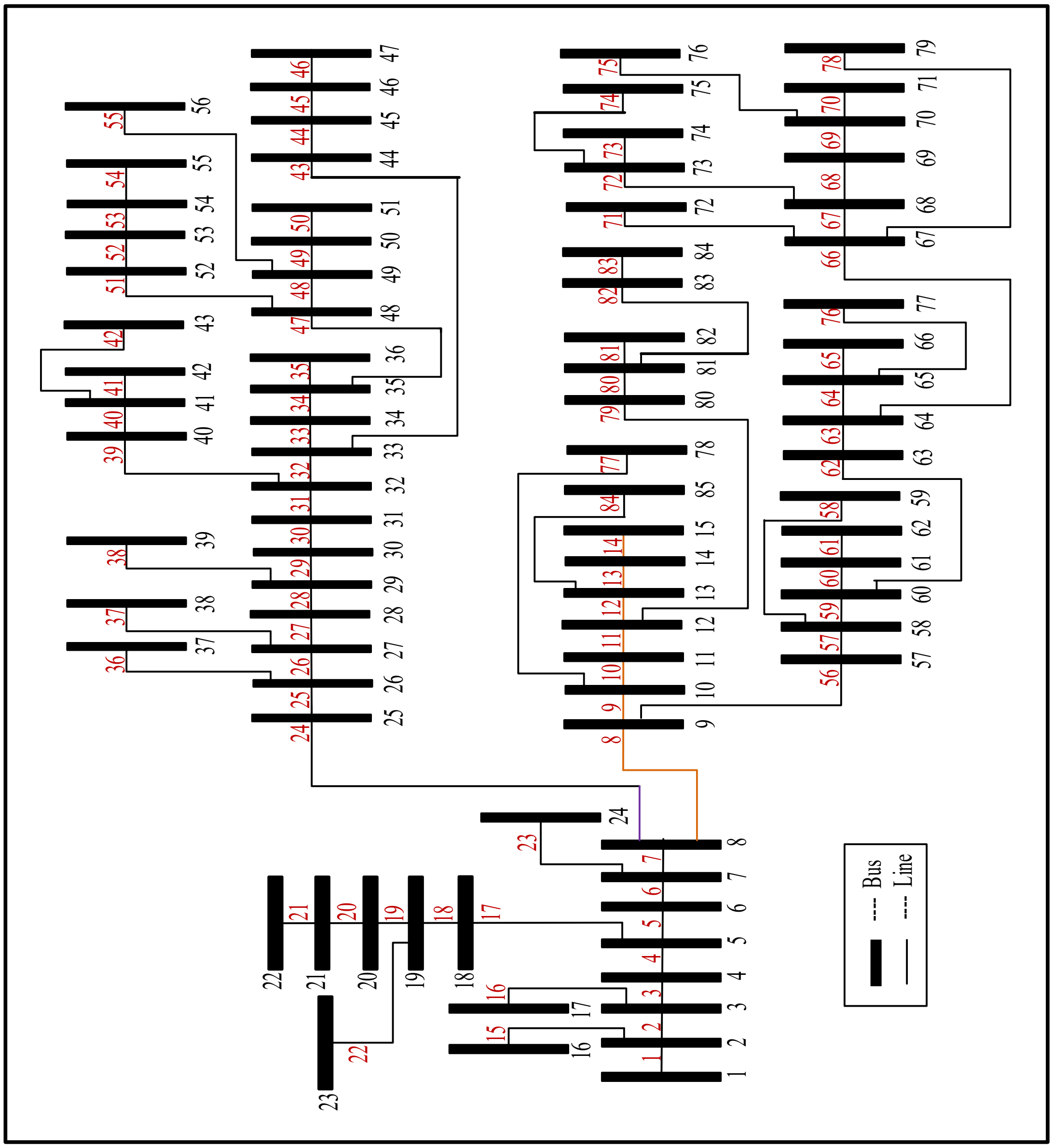

Fig-A2.1 85 Bus Distribution System

Table-A2.1 85 Bus Distribution System Line Data

Line No.	*From Bus*	*To Bus*	*R (Ohms)*	*X (Ohms)*
1	1	2	0.108	0.075
2	2	3	0.163	0.112
3	3	4	0.217	0.149
4	4	5	0.108	0.074
5	5	6	0.435	0.298
6	6	7	0.272	0.186
7	7	8	1.197	0.82
8	8	9	0.108	0.074
9	9	10	0.598	0.41
10	10	11	0.544	0.373
11	11	12	0.544	0.373
12	12	13	0.598	0.41
13	13	14	0.272	0.186
14	14	15	0.326	0.223
15	2	16	0.728	0.302
16	3	17	0.455	0.189
17	5	18	0.82	0.34
18	18	19	0.637	0.264
19	19	20	0.455	0.189
20	20	21	0.819	0.34
21	21	22	1.548	0.642
22	19	23	0.182	0.075
23	7	24	0.91	0.378
24	8	25	0.455	0.189
25	25	26	0.364	0.151
26	26	27	0.546	0.226
27	27	28	0.273	0.113
28	28	29	0.546	0.226
43	34	44	1.002	0.416
44	44	45	0.911	0.378
45	45	46	0.911	0.378
46	46	47	0.546	0.226
47	35	48	0.637	0.264
48	48	49	0.182	0.075
49	49	50	0.364	0.151
50	50	51	0.455	0.189
51	48	52	1.366	0.567
52	52	53	0.455	0.189
53	53	54	0.546	0.226
54	52	55	0.546	0.226
55	49	56	0.546	0.226
56	9	57	0.273	0.113
57	57	58	0.819	0.34
58	58	59	0.182	0.075
59	58	60	0.546	0.226
60	60	61	0.728	0.302
61	61	62	1.002	0.415
62	60	63	0.182	0.075
63	63	64	0.728	0.302
64	64	65	0.182	0.075
65	65	66	0.182	0.075
66	64	67	0.455	0.189
67	67	68	0.91	0.378
68	68	69	1.092	0.453
69	69	70	0.455	0.189
70	70	71	0.546	0.226

29	29	30	0.546	0.226	71	67	72	0.182	0.075
30	30	31	0.273	0.113	72	68	73	1.184	0.491
31	31	32	0.182	0.075	73	73	74	0.273	0.113
32	32	33	0.182	0.075	74	73	75	1.002	0.416
33	33	34	0.819	0.34	75	70	76	0.546	0.226
34	34	35	0.637	0.264	76	65	77	0.091	0.037
35	35	36	0.182	0.075	77	10	78	0.637	0.264
36	26	37	0.364	0.151	78	67	79	0.546	0.226
37	27	38	1.002	0.416	79	12	80	0.728	0.302
38	29	39	0.546	0.226	80	80	81	0.364	0.151
39	32	40	0.455	0.189	81	81	82	0.091	0.037
40	40	41	1.002	0.416	82	81	83	1.092	0.453
41	41	42	0.273	0.113	83	83	84	1.002	0.416
42	41	43	0.455	0.189	84	13	85	0.819	0.34

Table-A2.2 85 Bus Distribution System Bus Data

Bus No	P_{gen} (kW)	Q_{gen} $(kVAR)$	P_{load} (kW)	Q_{load} $(kVAR)$	***Bus No***	P_{gen} (kW)	Q_{gen} $(kVAR)$	P_{load} (kW)	Q_{load} $(kVAR)$
1	0	0	0.00	0.00	44	0	0	35.28	35.99
2	0	0	0.00	0.00	45	0	0	35.28	35.99
3	0	0	0.00	0.00	46	0	0	35.28	35.99
4	0	0	56.00	57.13	47	0	0	14.00	14.28
5	0	0	0.00	0.00	48	0	0	0.00	0.00
6	0	0	35.28	35.99	49	0	0	0.00	0.00
7	0	0	0.00	0.00	50	0	0	35.28	35.99
8	0	0	35.28	35.99	51	0	0	56.00	57.13
9	0	0	0.00	0.00	52	0	0	0.00	0.00
10	0	0	0.00	0.00	53	0	0	35.28	35.99
11	0	0	56.00	57.13	54	0	0	56.00	57.13
12	0	0	0.00	0.00	55	0	0	56.00	57.13
13	0	0	0.00	0.00	56	0	0	14.00	14.28

14	0	0	35.28	35.99
15	0	0	35.28	35.99
16	0	0	35.28	35.99
17	0	0	112	114.26
18	0	0	56.00	57.13
19	0	0	56.00	57.13
20	0	0	35.28	35.99
21	0	0	35.28	35.99
22	0	0	35.28	35.99
23	0	0	56.00	57.13
24	0	0	35.28	35.99
25	0	0	35.28	35.99
26	0	0	56.00	57.13
27	0	0	0.00	0.00
28	0	0	56.00	57.13
29	0	0	0.00	0.00
30	0	0	35.28	35.99
31	0	0	35.28	35.99
32	0	0	0.00	0.00
33	0	0	14.00	14.28
34	0	0	0.00	0.00
35	0	0	0.00	0.00
36	0	0	35.28	35.99
37	0	0	56.00	57.13
38	0	0	56.00	57.13
39	0	0	56.00	57.13
40	0	0	35.28	35.99
41	0	0	0.00	0.00
42	0	0	35.28	35.99
43	0	0	35.28	35.99

57	0	0	56.00	57.13
58	0	0	0.00	0.00
59	0	0	56.00	57.13
60	0	0	56.00	57.13
61	0	0	56.00	57.13
62	0	0	56.00	57.13
63	0	0	14.00	14.28
64	0	0	0.00	0.00
65	0	0	0.00	0.00
66	0	0	56.00	57.13
67	0	0	0.00	0.00
68	0	0	0.00	0.00
69	0	0	56.00	57.13
70	0	0	0.00	0.00
71	0	0	35.28	35.99
72	0	0	56.00	57.13
73	0	0	0.00	0.00
74	0	0	56.00	57.13
75	0	0	35.28	35.99
76	0	0	56.00	57.13
77	0	0	14.00	14.28
78	0	0	56.00	57.13
79	0	0	35.28	35.99
80	0	0	56.00	57.13
81	0	0	0.00	0.00
82	0	0	56.00	57.13
83	0	0	35.28	35.99
84	0	0	14.00	14.28
85	0	0	35.28	35.99

Table-A1.3 Generator Cost coefficients for 85 Bus Distribution System

Bus No	*Gen*	*a* (*\$/kW*^{2})	*b* (*\$/kW*)	*C* (*\$*)	P_{min} (kW)	P_{max} (kW)
1	G1	0.0248	35.60	33.12	0.0	800
6	G2	0.0468	40.12	22.02	0.0	100
19	G3	0.0268	31.60	39.69	0.0	400
25	G4	0.0288	25.16	39.20	0.0	600
32	G5	0.0681	12.441	32.01	0.0	500
48	G6	0.0253	25.55	24.39	0.0	300
11	G7	0.0268	31.60	39.69	0.0	500
60	G8	0.0681	32.44	32.01	0.0	800
67	G9	0.0288	20.16	39.20	0.0	400

Appendix-3:

Table-A3: MULTI-MICROGRID SYSTEM PARAMETER VALUES[52]

Model		Parameter Values
Wind Turbine Parameters	:	$K_{WTG} = 1,\ T_{WTG} = 1.5secs$
Solar PV System Parameters	:	$K_{PV} = 0.0075, T_{PV} = 0.03secs$
BESS Parameters	:	$K_{BES} = 1, T_{BES} = 0.1secs$
Valve Actuator Parameters	:	$T_1 = 0.025secs, T_2 = 2secs,$ $T_3 = 3secs$
Diesel Engine Generator Parameters	:	$K_E = 1, T_E = 3secs$
Speed Regulation Constant	:	$R_1 = 5\ \frac{Hz}{P.U.\ MW},\ \ R_2 = 5\frac{Hz}{P.U.\ MW}$
Synchronizing power coefficient	:	$T_{12} = 0.225\Pi secs$
Rotor Swing-1 Parameters	:	$K_{P1} = 60, T_{P1} = 18secs$
Rotor Swing-2 Parameters	:	$K_{P2} = 60, T_{P2} = 18$

Appendix-4:

CURRENT INJECTION BASED DISTRIBUTION SYSTEM LOAD FLOW STUDY

Algorithm:

1. Read the Distribution System data (i.e., No. of Buses(n), Slack bus, Line data, Bus data, epsilon, itermax).
2. Print the input data and cross check it.
3. Form the Y bus by Sparsity technique.
4. Calculate P_{inj} and Q_{inj} for i =1 to n.
5. Set iter=0
6. Set $Real(\Delta I)_{max} = 0$ and $Imag(\Delta I)_{max} = 0$.
7. Calculate $I_{sp}(i) = (P_{inj}(i) - Q_{inj}(i))/E(i)$, for i=1 to n.
8. Calculate $I_{cal}(i) = Y_{ii} * E_i + \sum_{\substack{j=1 \\ j\neq i}}^{n} E_q$
9. Calculate $\Delta I(i) = I_{sp}(i) - I_{cal}(i)$
10. Calculate $Real(\Delta I(i))$ and $Imag(\Delta I(i))$ for i=1 to n.
11. Evaluate $Real(\Delta I)_{max}$ and $Imag(\Delta I)_{max}$.
12. If $Real(\Delta I)_{max} < epsilon$ and $Imag(\Delta I)_{max} < epsilon$, go to step (17).
13. (a) Form Jacobian matrix A=$\begin{pmatrix} H & N \\ M & L \end{pmatrix}$

$$H_{pp} = b_p - B_{pp} \qquad H_{pq} = -B_{pq}$$

$$N_{pp} = -a_p - G_{pp} \qquad N_{pq} = -G_{pq}$$

$$M_{pp} = a_p - G_{pp} \qquad M_{pq} = -B_{pq}$$

$$L_{pp} = b_p + B_{pp} \qquad L_{pq} = B_{pq}$$

$$a_p = \frac{P_p(e_p^2 - f_p^2) + Q_p(2e_p f_p)}{V_p^4}$$

$$b_p = \frac{-Q_p(e_p^2 - f_p^2) + P_p(2e_p f_p)}{V_p^4}$$

(b) Set H(nslack, nslack)=10^{20} to make $\Delta e_{nslack} = 0$.

(c) Set L(n+nslack, n+nslack)=10^{20} to make $\Delta f_{nslack} = 0$.

14. Solve $\begin{bmatrix} \Delta I_{imag} \\ \Delta I_{real} \end{bmatrix} = \begin{pmatrix} H & N \\ M & L \end{pmatrix} * \begin{bmatrix} \Delta e \\ \Delta f \end{bmatrix}$

15. Update complex voltages (real and imaginary parts of voltage)
16. If iter $<$ itermax, go to step (6).
17. Print the Results.